AD-A110 963 LOCKHEED MISSILES AND SPACE CO INC PALO ALTO CA PALO --ETC F/G 1/3
PANEL OPTIMIZATION WITH INTEGRATED SOFTWARE (POIS). VOLUME I. P--ETC(U)
JUL 81 D BUSHNELL F33615-76-C-3105

UNCLASSIFIED AFWAL-TR-81-3073-VOL-1 NL

1 OF 3
AD A
110963

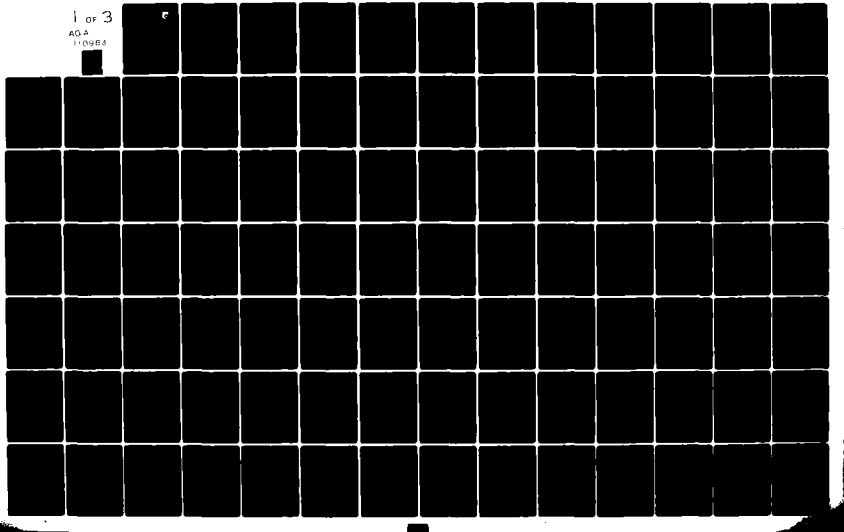

AFWAL-TR-81-3073
VOLUME I

PANEL OPTIMIZATION WITH INTEGRATED SOFTWARE (POIS)

PANDA--INTERACTIVE PROGRAM FOR PRELIMINARY MINIMUM WEIGHT DESIGN

DAVID BUSHNELL

LOCKHEED MISSILES AND SPACE COMPANY, INC.
3251 HANOVER STREET
PALO ALTO, CALIFORNIA 94304

JULY 1981

TECHNICAL REPORT AFWAL-81-3073, VOLUME I
Final Report for Period June 1976 - October 1980

Approved for public release; distribution unlimited.

FLIGHT DYNAMICS LABORATORY
AIR FORCE WRIGHT AERONAUTICAL LABORATORIES
AIR FORCE SYSTEMS COMMAND
WRIGHT-PATTERSON AIR FORCE BASE, OHIO 45433

NOTICE

When Government drawings, specifications, or other data are used for any purpose other than in connection with a definitely related Government procurement operation, the United States Government thereby incurs no responsibility nor any obligation whatsoever; and the fact that the government may have formulated, furnished, or in any way supplied the said drawings, specifications, or other data, is not to be regarded by implication or otherwise as in any manner licensing the holder or any other person or corporation, or conveying any rights or permission to manufacture use, or sell any patented invention that may in any way be related thereto.

This report has been reviewed by the Office of Public Affairs (ASD/PA) and is releasable to the National Technical Information Service (NTIS). At NTIS, it will be available to the general public, including foreign nations.

This technical report has been reviewed and is approved for publication.

Narendra S. Khot

NARENDRA S. KHOT,
Project Engineer

Fred H. Picchioni

FREDERICK A. PICCHIONI, Lt Col, USAF
Chief, Analysis & Optimization Branch

FOR THE COMMANDER

for

RALPH L. KUSTER, JR., Col, USAF
Chief, Structures & Dynamics Div.

"If your address has changed, if you wish to be removed from our mailing list, or if the addressee is no longer employed by your organization please notify AFWAL/FIBR, W-PAFB, OH 45433 to help us maintain a current mailing list".

Copies of this report should not be returned unless return is required by security considerations, contractual obligations, or notice on a specific document.

AIR FORCE/56780/3 February 1982 — 260

SECURITY CLASSIFICATION OF THIS PAGE (When Data Entered)

REPORT DOCUMENTATION PAGE	READ INSTRUCTIONS BEFORE COMPLETING FORM
1. REPORT NUMBER: AFWAL-TR-81-3073, Vol. I	2. GOVT ACCESSION NO.: AD-A110 963
3. RECIPIENT'S CATALOG NUMBER:	
4. TITLE (and Subtitle): PANEL OPTIMIZATION WITH INTEGRATED SOFTWARE (POIS) Volume I - PANDA--INTERACTIVE PROGRAM FOR PRELIMINARY MINIMUM WEIGHT DESIGN	5. TYPE OF REPORT & PERIOD COVERED: Final Report
	6. PERFORMING ORG. REPORT NUMBER:
7. AUTHOR(s): DAVID BUSHNELL	8. CONTRACT OR GRANT NUMBER(s): F33615-76-C-3105
9. PERFORMING ORGANIZATION NAME AND ADDRESS: Lockheed Palo Alto Research Laboratories 3251 Hanover Street Palo Alto, California 94304	10. PROGRAM ELEMENT, PROJECT, TASK AREA & WORK UNIT NUMBERS: 61102F 2307 N1 02
11. CONTROLLING OFFICE NAME AND ADDRESS: Flight Dynamics Laboratory (AFWAL/FIBRA) Air Force Wright Aeronautical Laboratories Wright-Patterson AFB, OH 45433	12. REPORT DATE: July 1981
	13. NUMBER OF PAGES: 253
14. MONITORING AGENCY NAME & ADDRESS(if different from Controlling Office)	15. SECURITY CLASS. (of this report): UNCLASSIFIED
	15a. DECLASSIFICATION/DOWNGRADING SCHEDULE
16. DISTRIBUTION STATEMENT (of this Report): APPROVED FOR PUBLIC RELEASE; DISTRIBUTION UNLIMITED	
17. DISTRIBUTION STATEMENT (of the abstract entered in Block 20, if different from Report)	
18. SUPPLEMENTARY NOTES	
19. KEY WORDS (Continue on reverse side if necessary and identify by block number): panel, optimization, weight, stiffened, composite, interactive, elastic-plastic	

20. ABSTRACT (Continue on reverse side if necessary and identify by block number)
An analysis and an interactive computer program are described through which minimum weight designs of composite, stiffened, cylindrical panels can be obtained subject to general and local buckling constraints and stress and strain constraints. The panels are subjected to arbitrary combinations of in-plane axial, circumferential, and shear resultants. Nonlinear material effects are included if the material is isotropic or has stiffness in only one direction (as does a discrete or a smeared stiffener). Several types of general and local buckling modes are included as constraints in the optimization process, including general instability,

DD FORM 1 JAN 73 1473 EDITION OF 1 NOV 65 IS OBSOLETE

SECURITY CLASSIFICATION OF THIS PAGE (When Data Entered)

panel instability with either stringers or rings smeared out, local skin buckling, local crippling of stiffener segments, and general, panel, and local skin buckling including the effects of stiffener rolling. Certain stiffener rolling modes in which the panel skin does not deform but the cross section of the stiffener does deform are also accounted for. The interactive PANDA system consists of three independently executed modules that share the same data base. In the first module an initial design concept with rough (not necessarily feasible or accurate) dimensions are provided by the user in a conversational mode. In the second module the user decides which of the design parameters of the concept are to be treated by PANDA as decision variables in the optimization phase. In the third module the optimization calculations are carried out. Many examples are provided in which optimum designs obtained by PANDA are compared to those in the literature.

FOREWORD

This report was prepared by Lockheed Missiles and Space Company, Inc., Palo Alto Research Laboratories, 3251 Hanover Street, Palo Alto, California, in partial fulfillment of the requirements under Contract F33615-76-C-3105. The effort was initiated under Project 2307, "Research in Flight Vehicle Structures," Task 2307N102, "Research in the Behavior of Metallic and Composite Components of Air Frame Structures." The project monitor for the contract was Dr. Narendra S. Khot of the Structures and Dynamics Division (AFWAL/FIBRA).

The technical work under the contract was performed during the period June 1976 through October 1980. Review report was submitted in October 1980 and the final report in March 1981.

The other reports published under this contract are "Imperfection Sensitivity of Optimized Structures," (AFWAL-TR-80-3128), "Numerical Procedure for Analysis of Structural Shells," (AFWAL-TR-80-3129), "Panel Optimization with Integrated Software (POIS)," (AFWAL-TR-80-3073, Vol II), "Design of Composite Material Structures for Buckling, An Evaluation of State-of-the-Art," (AFWAL-TR-81-3102).

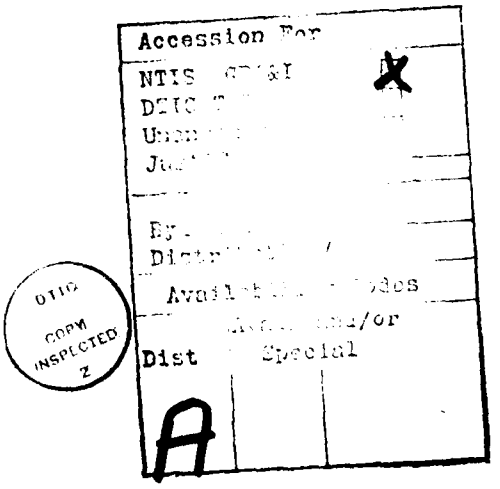

TABLE OF CONTENTS

TABLE OF CONTENTS (cont.)

TABLE OF CONTENTS (cont.)

ABSTRACT

An analysis and an interactive computer program are described through which minimum weight designs of composite, stiffened, cylindrical panels can be obtained subject to general and local buckling constraints and stress and strain constraints. The panels are subjected to arbitrary combinations of in-plane axial, circumferential, and shear resultants. Nonlinear material effects are included if the material is isotropic or has stiffness in only one direction (as does a discrete or a smeared stiffener). Several types of general and local buckling modes are included as constraints in the optimization process, including general instability, panel instability with either stringers or rings smeared out, local skin buckling, local crippling of stiffener segments, and general, panel, and local skin buckling including the effects of stiffener rolling. Certain stiffener rolling modes in which the panel skin does not deform but the cross section of the stiffener does deform are also accounted for. The interactive PANDA system consists of three independently executed modules that share the same data base. In the first module an initial design concept with rough (not necessarily feasible or accurate) dimensions are provided by the user in a conversational mode. In the second module the user decides which of the design parameters of the concept are to be treated by PANDA as decision variables in the optimization phase. In the third module the optimization calculations are carried out. Many examples are provided in which optimum designs obtained by PANDA are compared to those in the literature.

NOMENCLATURE

A	= stiffener cross section area
$\underset{\sim}{A}$	= 3 x 3 integrated constitutive matrix governing extensional (membrane) behavior, Eq. (4)
a_o, b_o	= distances between rings, stringers (Fig. 1)
a, b	= axial, circumferential, dimensions of panel
b_i	= width of ith segment of any stiffener (Fig. 4)
C_{ij}; i=1,6; j=1,6	= 6 x 6 integrated constitutive matrix governing extensional and bending behavior, Eqs. (37) and (40)
c	= slope of buckling nodal lines for panel that is long in the x-direction [Eqs.(51), Fig. 14a]
d	= slope of buckling nodal lines for panel that is long in the y-direction [Eqs.(51), Fig. 14b]
e	= strain or eccentricity, depending on context
$\bar{e}$	= effective strain
E, E_o	= Young's modulus
G, G_o	= shear modulus
$\bar{G}$	= reduced shear modulus, Eq. (41)
g	= plasticity factor, Eq. (30)
I	= stiffener bending moment of inertia
J	= stiffener torsional constant (e.g. $\sum_{i=1}^{N} b_i t_i^3/3$)
$\bar{n}$, $\bar{m}$	= halfwaves in axial, circumferential directions
n, m	= circumferential, axial wave indices, Eq. (52)
n_1, m_1, n_2, m_2	= wave indices, Eq. (51)
N, M	= stress, moment resultants
p	= pressure

R = radius of cylindrical panel

s = local coordinate shown in Fig. 18

t = thickness

u^*, v^*, w^* = displacement components referred to stiffener coordinates, Figs. 16, 17

u, v, w = displacement components of panel skin in x, y, z directions, respectively (Fig. 3)

x, y, z = shell surface coordinates, Fig. 2; or coordinates shown in Fig. 18, depending on context

$\bar{x}_i, \bar{y}_i$ = coordinates in the plane of the ith stiffener segment (Fig. 4)

$\bar{x}, \bar{y}, \bar{z}$ = coordinates shown in Fig. 16 and Fig. 17

x_{max}, y_{max} = defined just after Eq. (49)

β = rotation of flange, Fig. 18

γ = stiffener rolling angle, Fig. 17

λ = eigenvalue or load factor

κ = change in curvature or twist

ν = Poisson's ratio

ρ = density

σ = stress

$\bar{\sigma}$ = effective stress

ω = stiffener rotation components, Figs. 16, 17

ϕ = ratio (local buckling load factor)/(general buckling load factor), or angle from material coordinates of a lamina to the axial coordinate (Fig. 2), depending on context

Subscripts

eff = "effective"

1,2,11,12,22 = pertain to strain components and moduli with respect to the material coordinate directions, 1 and 2, shown in Fig. 2

b = pertaining to buckling analysis

b = bending energy [Eqs.(85,88,92,94)]

e = eigenvalue parameter

f = flange

i = stiffener segment number

m = membrane energy [Eqs.(81-83, 90,91,93]

pl = material proportional limit

PRE, fixed = prestress not multiplied by eigenvalue

s = secant modulus

skin = pertaining to part of the panel between stiffeners

T = tangent modulus

w = web

$\bar{x}$ = $\bar{x}$ - direction (Figs. 16, 17)

x = x - direction (Fig. 2); or along stiffener axis

y = y - direction (Fig. 2)

xy = in-plane shear (Fig. 2), or twist

( ),x = differentiation with respect to x; Eq. (5)

Superscripts

eff	= "effective"
b	= pertaining to buckling analysis
f	= flange
i	= stiffener segment number
j	= stiffener segment number
k	= layer index
o	= prebuckling condition at design load
r	= ring
s	= stringer
w	= web

LIST OF TABLES

LIST OF FIGURES

17. In-plane bending of a flange induced by rolling of the stiffener in the mode shown in Figure 6a

18. Stiffener coordinates and displacement components for rolling analysis of the types shown in Figs 6b and 6c (no participation of the panel skin)

19. Buckling loads of a composite, axially compressed cylindrical shell with an unbalanced laminate (0, 0, -0). Comparison of results from PANDA, STAGSC-1 [62], and Booton and Tennyson [57].

20. Ring and stringer stiffened cylindrical shell under pure torsion. The dimensions correspond to an optimum design obtained by Simitses and Giri [63] (See Table 4, Case 2)

21. Shallow curved panel under pure in-plane shear. Bottom portion shows bifurcation buckling pattern predicted by STAGSC-1 [62]. (See Table 4, Case 3)

22. Buckling modes predicted by BOSOR4 for axially compressed panels of lengths (a) 40 in., (b) 20 in., (c,d) 10 in. Dimensions of the cross sections were obtained by optimization analyses with PANDA.

23. Axially compressed ring and stringer stiffened cylindrical shell analysed by Block, Card, and Mikulas [65] and by Kicher and Wu [66]. (See Table 5)

24. Axially compressed, elastic-plastic, ring stiffened cylindrical shell. Comparison of critical loads from PANDA and from BOSOR5 [59].

25. Buckling of axially compressed composite panel with composite stringers. Comparison of results from PANDA and the analyses of Williams and Stein [24]. (see Table 6)

26. General (ring) instability of long, ring stiffened cylindrical shell under uniform external lateral pressure, and local instability (nonsymmetric sidesway or "tripping") of ring. Comparison of results from PANDA and results from BOSOR4 [58]. (See Table 7)

27. Externally pressurized ring stiffened cylindrical shell that fails by axisymmetric sidesway of the deep rings, (a) geometry, (b) results of linear bifurcation analyses with BOSOR4 (solid line) and PANDA (x's). (See Table 8)

28. Local and general buckling of ring stiffened cylinder under uniform lateral external pressure. Solid line is from BOSOR4 predictions; x's are from PANDA. (See Table 9)

29. Finite element model for local buckling under axial compression of a portion of the ring and stringer stiffened cylindrical shell shown in Fig. 9. Linear bifurcation buckling

load factors and an elastic-plastic collapse load were obtained through use of the STAGSC-1 program [62]. (See Table 10)

30. Elastic-plastic collapse of the axially compressed cylindrical shell shown in Figure 9, as predicted by BOSOR5 [59] and STAGSC-1 [62] (See Table 11)

31. Buckling modes obtained with BOSOR4 corresponding to optimum designs of hydrostatically compressed, ring stiffened cylindrcal shells The configuration (a) was obtained by Pappas and Allentuch [47]. The configuration (d) was obtained by PANDA. Design pressure p_o = 898 psi. (See Table 18)

32. Effective strains midway between adjacent rings at the buckling pressure for a hydrostatically compressed cylindrical shell with internal rectangular stiffeners. Configuration is shown in Fig. 34. Design pressure p_o = 4066 psi. (See Table 19)

33. Hydrostatically compressed, internally ring stiffened cylindrical shell: BOSOR5 model and predicted buckling modes and pressures corresponding to the analysis of Renzi [44]. (See Table 19)

34. Hydrostatically compressed, internally ring stiffened cylindrical shell: BOSOR5 model and predicted buckling modes and pressures corresponding to the optimum design determined by PANDA. (See Table 19)

35. Hydrostatically compressed, internally ring stiffened cylindrical shells: Modeling strategy for BOSOR5 analyses of the minimum weight designs obtained by PANDA for design pressures p_o ranging from p_o = 677 psi to p_o = 4743 psi. (See Table 20 for dimensions.)

36. Hydrostatically compressed, internally ring stiffened cylindrical shells: BOSOR5 discretized models corresponding to minimum weight designs obtained by PANDA for design pressures ranging from 677 psi to 4743 psi. (See Table 20)

37. Hydrostatically compressed, internally ring stiffened cylindrical shells: Midbay effective membrane strains at the design pressures for the optimized configurations shown in Figure 36.

38. Hydrostatically compressed, internally ring stiffened cylindrical shells: Comparison of buckling loads obtained from PANDA and from BOSOR5. This is a comparison because the critical loads from PANDA are all very near unity, as seen from Table 21.

39. Buckling modes predicted by BOSOR5 for the optimum design corresponding to p_o = 4743 psi.

40. Hydrostatically compressed, internally ring-stiffened

cylindrical shells optimized by PANDA for a design pressure of 2710 psi. Comparisons of buckling predictions from BOSOR5 and PANDA: (a) minimum weight design corresponding to a one-layered model in PANDA; (b) minimum weight design corresponding to a 5-layered model in PANDA.

41. Hydrostatically compressed, internally ring-stiffened cylindrical shell optimized by PANDA (5-layered model) for a design pressure of 2710 psi: Comparisons between BOSOR5 and PANDA of the prebuckling state (a) in the ring; (b) in the skin midway between rings.

SECTION I

INTRODUCTION

Objective

The objective of the development of PANDA has been to create an interactive computer program for engineers which derives minimum weight designs of stiffened cylindrical panels under combined in-plane loads, N_x , N_y , and N_{xy} . The loading of the stiffened panel is assumed in most cases to result in uniform membrane strain components e_x and e_y in both skin and stiffeners and uniform shear strain e_{xy} in the skin. Meridional bending between rings in the prebuckling phase is included for shells without axial stiffeners. Nonlinear material behavior is included in the prebuckling analysis if the material is isotropic or has strength only in one direction (smeared or discrete stiffeners).

Buckling loads are calculated by use of simple assumed displacement functions. For example, general instability of panels with balanced laminates and no shear loading is assumed to occur in the familiar $w(x,y) = C\sin(ny)\sin(mx)$ mode. In the presence of in-plane shear and/or unbalanced laminates, both local and general buckling patterns are assumed to have the form

$$w(x,y) = C\{ \cos[(n+mc)y - (m+nd)x] - \cos[(n-mc)y + (m-nd)x] \}$$

in which either c or d are zero, depending on the geometry and the stiffness of the entire panel or whatever portion of the panel is under consideration.

The skin is cylindrical with radius R and the stiffeners are composed of assemblages of flat plate segments the lengths of which are large compared to the widths and the widths of which are large compared to the thicknesses. These flat plate segments are oriented either normal or parallel to the plane of the panel skin.

Figure 1 shows an example of the panel geometry. The overall dimensions of the panel are (a,b) and the spacings of the stiffeners are (a_o ,b_o).

Material Properties

If the material is orthotropic or anisotropic, buckling is assumed to occur at stress levels for which this material remains elastic. Feasible designs are constrained by maximum stress or strain criteria. Plasticity with arbitrary strain hardening is permitted if the material is isotropic or if it has stiffness in one coordinate direction only, as does the continuum representation or each segment of a smeared stiffener. The cylindrical skin and stiffener segments can be composed of multiple la-

yers or isotropic or orthotropic material, as depicted in Fig. 2. Each layer has a unique angle of orthotropy relative in the case or the panel skin to the direction of the generator (x- direction) and in the case of a stiffener segment to the stiffener axis. In the buckling analysis the segments of the stiffeners are assumed to be monocoque and isotropic or orthotropic, not layered anisotropic. Therefore, equivalent orthotropic properties for stiffener segments are calculated from input data for the stiffener segment laminates provided by the program user.

Types or Buckling

Optimum designs with respect to weight are obtained in the presence of constraints due to local and general buckling, maximum tensile and compressive stress or strain, maximum shear strain, and lower and upper bounds on skin layer thicknesses, stiffener cross section dimensions, and stiffener spacings. Design parameters allowed to vary during the optimization phase include panel skin laminae thickness and winding angles, spacings of stiffeners, and thicknesses and widths of the segments of ring and stringer cross sections.

The buckling formulas are derived from Donnell's equations (Reference [1]) with a posteriori application of a reduction factor $(n_c^2 - 1)/n_c^2$ for panels in which the axial half wavelength of the buckling pattern is longer than the panel radius of curvature, R. The circumferential wave index, n_c, equals $n\pi R/b$

or $n\pi R/b_o$, with n being the number of half waves in the circumferential direction over the span b or b_o , respectively.

The many types of buckling included in the PANDA analysis are summarized in Table 1 and are briefly described next.

Skin Buckling

For the case of balanced laminates and no in-plane shear, local buckling of the skin is assumed to have the form

$$w_{skin} = C_{skin} \sin\left(\frac{\bar{n}_{skin}\pi y}{b_o}\right) \sin\left(\frac{\bar{m}_{skin}\pi x}{a_o}\right) \qquad (1)$$

in which $\bar{n}_{skin}$ and $\bar{m}_{skin}$ are the numbers of half-waves between stringers with spacing b_o and rings with spacing a_o , respectively. The coordinates and shell wall displacement components are shown in Fig. 3. Equation(1) implies simple support boundary conditions at stiffener lines of attachment. With shear present and/or unbalanced laminates the skin buckling pattern has the form given in the second paragraph under Objective.

General Instability

General instability buckling modes of panels with balanced laminates and no shear also have the form given in Eq.(1) with a_o , b_o , $\bar{n}_{skin}$, and $\bar{m}_{skin}$ replaced by quantities appropriate to the overall dimensions (a,b) of the panel. PANDA also calcu-

lates values for "semi-general" instability, that is buckling between rings with smeared stringers and buckling between stringers with smeared rings.

Buckling of Stiffeners

Local buckling of the ith stiffener segment implies

$$w^i_{stiff} = C^i_{stiff} \sin\left(\frac{\pi \bar{\bar{y}}_i}{b_i}\right) \sin\left(\frac{\bar{m}^i_{stiff} \pi \bar{x}}{\ell}\right) \tag{2}$$

for each stiffener segment with both long edges supported (called "internal" segments in Fig. 4). As shown in Fig. 4 the quantity $\bar{x}$ is the coordinate along the stiffener axis, $\bar{\bar{y}}_i$ is the coordinate perpendicular to $\bar{x}$ in the plane of the ith stiffener segment, b_i is the width of the stiffener segment, and ℓ is the length of the stiffener segment. ($\ell = a_o$ for stringers and $\ell = b_o$ for rings). For stiffener segments with only one long edge supported, (called "end" segments), the local buckling modal displacement is assumed to be in the form

$$w^i_{stiff} = C^i_{stiff} \bar{\bar{y}}_i \sin\left(\frac{\bar{m}^j_{stiff} \pi \bar{x}}{\ell}\right) \tag{3}$$

The stiffener segment buckling analysis is carried out with the assumption that each "internal" segment buckles with its own $\bar{m}^i$. This assumption implies that rotational incompatibility exists at junctions between segments with differing critical values of $\bar{m}^i$. "End" segments are assumed to buckle at the criti-

cal $\bar{m}^j$ of the segment to which they are joined. The buckling modes (2) and (3) are shown in Fig. 5.

Rolling Modes

Additional types of panel and stiffener buckling are considered here. These are called "rolling" modes. The first kind of rolling mode involves both skin and stiffeners and is local or "semi-general", the characteristic half-wave-length being integer fractions of the lengths (a_o ,b_o), or (a,b_o) or (a_o ,b). In these rolling modes the stiffener cross sections rotate about their lines of attachment to the panel skin as shown in Fig. 6a. The cross sections do not deform in the plane of the paper. They do warp, however. The other types of rolling instability do not involve the skin at all. Only the stiffener web deforms, the rest or the stiffener cross section displacing and rotating as a rigid body, as displayed in Fig. 6b. One of these rolling modes (Fig. 6b) occurs in both rings and stringers and in both curved and flat panels. In this mode the buckling deformations are nonuniform (sinusoidal) along the axis of the stiffener. The other rolling mode (Fig. 6c) occurs only in the cases of internal rings on cylindrical panels under external pressure and external rings on cylindrical panels underinternal pressure. In this mode buckling deformations are uniform along the axis of the ring. Stiffener rolling in the more general mode (Fig. 6b) is due to compression along the stiffener and is only weakly dependent on the curvature of this axis. On the other hand, the

local ring buckling depicted in Fig. 6c is axisymmetric and arises because of the circumferential curvature of the stiffener axis and prestress in the stiffener segments. It is interesting to note that axisymmetric rolling can occur even if there are no compressive stresses anywhere in the structure, as is the case for internally pressurized cylindrical shells with external rings.

Optimization

The subroutine CONMIN [2,3] is used in PANDA for finding minimum weight designs. This subroutine, written by Vanderplaats in the early 1970's, is based on a nonlinear constrained search algorithm due to Zoutendijk [4]. Briefly, the analytic technique used in CONMIN is to minimize an objective function (panel weight, for example) until one or more constraints, in this case buckling loads, maximum stress or strain, and upper and lower bounds on decision variables, become active. The minimization process then continues by following the constraint boundaries in decision variable space in a direction such that the value of the objective function continues to decrease. When a point is reached where no further decrease in the objective function is obtained, the process is terminated.

Imperfection Sensitivity

It should be emphasized that PANDA does not account expli-

citly for initial structural imperfections. As the code is now written, the user should design a panel to higher loads than those actually to be seen in service; the deleterious effects of initial imperfections can be accounted for in this way.

SECTION II

BRIEF REVIEW OF PREVIOUS WORK ON OPTIMIZATION OF STIFFENED SHELLS AND PANELS UNDER DESTABILIZING LOADS

This review is concerned with optimization of stiffened shells and panels under destabilizing loads. Optimization techniques per se are not discussed or referenced here. Venkayya [5] has written an excellent survey with an extensive bibliography on this subject.

Most of the work on optimization of stiffened shells and panels under compressive loads has been motivated by the wish to find minimum weight designs of aerospace vehicles. Minimum weight design of ship decks and submarine pressure hulls has also been studied. In recent years computer programs for optimizing aerospace structures have been written for application to laminated wall construction. Design variables include laminae thicknesses and winding angles. Computer programs for optimizing ship structures, especially submarine pressure hulls, have been written to include nonlinear material behavior.

Optimization algorithms have tended to follow either of two strategies: 1. calculation of optimum designs from linear or nonlinear programming techniques created to find minima of an objective function in design space, and 2. calculation of opti-

mum designs from formulas derived from the condition that different types of failures should occur at a given load. (See Venkayya [5] for further details.)

One of the earliest papers on optimum design of stiffened panels is by Catchpole[5a]. Schmit and his colleagues have written several papers on optimization of stiffened plates and cylindrical shells subject to combined in-plane loading [6-10]. Optimization is by various nonlinear programming methods. In an early work, Schmit, Kicher, and Morrow [6] found minimum weight designs of rectangular, simply supported waffle plates. Buckling constraint conditions include general instability, local instability between stiffeners, and stiffener instability. Bronowicki, et al [10] optimized a cylindrical shell with internal T-shaped rings subject to uniform external hydrostatic pressure. They found minimum weight designs with maximum separation of the lowest two frequencies and with maximum separation of the lowest two frequencies with primarily axial content. Gross buckling is prevented by specification of a minimum natural frequency. Additional constraints preclude yielding, buckling of panels between rings, and buckling of stiffeners or stiffener segments. Optimization is by use of a sequential unconstrained minimization technique.

Several papers were written by Burns and his colleagues [11-15]. The primary motivation was to produce minimum weight designs of rocket boosters. The structures were optimized

through application of formulas which dictate that local and general instability occur at the same load.

Many articles and computer programs have been written under the sponsorship of NASA or used by NASA personnel [16-26]. The motivation has been to design minimum weight structures and to provide computer programs for such designs for rocket boosters and airplane fuselages and wings.

The latest in the series of NASA programs for optimization of aerospace structures is the PASCO program [26, 27] written by Anderson, Stroud, and others at NASA. This program calculates minimum weight designs of composite stiffened panels. A panel is considered to be built up of an assemblage of flat plate segments, each of which may have laminated wall construction. The buckling analysis is exact within the limitations of Kirchoff-Love theory. Thus, complex buckling modes are included in the optimization process, modes for example in which general and local waviness are combined. The panels must be simply supported at the top and bottom and be stiffened only in the axial direction. The effect of bow-type imperfections are included, both in the stress and local buckling analyses. PASCO is a combination of a structural program VIPASA written by Wittrick and Williams [23] for the local and general buckling of stiffened flat panels and the previously mentioned optimization routine CONMIN written by Vanderplaats [2].

Recent advances in the application of laminated composite materials to aerospace structures has led to many papers on the optimization of stiffened composite panels and wings, among them [28-31].

Several papers on optimization of stiffened cylinders have been written recently by Simitses and his colleagues [32-36]. Their primary motivation has been to produce a computerized capability to design minimum weight fuselages for large aircraft. These structures are subjected to combined axial compression, shear, and internal pres- sure. In the papers by Simitses, et al, the buckling equations are based on Donnell's shell theory [1]. The Galerkin procedure is used to obtain buckling loads. The series expansion for the buckling modal displacement is valid for simply supported panels. Local buckling of stiffener segments is included, and both rings and stringers may be present. The von Mises yield criterion is used for the maximum stress constraint. Optimization is by a variation of the Simplex method.

Papers have been written on the optimization of structures used in ships [39-47]. While recent developments in capabilities to create minimum weight designs of aerospace structures have emphasized laminated composites, recent developments of capabilities to create minimum weight designs of ships have included nonlinear material behavior [44]. Optimization programs for the minimum weight design of submarine pressure hulls (ring

stiffened cylinders) have been written by Pappas and his co-workers [45-47] and by Renzi [44]. Renzi's program, called DAPS3, essentially incorporates the structural analyses and concepts described in [40-43]. Pappas [47] includes in his optimization program general instability, buckling between rings, and crippling of the rings, which have T-shaped cross sections. The design is constrained by a maximum stress criterion and the material must remain elastic. Pappas performs an elaborate search in buckling modal wavelength space (m,n)-space in order to obtain reliably the minimum buckling load corresponding to general instability.

Under the sponsorship of the Air Force Flight Dynamics Laboratory, Almroth, et al [48] have created a system of computer programs that work together to create optimum designs of stiffened cylindrical panels. The PANDA code, based on simple buckling formulas and restricted to simply supported uniform panels, can be used to obtain an initial design. The parameters of this design are stored on a file which can be read by other programs requiring more computer time than PANDA but not restricted as to boundary conditions and uniformity of thickness, stiffener spacing, loading, and buckling mode shapes.

Other papers on optimization subject to constraints other than buckling and stress include Refs. [49] and [50].

SECTION III

FLOW OF CALCULATIONS IN PANDA

Figures 7 and 8 show the flow of calculations in PANDA. Each of the top two boxes in Figure 7 represents a separate interactive computer program. In the first program (called BEGIN) the user, with a specific concept in mind (e.g. knowing in advance that he wants to find the minimum weight design of a composite cylindrical shell of 7 layers stiffened by T-shaped composite internal rings and I-shaped aluminum external stringers) provides the material properties, loads, and starting design in a "conversational" mode.

In the second program (called DECIDE) the user decides whether he wants to do simply a buckling analysis of the starting design or whether he wants to do an optimization analysis. If he wants to do an optimization analysis, the user is then asked, also in this second program, to identify which of the design parameters are to be allowed to vary during the optimization process, that is which of the design parameters are to be "decision variables" and what are the lower and upper bounds of these decision variables. The user can also specify at this time that certain of the design parameters be "linked" to (to vary in proportion with) certain of the decision variables. For example, in laminated composite wall construction the

thicknesses of layers with plus winding angles are usually taken to be equal to those with minus the same winding angles; the width of Segment 3 of a T-shaped stiffener is equal to that of Segment 2 (Fig.4a).

When the first two programs have been executed (through commands "RUN BEGIN" and "RUN DECIDE", respectively), the user next executes the main analysis module through the command "RUN PANCON", which performs, with some on-line interaction with the user, the rest of the calculations indicated in Figures 7 and 8.

It is easy to see from Fig. 7 that if there are a large number, NDV, of decision variables (NDV > 6, say) many, many buckling load factors must be computed, especially if the case is complicated so that many different kinds of buckling modes must be considered. For example, in the case displayed in Fig. 9, for which 11 different types of buckling are investigated, as listed in Table 1, there might be as many as 7 decision variables: t, a_o, b_o, t^s, b^s, t^r, and b^r (identified in Figure 9). Thus, each execution of the loop, (I = 1, NDV), in Figure 7 requires calculation of NDV * 11 = 77 critical buckling load factors. Each of the 77 critical buckling load factors represents the results of minimization of the potential energy with respect to the wave indices $\bar{m}$ and $\bar{n}$ and the buckling nodal line slopes c or d. In order to save computer time in PANDA the buckling modal parameters, $\bar{m}(i)$, $\bar{n}(i)$, c(i), and d(i), i = 1, 2 .. 11 corresponding to the 11 critical modes for the current

"baseline" design (X(J), J = 1, NDV) are held constant for the slightly perturbed designs Y investigated in the loop over NDV. These perturbed designs must be evaluated with regard to stress and buckling in order to generate gradients of weight and constraint conditions needed by the optimizer CONMIN [2,3].

Simple Example

The PANDA program is completely interactive, with the user's instructions embedded in the three modules, BEGIN, DECIDE, and PANCON. The user has two choices in the preprocessor BEGIN:

(1) The user can choose the long form of the description of the input data, which provides details needed by those who have never before used PANDA or by those who would like to have their memories refreshed; or

(2) The user can choose the short form of the description of the input data, which simply calls for the input data by name, without giving additional description as to what the data are.

Table 2a is a list of a runstream generated with use of the short form for a very simple case with an intuitively obvious answer. The table first illustrates how the three modules of PANDA are exercized simply to calculate a buckling load for a

given design (pages 1-6 of Table 2a). This calculation is followed by an optimization analysis (pages 7-12 of Table 2a). The geometry is for an unstiffened cylinder of radius R = 100 in. and length L = 200 in., with a wall consisting of two layers, each of a different elastic material, loaded in hydrostatic compression with a design pressure of p_o = 20 psi. In the starting design the two layers are of equal thickness and the shell is unnecessarily heavy, that is, the buckling load factor corresponding to the starting design is 3.238 (p. 6 of Table 2a) whereas a load factor of 1.0 would still yield a feasible design.

The material of layer no. 2 (the outer layer) has been deliberately chosen, for the purpose of demonstration, so that its E/ρ is considerably lower than that of the material of layer no. 1. If the decision variables are the thicknesses of the two layers, if these thicknesses are essentially unbounded, and if the effective stress at buckling is less than the maximum specified for either material, then it is known for this simple problem that the optimum design must correspond to the cylinder being made entirely of the material of layer no. 1, with its thickness derived so that the buckling load multiplier (eigenvalue) is equal to unity.

Starting on page 7 of Table 2a are listed the results of a second execution of DECIDE, this for the purpose of choosing decision variables and upper and lower bounds for the optimization

phase of the example. The program module PANCON is subsequently executed again. Results from this second execution of PANCON, this time executed in the optimization mode, begin on page 9 of Table 2a. Design iterations are represented on pages 9 and 10 of Table 2a. Each line "PANEL WEIGHT = ..." corresponds to a trip around the outer loop in Fig. 7. After three sets of five iterations each it appears to the user from successive evaluations of the weight that convergence has been achieved for all practical purposes. The print-out of a summary of design information on page 10 of Table 2a reveals that indeed the outer layer has essentially disappeared and the buckling load factor is very close to unity. Further details of the optimized design can then, at the option of the user, be printed as appears on page 11 of Table 2a.

User's Input Responses Saved on Permanent Files

During executions of BEGIN and DECIDE the user must respond, especially in complex cases, to many requests for input data. It is possible that after he has already spent a considerable amount of time at the terminal he may hit the wrong key, change his mind about some previous input, or be called away from the terminal, or his link with the computer may for some reason be inadvertently destroyed. In order to eliminate the burdon of the user's having to repeat the entire interactive sequence, his responses to requests for input are instantaneously saved on permanent files, one file for BEGIN data and another

(with a different name) for DECIDE data. Examples of these files corresponding to the case in Table 2a are given in Tables 2b-2d. Note that the user can easily investigate cases that represent modifications of his original case by editing these files rather than having to go through the entire interactive sequence repeatedly. Editing the files is easy because each input datum is identified by a short phrase.

It should be emphasized here that during exploration of a given design concept (e.g. cylinder of given materials with two layers and internal T-shaped rings) it is not necessary for the user to execute BEGIN more than once. The user is given the opportunity to modify the design and the loading, as well as to change his mind concerning the choice of decision variables and upper and lower bounds in the program module DECIDE. Note, however, that the user must return to BEGIN if he wishes to change the material properties, the number of layers in the panel skin, or the number or orientation of the segments in either stringers or rings.

Complex Example

The appendix contains output from PANDA corresponding to use of the long form of the description of the input data. This case represents optimization of a composite panel stiffened by both stringers and rings. The stringers are composite. There are two load sets: 1. a combined axial compression and

in-plane shear which are eigenvalue parameters, and 2. an internal pressure ($N_{ypre} = 2N_{xpre}$) which represents a fixed load (not an eigenvalue parameter). Figures 10 and 11 show the geometry, stacking sequence, and loading on the panel. There are 11 decision variables, including

1. thickness t_1 of panel skin layer no. 1 (the other layers are linked to layer no. 1);

2. stringer spacing b_o ;

3. thickness t_{s1} of stringer segment no. 1;

4. thickness t_{s2} of stringer segment no. 2;

5. width (height) b_{s1} of stringer segment no. 1;

6. width (height) b_{s2} of stringer segment no. 2;

7. ring spacing a_o ;

8. thickness t_{r1} of ring segment no. 1;

9. thickness t_{r2} of ring segment no. 2;

10. width (height) b_{r1} of ring segment no. 1;

11. width (height) b_{r2} of ring segment no. 2.

One can see from the buckling load factors corresponding to the final design (see p. of the appendix) that three buckling modes are critical: general instability, local skin buckling, and buckling between stringers with smeared rings (a semi-general instability mode). In addition, the mode corresponding to buckling between rings with smeared stringers is close to being critical, exhibiting a margin of only 13 per cent.

SECTION IV

PREBUCKLING AND BUCKLING ANALYSIS ON WHICH PANDA IS BASED

Prebuckling Analysis

The prebuckling analysis is based on the assumption that the panel with smeared stiffeners is in a membrane state of strain $\underset{\sim}{e}^{\circ}$. The membrane strain components can be determined from:

$$\underset{\sim}{e}^{\circ} = \begin{Bmatrix} e_x^{\circ} \\ e_y^{\circ} \\ e_{xy}^{\circ} \end{Bmatrix} = \overset{3 \times 3}{\begin{bmatrix} & A & \end{bmatrix}}^{-1} \begin{Bmatrix} N_x^{\circ} \\ N_y^{\circ} \\ N_{xy}^{\circ} \end{Bmatrix} \tag{4}$$

in which N_x°, N_y°, N_{xy}° represent the load combination for which the panel is being designed and $\underset{\sim}{A}$ is the 3 x 3 integrated constitutive matrix for extensional deformation of the panel with smeared stiffeners. If the materials of the skin and stiffeners remain elastic at the load level specified by the designer, then the entire prebuckling analysis consists of:

1. an approximate determination of the circumferential strain midway between rings and circumferential strain at ring centroids for panels stiffened by rings only, and
2. a computation from the known strain field and known material properties of how much of the total load N_x°, N_y° is carried by the skin and how much is carried by the stiffeners. (The in-plane shear load N_{xy}° is carried only by the skin.)

Calculation of Midbay Circumferential Strain: In the case of panels or complete cylindrical shells stiffened by rings and subjected to uniform lateral pressure, the stress in the skin midway between rings can be rather sensitive to the ring cross section area and spacing for

configurations with rather closely spaced rings. Such configurations represent optimum designs of submarine pressure hulls, for example. The buckling pressure corresponding to local instability depends directly on the midbay circumferential stress. When the material behavior is nonlinear, the buckling pressure corresponding to general instability also depends on the state of strain at midbay because the reduced moduli of the skin there naturally act to decrease the coefficients C_{ij} of the integrated constitutive law which appear in the buckling equations.

The differential equation governing the axisymmetric prebuckling behavior of a composite cylindrical shell supported in any way at its ends is derived by Jones and Hennemann [51]:

$$Aw,^{\circ}_{xxxx} + Bw,^{\circ}_{xx} + Dw^{\circ} + E = 0 \tag{5}$$

with the coefficients A, B, D, and E given by:

$$\begin{aligned} A &= C_{44} - C_{14}^2 / C_{11} \\ B &= -N_x^{\circ} + 2(C_{12}C_{14} - C_{11}C_{15}) / (C_{11}R) \\ D &= (C_{22} - C_{12}^2 / C_{11}) / R^2 \\ E &= C_{12}N_x^{\circ} / (C_{11}R) - N_y^{\circ} / R \end{aligned} \tag{6}$$

in which the C_{ij} are coefficients of the integrated constitutive law relating reference surface strains and changes in curvature of the panel skin to stress and moment resultants in the panel skin (no smeared stiffeners). The homogeneous form of Eq. (5) can be written as:

$$w,^{\circ}_{xxxx} + 4Sw,^{\circ}_{xx} + 4T^2w^{\circ} = 0 \tag{7}$$

where:

$$S = B / (4A) \qquad T = (D/A)^{\frac{1}{2}} / 2 \tag{8}$$

In Eqs. (5) and (7), the axial coordinate x is zero at the mid-length of the cylinder (midbay). The particular solution of Eq. (5) is:

$$w_p^o = -(C_{12}N_x^o - C_{11}N_y^o)R / (C_{11}C_{22} - C_{12}^2) \tag{9}$$

Almroth [52] gives the following expression for the axisymmetric normal displacement of a clamped or a simply-supported uniformly loaded cylindrical shell:

$$w^o = w_p^o\left[1 + F_1 \sin(a_1x)\sinh(a_2x) + F_2 \cos(a_1x)\cosh(a_2x)\right] \tag{10}$$

in which:

$$a_1 = (T + S)^{\frac{1}{2}} \qquad a_2 = (T - S)^{\frac{1}{2}} . \tag{11}$$

Equation (10) can be applied to the case of a ring stiffened panel. For this configuration Eq. (10) applies to the portion of the panel between adjacent rings. The axial coordinate x is zero midway between rings and equal to $\pm a_o/2$ at the rings. Expression (10) satisfies the symmetry condition at x = 0. The unknown coefficients F_1 and F_2 can be obtained from the two conditions:

$$\frac{dw^o}{dx} = 0 \qquad \text{at} \quad x = a_o/2 \tag{12}$$

$$\frac{2}{a_o}\int_0^{(a_o/2)} w^o dx = e_y^o R \tag{13}$$

where e_y^o is the average circumferential strain [Eq.(4)] calculated from the model in which the stiffeners have been smeared out. The first condition is a symmetry condition and the second condition states that the average radial displacement is equal to that calculated from the smeared ring model [Eq. (4)]. Conditions (12) and (13) lead to:

$$F_1 = -B_{22}(a_1^2 + a_2^2)L/\Delta$$
$$F_2 = B_{21}(a_1^2 + a_2^2)L/\Delta \tag{14}$$

with:

$$L \equiv a_o/2$$
$$\Delta \equiv B_{11}B_{22} - B_{12}B_{21}$$
$$B_{11} = a_2\sin(a_1L)\cosh(a_2L) - a_1\cos(a_1L)\sinh(a_2L)$$
$$B_{12} = a_2\cos(a_1L)\sinh(a_2L) + a_1\sin(a_1L)\cosh(a_2L)$$
$$B_{21} = a_2\sin(a_1L)\cosh(a_2L) + a_1\cos(a_1L)\sinh(a_2L) \tag{15}$$
$$B_{22} = a_2\cos(a_1L)\sinh(a_2L) - a_1\sin(a_1L)\cosh(a_2L)$$

the prebuckling radial displacements at x = 0 (midway between rings) and at the ring attachment stations are :

$$w^o(x = 0) = w_p^o + F_2(w_p^o - e_y^o R) \tag{16}$$

$$w^o(x = L = a_o/2) = w_p^o + (w_p^o - e_y^o R)\left| F_1 \sin(a_1 L)\sinh(a_2 L) + F_2 \cos(a_1 L)\cosh(a_2 L)\right| \tag{17}$$

In certain cases it is important to include the effect of prebuckling axial bending midway between rings. This bending contributes to further plastic straining at the outer fiber of a ring-stiffened, externally pressurized cylindrical shell, leading to a reduction in the instantaneous stiffness coefficients governing stability. The change in axial curvature $w^o_{,xx}$ at $x = 0$ is given by:

$$w^o_{,xx}(x = 0) = (w_p^o - e_y^o R)\left|F_1 2a_1 a_2 + F_2(a_2^2 - a_1^2)\right| \tag{18}$$

The circumferential strains midway between rings and at ring attachment stations are:

$$\begin{aligned} e^o_{yskin}(x = 0) &= w^o(x = 0)/R \\ e^o_{yskin}(x = a_o/2) &= w^o(x = a_o/2)/R. \end{aligned} \tag{19}$$

Loads in the Skin and in the Stiffeners: The stress resultants along the axis $\bar{x}$ of each stiffener segment are calculated from the axial strains in these segments, which are available from Eqs. (4) and (19b). Knowing the strains along the axis of each set of stiffeners and the stress-strain curves of the materials from which these segments are fabricated, one can calculate the stress resultants $N^{oi}_{\bar{x}}$ from:

$$N_{\bar{x}}^{oi} = \sigma_{\bar{x}}^{oi} t^i = E_s^i e_{\bar{x}}^{oi} t^i \tag{20}$$

in which E_s^i is the secant modulus, $e_{\bar{x}}^i$ is the strain of the stiffener axis, and t^i is the thickness of the ith stiffener segment.

If local bending of the skin between rings is ignored, the resultants (N_{xskin}^o, N_{yskin}^o) of the skin are given by:

$$N_{xskin}^o = N_x^o - \sum_{i=1}^{N^s} N_{\bar{x}}^{oi}(\text{stringer})/b_o \tag{21}$$

$$N_{yskin}^o = N_y^o - \sum_{i=1}^{N^r} N_{\bar{x}}^{oi}(\text{ring})/a_o \tag{22}$$

where N^s and N^r are the numbers of stringer segments and ring segments, respectively. If local bending of the skin between rings is accounted for, the circumferential resultant carried by the skin midway between rings is given by:

$$N_{yskin}^o = C_{12} N_{xskin}^o / C_{11} + e_{yskin}^o (x = 0) \left| C_{22} - C_{12}^2 / C_{11} \right| \tag{23}$$

with e_{yskin}^o being computed from Eq. (19a).

Inclusion of Plasticity: The flow of calculations in the prebuckling phase is displayed in Fig. 12. As can be seen from this flow, the process is iterative. The objectives of the prebuckling computations are:

1. to compute instantaneous values for the moduli E_{11}^k, E_{12}^k, F_{22}^k, and G^k, k = 1,2, .. N^L, where N^L is the number of layers in the panel skin (these

moduli are used in the calculation of the integrated constitutive law governing stability);

2. to compute instantaneous values for the corresponding moduli of the segments of the rings and stringers;

3. to compute how much load is carried by the skin and how much is carried by the stiffeners.

These goals are summarized in the two boxes in the lower left-hand corner of Fig. 12.

The contents of the boxes on the right-hand-side of Fig. 12 will next be described.

The strain components in the kth lamina in material coordinates are calculated from:

$$\begin{Bmatrix} e_1^k \\ e_2^k \\ e_{12}^k \end{Bmatrix} \begin{bmatrix} c^2 & s^2 & sc \\ s^2 & c^2 & -sc \\ -2sc & 2sc & (c^2-s^2) \end{bmatrix} \begin{Bmatrix} e_x^o - zw^o_{,xx} \\ e^o_{yskin} \\ e^o_{xy} \end{Bmatrix} \tag{24}$$

in which:

$$c \equiv \cos\phi \qquad s \equiv \sin\phi, \ (\phi \text{ is shown in Fig. 2}), \tag{25}$$

z is the positive outward coordinate normal to the shell reference surface, $w^o_{,xx}$ is given by Eq. (18), and e^o_{yskin} is given by Eq. (19a). The corresponding stress components are:

$$\begin{aligned} \sigma_1^k &= E_{11}^k e_1^k + E_{12}^k e_2^k \\ \sigma_2^k &= E_{12}^k e_1^k + E_{22}^k e_2^k \\ \sigma_{12}^k &= G^k e_{12}^k . \end{aligned} \tag{26}$$

The moduli E_{11}^k, E_{12}^k, E_{22}^k, and G^k may be reduced from the elastic values because of plastic flow. J_2-deformation theory [53] is used as described next. Hutchinson [53] gives further details.

The effective stress can be calculated from the stress components σ_1^k, σ_2^k, σ_{12}^k:

$$\bar{\sigma}^k = \left| (\sigma_1^k)^2 + (\sigma_2^k)^2 - (\sigma_1^k \sigma_2^k) + 3(\sigma_{12}^k)^2 \right|^{1/2} \tag{27}$$

If $\bar{\sigma}^k$ is less than the proportional limit stress, σ_{pl}^k, no more calculations are performed for the kth layer in this iteration. If $\bar{\sigma}^k > \sigma_{pl}^k$, the effective strain $\bar{e}^k$ is computed from:

$$\bar{e}^k = 0.4714 \left| (e_1^k - e_2^k)^2 + (e_1^k - e_3^k)^2 + (e_2^k - e_3^k)^2 + 3(e_{12}^k)^2/2 \right|^{1/2} \tag{28}$$

The strain e_3^k normal to the reference surface is calculated from:

$$e_3^k = -(e_1^k + e_2^k)(\nu + g/3)(1 - \nu + g/3) \tag{29}$$

in which:

$$g = 1.5(E^k/E_s^k - 1) \tag{30}$$

where E_s^k is the secant modulus obtained from the previous iteration. The effective strain $\bar{e}^k$ is compared with $\bar{e}_I^k$, where:

$$\bar{e}_I^k = e_I^k - (1-2\nu)\sigma_I^k/(3E^k). \tag{31}$$

In Eq. (31) e_I and σ_I are coordinates of the stress-strain curve for the material of the kth layer. These are provided by the user of PANDA. The values of e_I^k and σ_I^k that lie on the stress-strain curve and produce $\bar{e}_I^k$ equal to $\bar{e}^k$ from Eq. (28) are used to determine new estimates of the tangent and secant moduli E_T^k and E_s^k, respectively:

$$E_T^k = d\sigma_I^k/de_I^k \; ; \quad E_s^k = \sigma_I^k/e_I^k \tag{32}$$

The new estimate of the effective stress is, of course, σ_I^k. In PANDA the stress-strain curve is represented in a piecewise linear fashion, the linear segments connecting coordinates (e_j, σ_j), $j = 1, 2, \ldots$ that are supplied by the program user. A smoothing technique is used in the determination of E_T^k in order to prevent oscillatory behavior in the optimization phase associated with corners between line segments of the stress-strain curve.

New values of the moduli E_{11}^k, E_{12}^k, E_{22}^k, and G^k are computed from J_2-deformation theory [53]:

$$\begin{aligned} E_{11}^k &= a/\Delta & E_{12}^k &= b/\Delta \\ E_{22}^k &= E_{11}^k & G^k &= G_e^k(1 + \nu)/(1 + \nu + g) \end{aligned} \tag{33}$$

in which G_e^k is the elastic shear modulus of the kth layer and

$$\begin{aligned} a &\equiv (1 + 2g/3)/E^k \\ b &\equiv (\nu + g/3)E^k \\ g &\equiv 1.5(E^k/E_s^k - 1) \\ \Delta &\equiv a^2 - b^2 \; . \end{aligned} \tag{34}$$

The above calculations are repeated for every layer in the laminate.

The reduced moduli of the stiffener segments are determined in a completely analogous fashion, except that the effective strain [Eq. (28)] is replaced by:

$$\bar{e} = e^{\circ}_{\bar{x}} \tag{35}$$

for all stringer segments and:

$$\bar{e} = (R/R_{c.g.})e^{\circ}_{yskin}(x = a_o/2) \tag{36}$$

for all ring segments. The quantity $R_{c.g.}$ is the radius to the ring centroid and $e^{\circ}_{yskin}(x = a_o/2)$ is the strain in the skin at the ring attachment point [Eq. (19b)].

Integrated Constitutive Law: The integrated constitutive law for the laminated panel skin, for both the prebuckling analysis and the stability analysis, has the form:

$$\begin{Bmatrix} N_x \\ N_y \\ N_{xy} \\ M_x \\ M_y \\ M_{xy} \end{Bmatrix} = \left[\begin{array}{ccc:ccc} A_{11} & A_{12} & A_{16} & B_{11} & B_{12} & B_{16} \\ A_{12} & A_{22} & A_{26} & B_{12} & B_{22} & B_{26} \\ A_{16} & A_{26} & A_{66} & B_{16} & B_{26} & B_{66} \\ \hdashline B_{11} & B_{12} & B_{16} & D_{11} & D_{12} & D_{16} \\ B_{12} & B_{22} & B_{26} & D_{12} & D_{22} & D_{26} \\ B_{16} & B_{26} & B_{66} & D_{16} & D_{26} & D_{66} \end{array}\right] \begin{Bmatrix} e_x \\ e_y \\ e_{xy} \\ \kappa_x \\ \kappa_y \\ 2\kappa_{xy} \end{Bmatrix} = \underset{\sim}{C}\underset{\sim}{e} \tag{37}$$

in which N_x, N_y, ... M_{xy} are the stress and moment resultants and e_x, e_y, ... κ_{xy} are the reference surface strains, changes in curvature, and twist. The A_{ij}, B_{ij}, and D_{ij} are given by Jones [54]:

$$A_{ij} = \sum_{k=1}^{N^L} (\bar{Q}_{ij})_k \, (z_k - z_{k-1})$$

$$B_{ij} = \frac{1}{2} \sum_{k=1}^{N^L} (\bar{Q}_{ij})_k \, (z_k^2 - z_{k-1}^2) \qquad (38)$$

$$D_{ij} = \frac{1}{3} \sum_{k=1}^{N^L} (\bar{Q}_{ij})_k \, (z_k^3 - z_{k-1}^3)$$

in which the z_k are measured from the reference surface. The $\bar{Q}_{ij}$ for each lamina are given by Jones as:

$$\begin{aligned}
\bar{Q}_{11} &= E_{11}c^4 + 2(E_{12} + 2G)s^2c^2 + E_{22}s^4 \\
\bar{Q}_{12} &= (E_{11} + E_{22} - 4G)s^2c^2 + G(s^4 + c^4) \\
\bar{Q}_{22} &= E_{11}s^4 + 2(E_{12} + 2G)s^2c^2 + E_{22}c^4 \\
\bar{Q}_{16} &= (E_{11} - E_{12} - 2G)sc^3 + (E_{12} - E_{22} + 2G)s^3c \\
\bar{Q}_{26} &= (E_{11} - E_{12} - 2G)s^3c + (E_{12} - E_{22} + 2G)sc^3 \\
\bar{Q}_{66} &= (E_{11} + E_{22} - 2E_{12} - 2G)s^2c^2 + G(s^4 + c^4).
\end{aligned} \qquad (39)$$

For the prebuckling phase, E_{11}, E_{12}, E_{22}, and G are the reduced moduli defined in Eqs. (33), c and s are defined in Eq. (25), and ϕ is the angle from the axial direction to the fiber axis of the lamina (direction in which the modulus E_1 is measured: Fig. 2).

"Smeared" Stiffeners: For the calculation of the average prebuckling strain components from Eq. (4), the stiffeners must be treated as part of the skin, that is, "smeared out" over the panel surface. This

"smearing" is accomplished via a theory used by Baruch and Singer [55] as described in the text by Brush and Almroth [56]. To certain of the constitutive coefficients A_{ij}, B_{ij}, and D_{ij} in Eq. (37) are added terms that reflect the extensional, bending, and torsional rigidities of the rings and stringers. For example, with external rings and external stringers (positive eccentricities), all of the segments which are of the same material, new constitutive coefficients C_{ij} are obtained as follows:

$$
\begin{aligned}
C_{11} &= A_{11} + E_s^s A^s / b_o \\
C_{22} &= A_{22} + E_s^r A^r / a_o \\
C_{14} &= B_{11} + e^s E_s^s A^s / b_o \\
C_{25} &= B_{22} + e^r E_s^r A^r / a_o \\
C_{44} &= D_{11} + E_s^s I^s / b_o \\
C_{55} &= D_{22} + E_s^r I^r / a_o \\
C_{66} &= D_{66} + (\bar{G}^s J^s / b_o + \bar{G}^r J^r / a_o)/4
\end{aligned}
\tag{40}
$$

in which superscripts s and r denote "stringer" and "ring", respectively; subscript s denotes "secant modulus"; $\bar{G}$ is the effective elastic-plastic shear modulus:

$$
\bar{G} = G_e \, (1 + \nu)/(1 + \nu + g) \tag{41}
$$

with g given by Eq. (34c); and J is the torsion constant for the stiffener cross section. The quantities e^s and e^r are the distances from the skin reference surface to the centroidal axes of the stringers and rings, respectively, positive when these axes lie on the outside of the shell.

The new prebuckling C_{ij} in Eq. (40) are used to calculate new average strain components from Eq. (4), as indicated in Fig. 12. Eqs. (5-41) are solved again. Iterations continue until the prebuckling strain components e_x°, e_{yskin}°, e_{xy}° change no more than 0.01 % from their values as of the previous iteration. Figure 13 shows the results of several prebuckling iterations applied to a ring-stiffened submarine hull subject to uniform external hydrostatic compression. Quadratic extrapolation of the strain components is used every four iterations.

Instantaneous Moduli for Stability Analysis: Once convergence of the prebuckling strain components has been achieved, the instantaneous moduli (tangent moduli) governing stability are calculated. The instantaneous moduli for the kth layer of the panel skin can be calculated with use of J_2-deformation theory [53]:

$$E_{11b}^k = a/\Delta \qquad E_{12b}^k = b/\Delta \qquad E_{22b}^k = c/\Delta$$
$$G_b^k = G_e^k\,(1+\nu)/\left|1 + \nu + g + 2g'(\sigma_{12}^k)^2\right| \tag{42}$$

in which:

$$a \equiv (1 + 2g/3 + g's_2^2)/E^k$$
$$b \equiv (\nu + g/3 - g's_1s_2)/E^k$$
$$c \equiv (1 + 2g/3 + g's_1^2)/E^k \tag{43}$$
$$\Delta \equiv ac - b^2$$

with g given by Eq. (34c),

$$g' = 2.25E^k(1/E_T^k - 1/E_s^k)/\bar{\sigma}^2 \tag{44}$$

and the stress deviators s_1 and s_2 given by:

$$s_1 = (2\sigma_1^k - \sigma_2^k)/3 \qquad s_2 = (2\sigma_2^k - \sigma_1^k)/3. \tag{45}$$

Analogous formulas are used for the instantaneous moduli of the stiffener segments. The instantaneous moduli given in Eq. (42) are used in Eqs. (39), which through Eqs. (38), yield new coefficients A_{ij}^b, B_{ij}^b, and D_{ij}^b in Eq. (37), that apply during the buckling phase of the analysis. Superscript b denotes "value during buckling modal deformation".

For the calculation of general instability and "semi-general" instability, at least one set of stiffeners must be smeared out over whatever domain within the panel [(a,b), (a_o,b), (a,b_o)] is being considered during the current buckling analysis. Formulas for the instantaneous stiffness coefficients C_{ij}^b are similar to those given for C_{ij} in Eq. (40), with the secant moduli E_s^s, E_s^r for the stringers and rings being replaced by the tangent moduli E_T^s, E_T^r; and the A_{ij}, B_{ij}, D_{ij} being replaced by A_{ij}^b, B_{ij}^b, D_{ij}^b.

General, "Semi-General," and Local Instability of Panel

Governing Equations: For layered and stiffened shells with membrane-bending coupling, Eqs. (37), as modified in accordance with Eqs. (40,42), may be written in the form:

$$\begin{Bmatrix} N^b \\ M^b \end{Bmatrix} = \begin{bmatrix} A & B \\ B & D \end{bmatrix} \begin{Bmatrix} e^b \\ \kappa^b \end{Bmatrix} = \underset{\sim}{\overset{6x6}{C}}\, e^b \tag{46}$$

where superscript b denotes "value due to buckling modal deformation";

A, B, and D are 3 x 3 symmetric full matrices containing the instantaneous stiffness coefficients just derived (superscript b dropped for convenience); and:

$$\begin{aligned} \left\lfloor N^b;\ M^b \right\rfloor &\equiv \left\lfloor N_x^b,\ N_y^b,\ N_{xy}^b;\ M_x^b,\ M_y^b,\ M_{xy}^b \right\rfloor \\ \left\lfloor e^b;\ \kappa^b \right\rfloor &\equiv \left\lfloor e_x^b,\ e_y^b,\ e_{xy}^b;\ \kappa_x^b,\ \kappa_y^b, 2\kappa_{xy}^b \right\rfloor = e^b \end{aligned} \tag{47}$$

The strain energy U and work W done by the prebuckling in-plane loads N_x°, N_y°, N_{xy}° during the buckling process are given by:

$$U = \frac{1}{2} \int_0^{y_{max}} \int_0^{x_{max}} e^{b^T} C\, e^b dx\, dy \tag{48}$$

$$W = \frac{1}{2} \int_0^{y_{max}} \int_0^{x_{max}} \left(N_x^\circ w_x^{b^2} + N_y^\circ w_y^{b^2} + 2N_{xy}^\circ w_x^b w_y^b \right) dx\, dy \tag{49}$$

in which the upper limits of integration x_{max} and y_{max} depend on what kind of instability is being investigated, general, "semi-general," or local, as follows:

Type of Instability	x_{max}	y_{max}
general	a	b
between rings, smeared stringers	a_o	b
between stringers, smeared rings	a	b_o
local	a_o	b_o

In the domains (x, y) bounded by (a, b) or (a_o,b) or (a, b_o) or (a_o, b_o), the buckling modal displacement components u^b, v^b, w^b are assumed to have the general form:

$$\begin{aligned} u^b &= A(n_2^2 m_1 \sin(n_1 y - m_1 x) + n_1^2 m_2 \sin(n_2 y + m_2 x)) \\ v^b &= B(\quad n_2 \sin(n_1 y - m_1 x) - \quad n_1 \sin(n_2 y + m_2 x)) \\ w^b &= C(\quad \cos(n_1 y - m_1 x) - \quad \cos(n_2 y + m_2 x)) \end{aligned} \tag{50}$$

in which:

$$\begin{aligned} n_1 &= n + mc \qquad & m_1 &= m + nd \\ n_2 &= n - mc \qquad & m_2 &= m - nd \end{aligned} \tag{51}$$

The displacement functions (50) were chosen to permit nearly inextensional reference surface buckling strain components, e_x^b, e_y^b, and e_{xy}^b, and to allow reasonably accurate determination of buckling loads in the presence of shear and unbalanced laminates without the need for series expansions. The wave indices n and m are:

$$n \equiv \bar{n}\pi/y_{max} \qquad\qquad m \equiv \bar{m}\,\pi/x_{max} \tag{52}$$

in which the quantities $\bar{m}$ and $\bar{n}$ are the numbers of half-waves over the arc lengths x_{max} and y_{max}, respectively. The reference surface buckling strains and changes in curvature from Donnell's theory [1] are given by:

$$\begin{aligned} e_x^b &= u^b_{,x} \qquad & e_y^b &= v^b_{,y} + w^b/R \qquad & e_{xy}^b &= u^b_{,y} + v^b_{,x} \\ \kappa_x^b &= -w^b_{,xx} \qquad & \kappa_y^b &= -w^b_{,yy} \qquad & \kappa_{xy}^b &= -w^b_{,xy} \end{aligned} \tag{53}$$

where $(\ )_{,x}$ and $(\ )_{,y}$ indicate differentiation.

Insertion of Eqs. (50) into Eqs. (53) and Eqs. (48, 49) leads to an expression for the total potential energy, U-W, of the form:

$$U - W = \begin{bmatrix} A, & B, & C \end{bmatrix} \begin{bmatrix} a_{11} & a_{12} & a_{13} \\ a_{12} & a_{22} & a_{23} \\ a_{13} & a_{23} & a_{33} \end{bmatrix} \begin{Bmatrix} A \\ B \\ C \end{Bmatrix} \tag{54}$$

in which:

$$\begin{aligned}
a_{11} &= C_{11}(n_2^4 m_1^4 + n_1^4 m_2^4) + C_{33}(n_2^4 n_1^2 m_1^2 + n_1^4 n_2^2 m_2^2) \\
&\quad + \underline{2C_{13}(-n_2^4 m_1^3 n_1 + n_1^4 m_2^3 n_2)} \\
a_{12} &= -(C_{12} + C_{33})(n_2^3 n_1 m_1^2 + n_1^3 n_2 m_2^2) + C_{13}(n_2^3 m_1^3 - n_1^3 m_2^3) \\
&\quad + \underline{C_{23}(n_2^3 n_1^2 m_1 - n_1^3 n_2^2 m_2)} \\
a_{22} &= 2C_{22} n_1^2 n_2^2 + C_{33}(n_2^2 m_1^2 + n_1^2 m_2^2) + \underline{2C_{23}(-n_1 n_2^2 m_1 + n_1^2 n_2 m_2)} \\
a_{13} &= -C_{12}(n_2^2 m_1^2 + n_1^2 m_2^2)/R - C_{14}(n_2^2 m_1^4 + n_1^2 m_2^4) \\
&\quad -(C_{15} + 2C_{36}) n_1^2 n_2^2 (m_1^2 + m_2^2) + \underline{(2C_{16} + C_{34})(n_2^2 n_1 m_1^3 - n_1^2 n_2 m_2^3)} \\
&\quad + \underline{C_{23}(n_2^2 n_1 m_1 - n_1^2 n_2 m_2)/R + C_{35}(n_2^2 n_1^3 m_1 - n_1^2 n_2^3 m_2)}
\end{aligned} \tag{55}$$

$$a_{23} = n_1 n_2 \Big[2C_{22}/R + (C_{24} + 2C_{36})(m_1^2 + m_2^2) + C_{25}(n_1^2 + n_2^2) \Big]$$
$$+ (2C_{26} + C_{35})(-n_1^2 n_2 m_1 + n_2^2 n_1 m_2) + C_{23}(-n_2 m_1 + n_1 m_2)/R$$
$$+ C_{34}(-n_2 m_1^3 + n_1 m_2^3) \qquad (55)$$

$$a_{33} = 2C_{22}/R^2 + 2C_{24}(m_1^2 + m_2^2)/R + 2C_{25}(n_1^2 + n_2^2)/R$$
$$+ C_{44}(m_1^4 + m_2^4) + C_{55}(n_1^4 + n_2^4) + (2C_{45} + 4C_{66})(n_1^2 m_1^2 + m_2^2 n_2^2)$$
$$+ N_{XPRE}(m_1^2 + m_2^2) + N_{YPRE}(n_1^2 + n_2^2) + 2N_{XYPRE}(n_2 m_2 = n_1 m_1)$$
$$+ 4C_{26}(-n_1 m_1 + n_2 m_2)/R + 4C_{46}(-n_1 m_1^3 + n_2 m_2^3) + 4C_{56}(-n_1^3 m_1 + n_2^3 m_2)$$

In Eqs. (55), the C_{ij} are coefficients of the integrated constitutive law $\underset{\sim}{C}$ relating buckling modal stress and moment resultants to buckling modal reference surface strains and changes in curvature [Eqs. (37,40,46)]. N_{XPRE}, N_{YPRE}, and N_{XYPRE} are in-plane loads that are not multiplied by the load factor (eigenvalue) λ, but represent a fixed prestressed state. The total prebuckling in-plane load components, N_x^o, N_y^o, N_{xy}^o, which appear in Eq. (49) are given by:

$$N_x^o = N_{XPRE} + \lambda N_{xe}$$
$$N_y^o = N_{YPRE} + \lambda N_{ye} \qquad (56)$$
$$N_{xy}^o = N_{XYPRE} + \lambda N_{xye}$$

in which λ is a load factor to be calculated in the buckling analysis and subscript "e" denotes "eigenvalue parameter". One finds the eigenvalue λ by setting the determinant of the a-matrix on the right-hand-side of Eq. (54) equal to zero. The resulting expression for λ is:

$$\lambda = \frac{a_{33} + \dfrac{\left[a_{23}(a_{12}a_{13} - a_{11}a_{23}) + a_{13}(a_{12}a_{23} - a_{13}a_{22})\right]}{\left(a_{11}a_{22} - a_{12}^2\right)}}{-N_{xe}(m_1^2 + m_2^2) - N_{ye}(n_1^2 + n_2^2) - 2N_{xye}(m_2n_2 - m_1n_1)} \tag{57}$$

The constraint imposed on the design during the optimization process is that λ should be greater than unity. Equations (46-57) apply to any kind of shell buckling: general, "semi-general", or local. The load factors λ corresponding to the various types of instability are calculated with use of appropriate C_{ij}, x_{max}, and y_{max} pertaining to whatever portion of the structure is being investigated. For general instability both rings and stringers are smeared out; for "semi-general" buckling, either rings or stringers are smeared out; and, for local skin buckling, neither set of stiffeners is smeared out. All buckling load multipliers λ are calculated with the assumption that the boundaries of the portion of the structure under investigation are simply supported. Note that the simple-support condition is violated if either c or d in Eqs. (51) are not equal to zero.

The expression for λ contains unknown quantities m, n, c, and d. When in-plane shear N_{xy}^{o} is present or when any of the terms A_{i6}, B_{i6}, D_{i6},

$i \neq 6$ [see Eq. (37)] is non-zero, the minimum value of λ for fixed m and n with respect to the slope, c or d, of the buckling nodal lines is found. In the calculation of this minimum it is always assumed that either c or d is zero. Figure 14 shows the model. For each kind of buckling: general, semi-general, or local, a test is made to see in which coordinate direction the panel is "long". The test is based on the quantity:

$$\bar{L} = \left(x_{max} / y_{max} \right) \left(C_{55} / C_{44} \right)^{1/2} \tag{58}$$

If the panel is shallow ($R/y_{max} > 1.0$) and if $\bar{L} \geq 1.0$, the panel is effectively "long" in the x-direction and the model shown in Fig. 14(a) is used. If the panel is not shallow ($R/y_{max} < 1.0$) or if $\bar{L} < 1$, the opposite is true and the model shown in Fig. 14(b) is used. In this way, the boundary conditions are satisfied along the edges that span the least number of buckling modal half-waves while the correct solution is obtained for buckling of a long cylinder under pure torsion. The boundaries along which the simple support conditions are violated span the largest number of half-waves and hence the conditions there least affect the critical load. The utility of the approximate expressions (50) is thereby maximized. Such a strategy is advantageous because the buckling loads must be calculated very often in the optimization analysis. Since the optimum design is being obtained interactively, it is necessary to avoid discouraging or boring the program user by making him wait a long time at the terminal while elaborate buckling calculations proceed for each new trial design.

To increase the efficiency of the subroutine that calculates buckling loads, the terms in Eqs. (55) are arranged so that those which are often zero (e.g., the terms underlined in Eqs. (55))are not calculated if it is known in advance that they are zero.

The eigenvalue is modified by a factor "DONNEL" = $(n_c^2 - 1)/n_c^2$ under certain conditions for which the Donnell theory [Eqs. (49, 53)] yields inaccurate results, such as buckling of a complete cylindrical shell under uniform external pressure for which n_{cr} is less than 4 or 5 half-waves over 180° of the circumference. The factor "DONNEL" is not applied if $n_c = 1$ or if the axial half-wavelength of the buckling pattern is less than the radius R of the cylinder.

Strategy for finding the minimum buckling load with respect to $\bar{m}$, $\bar{n}$, c, or d: For each wave index combination, $\bar{m}$ and $\bar{n}$, the minimum λ with change in the buckling nodal line slope c or d is found (only in cases for which shear loading is present or any A_{i6}, B_{i6}, or $D_{i6} \neq 0$; $i \neq 6$) by variation of c or d in equal increments or decrements of 0.01 if its absolute value is less than 0.1 and by a factor of 1.2 if its absolute value is greater than 0.1. The buckling nodal line slopes are shown in Fig. 14.

The minimum λ with respect to the wave indices $\bar{m}$ and $\bar{n}$ is found with due attention to the fact that for a given geometry and loading this minimum may be non-unique, as pointed out by Burns [14] and by Pappas and Allentuch [47]. Four regions in $(\bar{m}, \bar{n})$ space are searched for minima in the function $\lambda(\bar{m}, \bar{n})$: low $\bar{m}$, low $\bar{n}$; low $\bar{m}$, high $\bar{n}$; high $\bar{m}$, low $\bar{n}$; and high $\bar{m}$, high $\bar{n}$. Figure 15 shows the results of such a search for an axially compressed composite unstiffened cylindrical shell, the dimensions and properties of which are from Booton and Tennyson's

paper [57].

For low $\bar{m}$ ($\bar{m} = 1$), the search begins at:

$$\bar{n}_{start_1} = (y_{max}/x_{max})(C_{44}/C_{55})^{\frac{1}{4}} \qquad \text{or} \quad \bar{n}_{start_1} = 1 \tag{59}$$

whichever is larger. With $\bar{m} = 1$, a minimum $\lambda(1, \bar{n})$ is sought. The region in $(\bar{n}, \bar{m})$ space surrounding this minimum is then explored by variation of both $\bar{m}$ and $\bar{n}$. When a local minimum $\lambda_1(\bar{m}_{L1}, \bar{n}_{L1})$ has been found, $\bar{m}$ is reset to unity and a new minimum $\lambda_1(1, \bar{n})$ is sought in whichever region was not covered by the initial search that began at $\bar{n}_{start}$ given by Eq. (59). If the minimum $\bar{n}$ covered in the search for $\lambda_1(\bar{m}_{L1}, \bar{n}_{L1})$ is greater than or equal to 3, the low-$\bar{n}$ range is next covered, starting at $\bar{n} = 1$. If the low-$\bar{n}$ range was covered in the search for $\lambda_1(\bar{m}_{L1}, \bar{n}_{L1})$, the high-$\bar{n}$ range is next covered, starting at:

$$\bar{n}_{start_2} = y_{max}/(0.2R) \tag{60}$$

As before, a minimum $\lambda_2(1, \bar{n})$ is sought, after which the region in $(\bar{m}, \bar{n})$ space about this minimum is explored as before in order to find $\lambda_2(\bar{m}_{L2}, \bar{n}_{L2})$, in which subscript L again denotes "local minimum".

For high $\bar{m}$, low $\bar{n}$, the search for $\lambda_3(\bar{m}_{L3}, \bar{n}_{L3})$ begins at $\bar{n} = 1$ and $\bar{m}$ equal to the larger of the following:

$$\bar{m}_{start} = x_{max}/\left[\pi(R^2 C_{44}/C_{22})^{\frac{1}{4}}\right] \tag{61}$$

or:

$$\bar{m} = (x_{max}/y_{max})(C_{55}/C_{44})^{\frac{1}{4}} \tag{62}$$

Equation (61) yields approximately the number of axial waves in a cylinder of length x_{max} which buckles axisymmetrically and Eq. (62) yields approximately the number of axial waves in an axially compressed flat plate of aspect ratio x_{max}/y_{max}. During the search process $\bar{n}$ is increased monotonically. For each $\bar{n}$ a minimum $\lambda_3(\bar{m}, \bar{n})$ is found, eventually leading to $\lambda_3(\bar{m}_{L3}, \bar{n}_{L3})$. The final region, high $\bar{m}$, high $\bar{n}$, is searched for a local minimum $\lambda_4(\bar{m}_{L4}, \bar{n}_{L4})$ starting with:

$$\bar{m}_{start_2} = \bar{m}_{L3} \qquad \bar{n}_{start_3} = y_{max}/(0.4R) \tag{63}$$

In Figure 15, the four regions searched are outlined in dashed boxes. It turns out that in this case each of the four regions contains a local minimum load multiplier λ. PANDA selects the lowest of these minima, as the critical load multiplier. In this case, $\lambda_{cr} = \lambda_2(\bar{m}_{L2}, \bar{n}_{L2}) = \lambda_2(1, 9) = 7.33$. The dotted curve in Fig. 15 represents constant values of the quantity:

$$\left| (\bar{m}\pi R/x_{max})^2 + \bar{n}^2 \right|^2 / (\bar{m}\pi R/x_{max})^2 \tag{64}$$

which appears in Eqs. (5.50) and (5.51) of Brush and Almroth [56]. In the context of Donnell's theory, minimization of the axial buckling load of an isotropic monocoque cylindrical shell with respect to this quantity yields the formula:

$$\frac{P_{cr}}{2\pi R} = \frac{Et^2/R}{\left|3(1 - \nu^2)\right|^{\frac{1}{2}}} \tag{65}$$

in which P_{cr} is the total critical axial load on the cylinder.

If the quantity (64) is set equal to its value corresponding to the minimum $\lambda(\bar{m},\bar{n})$ along the $\bar{m}$-axis in Fig. 15 ($\bar{m} = 9$, $\bar{n} = 0$, value of Quantity (64) = 400) then the dashed curve in Fig. 15 is obtained for the various $(\bar{m}, \bar{n})$ combinations that yield this same value, 400. It is seen that the dashed curve passes close to all of the minima found by PANDA in $(\bar{n}, \bar{m})$ space.

In the optimization analysis it is necessary not only to find the various buckling loads (local, semi-general, general) at a given design point, but to determine how these loads vary with a small change in each decision variable from this design point. In PANDA the small change is equal to 5.0 percent of the current value of the decision variable. Much computer time is saved by use of whatever values of $\bar{m}$, $\bar{n}$, c, and d exist at the design point for calculation of the eigenvalue λ at these neighboring points also. This strategy is indicated in Fig. 7.

Local Buckling (Crippling) of Stiffener Segments

There are two types of stiffeners, those along cylinder generators called stringers and those along circumferences called rings (Fig. 1). Each type of stiffener is assumed to consist of an assemblage of rectangular pieces of width b_i and thickness t_i. The rectangular pieces of each stiffener type are divided into two classes: those that are "internal" or "interior" and those that are "ends". Figure 4 shows examples. "Internal" stiffener segments are those which have both edges connected to other stiffener segments or the panel skin. "Ends" are stiffener segments only one edge of which is connected to another structural part. All stiffener segments are assumed to be flat and long compared to their widths. Thus, for stringers $a_o >> b_i^s$ and for ring segments $b_o >> b_i^r$. The curvatures of the ring segments are neglected.

Effective stiffener segment material properties: The theory for crippling of stiffener segments is based on the assumption that these segments are monocoque

and orthotropic, not layered anisotropic. Thus, the terms in Eq. (37), A_{i6} and D_{i6}; $i \neq 6$, are assumed to be zero and all of the B_{ij} are assumed to be zero when applied to the crippling or rolling analyses of stiffener segments. The PANDA program allows the user to provide input as if the stiffener segments were layered anisotropic. From initial values of A^i_{11}, A^i_{12}, A^i_{22}, and A^i_{66} computed from the anisotropic theory for the ith stiffener segment laminate corresponding to the user's starting design, effective moduli and Poisson's ratio are derived from:

$$E^{i(eff)}_{11} = A^i_{11}/t^i; \qquad E^{i(eff)}_{22} = A^i_{22}/t^i$$

$$\nu^{i(eff)}_{12} = A^i_{12}/A^i_{22}; \qquad G^{i(eff)} = A^i_{66}/t^i \tag{66}$$

in which:

$$t^i = \sum_{k=1}^{N} t^i_k \tag{67}$$

During the optimization phase the total thickness t^i of the ith stiffener segment laminate may be a decision variable; the thicknesses of each lamina are not decision variables. If the stiffener material is isotropic and if $t^i = t^1_k$ (N = 1 layer), the effect of nonlinear material behavior is included in the analysis. The A^i_{jk} in Eq. (66) are the instantaneous coefficients referred to in the discussion associated with Eqs. (42-45).

Local Buckling of "Internal" Segments: For "internal" segments the critical load factors λ_i can be calculated from Eqs. (55)-(57) with c = d = $N^\circ_{xy} = N^\circ_y = 0$, $R \to \infty$, and the "anisotropic" $C^i_{ij} = 0$. The axial prebuckling

resultant in Eq. (56a) $|N_x^\circ|$ is interpreted to mean the prebuckling stress resultant along the axis of the stiffener and the wave index m_i is given by $m_i = \bar{m}_i \pi/\ell$ in which $\bar{m}_i$ is the number of half-waves along ℓ, where ℓ is $a_\circ$ for a stringer segment and $b_\circ$ for a ring segment. With these simplifications and definitions the terms a_{13} and a_{23} in Eqs. (55) vanish and Eq. (57) becomes:

$$\lambda_i = \frac{\left| C_{44}^i m_i^2 + C_{55}^i (n_i^4/m_i^2) + (2C_{45}^i + 4C_{66}^i) n_i^2 + N_{XPRE}^i \right|}{-N_{xe}^i} \tag{68}$$

If it is assumed that the internal stiffener segment buckles with one-half wave ($\bar{n}_i = 1$) across its width b_i, as shown in Fig. 5, then it can be shown that:

$$m_i = n_i (C_{55}^i/C_{44}^i)^{\frac{1}{4}} = (\pi/b_i)(C_{55}^i/C_{44}^i)^{\frac{1}{4}} \tag{69}$$

The quantities C_{44}^i, C_{55}^i, C_{45}^i and C_{66}^i in Eqs. (68, 69) are given by:

$$\begin{aligned} C_{44}^i &= E_{11}^{i(eff)} t^{i\,3}/12 \; ; & C_{55}^i &= E_{22}^{i(eff)} t^{i\,3}/12 \; ; \\ C_{45}^i &= \nu_{12}^{i(eff)} E_{11}^{i(eff)} t^{i\,3}/12 \; ; & C_{66}^i &= G^{i(eff)} t^{i\,3}/12 \end{aligned} \tag{70}$$

Use of Eq. (69) with $n_i = \pi/b_i$ in Eq. (68) yields:

$$\lambda_i = \frac{\left| 2(\pi/b_i)^2 \left| (C_{44}^i C_{55}^i)^{\frac{1}{2}} + C_{45}^i + 2C_{66}^i \right| + N_{XPRE}^i \right|}{-N_{xe}^i} \tag{71}$$

in which:

$$N^i_{XPRE} \equiv N^i_{\bar{x}pre} \tag{72}$$

$$N^i_{xe} = N^{io}_{\bar{x}} - N^i_{\bar{x}pre} \tag{73}$$

where $N^{io}_{\bar{x}}$, given by Eq. (20), is the total prebuckling axial resultant (lb/in) carried by the ith stiffener segment and $N^i_{\bar{x}pre}$ is that portion of the prebuckling axial resultant carried by the ith stiffener segment that is not to be multiplied by the load factor λ_i.

Local Buckling of "end" segments: It is assumed here that the stiffener "end" segment cross-section does not deform in the buckling mode (Fig. 5, Segment 3). The assumed displacement function is:

$$\begin{aligned} w^i &= C\bar{v}_i \sin\left[\bar{m}^j \pi \bar{x}/\ell\right] = C\bar{v}_i \sin\left[m^j \bar{x}\right] \\ u^i &= 0 \\ v^i &= 0 \end{aligned} \tag{74}$$

Use of Eqs. (74) in Eqs. (48, 49, 53) leads to the following expressions for strain energy of and work done on the ith segment:

$$U^i = C^2 \frac{\ell}{4}\left[C^i_{44}(m^j)^4 b_i^3/3 + 4C^i_{66}(m^j)^2 b_i\right] \tag{75}$$

$$W^i = C^2 \frac{\ell}{4}\left[N^{oi}_{\bar{x}}(m^j)^2 b_i^3/3\right] \tag{76}$$

In Eq. (74), $\bar{\bar{y}}_i$ is the distance along the width of the "end", as shown in Fig. 4, and $\bar{m}^j$ is the number of half-waves in the local critical buckling pattern of the structural segment to which the end segment is attached (Segment j). For example, with reference to Fig. 5, for stiffener Segment 3 (i = 3, j = 2), m^j is given by:

$$m^{(j)} = \bar{m}^{(2)} = (\pi/b_2)\left|C^{(2)}_{55}/C^{(2)}_{44}\right|^{\frac{1}{4}} \tag{77}$$

For blade stiffeners, such as shown in Fig. (4c):

$$m^j = \bar{m}_{skin}\pi/\lambda \tag{78}$$

With the total pre-stress resultant $N^{oi}_{\bar{x}}$ in the end segment defined by Eq. (73), minimization of the total potential energy, $U^i - W^i$, with respect to the undetermined coefficient C in Eqs. (75,76) yields the following equation for the buckling load factor λ_i:

$$\lambda_i = \frac{C^i_{44}(m^j)^2 b_i^3 + 12C^i_{66}b_i + N^i_{\bar{x}pre}\, b_i^3}{-N^i_{\bar{x}e}\, b_i^3} \tag{79}$$

If more than one "end" segment is attached to the same "internal" segment or to the skin, the buckling criterion is:

$$-\sum_{k=1}^{K_e}(N^k_{\bar{x}pre} + \lambda N^k_{\bar{x}e})b_k^3 = \sum_{k=1}^{K_e}\left[(m^j)^2 C^k_{44}b_k^3 + 12C^k_{66}b_k\right] \tag{80}$$

in which K_e is the number of "end" segments attached to the jth "internal"

segment or to the panel skin.

Rolling Modes

Three types of rolling modes of instability have been described in the summary and are illustrated in Fig. 6. PANDA accounts for these three types of rolling, one (Fig. 6a) in which the panel skin participates and two (Fig. 6b, c) in which it does not.

Rolling with Participation of the Panel Skin

For panels stiffened by both rings and stringers, there are three eigenvalues (buckling load factors λ) corresponding to the type of rolling in which the panel skin participates. These modes are characterized by (1) local rolling between rings and stringers, with both sets of stiffeners twisting about nodal lines of the buckling pattern; (2) rolling in which the stringers are smeared out and the rings twist about nodal lines of the buckling pattern; and (3) rolling in which the rings are smeared out and the stringers twist about nodal lines in the buckling pattern.

Figures 16 and 17 show in more detail the geometry of the type of rolling deformation depicted in Figure 6a. This deformation is assumed to be either local, that is, the distances x_{max} and y_{max} considered in the rolling instability mode are the spacings a_o and b_o between the rings and stringers, respectively, or "semi-general," that is, the distances x_{max} and y_{max} apply to subdomains of the structure with either rings or stringers smeared and the opposite set of stiffeners twisting along simply-supported boundaries. The widths of the stiffener

segments are assumed to be small compared to the half-wavelength, $\ell/\bar{m}$, of the rolling buckling modes. For local rolling the quantity ℓ is the distance a_o between rings in the rolling analysis of stringers and ℓ is the distance b_o between stringers in the rolling analysis of rings. All stiffener segments are assumed to be perpendicular or parallel to the plane of the skin. The effect of curvature of the ring segments on cylindrical panels is neglected.

The assumed deflection field given in Fig. 17 leads to zero in-plane shear of each stiffener segment. Although Fig. 16 may seem to imply that the following analysis applies only to stringers, this is not so. It is emphasized that the analysis of this section applies to rings as well. Figure 17 shows the $\bar{x}$, $\bar{y}$, $\bar{z}$ coordinate system and associated displacement components, u^*, v^*, w^*, and rotation components, $\omega_{\bar{y}}$ and $\omega_{\bar{z}}$.

The rolling deformations depicted in Figs. 16 and 17 cause inextensional bending and twisting of the stiffener web and extensional deformation of the flange. The strain energy of the extensional (membrane) deformation of the flange is large compared to its inextensional (bending and twisting) strain energy. Therefore, in the discussion that follows, the inextensional strain energy of the flange is neglected.

Membrane Energy: That portion of the strain energy of the stiffener associated with membrane-type deformations of the ith stiffener segment deforming in the rolling mode is:

$$U_m^i = \frac{1}{2} \int_{\bar{y}_i=0}^{b_i} \int_{\bar{x}=0}^{\ell} u_{,\bar{x}}^{*2} C_{11}^i d\bar{x} d\bar{y}_i \qquad (i \neq \text{web}) \qquad (81)$$

in which $\bar{\bar{y}}_i$ is the local coordinate shown in Fig. 4, $u^*_{\bar{x}}$ is the axial strain in this segment, C^i_{11} is the instantaneous stiffness coefficient [same as A^i_{11} in Eq. (66)], b_i is the width of the segment and ℓ is the length of whatever portion of the panel is being investigated, as follows:

Type of Rolling Instability	ℓ	Eq. (81) applies to:
local stringer	a_o	stringer energy
local ring	b_o	ring energy
smeared stringers	b	ring energy
smeared rings	a	stringer energy

The total membrane energy of the stiffener is:

$$U_m = \sum_{\substack{i=1 \\ i \neq \text{web}}}^{N} U^i_m \qquad \begin{array}{l} i \neq \text{web or other segments attached} \\ \text{along the line } \bar{y} = \bar{z} = 0. \text{ (Fig. 17)} \end{array} \qquad (82)$$

in which N is the number of segments in the stiffener cross-section.

The corresponding "membrane" work done by the prebuckling stress resultant $N^{oi}_{\bar{x}}$ in the ith segment during rolling deformations is:

$$W^i_m = \frac{1}{2} \int_{\bar{\bar{y}}_i=0}^{b_i} \int_{\bar{x}=0}^{\ell} N^{oi}_{\bar{x}} (\omega^2_{\bar{z}} + \omega^2_{\bar{y}}) d\bar{x} d\bar{\bar{y}}_i \qquad (83)$$

($i \neq$ web or other segments attached along $\bar{y} = \bar{z} = 0$)

The quantities $\omega_{\bar{z}}$ and $\omega_{\bar{y}}$ are the rotations about the $\bar{z}$ axis and $\bar{y}$ axis,

respectively, and are given by:

$$\omega_{\bar{z}} = \frac{1}{2}\left(\frac{\partial v^*}{\partial \bar{x}} - \frac{\partial u^*}{\partial \bar{y}}\right) \quad ; \qquad \omega_{\bar{y}} = \frac{1}{2}\left(\frac{\partial u^*}{\partial \bar{z}} - \frac{\partial w^*}{\partial \bar{x}}\right) \tag{84}$$

Bending and Twisting Energy: In addition to the membrane-energy-related modes just described, the stiffener rolling deformations involve bending and twisting energy, that is, strain energy related to strains which vary through the thickness of each segment, and work done by the prebuckling stress resultant related to out-of-plane rotations of each stiffener segment. Only the bending and twisting energy of the stiffener web and other segments attached along the line $\bar{y} = \bar{z} = 0$ are included, since these components of energy are negligible compared to U_m^i [Eq. (81)] for the remainder of the stiffener cross section. The bending and twisting strain energy of the web shown in Figs. 16 and 17 is given by:

$$U_b^i = \frac{1}{2}\int_{\bar{y}_i=0}^{b_i}\int_{\bar{x}=0}^{\ell}\left[\kappa_{\bar{x}},\ \kappa_{\bar{z}},\ 2\kappa_{\bar{x}\bar{z}}\right]\left[D^i\right]\begin{Bmatrix}\kappa_{\bar{x}}\\ \kappa_{\bar{z}}\\ 2\kappa_{\bar{x}\bar{z}}\end{Bmatrix} d\bar{x}d\bar{y}_i \tag{85}$$

(i = web or other segment attached along the line $\bar{y} = \bar{z} = 0$.)

The coefficients of the 3 x 3 flexural rigidity matrix D^i are called C_{44}^i, C_{45}^i, C_{55}^i, C_{66}^i in Eq. (68); they are given by Eqs. (70). Thus:

$$\left[D^i\right] \equiv \begin{bmatrix} D^i_{11} & D^i_{12} & 0 \\ D^i_{12} & D^i_{22} & 0 \\ 0 & 0 & D^i_{66} \end{bmatrix} \equiv \begin{bmatrix} C^i_{44} & C^i_{45} & 0 \\ C^i_{45} & C^i_{55} & 0 \\ 0 & 0 & C^i_{66} \end{bmatrix} \tag{86}$$

These are the instantaneous flexural and twist rigidities of the ith stiffener segment, analogous to those for the panel skin referred to in the discussion associated with Eqs. (42-46). The expressions for changes in curvature and twist of the web are analogous to those for the panel skin:

$$\kappa_{\bar{x}} = -v^*_{,\bar{x}\bar{x}} \quad ; \quad \kappa_{\bar{z}} = -v^*_{,\bar{z}\bar{z}} \quad ; \quad \kappa_{\bar{x}\bar{z}} = -v^*_{,\bar{x}\bar{z}} \tag{87}$$

where v^* is the displacement in the $\bar{y}$ direction, indicated in Figs. 16 and 17. The work done by the prebuckling stress resultant during buckling of the web is:

$$W^i_b = \frac{1}{2} \int_{\bar{y}_i=0}^{b_i} \int_{x=0}^{\ell} N^{oi}_{\bar{x}} \, v^{*2}_{,\bar{x}} \, d\bar{x} d\bar{y}_i \tag{88}$$

(i = web or other segments attached along the line $\bar{y} = \bar{z} = 0$)

In PANDA rolling modes are assumed to occur only if the stiffener has a web which is perpendicular to the panel skin. The expressions (81) and (83) apply only to the portion of the stiffener attached to the end of this web. The cross-sections of these flange segments remain undeformed

and initially plane sections of them remain plane during buckling deformations. However, note from Figs. 16 and 17 that this plane rotates about the normal to the shell wall at the web attachment line. Therefore the entire cross-section of the stiffener (web and flange taken together) clearly warps. The expressions (85) and (88) apply only to the web. The bending and twisting energy of the rest of the stiffener cross-section is neglected compared to the membrane energy of the flange represented by Eq. (81). This approximation seems valid as long as the segments are slender (width >> thickness).

Introduction of Displacement Functions: The various components of energy associated with the rolling mode shown in Figs. 6, 16 and 17 are derived from Eqs. (81) to (88) with the assumed displacement field given in Fig. 17 and repeated here:

$$\begin{aligned} u^* &= -m\,\gamma\,\bar{y}\,\bar{z}\cos m\,\bar{x} \\ v^* &= +\gamma\,\bar{z}\sin m\,\bar{x} \qquad\qquad m = \bar{m}\,\pi/s \\ w^* &= -\gamma\,\bar{y}\sin m\,\bar{x} \end{aligned} \tag{89}$$

If the height (width) of the web is called b_w and one inserts the right-hand side of Eq. (89a) with (with $\bar{z} = b_w$) into Eq. (81), one obtains for the membrane-type energy of each segment of the stiffener attached to the end of the web:

$$U_m^i = \frac{\ell}{4} (\gamma b_w)^2 m^4 \int_{\bar{\bar{y}}_i=0}^{b_i} C_{11}^i \bar{y}^2 \, d\bar{\bar{y}}_i \qquad (i \neq \text{web}) \tag{90}$$

U_m^i can be evaluated once $\bar{y}$ as a function of $\bar{\bar{y}}$ is known. For example, in the case of the T-shaped stiffener shown in Fig. (4a), $\bar{y} = \bar{\bar{y}}_2$ in Segment 2 and $\bar{y} = -\bar{\bar{y}}_3$ in Segment 3. Therefore:

$$U_m^i = \frac{\ell}{4} (\gamma b_w)^2 m^4 C_{11}^i b_i^3/3 \qquad (i = 2, 3) \tag{91}$$

If $C_{11}^{(2)} = C_{11}^{(3)}$, the total membrane energy $U_m = 2U_m^{(2)}$. This energy is simply the "EI" bending energy of a beam of depth equal to the width of the flange ($b_2 + b_3$ in Fig. 4a) deforming in its plane in a mode $(\gamma b_w)\sin m\bar{x}$. The bending and twisting energy of the web can be found, with use of Eqs. (85) and (87), to be:

$$U_b^i = \frac{\ell}{4} \left[C_{44}^w m^4 \gamma^2 \frac{b_w^3}{3} + 4C_{66}^w m^2 \gamma^2 b_w \right] \qquad \begin{matrix} (w = \text{"web"}) \\ (i = \text{"web"}) \end{matrix} \tag{92}$$

The corresponding "work done" terms, W_m^i and W_b^i, are obtained from Eqs. (83), (84), and (88):

$$W_m^i = \frac{m^2 \ell}{4} (\gamma b_w)^2 \int_{\bar{\bar{y}}=0}^{b_i} N_{\bar{x}}^{oi} \, d\bar{\bar{y}}_i \qquad (i \neq \text{web}) \tag{93}$$

$$W_b^i = \frac{m^2 \ell}{4} (\gamma b_w)^2 N_{\bar{x}}^{oi} b_w/3 \qquad (i = \text{web}) \tag{94}$$

Relation to Panel Skin Deformation: With no shear loading and the A_{i6}, B_{i6}, $D_{i6} = 0$ for $i \neq 6$ in Eq. (37), the rotation γ, shown in Fig. 16, is related to the amplitude C of the sinusoidal deformation of the panel skin, $w_{skin} = 2C \sin ny \sin mx$, [Eq. (50c) and Eq. (51) with $c = d = 0$] as follows:

$$\begin{aligned} &\text{For stringers:} \quad \gamma = -2Cn \\ &\text{For rings:} \quad \gamma = +2Cm \end{aligned} \tag{95}$$

in which n and m are given by Eqs. (52). Through Eqs. (95), the components of rolling mode energy and work done by the prebuckling compression during buckling can be expressed in terms of the undetermined skin buckling amplitude C. The total potential energy U - W has the same form as that given in Eq. (54). The only difference is that the array element a_{33}, given for the panel skin in Eq. (55f), has additional terms associated with stiffener deformations:

$$
\begin{aligned}
a_{33} = \left[a_{33}\right]_{skin} + \frac{2m^2n^2}{y_{max}} \Bigg[& m^2 b_w^2 \sum_{\substack{i=1 \\ i\neq web}}^{N^s} \left(\int_{\bar{\bar{y}}=0}^{b_i} C_{11}^i \left[\bar{y}(\bar{\bar{y}}_i)\right]^2 d\bar{\bar{y}}_i \right) \\
& + C_{44}^w m^2 b_w^3/3 + 4C_{66}^w b_w + b_w^2 \sum_{\substack{i=1 \\ i\neq web}}^{N^s} \left(\int_{\bar{\bar{y}}=0}^{b_i} N_{\bar{x}pre}^{oi} \, d\bar{\bar{y}}_i \right) \\
& + N_{\bar{x}pre}^{ow} b_w^3/3 \Bigg]_{stringer} \\
& + \frac{2m^2n^2}{x_{max}} \Bigg[n^2 b_w^2 \sum_{\substack{i=1 \\ i\neq web}}^{N^r} \left(\int_{\bar{\bar{y}}=0}^{b_i} C_{11}^i \left[\bar{y}(\bar{\bar{y}}_i)\right]^2 d\bar{\bar{y}}_i \right) \\
& + C_{44}^w n^2 b_w^3/3 + 4C_{66}^w b_w \\
& + b_w^2 \sum_{\substack{i=1 \\ i\neq web}}^{N^r} \left(\int_{\bar{\bar{y}}=0}^{b_i} N_{\bar{x}pre}^{oi} \, d\bar{\bar{y}}_i \right) + N_{\bar{x}pre}^{ow} b_w^3/3 \Bigg]_{ring}
\end{aligned}
\tag{96}
$$

in which $\bar{y}(\bar{\bar{y}}_i)$ indicates that $\bar{y}$ is a function of $\bar{\bar{y}}_i$. In Eq. (96), x_{max} and y_{max} have the meanings analogous to those in the discussion following Eq. (49):

Type of Rolling Instability	x_{max}	y_{max}
local	a_o	b_o
smeared stringers	a_o	b
smeared rings	a	b_o

The result in Eq. (96) is obtained after division of both skin and stringer terms, derived from energy expressions, by the quantity $x_{max}y_{max}/4$.

The denominator on the right-hand-side of Eq. (57) must also be modified by addition of the terms:

$$- \frac{2m^2n^2}{y_{max}} \left[b_w^2 \sum_{\substack{i=1 \\ i\neq web}}^{N^s} \left(\int_{\bar{\bar{y}}=0}^{b_i} \underline{\underline{N}}_{xe}^{oi} d\bar{\bar{y}}_i \right) + \underline{\underline{N}}_{xe}^{ow} b_w^3/3 \right]_{stringer}$$

$$- \frac{2m^2n^2}{x_{max}} \left[b_w^2 \sum_{\substack{i=1 \\ i\neq web}}^{N^r} \left(\int_{\bar{\bar{y}}=0}^{b_i} \underline{\underline{N}}_{xe}^{oi} d\bar{\bar{y}}_i \right) + \underline{\underline{N}}_{xe}^{ow} b_w^3/3 \right]_{ring} \qquad (97)$$

in which $\underline{\underline{N}}_{xe}^{oi}$ and $\underline{\underline{N}}_{xe}^{ow}$ are given by Eq. (73). Expressions (95-97) apply only if $c = d = 0$. However, the eigenvalues including stiffener rolling are expected to be reasonably accurate for most practical cases involving combined in-plane loads which include shear.

Rolling of Stiffeners without Participation of Panel Skin

Figure 18 shows the coordinate system and positive displacement components v, u^w, w^w, u^f, w^f in the web and flange. The following

analysis is limited to stiffeners with T-shaped or L-shaped cross-sections. A special case of such a stiffener is a blade, which is a T or L-shaped cross-section with a vanishingly small flange. The analysis is based on treatment of the web as a flexible annulus (a type of shell) and the flange as a very short cylindrical shell. Although Fig. 18 depicts the geometry for a ring, the analysis applies to stringers as well. In that case the radius of the short cylindrical shell that represents the flange is set equal to a very large number in PANDA.

Assumptions: The following assumptions are made with regard to the prebuckling and buckling modal strains and displacements:

1) The prebuckling strains are assumed to be uniform over the web and uniform over the flange (although different prebuckling strain states exist in the web and flange).

2) The buckling modal state is characterized by,

For the web:

$$w_b^w(x, y) = \left[Cx^2 + Dx^2(1 - x/b_w)\right] \sin(\bar{n}\pi y/\ell) \tag{98}$$

$$e_x^b = 0 \tag{99}$$

$$e_{xy}^b = 0 \tag{100}$$

For the Flange:

$$w_b^f(s, y) = u_b^w(x = b_w, y) + s\beta \sin(\bar{n}\pi y/\ell) \tag{101}$$

$$u_b^f(s, y) = \mp w_b^w(x = b_w, y) = u_b^f(y) \tag{102}$$

$$e_s^b = 0; \qquad e_{sy}^b = 0 \tag{103}$$

in which C and D are coefficients to be determined by minimization of the total energy in the rolling stiffener. Quantities such as x, y, s and $\bar{s}$ and the various web and flange displacement components are indicated in Fig. 18 for both external and internal stiffeners. In terms preceeded with $\pm$ or $\mp$, the top sign corresponds to external stiffening and the bottom to internal stiffening. The quantity $u_b^w(x = b_w, y)$ signifies the value of u^w evaluated at $x = b_w$ (see Fig. 18b, for example).

Strain energy: The total strain energy of the stiffener is:

$$U = \frac{1}{2}\int_{y=0}^{\ell}\left(\sum_{i=1}^{N}\int_{\bar{\bar{y}}_i=0}^{b_i}(\underset{\sim}{e}_{pre} + \underset{\sim}{e}^b)^T\left[C^i\right](\underset{\sim}{e}_{pre} + \underset{\sim}{e}^b)\,d\bar{\bar{v}}_i\right)dy \tag{104}$$

in which N is the number of stiffener segments, $\bar{\bar{y}}_i$ is the local stiffener segment coordinate shown in Fig. 4 ($\bar{\bar{y}}_i = x$ in the web; $\bar{\bar{y}}_i = s$ in the flange), and:

$$(\underset{\sim}{e}_{pre})^T = \left\lfloor 0,\ e_y^o,\ 0,\ 0,\ 0,\ 0 \right\rfloor \tag{105}$$

$$(\underset{\sim}{e}^b)^T = \left\lfloor 0,\ e_y^b,\ 0,\ \kappa_{\bar{\bar{y}}}^b,\ \kappa_y^b,\ 2\kappa_{\bar{\bar{y}}y}^b \right\rfloor \tag{106}$$

Using Eqs. (104-106), one can write the strain energy of the ith segment of the stiffener in the simpler form:

$$U^i = \frac{1}{2}\int_{y=0}^{\ell}\int_{\bar{y}_i=0}^{b_i}\left[C^i_{22}(e^b_y + e^b_v)^2 + C^i_{44}(\kappa^b_{\bar{v}})^2 + 2C^i_{45}\kappa^b_{\bar{v}}\kappa^b_y + C^i_{55}(\kappa^b_v)^2 + C^i_{66}(2\kappa^b_{\bar{y}y})^2\right]d\bar{y}dy \tag{107}$$

Note that because the web and flange are here being treated as shell components, C^i_{22} and C^i_{55} are identified with the long dimension, ℓ, of the stiffener while C^i_{44} is identified with the width, b_i. This is the opposite nomenclature from that used in the previous section.

Strain-Displacement Relations for Buckling Analysis: The strain displacement relations to be used here are of the Novoshilov-Sanders type. They are the same as those used in BOSOR4 [58] and BOSOR5 [59].

For the web:

$$\begin{aligned}
e_x &= u' + (w'^2 + \gamma^2)/2 = 0\\
e_y &= \dot{v} - u/r + (\zeta^2 + \gamma^2)/2\\
e_{xy} &= \dot{u} + r(v/r)' + w'\dot{w} = 0\\
\kappa_x &= w''\\
\kappa_y &= \ddot{w} - w'/r\\
2\kappa_{xy} &= 2(-w'\dot{} \pm \dot{w}/r)
\end{aligned} \tag{108}$$

$$\zeta = \dot{w}$$

$$\gamma = (\dot{u} - v' + v/r)$$

in which $(\ )' \equiv d(\ )/dx$ and $(\dot{\ }) \equiv d(\ )/dv$.

For the flange:

$$e_s = 0$$

$$e_y = \dot{v} + w/R_f + (\zeta^2 + \gamma^2)/2$$

$$e_{sy} = \dot{u} + r(v/r)' + w'(\dot{w} - v/R_f) = 0$$

$$\kappa_s = w'' \qquad (109)$$

$$\kappa_y = \ddot{w} - \dot{v}/R_f$$

$$2\kappa_{sy} = 2(-\dot{w}' + v'/R_f)$$

$$\zeta = \dot{w}$$

$$\gamma = (\dot{u} - v')/2$$

in which $(\ )' \equiv d(\ )/ds$ and $(\dot{\ }) \equiv d(\ )/dv$ and in which superscript b has been dropped for convenience.

Analysis of the Web: The assumptions that $e_x = e_{xy} = 0$ [Eqs. (99, 100)] along with Eqs. (108a) and (108c) can be used to determine u^W and v^W, given w^W [Eq. (98)]. After some algebraic manipulations one obtains:

$$u^w = \left[-2(C + D)^2 x^3/3 + 3(C + D)Dx^4/(2b_w) - 9(D/b_w)^2 x^5/10\right] \sin^2(\bar{n}\pi y/b_w) \tag{110}$$

$$v^w = -(\bar{n}\pi/b_w)\left[(C + D)^2 x^4/6 - 2(C + D)Dx^5/(5b_w) + (D/b_w)^2 x^6/5\right] \sin(\bar{n}\pi y/b_w)\cos(\bar{n}\pi y/b_w) \tag{111}$$

With use of Eqs. (107), (108), (110) and (111), one obtains for the strain energy of the web (including the effect of the prebuckling stress resultant in the y-direction, N^{ow}):

$$U^{web} = \frac{1}{4}\left\{C^2\left[p_1 + p_2 + 4C^w_{44}b_w + q_1 + q_2 + 4q_3 - s_1 + s_2\right] + CD\left[p_1/5 + p_2/3 - 4C^w_{44}b_w + q_1/3 - q_3 + s_1 - s_2\right] + D^2\left[p_1/10 + p_2/21 + 4C^w_{44}b_w + q_1/21 + 2q_3/5 + s_1/5 + s_2/4\right]\right\} \tag{112}$$

in which:

$$p_1 = \mp N^{ow}b_w^4/(3r_{ave}) \quad ; \quad p_2 = n^2N^{ow}b_w^5/5$$

$$q_1 = b_w^5(C^w_{55}n^4 + 4C^w_{66}n^2/r^2_{ave})/5 \quad ; \quad s_1 = 4C_{45}n^2b_w^3/3$$

$$q_2 = \mp b_w^4n^2(C^w_{55} + 4C^w_{66})/r_{ave} \quad ; \quad s_2 = -4C_{45}b_w^2/r_{ave} \tag{113}$$

$$q_3 = b_w^3(C^w_{55}/r^2_{ave} + 4C^w_{66}n^2)/3$$

where r_{ave} is the average radius of the web,

$$r_{ave} = (R + R_f)/2 \tag{114}$$

and n is given by:

$$n = \bar{n}\pi/\ell \tag{115}$$

In Eq. (113 a, b) the stress resultant in the web N^{ow} is comprised of two parts, a fixed part and a part to be multiplied by the eigenvalue,

$$N^{ow} = N^{ow}_{PRE} + \lambda N^{ow}_{e} \tag{116}$$

Analysis of the Flange: From the assumption that $e_{sy} = 0$ [Eq. (103)] along with Eq. (109c) and Eq. (102), an expression for v can be derived. From Eq. (102), it is known that:

$$u^f = \mp Cb_w^2 \sin(\bar{n}\pi y/\ell) \quad . \tag{117}$$

Integration of Eq. (109c) yields:

$$v^f = \pm (n\pi/\ell) Cb_w^2 s \cos(\bar{n}\pi y/\ell) + v^w(x = b_w) \tag{118}$$

in which $v^w(x = b_w)$ signifies the value of v^w evaluated at $x = b_w$ (see Fig. 18). The last term on the right-hand-side of Eq. (118) drops out when integration over y is performed.

With use of Eqs. (107), (109), (117), and (118), one obtains for the strain energy of the flange (including the effect of the prebuckling stress

resultant in the y-direction N^{of}):

$$U^f = \frac{1}{4}\left\{C^2\left[f_1c_2 + f_2c_3 + f_3c_4^2 + c_5(2+e)^2\right] + CD\left[-f_1c_6 - f_3(2e)c_4 - 2(2+e)c_5 + c_7\right] + D^2\left[f_1c_1 + f_3e^2 + c_5 - .4c_7\right]\right\} \tag{119}$$

in which:

$$f_1 = \sum_{\substack{i=1 \\ i\neq web}}^{N} N_i^{of} b_i^3/3 \qquad f_2 = \sum_{\substack{i=1 \\ i\neq web}}^{N} N_i^{of} b_i$$

$$f_3 = \sum_{\substack{i=1 \\ i\neq web}}^{N} C_{22}^i b_i^3/3 \qquad f_4 = \sum_{\substack{i=1 \\ i\neq web}}^{N} C_{55}^i b_i^3/3 \tag{120}$$

$$f_5 = \sum_{\substack{i=1 \\ i\neq web}}^{N} C_{66}^i b_i$$

and:

$$c_1 = n^2 b_w^2 \qquad c_2 = c_1(2+e)^2$$

$$c_3 = c_1 b_w^2 \mp 4b_w^3/(3R_f) \qquad c_4 = c_1 + 2e \tag{121}$$

$$c_5 = c_1(n^2 f_4 + 4f_5) \qquad c_6 = c_1 2(2+e)$$

$$c_7 = \pm f_2 b_w^3/(3R_f)$$

with:

$$e = \mp b_w/R_f \tag{122}$$

where R_f is the radius of the very short cylindrical shell that represents the flange.

As in the case of the web, the prebuckling stress resultant in the flange is comprised of two parts, a fixed part and a part to be multiplied by the eigenvalue:

$$N_i^{of} = N_{iPRE}^{of} + \lambda N_{ie}^{of} \tag{123}$$

Lowest Eigenvalue: The lowest eigenvalue λ for stiffener rolling instability without participation of the skin can be obtained by insertion of the right-hand-side of Eq. (116) into Eq. (112), insertion of the right-hand-side of Eq. (123) into Eq. (119), minimization of the sum of U^{web} and U^f with respect to the coefficients C and D, and determination of the lowest root of the quadratic equation in λ that represents the vanishing of the determinant of the coefficient matrix of the two simultaneous homogeneous equations in C and D.

Axisymmetric Rolling Instability: Axisymmetric rolling instability of rings can be calculated by the setting of n in Eqs. (113) and (121) equal to zero. It is interesting to note that rolling instability is possible in the case of internally pressurized cylindrical shells with external rings even though the stresses everywhere in the shell, web, and flange are tensile.

SECTION V

EXAMPLES OF BUCKLING PREDICTIONS FROM PANDA

Purpose of this Section

The purpose of this section is to provide the user of PANDA with an appreciation of the quality of the estimates of buckling loads for the many kinds of instability summarized in Table 1 and in the Introduction. Results obtained by PANDA are compared to results in the literature and to results from other computer programs.

The strengths as well as the weaknesses of PANDA are revealed. It is emphasized that the accuracy of PANDA buckling predictions is case dependent; expressions such as (50) cannot lead to predictions with uniform accuracy for differing configurations. The emphasis during the development of PANDA was on the creation of an interactive preliminary design tool that includes many kinds of buckling yet responds rapidly on a minicomputer such as the VAX. PANDA can be used very effectively to reduce greatly the vast expanse of feasible design space to a manageable region. This region can subsequently be explored further with the use of more elaborate design programs that require more computer time, such as that described in Reference [48].

Buckling Loads of Unstiffened Panels

Table 3 lists results for buckling modes under pure shear and combined shear and axial tension or compression of curved isotropic panels long in the circumferential direction (Cases 1-4), panels long in the axial direction (Cases 6-8), and squarish panels (Cases 5, 9, 10). For panels long in the circumferential direction PANDA predictions, which are based on the assumed displacement functions (50), agree very well with the predictions of Simitses, Giri, and Sheinman [61], which are based on multi-term, two-dimensional trigonometric expansions. PANDA overestimates the shear buckling loads for curved panels that are thin and long in the axial direction (Cases 6, 7, 8). (The result of Simitses, et al [61] for Case 8 is confirmed by a linear bifurcation analysis performed with use of STAGSC-1 [62]. PANDA underestimates shear buckling loads for curved panels that are squarish and that buckling in less than three half waves in the "long" direction. (Cases 5, 9, 10). This underestimation is due to violation of the simply supported boundary conditions along the two short edges.

Figure 19 shows buckling loads of an axially compressed, three-layered composite cylinder, the dimensions and material properties of which are given in Fig. 15. The C_{ij} matrix [Eq. (46)] for this unbalanced laminate is full. Results from PANDA, STAGSC-1 [62], and the analysis of Booton and Tennyson [57] are superposed. The STAGSC-1 results correspond to a linear bifur-

cation model with the assumption of a uniform membrane prebuckling state.

It is seen that application of the aforementioned "Donnell factor", $(n_c^2 - 1)/(n_c^2)$, to compensate for the unconservativeness of Donnell's shallow shell theory leads to a rather conservative estimate of the buckling load over a wide range of winding angle ϕ in this case. This is because the factor $(n_c^2 - 1)/n_c^2$ is applied to every $\lambda(\bar{n},\bar{m})$ calculated during the search over $\bar{m}$ and $\bar{n}$ for $\lambda_{cr}(\bar{m}_{cr},\bar{n}_{cr})$, not just to the minimum $\lambda_{cr}(\bar{m}_{cr},\bar{n}_{cr})$ determined from Donnell's theory. Since $\lambda(\bar{m},n)$ for axially compressed shells is weakly dependent on $\bar{m}$ and n, application of the factor $(n_c^2 - 1)/n_c^2$ to every $(\bar{m},\bar{n})$ leads to predictions that buckling will occur with $\bar{n} = 2$ over a wide range of winding angles ϕ (10 deg. $< \phi <$ 75 deg.). Were the minimum $\lambda_{cr}(\bar{m}_{cr},\bar{n}_{cr})$ to be calculated from Donnell's theory first and the "Donnell factor" applied only to the final minimum value of λ determined <u>after</u> the search over $\bar{m}$ and $\bar{n}$, the results would agree fairly closely with those labelled "Donnell theory" over the entire range of winding angle ϕ. However, in order to obtain reasonably conservative estimates of buckling load factors for perfect shells in other situations, especially in the case of ring-stiffened cylinders under uniform external pressure, it is felt that the "Donnell factor" should be applied to every $\lambda(\bar{m},n)$ during the search for $\lambda_{cr}(\bar{m}_{cr},n_{cr})$ rather than only to the final $\lambda_{cr}(\bar{m}_{cr},\bar{n}_{cr})$ calculated from Donnell's theory.

Case No. 1 in Table 4 lists buckling load predictions from PANDA and STAGS-C1 [62] for positive and negative pure torsion on the unbalanced composite cylindrical shell sketched in Fig. 15. Agreement between the two programs is very good.

Buckling Loads of Stiffened Shells and Panels

Pure Shear: Case 2 in Table 4 pertains to a complete cylindrical shell stiffened by both stringers and rings (Fig. 20) and Case 3 pertains to a shallow cylindrical panel stiffened by stringers only (Fig. 21). Both structures are subjected to pure in-plane shear loading, N_{xy}. Case 2 represents an optimum design obtained by Simitses and Giri [63]. Results from PANDA and STAGS-C1 are in reasonably good agreement. (The stiffeners are smeared out in both models in this case.) The PANDA results are compared to the results of Reference [63] in the section on optimization examples.

Case 3 in Table 4 represents a near-optimum design obtained by PANDA. The general instability buckling load factor calculated by STAGS-C1 with use of a model in which the stringers are treated as discrete is much lower than that obtained with a model in which the stringers are smeared, for which PANDA and STAGS-C1 exhibit reasonably good agreement. Figure 21 shows the bifurcation buckling mode shape from the STAGS-C1 model with discrete stringers. Note that the nodal lines (dash-dot) are curved, a situation that cannot be duplicated with use of the

simple assumed modal displacement pattern [Eq. (50)] on which the PANDA analysis is based.

Axial Compression: Figure 22 shows an analogous phenomenon for axially compressed, 60-in.-wide, flat panels of three lengths stiffened by stringers of rectangular cross section. The results displayed in Fig. 22 were obtained from BOSOR4 [58]. The panels, discretized models of the cross sections of which are plotted in Fig. 22, are subjected to uniform compression normal to the plane of the paper. The geometries shown in Fig. 22 represent designs that have been optimized by PANDA such that the load factor λ is 1.0 for both general and local instability. Figure 22 shows load factors λ and bifurcation buckling modes obtained from the BOSOR4 computer program [58] for PANDA-optimized panels of three lengths normal to the plane of the paper: 40 in., 20 in., and 10 in. Note that as the panel becomes shorter, the general instability mode shape as predicted by BOSOR4 consists of an increasingly obvious superposition of a local and global pattern that is not well represented by the displacement field [Eq. (50)] used in the PANDA analysis. Therefore, PANDA overestimates the critical axial load in such cases. For the 10-inch-long panel, for example, PANDA overestimates the critical general instability load by about 30 per cent (Fig. 22c). The mode shape corresponding to local instability, shown only in Fig. 22d, is accurately represented in the PANDA analysis for all three panels, however. Therefore the load factor λ = 1.0 obtained from PANDA agrees well in all

three cases with those obtained from BOSOR4 corresponding to local buckling of the skin.

The deleterious effect on λ of the combined local-general mode is most pronounced in cases for which the axial wavelengths of the two modes approach each other. This phenomenon has been previously noted [64]. It is being emphasized here in order to warn the user of PANDA to check optimum designs obtained therefrom with more elaborate analyses and to urge the user to design to higher loads than those the structure will actually see in service in order to compensate for the approximations inherent in the simplified PANDA model as well as for initial imperfections.

Table 5 lists bifurcation buckling load factors for an axially compressed ring and stringer stiffened complete elastic cylindrical shell with various combinations of external and internal stiffening. The geometry and material properties are given in Fig. 23. Excellent agreement is obtained with the analyses of Block, Card, and Mikulas [65] and Kicher and Wu [66].

Plastic Buckling: Figure 24(a) shows a ring stiffened cylindrical shell subjected to uniform axial compression. The stress-strain curve is plotted in Fig. 24(b). Axisymmetric collapse is predicted by BOSOR5 [59] to occur at N_{xx} = 570 lb/in and local bifurcation buckling between rings with n equal one

circumferential wave is predicted by PANDA to occur at N_x = 550 lb/in. In the PANDA model the rings are assumed to be equally spaced on 2.5-in. centers. The prediction with PANDA of non-symmetric local (between rings) bifurcation buckling with only one circumferential wave is tantamount to a prediction of axi-symmetric collapse, since the buckling load is essentially independent of the number of circumferential waves for local shell buckling modes with waves that are very long in the circumferential direction compared to the ring spacing. Figure 24(b) demonstrates that at N_x = 550 lb/in the shell material is stressed well beyond its proportional limit.

Examples of Buckling Including Stiffener Crippling and Rolling

Tables 6-11 and Figures 25-30 pertain to examples which involve all of the types of instability covered by the PANDA computer program. The buckling loads predicted by PANDA are compared to results from other computer programs. None of these examples corresponds to an optimum design. That will be covered in another section. The purposes of these examples are:

(1) to verify the PANDA buckling analysis,

(2) to provide the PANDA user with a physical "feel" for various types of buckling that might occur in these structures, and

(3) to provide the user with an evaluation of the quality of buckling predictions obtained with PANDA.

Axially Compressed, Blade Stiffened, Composite Plate: The configuration of a single module of the plate (stringer plus a portion of the plate equal to the spacing between stringers) is shown in Figure 25. The plate is loaded by uniform axial shortening (normal to the plane of the paper). In the PANDA model the length L = a of the panel in the axial direction is 76 cm and the span b is 1144 cm, that is, the panel is taken to be so wide that the general instability load with simply-supported longitudinal edges closely approaches the wide column buckling load. The axial stress resultant $\bar{N} = N_x^0$ is 15730 N/m. The buckling load multipliers (eigenvalues) associated with the various modes of buckling included in the PANDA analysis for this particular configuration are listed in Table 6. Certain of the buckling strains are plotted in Figure 25 for comparison with the results of Williams and Stein [24].

In addition to the buckling load factors and critical wave numbers, which are provided as output from PANDA, the equation numbers on which the calculations are based are listed in Table 6. The general instability eigenvalue 1.33 corresponds in this case to the column buckling mode indicated in Figure 25. The local skin buckling eigenvalue 1.135 corresponds to buckling of an axially compressed, unstiffened flat plate of width 11.44 cm simply supported on all four edges and loaded by N_{xskin}^0 = 6114

N/m, which is the share of the total axial resultant N_x^0 = 15730 N/m that is carried by the skin. The factor 1.207 corresponding to buckling of stringer segment no. 1 is calculated from the assumptions that:

(1) the stringer cross section does not deform, as shown for the "end" segment, Seg. 3 in Fig. 5, and

(2) the stringer buckles with the same number of axial half-waves, m = 7, that governs local skin buckling.

The factor 1.029 in Table 6, corresponding to local rolling with skin buckling between stiffeners (Fig. 16) is actually the best estimate of local buckling in this simple elastic case. The local skin buckling load factor, 1.135, is calculated neglecting two counteracting effects,

(1) the resistance of the stringer to twisting about its attachment line to the skin, which of course would tend to increase this load factor, and

(2) the work done by the axial compression in the stringer as it deforms in the buckling mode, which would tend to decrease this load factor.

The buckling load factor, 1.207, associated with the stringer buckling by itself is calculated with the constraint

that the number of axial half waves, m = 7, is the same as that for local buckling of the skin, whereas in fact the stringer, were it hinged along its line of attachment to the skin, would "want" to buckle in fewer axial waves (1 half wave, to be exact). The skin "wants" to buckle in 7 half waves. The two parts of the structure, skin and stringer, reach a compromise at 5 half waves and a load factor of 1.029. Thus, the approximate local buckling load factor of 1.135, based on the assumption of simple support along stringer lines of attachment, is slightly unconservative due to the important contribution of the "work done" terms in Eq. (97). The significant effect of these terms has been discussed previously. (See Reference 64, in particular Figs 4 and 7 and the associated discussion in that reference.)

The load factor 1.834 in Table 6 corresponds to buckling deformations of the type shown in Fig. 18, in which the cross section of the web deforms but the skin does not participate. This mode is not critical in this case because the blade-shaped (rectangular) stringer is rather thick.

Were the blade stiffened panel to be optimized, all of the buckling load factors appearing in Table 6 might constrain the design at various iterations during the optimization process. The question arises, why include the local skin buckling (1.135) and buckling of stringer segment no. 1 (1.207) as potential constraints when the local-rolling-with-skin-buckling load factor (1.029) represents a better estimate of the actual phenome-

AD-A110 963 LOCKHEED MISSILES AND SPACE CO INC PALO ALTO CA PALO --ETC F/G 1/3
PANEL OPTIMIZATION WITH INTEGRATED SOFTWARE (POIS). VOLUME I. P--ETC(U)
JUL 81 D BUSHNELL F33615-76-C-3105

UNCLASSIFIED AFWAL-TR-81-3073-VOL-1 NL

2 OF 3
AD A
110963

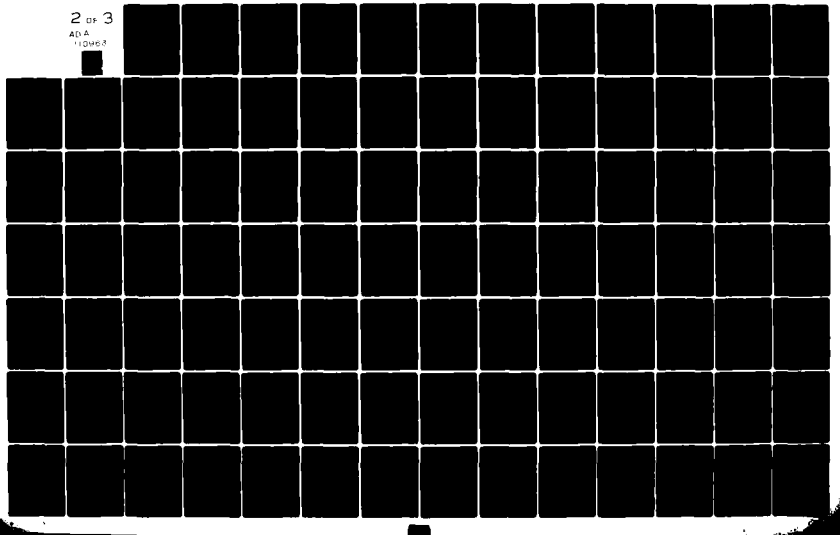

non in this case than either of the former two estimates? The answer is that the accuracy with which the various loads are determined is case-dependent. All the formulas are approximate, and for more complex stiffener cross sections or cases involving nonlinear material behavior, the local-rolling-with-skin- buckling phenomenon may not be as accurately represented as the local skin buckling phenomenon, for example.

This statement holds especially for cases in which there is more than one half wave between stiffeners in the critical buckling modes or in which plastic flow occurs before buckling. If there is more than one half wave between stiffeners in any of the buckling modes, the stiffener -rolling-with-skin-buckling model will overestimate the influence of the stiffener terms [Eqs. (96,97)]. In cases involving prebuckling plastic flow plastic hinges may form at stiffener lines of attachment, perhaps rendering the local-skin-buckling model with simple supports at stiffener lines of attachment a better representation of the actual local buckling phenomenon than the more complex local-rolling-with-skin-buckling model, even for modes with only one half wave between stiffeners in either or both of the coordinate directions. Since computer time is not important in applications of PANDA, it is safest to include all of the possible buckling modes as constraints.

Externally Pressurized Ring-Stiffened Cylindrical Shell: The configuration of a single module of the ring-stiffened cyl-

inder (ring plus a portion of the cylinder equal to the spacing between rings) is shown in Figure 26. The cylinder is loaded by a unit uniform external pressure which gives rise to a circumferential compression N_y^o of 5.218 lb/in. (No axial compression, $N_x^o = 0.$) In the PANDA model the length "a" of the "panel" in the axial direction is 100 inches, that is, the cylinder is taken to be long enough such that the general instability pressure with the assumption of simply supported ends closely approaches the ring buckling load, $EI(\bar{n}^2 - 1)/R_c$, in which I is the area moment of the entire cross section AA shown at the top of Figure 26 and R_c is the radius to the centroid of this cross section. The length b in the circumferential direction is taken to be $\pi * R$, which permits simulation of the behavior of a complete (360 deg.) cylindrical shell, with the number of circumferential half waves in the PANDA model being equal to the number of circumferential full waves in the complete cylinder.

The buckling load multipliers (eigenvalues) associated with various modes of buckling included in the PANDA analysis for this particular case are listed in Table 7. Buckling pressures corresponding to two of these factors are plotted in Figure 26 for comparison with results calculated with the BOSOR4 computer program [58]. The main purpose of this case is to verify the analysis of ring rolling without participation of the shell. The analysis is contained in Eqs. (98-123). The PANDA estimate for this buckling mode is about 12 per cent higher than that from BOSOR4.

Hydrostatically Compressed Ring Stiffened Cylindrical Shell with Slender Webs: The configuration analyzed by use of BOSOR4 [58] is shown in Figure 27(a). In the PANDA model the cylinder is taken to be 23.2 in. long with rings on 4.64-in centers. The axial and circumferential stress resultants corresponding to a unit external pressure are N_x^o = - 10.21 lb/in. and N_y^o = - 20.42 lb/in., respectively. Table 8 lists the buckling load multipliers from PANDA, and Fig. 27(b) shows a comparison of the three lowest buckling loads with predictions from BOSOR4. The ring sidesway modes of failure (n = 0 and n = 1 circumferential waves) are very accurately predicted by PANDA and the local web crippling load is about 10% too high. The modes involving skin buckling are much higher in this case. The purpose of the case is to check the low - $\bar{n}$ ring sidesway phenomenon in which the shell skin does not participate.

Another Ring-Stiffened Cylinder under External Pressure: This case is similar to that shown in Figure 26, except that in it the types of local and rolling buckling displayed in Figure 25 are also of interest. The configuration is shown in Figure 28 and the buckling load factors predicted with PANDA are listed in Table 9. The length of the cylindrical shell is 200 inches, the radius R is 100 inches, and the thickness is 1.0 in. The internal rings are spaced 25 in. apart. Comparisons between BOSOR4 and PANDA are plotted in Figure 28, which is taken from Reference [64]. The various curves labelled (1) - (6) in Figure 28 are discussed in [64]. Notice that the relationship of the

local skin buckling mode ($\bar{n}$ = 16) to the local -rolling-with-skin-buckling mode is similar here to that shown in Figure 25. The agreement with the 3-branch shell model of BOSOR4 is very good in all modes except for the non-symmetric ring sidesway mode ($\bar{n}$ = 6), for which PANDA predicts a critical load about 14% higher than that predicted by BOSOR4.

Elastic Buckling of a Ring and Stringer-Stiffened Cylinder: Figure 9 displays the geometry and Table 10 lists the various buckling load factors and critical wave numbers ($\bar{m}$, $\bar{n}$). The loading is uniform axial compression, N_x^o = 1.0 lb/in. This example is chosen because buckling can occur in any or all of the types of modes that are included as constraints in the PANDA optimization analysis.

Results from STAGSC-1 linear bifurcation computer runs on models with smeared and discrete stiffeners are also listed in Table 10. The STAGSC-1 model with discrete stiffeners is displayed in Figure 29(a) and (b). The lowest two eigenvalues from this model, which contains appropriate symmetry and antisymmetry boundary conditions for prebuckling and buckling phases, correspond to buckling (rolling) with smeared stringers [Fig. 29(c)] and local rolling with skin buckling between stiffeners [Fig. 29(d)].

Notice that the local skin buckling load factor, 58149 in Table 10, is about 20% less than the local rolling load factor,

70919, which corresponds to the same mode, $(\bar{m}, \bar{n}) = (21, 59)$. The stringers, being rather thick for their height (1 in. x 6 in.), stabilize the shell in the local mode because the strain energy terms [Eq. (96)] outweigh the "work done" terms [Eq. (97)] in their contributions to the array element a_{33} of the stability matrix [Eq. (54)].

The local buckling mode $(\bar{m}, \bar{n}) = (21, 59)$ half waves over the (axial, circumferential) dimensions of the entire (180 deg.) panel corresponds to $(\bar{m}, \bar{n}) = (3, 1)$ over the 120-in long, 37.7-in wide portion of the shell between adjacent stiffeners. (See Fig. 9.) The buckling modes predicted by STAGSC-1 agree with those predicted by PANDA in all of the modes investigated for this example.

Plastic Buckling for the Same Example: The example shown in Fig. 9 represents a typical design for a section of a steel containment vessel for a nuclear reactor. Large shells such as these are fabricated of a low carbon steel which has a low strain at yield and little post-yield strain hardening. Thus "thin" stiffened shells with large R/t_{skin}, as is the case for the design displayed in Fig. 9, buckle at stresses beyond the material proportional limit. In this case the material is taken to be elastic-perfectly-plastic with a yield stress of 38000 psi.

It is clear that for any case involving nonlinear material properties, actual buckling loads cannot be calculated simply by

multiplication of the load factors by the applied load. Plastic buckling loads of a structure with a given design must be found by variation of the applied load, N_x^o for example, until two successively increasing values of N_x^o yield load factors greater than unity and less than unity, respectively. In optimization problems, for which the load is fixed and the design is changing, the actual value of the load multiplier is not important, only whether it is greater than or less than unity.

Table 11 and Figure 30 pertain to plastic buckling of the stiffened shell shown in Figure 9 as predicted by PANDA, BOSOR5 [59], and STAGSC-1 [62]. Table 11 is divided into four sections (a-d), each section containing load multipliers corresponding to the applied axial load N_x^o appearing near the right-hand margin. PANDA predicts plastic buckling between N_x^o = -40185 lb/in. and N_x^o = -40200 lb/in. in the three modes indicated by boxes in Sections (a) and (b). The very large change in load multipliers and of the critical number of axial half waves in the general instability mode associated with the very small change in applied load is due, of course, to the abrupt yielding of shell and stiffener material with a drop in tangent modulus from E to E/100. Plastic local skin buckling occurs very near N_x^o = -40600 lb/in., followed by local rolling with skin buckling at N_x^o = -41200 lb/in.

Figure 30 shows results from analyses with BOSOR5 and STAGSC-1. In the BOSOR5 model the stringers are smeared out,

that is treated as an elastic-plastic shell wall layer of thickness equal to the stringer height b^s with a stress-strain curve with the stress coordinates multiplied by the ratio (t^s/b_o) of stringer thickness to stringer spacing, an axial modulus $E_1 = E^s(t^s/b_o)$, hoop modulus $E_2 = 0$, shear modulus $G = 0$, and density $\rho = \rho^s(t^s/b_o)$. The rings are treated as flexible shell branches. The STAGSC-1 model corresponding to the load-deflection curve in Figure 30(c) is given in Figs. 29(a) and (b). BOSOR5 and STAGSC-1 both predict instability at about $N_x^o = -38000$ lb/in. corresponding to axisymmetric collapse between rings.

The PANDA model predicts bifurcation buckling in this inter-ring- smeared-stringer mode at about $N_x^o = -40200$ lb/in. with 24 circumferential waves. However, note that the axial general instability mode, which occurs at the same load and has essentially an indeterminate number of axial waves, corresponds to $\bar{n} = 1$ circumferential wave. ($\bar{n}$ cannot be zero in PANDA in this mode because of the assumption of simply supported boundaries on all four edges of the panel). Also, note that at a slightly higher axial load, $N_x^o = -40600$ lb/in., the rolling mode with smeared stringers has $\bar{n} = 1$. As mentioned previously $\bar{n} = 1$ essentially signifies axisymmetric collapse in this case because the inter-ring buckling wave is long in the circumferential direction compared to its length in the axial direction and the bifurcation load is only very weakly dependent on $\bar{n}$ for buckles of this shape. Thus, the critical load and mode pred-

icted by PANDA agree well with those predicted by BOSOR5 and STAGSC-1, even though axisymmetric collapse is not explicitly included as one of the PANDA buckling modes. Any optimization analysis which includes the modes listed in Table 11 as constraint conditions will lead to a design that will be safe regarding nonlinear axisymmetric collapse as well. This statement is confirmed by the results of a parameter study given later.

SECTION VI

EXAMPLES OF OPTIMIZATION ANALYSIS WITH PANDA

Elastic Material

Tables 12-18 and Fig. 31 give results of the application of PANDA to problems that have previously been solved by others [6, 14, 33, 35, 47, 61, 63]. All of the examples except one involve stiffened complete (360 deg.) cylindrical shells. These are modelled in applications of PANDA as deep cylindrical "panels" that span 180 deg. Such a model, given the simple support condition along generators, is equivalent to treatment of the full 360 deg. cylindrical shell: the number of half waves along the circumferential coordinate of the 180-deg. "panel" is equivalent to the number of full waves around the circumference of the complete cylinder.

Each of Tables 12-18 is horizontally divided into three sections: dimensions, design load combination, and material properties are given in the top section; decision variables for optimization are listed in the middle section; and buckling load factors and wave numbers are listed in the bottom section. Optimum designs from PANDA are listed on the left and those from the referenced analysis are listed on the right. Buckling load factors and modes for both left and right sides were calculated

with PANDA.

The data in each of Tables 12-18 were generated in the following way: Simple buckling analyses were first performed with PANDA, corresponding to the dimensions found by the referenced investigation to be an optimum design. The buckling runs are analogous to that listed on the first six pages of Table 2a. The dimensions found to be optimum by the referenced investigation and the buckling load factors and modes computed by PANDA are listed in the right-hand columns of Tables 12-18. These "optimum" designs were then used as starting designs in the optimization process with PANDA, a process that is analogous to that listed on pages 7-10 of Table 2a. Through execution of the program module "DECIDE", the design variables listed in Tables 12-18 were chosen as decision variables for the optimization analysis with PANDA. Following execution of "DECIDE", the program module "PANCON" was run again, this time in the optimization mode. The results listed in the left-hand columns represent the converged optimum designs. They are generally obtained after two or three sets of five iterations each, much as is shown on pages 9 and 10 of Table 2a.

As seen from Tables 12-18 the minimum weight obtained by PANDA, consistent with the many buckling, stress, and strain constraints listed in the tables, is often less than the minimum weight determined by previous investigators. In cases for which the designs obtained by PANDA differ greatly from those obtained

by the referenced investigations, the results of both were checked with use of BOSOR4 [58] or STAGSC-1 [62]. Some specific remarks concerning these test cases follow:

Table 12: Local buckling is not critical in this example because the skin thickness is fixed at .05 in. and a limit is imposed on the stiffener height.

Table 13: The minimum weight and buckling loads from PANDA agree rather well with those from the analysis of Ref. [33] for this case. In the PANDA design the stringer is quite a bit thinner than is the case in the Ref. [33] optimum. This difference arises from the way that local stringer (or ring) buckling is handled (see the fifth load factor from the top, 1.6029 for the Ref. [33] dimensions): In both codes the stiffeners are assumed to be simply supported along their lines of attachment to the shell. However, in PANDA, for stiffeners of rectangular cross section, the number of waves along the stiffener axis must be equal to that governing local buckling of the skin. Inclusion in PANDA of the modes with the word "rolling" in them compensates for any unconservativeness that may be present because of this approach. In many other codes, including that on which the results of Ref. [33] are based, the minimum buckling load with respect to the number of waves along the stiffener axis is found without regard to the compatibility of stiffener and shell rotations. This minimum usually occurs at a lower wave number than that corresponding to local skin buck-

ling, and at a lower stress, leading to the appearance of a need for stockier stiffeners.

Table 14: There is a striking discrepancy between the results of Ref. [63] and those of PANDA for this case of buckling under pure in-plane shear. In particular, the general instability load factor predicted by PANDA is 4.74, whereas the analysis of Ref. [63] yields a load factor of 1.0 for the same dimensions. Both analyses are based on models with smeared stiffeners. As shown in Table 4, Case 2, the buckling load factors from PANDA agree reasonably well with those from a finite element program, STAGSC-1 [62]. The optimum design from PANDA is considerably lighter than that from Ref. [63], doubtless because of the discrepancy in the general instability load. Note that the height of the stringer web is more than an order of magnitude less in the PANDA design than it is in the design of Ref. [63], and that the stringer flange essentially disappears at the PANDA optimum. [Stringer Segment 2 represents half of the flange, as shown in Fig. 4(a).]

Table 15: The same basic geometry as for Table 14 is investigated here also. This case involves combined axial compression and torsion, and it is primarily the axial compression load component that "designs" the structure. Unlike the results of Table 14, the results from PANDA and Ref. [61] show reasonably good agreement. Note that certain stress and strain constraints are printed out at the bottom of the table. These are

printed out by PANDA whenever they are less than 2.0.

Table 16: The basic geometry is the same here as for the previous two tables. This case involves the same combined loads as those represented in Table 15, except that a constant internal pressure (not an eigenparameter) is also present, such as would be the case in a pressurized aircraft fuselage flying at high altitude. In comparing Table 16 with Table 15, note that two counteracting effects exist: The design is somewhat lighter because the internal pressure represents a stabilizing influence, but it is not a great deal lighter because the stress constraint for stress in the skin has become active.

Table 17: This is the only test case for a flat panel. According to PANDA the optimum design obtained by the analysis of Ref. [6] is not feasible (local skin buckling load factor is less than unity). However, the formulas used in PANDA for buckling of a flat plate in shear tend to be most conservative when there is only one half wave in each coordinate direction between stiffeners, which is the case in this example. (See also Table 3, Case 9 for a similar situation.)

Table 18: PANDA finds the design of Ref. [47] to be unfeasible, both with regard to general instability and local instability. The results from application of the BOSOR4 computer program [58] to the two designs in Table 18 confirm the PANDA analysis. The BOSOR4 predictions are shown in Fig. 31.

Because of the large number of rings in the optimum design of Ref. [47], most of them were treated as discrete beam-type structures rather than as branched shells. The positions of the ring centroids and ring attachment points are indicated in Fig. 31(b). Note that, corresponding to general instability, the critical pressure for the optimum design determined in Ref. [47], as calculated by BOSOR4, is 484 psi, which is .539 times the design pressure, p_o = 898 psi. This is in excellent agreement with the load factor .538 determined by PANDA. (See right-hand column in Table 18.) The results from BOSOR4 applied to the new optimum design determined by PANDA (left portion of Table 18, right portion of Fig. 31) indicate the presence of two general instability modes and a local instability mode within a few per cent of the load factors near unity predicted by PANDA for this optimum. In the case of hydrostatically compressed ring stiffened cylindrical shells it usually happens that in the neighborhood of the minimum weight design there are two general instability modes at about the same pressure, one of the type shown in Fig. 31(f) and the other of the more commonly recognized type shown in Fig. 31(g).

Elastic-Plastic Material

Table 19 and Figures 32-34 pertain to a hydrostatically compressed cylinder with internal rings of rectangular cross section. The PANDA optimum design has fewer, deeper rings than does the optimum predicted by the analysis of Ref. [44], but

the minimum weight is essentially the same. Figure 32 demonstrates that at the design pressure p_o = 4066 psi the material of the cylindrical shell is stressed well beyond its proportional limit.

Although PANDA indicates that the Ref. [44] design is unsafe with regard to general instability (load multiplier less than unity), an analysis of this configuration with use of the BOSOR5 computer program [59], results of which are shown in Figs. 32 and 33, show that the hull would survive the design pressure if it had no imperfections. BOSOR5 predicts axisymmetric collapse of the Ref. [44] design at a lower pressure than that corresponding to local nonsymmetric buckling. (The local nonsymmetric buckling mode is not shown in Fig. 33.)

Figure 34 shows the results of application of BOSOR5 to the optimum design derived by PANDA, dimensions of which are listed in the left-hand column of Table 19. For this design, local nonsymmetric buckling occurs at the lowest pressure, and slight margins exist in the general and local instability pressures of the perfect structure.

Imperfection Sensitivity

It should be emphasized that PANDA does not account for imperfection sensitivity. As the code is now written, it is up to the user to design a panel to higher loads than those actually

to be seen in service, such that the deleterious effects of initial imperfections will be allowed for. For discussions of imperfection sensitivity the reader is referred to [15, 53, 56, 67] and the references therein.

Parameter Study: Optimum Design of Elastic-Plastic, Ring-Stiffened Cylinders under Hydrostatic Compression

Tables 20-22 and Figures 35-41 pertain to this investigation. The main purpose of the study is to compare PANDA buckling predictions for optimum designs and BOSOR5 predictions for the same designs for a range of loading over which the amount of prebuckling plastic flow varies. BOSOR5 is an appropriate standard of comparison for ring stiffened cylindrical shells stressed under hydrostatic compression beyond the material proportional limit; there exist numerous comparisons with test results [68].

PANDA Results: The optimum designs and buckling pressure factors and modes from PANDA are listed in Tables 20 and 21. The configurations are similar to those shown in Figs. 33 and 34, except that the internal rings have flanges, as shown in Fig. 35(a). The results for each design pressure in Table 20 were obtained by first optimizing such that the ring spacing was included as a decision variable. The ring spacing was then set to a new value as near the optimum value as possible consistent with the condition that there be an integral number of rings

within the cylinder length of 172 inches. A new optimum was calculated corresponding to this new value of ring spacing, which was not allowed to vary during this second optimization process. It is seen from Table 21 that for a wide range of design pressures the optimum design is characterized by many nearly simultaneous buckling modes.

BOSOR5 Models: Figures 35 and 36 show the BOSOR5 models, which are similar to that depicted in Figs. 31(d) and 31(e) except for the different dimensions and the inclusion of elastic-plastic effects. Half the length of the shell is modeled, with symmetry conditions imposed at the mid length. The reference surface of the cylindrical shell is taken to be the inner surface. The web of each ring, treated as a flexible shell branch, is assumed to penetrate the flange to the middle surface of the flange. The material of the ring at the structural plane of symmetry at the bottom in Fig. 35 has half the stiffness of the other rings. All flanges except the two nearest the midlength of the shell (plane of symmetry at the top in Fig. 35) are modeled as discrete rings; the top two flanges are modeled as flexible shell branches. The stress-strain curve for the material is given in Table 19. Figure 36 shows the nodal points in the discretized BOSOR5 models of the optimum designs corresponding to each of the design pressures p_o listed in Tables 20-22. Nodal points are concentrated in the portion of the structure nearest the plane of symmetry in order to obtain converged buckling pressures for local shell, web, and flange

buckling modes.

Figure 37 demonstrates that all of the optimum designs are stressed beyond the material proportional limit at design pressures p_o from 677 to 4743 psi. It is interesting that for optimum designs with p_o from 2710 to 4743 psi the effective plastic strains at the midsurface halfway between rings are close to the 0.2 per cent yield strain, a result obtained from a rather rigorous analysis that confirms the appropriateness of earlier engineering design practice.

Comparison of PANDA and BOSOR5 Buckling Pressures: Figure 38 represents (indirectly) a comparison between PANDA and BOSOR5 buckling predictions because the lowest buckling load factor for each optimum design predicted by PANDA is very close to unity (p_{cr} = design pressure, p_o). Typical buckling modes from BOSOR5 are plotted in Fig. 39.

Figure 38 indicates that PANDA yields slightly unconservative local skin buckling loads and web buckling loads for optimum designs for pressures p_o in the range from 677 to 3388 psi. This slight unconservativeness is an effect of nonlinear material behavior. It is caused in large part by the neglect in the one-layer PANDA models of the variation of axial strain through the shell wall thickness half way between rings. One can see from the pre-bifurcation deflected shape shown in Fig. 39(a), for example, that there is more axial compression and hence gre-

ater effective strain at the outer fiber of the shell wall than at the middle fiber, to which the solid points on the stress-strain curve in Fig. 37 correspond. This bending effect is not included in the results shown in Fig. 38 because the shell wall in the PANDA models from which Fig. 38 was generated was assumed to consist of only one layer. The instantaneous (tangent) stiffness coefficients C_{ij} for the stability analysis are calculated only at the middle surface of each layer, so that in the case of a one-layered model axial bending is not accounted for.

Table 22 and Figure 40 demonstrate the effect of modeling the shell wall in the PANDA analysis as if it consisted of 5 layers of equal thickness. The data listed in the fourth column of Table 22 (5-layer models) are generated by performing simple buckling analyses (no optimization) with PANDA of the optimum designs to which Fig. 38 corresponds, except now the shell is modeled as if it had five layers each of thickness 0.1607 in. rather than one layer of thickness 0.807 in.

The buckling load factor decreases because of the term $(-zw,^{o}_{xx})$ in the expression for e_1^k in Eq. (24): In the one-layer model z is zero at the layer middle surface, so there is no contribution to e_1 due to axial bending. In the five-layer model, however, the two layers, 4 and 5, lying outside the shell middle surface have positive z, so that $e_1^{(4)}$ and $e_1^{(5)}$ are larger (in absolute value) than $e_1^{(1)}$, $e_1^{(2)}$, or

$e_1^{(3)}$. For shells that are stressed only a small amount beyond the material proportional limit, particularly if an elastic-plastic interface exists within the shell wall thickness that is oriented parallel to the middle surface, the absolute increases in $e_1^{(4)}$ and $e_1^{(5)}$ above the absolute value of middle surface strain $e_1^{(3)}$, cause a greater decrease in the instantaneous integrated stiffness coefficients C_{ij} [Eq. (37)] governing stability than the increase of C_{ij} caused by the decrease in $e_1^{(1)}$, and $e_1^{(2)}$ below the absolute value of $e_1^{(3)}$.

Figure 40 gives comparisons for the case p_o =2710 psi between BOSOR5 and PANDA buckling pressures as functions of the number of circumferential waves $\bar{n}$. Figure 40(a) displays this comparison for the optimum design corresponding to use of a one-layer PANDA model (Table 20, fourth row), and Fig. 40(b) gives comparisons for the slightly different optimum design (Table 20, fifth row) obtained by PANDA with use of a five-layer model. In the five-layer model the degree of unconservativeness of the PANDA predictions corresponding to local skin buckling has been reduced by about half and the PANDA prediction of the pressure at which local web buckling occurs is no longer greater than the BOSOR5 prediction for this mode.

Figure 41(a) shows a comparison between PANDA and BOSOR5 predictions of prebuckling circumferential strain and circumferential resultant in a typical web and flange for the 5-layer model at the design pressure of 2710 psi. The pronounced varia-

tion along the flange predicted by BOSOR5 is caused by local axisymmetric bending of the flange, as shown in Fig. 39(a): the flange acts as a very short cylindrical shell "pinched" at its midlength by an axisymmetric radial line load produced by the inward movement of the web as the external pressure is increased.

Figure 41(b) shows the midbay axial strain distributions as predicted by BOSOR5 and PANDA. The predicted circumferential strain is constant through the thickness and equal to -.646 per cent in both the PANDA and BOSOR5 analyses.

SECTION VII

CONCLUSIONS

Accuracy with which Buckling Loads are Computed by PANDA

The PANDA system was developed on a minicomputer. In order to obtain interactively optimum designs of stiffened panels in the presence of many decision variables and many buckling constraints, buckling loads and mode shapes have to be calculated extremely rapidly. Therefore, buckling formulas are derived from simple assumed displacement fields, such as those for the shell in Eqs. (50) and for the stiffeners in Eqs.(89) and (98).

Cases in which the assumed displacement patterns lead to rather poor estimates of the buckling loads have been described. They include buckling of certain unstiffened curved panels under pure in-plane shear (Table 3, Cases 8-10); buckling under pure axial compression of a wide, short stiffened panel (Fig. 22c); and rolling instability of the internal rings of a hydrostatically compressed cylindrical shell (Fig. 26). It is felt, however, that so many buckling constraints are included in the optimization analysis that at or near the optimum design the degree of unconservatism inherent in the one-term Ritz-type analysis on which PANDA is based has less impact than might appear to be the case from a simple buckling analysis of a

non-optimized design.

In order to compensate for possible unconservativeness in the PANDA analysis, the user should:

1. increase the in-plane loads to which the panel is being designed and,

2. check the load-carrying capability of the optimum design obtained with PANDA with use of a more rigorous buckling analysis, such as provided by a finite element program (References [48, 58, 59, 62]).

Even if the approximate nature of the buckling analysis in PANDA is disregarded, the loads applied in the design analysis must be greater than the operating loads in order to compensate for initial imperfections, which are not otherwise accounted for. The failure of PANDA to predict accurate buckling loads in all situations is less significant when viewed from this perspective. It should also be emphasized that PANDA is intended to be used for preliminary design.

In a few instances discrepancies between the buckling predictions of PANDA and those from the literature were investigated further with the use of BOSOR4, BOSOR5, or STAGSC-1. The predictions from these more rigorous computer codes often tend to confirm the PANDA results. Particularly good agreement is exhi-

bited between PANDA and BOSOR5 for elastic-plastic buckling of optimized, hydrostatically compressed, ring-stiffened cylindrical shells optimized for external pressures from about 700 to about 4700 psi.

How PANDA Performs on the VAX Computer

PANDA operates at a reasonable speed for interactive computing on a minicomputer such as the VAX. For example, the optimum design of the ring and stringer-stiffened cylindrical shell shown in Fig. 20, to which the results in Table 14 correspond, is obtained in four sets of five iterations each, the first set requiring 22 seconds at the terminal, the second 18 seconds, the third 15 seconds, and the fourth 12 seconds. (Three such sets of iterations are listed for example on pages 9 and 10 of Table 2a.) This means that every two to four seconds a new design is generated as iterations progress toward the optimum, a reasonable speed at which to obtain optimum designs in a conversationally interactive mode. Approximately the same amount of time at the terminal is required for determination of the optimum design of the ring-stiffened cylindrical shell depicted in Fig. 35a. This shell is subjected to an external hydrostatic pressure of 4066 psi and buckles in the plastic range, as shown in Fig. 37.

Possible Future Enhancements of the Capability of PANDA

...der combined loads," AFOSR TR-76-0930, Georgia Institute of

There are many ways in which PANDA could be improved with retention of its computationally interactive nature:

1. The effect of imperfections could be incorporated explicitly in PANDA through the use of semiempirical formulas of the type derived by Miller and Tsai for the ASME code [69], for example.

2. New buckling modal displacement functions could be introduced such that other than simple support boundary conditions could be imposed. This would be especially important for the case of axially stiffened panels clamped at the edges and buckling in the general instability mode. In order to obtain reasonably optimum designs for a test environment, in which the loaded edges are usually clamped rather than simply supported, one would have to be able to apply clamping for the general instability mode and simple support for the local modes.

3. Optimization could be performed for ranges of in-plane load components, rather than just for a single in-plane load combination. This might be done by first computing the buckling load interaction surfaces

$$f(N_x^o \ , \ N_y^o \ , \ N_{xy}^o \ ) = 0$$

for each design iteration and for each type of buckling mode that span the range of load components provided by the program user and then introducing only that load combination for each buckling mode which is most critical relative to the corresponding load interaction surface.

4. PANDA could be expanded to handle other than cylindrical geometry. Here the difficult task would be to choose appropriate displacement functions for the approximate buckling analysis.

5. The general instability analysis could be improved in the case of stiffened panels by use of a more elaborate assumed displacement field, one that reflects the local-general nature of general instability buckling modes such as that shown in Fig. 22c. Such an improvement would require of PANDA the capability to handle the stiffeners as discrete in calculations of general or semi-general instability load factors and mode shapes.

6. Panels for aircraft fuselages and ship decking are often designed so that local buckling of the skin between adjacent stiffeners is permitted. PANDA could be improved by use of effective stiffness of the skin in its post-buckled state. A difficult task here would be to calculate maximum strains in the loaded, post-buckled skin.

7. Composite materials exhibit a great variety of failure modes and some nonlinear material behavior. Some of this new knowledge should be incorporated into PANDA, which, in the case of anisotropic laminates, now simply checks for maximum stress or strain of each layer and is restricted to linear material behavior if the material is orthotropic.

8. Sanders' equations could be used rather than Donnell's.

9. The scope of PANDA could be broadened to include optimization with respect to individual lamina properties of laminated stiffeners.

10. PANDA is now limited to the analysis of panels with open-section stiffeners. The capability could be expanded to permit optimization of corrugated panels or panels with hat stiffeners.

REFERENCES

[1] L. H. Donnell, "A new theory for the buckling of a thin cylinder under axial compression and bending", Trans. ASME Vol. 56, No. 11, 795-806 (1934)

[2] G. N. Vanderplaats, "CONMIN--a FORTRAN program for con- strained function minimization," NASA TM X-62-282, version updated in March 1975, Ames Research Center, Moffett Field, CA (Aug. 1973)

[3] G. N. Vanderplaats and F. Moses, " Structural optim-ization by methods of feasible directions," Computers and Structures, Vol. 3, pp 739-755 (1973)

[4] Zoutendijk, G., Methods of feasible directions, Elsev-ier Publishing Company, Amsterdam, 1960.

[5] V. B. Venkayya, "Structural optimization: a review and some recommendations," International Journal of Numerical Methods in Engineering, Vol. 13, pp 203-228 (1978)

[5a] E. J. Catchpole, "The optimum design of compression surfaces having unflanged integral stiffeners," Journal of Royal

Aerospace Society, Vol. 58, p 765 (1954)

[6] L. A. Schmit, T. P. Kicher, and W. M. Morrow, "Structural synthesis capability for integrally stiffened waffle plates," AIAA J, Vol. 1, 2820-2836 (1963)

[7] W. M. Morrow and L. A. Schmit, "Structural synthesis of a stiffened cylinder," NASA CR-1217 (Dec 1968)

[8] T. P. Kicher, "Structural synthesis of integrally stiffened cylinders," Journal of Spacecraft and Rockets, Vol. 5, pp 62-67 (1968)

[9] L. D. Hofmeister and L. P. Felton, "Synthesis of waffle plates with multiple rib sizes," AIAA J, Vol. 5, pp 2193-2199, (1969)

[10] R. J. Bronowicki, R. B. Nelson, L. P. Felton, and L. A. Schmit, Jr., "Optimization of ring stiffened cylindrical shells," AAIA J, Vol. 13, pp 1319-1325 (1975)

[11] R. F. Crawford and A. B. Burns, "Minimum weight potentials for stiffened plates and shells," AAIA J, Vol. 1, pp 879-886 (1963)

[12] A. B. Burns and J. Skogh, "Combined loads minimum weight analysis of stiffened plates and shells," Journal of

Spacecraft and Rockets, Vol. 3, pp 235-240 (1966)

[13] A. B. Burns and B. O. Almroth, "Structural optimization of axially compressed cylinders, considering ring-stringer eccentricity effects," Journal of Spacecraft and Rockets, Vol. 3, pp 1263-1268 (1966)

[14] A. B. Burns, "Optimum stiffened cylinders for combined axial compression and internal or external pressure," Journal of Spacecraft and Rockets, Vol. 5, pp 690-699 (1968)

[15] B. O. Almroth, A. B. Burns, and E. V. Pittner, "Design criteria for axially loaded cylindrical shells," Journal of Spacecraft and Rockets, Vol. 7, pp 714-720 (1970)

[16] G. A. Cohen, "Optimum design of truss-core sandwich cylinders under axial compression," AAIA J, Vol. 1, pp 1626-1630 (1963)

[17] G. Gerard, "Optimum structural design concepts for aerospace vehicles," Journal of Spacecraft and Rockets, Vol. 3, pp 5-18 (1966)

[18] W. J. Stroud and N. P. Sykes, "Minimum-weight stiffened shells with slight meridional curvature designed to support axial compressive loads," AIAA J, Vol. 7, pp 1599-1601 (1969)

[19] C. Laksnmikantham and G. Gerard, "Minimum weight design of stiffened cylinders," Aerospace Quarterly, pp 49-68 (Feb 1970)

[20] D. L. Block, "Minimum weight design of axially compressed ring and stringer stiffened cylindrical shells," NASA CR-1766 (Jul 1971)

[21] J. L. Shideler, M. S. Anderson, and L. R. Jackson, "Optimum mass- strength analysis for orthotropic ring-stiffened cylinders under axial compression," NASA TND-6772 (Jul 1972)

[22] A. V. Viswanathan and M. Tamekuni, "Elastic buckling analysis for composite stiffened panels and other structures subjected to biaxial inplane loads," NASA CR-2216 (Mar 1973)

[23] W. H. Wittrick and F. W. Williams, "Buckling and vibration of anisotropic or isotropic plate assemblies under combined loadings," International Journal of Mechanical Sciences, Vol. 16, pp 209-239 (1974)

[24] J. G. Williams and M. Stein, "Buckling behavior and structural efficiency of open-section stiffened composite compression panels," AIAA J, Vol. 14, pp 1618-1626 (1976)

[25] B. L. Agarwal and L. H. Sobel, "Weight comparisons of optimized stiffened, unstiffened, and sandwich cylindrical shells," Journal of Aircraft, Vol. 14, pp 1000-1008 (1977)

[26] M. S. Anderson and W. J. Stroud, "General panel sizing computer code and its application to composite structural panels," AIAA J, Vol. 17, pp 892-897 (1979)

[27] G. G. Weaver and J. R. Vinson, "Minimum-mass designs of stiffened graphite/polymide compression panels, in Modern Developments in Composite Materials and Structures," ASME 1979 Winter Annual Meeting, pp 215-233 (Dec 1979)

[28] L. A. McCullers, "Automated design of advanced composite structures," ASME AMD, Vol. 7, pp 119-130 (Nov 1974)

[29] T. Hayashi, "Optimization for elastic buckling strength of fiber- reinforced composite structures--columns, plates and cylinders," Proc. Mech. Behavior of Materials, Soc. of Material Science, Japan, pp 399-405 (Aug 1974)

[29a] M. Aswani, "Optimization of stiffened cylinder subject to destabilizing load," Proc. Advances in Civil Eng. Through Engrg. Mech., ASCE, New York, pp 456-459 (May 1977)

[30] N. S. Khot, "Computer Program (OPTCOMP) for optimization of composite structures for minimum weight design,"

AFFDL-TR-76-149 (1977)

[31] J. H. Starnes, Jr., and R. T. Haftka, "Preliminary design of composite wings for buckling strength, and displacement constraints," Journal of Aircraft, Vol. 16, pp 564-570 (1979)

[32] G. J. Simitses and V. Ungbhakorn, "Weight optimization of stiffened cylinders under axial compression," Comp _ Struct, Vol. 5, pp 305-314 (1975)

[33] G. J. Simitses and V. Ungbhakorn, "Minimum-weight design of stiffened cylinders under axial compression," AIAA J, Vol. 13, pp 750-755 (1975)

[34] I. Sheinman and G. J. Simitses, "Buckling analysis of geometrically imperfect stiffened cylinders under axial compression," AIAA J, Vol. 15, pp 374-382 (1977)

[35] G. J. Simitses and J. Giri, "Optimum weight design of stiffened cylinders subjected to torsion combined with axial compression with and without lateral pressure," Comp _ Struct, Vol. 8, pp 19-30 (1978)

[36] G. J. Simitses and I. Sheinman, "Optimization of geometrically imperfect stiffened cylindrical shells under axial compression," Comp. Struct, Vol. 9, pp 377-381 (1978)

[37] M. Isreb, "Wing center section optimization with stress and local instability constraints," Comp Struct, Vol. 10, pp 855-861 (1979)

[38] A. Libai, "Optimization of a stiffened square panel subjected to compressive edge loads," AIAA J, Vol. 17, pp 1379-1380 (1979)

[39] J. B. Caldwell and A. D. Hewitt, "Cost effective design of ship structures," Met Constr, Vol. 8, pp 64-67 (1976)

[40] J. G. Pulos and M. A. Krenzke, "Recent developments in pressure hull structures and materials for hydrospace vehicles," David Taylor Model Basin Rep. 2137, Washington, D. C. (Dec 1965)

[41] M. E. Lunchick, "Plastic axisymmetric buckling of ring- stiffened cylindrical shells fabricated from strain-hardening materials and subjected to external hydrostatic pressure," David Taylor Model Basin rep. 1393, Washington, D. C. (Jan 1961)

[42] M. E. Lunchick, "Plastic general-instability pressure of submarine pressure hulls," ASME Paper 62-WA-262 (1962)

[43] L. Boichot and T. E. Reynolds, "Inelastic buckling tests of ring-stiffened cylinders under hydrostatic pressure,"

David Taylor Model Basin rep. 1992, Washington, D. C. (May 1965)

[44] J. R. Renzi, "Optimization of orthotropic, non-linear, ring- stiffened cylindrical shells under external hydrostatic pressure as applied to mmc materials," Naval Surface Weapons Center, NSWC TR 79-305, (Sept. 1979). See also, J. R. Renzi, "Axisymmetric stresses and deflections, inter-bay buckling, and general instability of orthotropic, hybrid, ring-stiffened cylindrical shells under external hydrostatic pressure, Naval Surface Weapons Center, NSWC TR-80-269, April 1981

[45] M. Pappas and C. L. Amba-Rao, "A direct search algorithm for automated optimum structural design," AIAA J, Vol. 9, pp 387-393 (1971)

[46] M. Pappas and A. Allentuch, "Structural synthesis of frame reinforced submersible circular cylindrical hulls," Computers and Structures, Vol. 4, pp 253- 280 (1974)

[47] M. Pappas and A. Allentuch, "Pressure hull optimization using general instability equation admitting more than one longitudinal buckling half-wave," Journal of Ship Research, Vol. 19, pp 18-22 (1975)

[48] B. O. Almroth, P. Stern, and D. Bushnell, "Imper-

fection sensitivity of optimized structural panels," AFWAL-TR-80-3182, March 1981

[49] S. N. Patnaik and M. Maiti, "Optimum design of stiffened structures with constraint on the frequency in the presence of initial stresses," Computer Meth. Appl. Mech. Eng., Vol. 7, pp 303-322 (1976)

[50] M. W. Dobbs and R. B. Nelson, "Minimum weight design of stiffened panels with fracture constraints," Computers and Structures, Vol. 8, pp 753-759 (1978)

[51] R. M. Jones and J. C. F. Hennemann, "Effect of prebuckling deformations on buckling of laminated composite circular cylindrical shells," AIAA J, Vol. 18, pp 110-115 (1980), see also, Proc. AIAA/ASME 19th SDM conf, pp 370-379 (1978)

[52] B. O. Almroth, "Influence of edge conditions on the stability of axially compressed cylindrical shells," AIAA J, Vol. 4, pp 134-140 (1966)

[53] J. W. Hutchinson, "Plastic buckling," Advances in Applied Mechanics, Vol. 14, edited by C. S. Yih, Academic Press, Inc., pp 69-144 (1974)

[54] R. M. Jones, Mechanics of Composite Materials, McGraw-Hill Book Co., New York (1975)

[55] M. Baruch and J. Singer, "Effect of eccentricity of stiffeners on the general instability of stiffened cylindrical shells under hydrostatic pressure," J. Mech. Eng. Sci., Vol. 5, No. 1, pp 23-27 (1963)

[56] D. O. Brush and B. O. Almroth, Buckling of Bars, Plates and Shells, McGraw-Hill Book Co., New York (1975)

[57] M. Booton and R. C. Tennyson, "Buckling of imperfect anisotropic circular cylinders under combined loading," AIAA J, Vol. 17, No. 3, pp 278-287 (Mar 1979)

[58] D. Bushnell, "Stress, stability, and vibration of complex, branched shells of revolution," Computers and Structures, Vol. 4, pp. 399-435 (1974)

[59] D. Bushnell, BOSOR5--program for buckling of elastic-plastic complex shells of revolution including large deflections and creep," Computers and Structures, Vol. 6, pp. 221-239 (1976)

[60] G. J. Simitses and I. Sheinman, "Accurate prediction of critical conditions for shear-loaded panels," AIAA J, Vol. 14, No. 5, pp 683-685 (May 1976)

[61] G. J. Simitses, J. Giri and I. Sheinman, "Minimum weight design of stiffened cylinders and cylindrical panels

under combined loads," AFOSR TR-76-0930, Georgia Institute of Technology, Atlanta, GA (1976)

[62] B. O. Almroth and F. A. Brogan, "The STAGS computer code," NASA Langley Research Center, NASA CR 2950, Feb. 1978

[63] G. J. Simitses and J. Giri, "Minimum weight design of stiffened cylinders subjected to pure torsion," Computers and Structures, Vol. 7, pp667-677 (1977)

[64] D. Bushnell, "Evaluation of various analytical models for buckling and vibration of stiffened shells," AIAA Journal, Vol. 11, No. 9, pp. 1283-1291 (1973)

[65] D. W. Block, M. F. Card, and M. F. Mikulas,Jr., "Buckling of eccentrically stiffened orthotropic cylinders," NASA Langley Research Center, NASA TND 2960, Aug. 1965

[66] T. P. Kicher and C-H Wu, "Buckling of anisotropic circular cylindrical shells," AFML Rept. TR-71-260, Nov. 1971

[67] D. Bushnell, "Buckling of shells--pitfall for designers," to appear in AIAA Journal, September or October, 1981

[68] D. Bushnell, "Buckling of elastic-plastic shells of revolution with discrete elastic-plastic ring stiffeners,"

International Journal of Solids and Structures, Vol. 12, pp. 51-66 (1976)

[69] C. D. Miller, Code Case N-284, ASME Boiler and Pressure Vessel Code, 1980 Code Cases, Nuclear Components, American Society of Mechanical Engineers, New York, pp. 633-656 (July 1980)

Table 1 Buckling Modes Included in the PANDA Analysis

TYPE OF BUCKLING	MODEL USED FOR ESTIMATE
1. General instability Fig. 1; Eq. (57)	Buckling of skin and stiffeners together with smeared rings and stringers. Panel is simply supported along the edges $x = y = 0$, $x = a$, and $y = b$.
2. Local instability Fig. 3; Eq. (57)	Buckling of skin between adjacent rings and adjacent stringers. Portion of panel bounded by adjacent stiffeners is simply supported. Stiffeners take their share of the load in the prebuckling analysis but are disregarded in the stability analysis.
3. Panel instability	
(a) between rings with smeared stringers Fig. 1; Eq. (57)	Buckling of skin and stringers between adjacent rings. Portion of panel bounded by adjacent rings is simply supported. Stringers are smeared. Simple support conditions imposed at $y = 0$ and at $y = b$. Rings take their share of the load in the prebuckling analysis, but are disregarded in the stability analysis.
(b) between stringers with smeared rings Fig. 1; Eq. (57)	Buckling of skin and rings between adjacent stringers. Portion of panel between adjacent stringers is simply supported. Rings are smeared. Simple support conditions imposed at $x = 0$ and at $x = a$. Stringers take their share of the load in the prebuckling analysis, but are disregarded in the stability analysis.
4. Local crippling of stiffener segments	
(a) "internal" segments Figs. 4,5; Eq. (71)	Individual stiffener segment buckles as if it were a long flat strip simply supported along its two long edges. Loading is compression along the stiffener axis. Curvature of ring segments ignored.
(b) "end" segments Figs. 4,5; Eq. (79)	Individual stiffener segment buckles as if it were a long flat strip simply supported along the long edge at which it is attached to its neighboring segment or to the panel skin and free along the opposite edge. Loading is compression along the stiffener axis. Number of half waves along the stiffener axis is the same as that of the part of the structure to which the "end" is attached. Curvature of ring segments ignored.

Table 1 (continued)

TYPE OF BUCKLING	MODEL USED FOR ESTIMATE
5. Local rolling with skin buckling between stiffeners Fig. 6a; Eqs, (57,96,97)	Same as "Local instability" except that strain energy in stiffeners and work done by prebuckling compression in stiffeners are included in the buckling formula. Stiffener cross sections do not deform as stiffeners twist about their lines of attachment to the panel skin.
6. Rolling instability	
(a) with smeared stringers Fig. 6a; Eqs. (57,96,97)	Same as "Panel instability", Type (a), except that strain energy of rings and work done by prebuckling compression along the ring centroidal axis are included in the buckling formula. Ring cross section does not deform as ring twists about its line of attachment to the panel skin.
(b) with smeared rings Fig. 6a; Eqs. (57,96,97)	Same as "Panel instability", Type (b), except that strain energy of stringers and work done by prebuckling compression along the stringer centroidal axis are included in the buckling formula. Stringer cross section does not deform as it twists about its line of attachment to the panel skin.
7. Rolling of stringers, no buckling of skin Fig. 6b; Eqs. (112,119)	Stringer web cross section deforms but the flange cross section does not. Buckling mode has waves along stiffener axis.
8. Rolling of rings, no buckling of skin Fig. 6b; Eqs. (112,119)	Ring web cross section deforms but the flange cross section does not. Buckling mode has waves along the ring axis. This mode is sometimes called "frame tripping" by those interested in submarine structures.
9. Axisymmetric rolling of rings, no skin buckling Fig. 6c; Eqs. (112,119)	Same as "Rolling of rings", except that the buckling mode has zero waves around the circumference of the panel.

TABLE 2a (12 pages)

```
SAMPLE PANDA RUN STREAM: HYDROSTATICALLY COMPRESSED, UNSTIFFENED,
    TWO-LAYERED CYLINDRICAL SHELL...buckling and optimization

$ RUN BEGIN              (Provide initial design)

 THE INPUT DATA PROVIDED BY YOU DURING EXECUTION
 OF THIS PROGRAM ARE SAVED ON A PERMANENT FILE. PLEASE
 PROVIDE THE NAME (9 CHARACTERS OR LESS AND ONE WORD) FOR THIS
 FILE.

 PERMANENT FILE NAME =
 PERMANENT FILE NAME =SAMPLECYL.DAT

 IS PART OR ALL OF THE INPUT FOR THIS CASE STORED ON
 THIS FILE YET?
 Y

 PLEASE TYPE A SHORT TITLE ON THE NEXT LINE..
  BUCKLING OF UNSTIFFENED CYLINDER WITH TWO LAYERS

  DO YOU WANT MORE INFORMATION ABOUT PANDA (Y or N)
 N
  DO YOU WANT LONG PROMPTS?
 N

 IS THE PANEL FLAT  (YES OR NO)...
 N
  AXIAL RESULTANT, NX =
  IS THE AXIAL LOAD COMPRESSIVE...(Y or N)
 Y
 NX =-0.100E+04 <-------------------------- P0R/2
  IS  NX  OKAY...(Y or N)
 Y
  CIRCUMFERENTIAL RESULTANT, NY =
  IS THE CIRCUMFERENTIAL LOAD COMPRESSIVE...(Y or N)
 Y
 NY =-0.200E+04 <-------------------------- P0R
  IS  NY  OKAY...(Y or N)
 Y
  IN-PLANE SHEAR RESULTANT, NXY =
 NXY = 0.000E+00
  IS  NXY  OKAY...(Y or N)
 Y

 DO YOU WANT TO READ VALUES FOR AXIAL RESULTANT AND
 HOOP RESULTANT  (NXFIXED, NYFIXED) WHICH ARE NOT BUCKLING
 PARAMETERS BUT REPRESENT A FIXED PRESTRESSED STATE...
 (THE USUAL ANSWER IS NO)
 N

 CYLINDRICAL PANEL RADIUS OF CURVATURE=
 CYLINDRICAL PANEL RADIUS, R=  100. <------- R
```

P_0 = design pressure

Table 2a (continued)

```
 IS  THE PANEL RADIUS R OKAY...(Y or N)
Y
 AXIAL LENGTH OF PANEL =
AXIAL LENGTH OF PANEL =  200.
 IS THE AXIAL LENGTH OKAY...(Y or N)
Y
 CIRCUMFERENTIAL LENGTH OF PANEL =
CIRCUMFERENTIAL LENGTH OF PANEL =  314.
 IS THE CIRCUMFERENTIAL LENGTH OKAY...(Y or N)
Y

NUMBER OF LAYERS IN PANEL SKIN=
NUMBER OF LAYERS IN PANEL SKIN=  2
 IS THE NUMBER OF LAYERS OKAY...(Y or N)
Y

PANEL SKIN LAYER THICKNESSES (INNER LAYER IS FIRST)

TLAYER( 1) = ...
TLAYER( 1) =  0.500
IS TLAYER( 1) OKAY....(Y or N)
Y

TLAYER( 2) = ...
TLAYER( 2) =  0.500
IS TLAYER( 2) OKAY....(Y or N)
Y

PANEL SKIN LAYER WINDING ANGLES (DEGREES)

 ALPHA( 1) = ...
 ALPHA( 1) =  0.000E+00
IS  ALPHA( 1) OKAY....(Y or N)
Y

 ALPHA( 2) = ...
 ALPHA( 2) =  0.000E+00
IS  ALPHA( 2) OKAY....(Y or N)
Y

PANEL SKIN LAYER MATERIAL TYPES (1, 2, 3, ...)

  MATL( 1) = ...
  MATL( 1) =   1
IS   MATL( 1) OKAY....(Y or N)
Y

  MATL( 2) = ...
  MATL( 2) =   2
IS   MATL( 2) OKAY....(Y or N)
Y

IS THE PANEL STIFFENED...  (YES OR NO)
N
```

```
NEXT PROVIDE MATERIAL PROPERTIES...
NUMBER OF DIFFERENT MATERIALS SPECIFIED = 2

MATERIAL PROPERTIES FOR MATERIAL TYPE 1
MODULI E1, E2, AND G; POISSONS RATIO NU; AND
DENSITY RHO ARE TO BE PROVIDED NOW FOR MATERIAL TYPE NO.  1

 MODULUS E1 IN MATL FIBER DIRECTION OR STIFFENER AXIS=
MATERIAL TYPE  1 AND  E1( 1) = 0.100E+08
 IS  THE MODULUS E1  OKAY...(Y or N)
Y
 IS THIS MATERIAL ISOTROPIC?
Y
 POISSONS RATIO NU =
MATERIAL TYPE  1 AND  NU( 1) = 0.300
 IS POISSONS RATIO NU OKAY...
Y
 WEIGHT DENSITY (e.g. LB/CUBIC INCH), RHO =
MATERIAL TYPE  1 AND RHO( 1) = 0.100
 IS THE DENSITY RHO OKAY...
Y
DO YOU WANT TO PROVIDE A STRESS-STRAIN CURVE FOR THIS MATERIAL..

N
FOR THIS MATERIAL YOU MAY SPECIFY EITHER A SINGLE
MAXIMUM ALLOWABLE EFFECTIVE STRESS  OR  FIVE ULTIMATE
STRAIN COMPONENTS.


DO YOU WANT TO SPECIFY A SINGLE MAXIMUM ALLOWABLE
EFFECTIVE STRESS...(Y or N)
Y
MAXIMUM ALLOWABLE EFFECTIVE STRESS =
MATL TYPE  1. MAX EFFECTIVE STRESS = 0.500E+05
 IS THE MAXIMUM VALUE OF EFFECTIVE STRESS OKAY...
Y

DO YOU WANT ANOTHER CHANCE TO PROVIDE MATERIAL
PROPERTIES FOR THIS MATERIAL TYPE..
N

MATERIAL PROPERTIES FOR MATERIAL TYPE 2
MODULI E1, E2, AND G; POISSONS RATIO NU; AND
DENSITY RHO ARE TO BE PROVIDED NOW FOR MATERIAL TYPE NO.  2

 MODULUS E1 IN MATL FIBER DIRECTION OR STIFFENER AXIS=
MATERIAL TYPE  2 AND  E1( 2) = 0.200E+08
 IS  THE MODULUS E1  OKAY...(Y or N)
Y
 IS THIS MATERIAL ISOTROPIC?
Y
 POISSONS RATIO NU =
MATERIAL TYPE  2 AND  NU( 2) = 0.300
 IS POISSONS RATIO NU OKAY...
Y
```

```
 WEIGHT DENSITY (e.g. LB/CUBIC INCH), RHO =
MATERIAL TYPE  2 AND RHO( 2) = 0.300
 IS THE DENSITY RHO OKAY...
Y
DO YOU WANT TO PROVIDE A STRESS-STRAIN CURVE FOR THIS MATERIAL..

N
FOR THIS MATERIAL YOU MAY SPECIFY EITHER A SINGLE
MAXIMUM ALLOWABLE EFFECTIVE STRESS  OR  FIVE ULTIMATE
STRAIN COMPONENTS.


DO YOU WANT TO SPECIFY A SINGLE MAXIMUM ALLOWABLE
EFFECTIVE STRESS...(Y or N)
Y
MAXIMUM ALLOWABLE EFFECTIVE STRESS =
MATL TYPE  2. MAX EFFECTIVE STRESS = 0.100E+06
 IS THE MAXIMUM VALUE OF EFFECTIVE STRESS OKAY...
Y

DO YOU WANT ANOTHER CHANCE TO PROVIDE MATERIAL
PROPERTIES FOR THIS MATERIAL TYPE..
N

IS THE RATIO PHI=(LOCAL/GENERAL) BUCKLING LOAD
DIFFERENT FROM UNITY...
N


WHEN YOUR TERMINAL SAYS

            READY

  PLEASE TYPE THE COMMAND

            -DECIDE
```

```
$ RUN DECIDE                (tell PANDA to do a simple buckling analysis)

 BUCKLING OF UNSTIFFENED CYLINDER WITH TWO LAYERS


INPUT DATA SUPPLIED INTERACTIVELY BY YOU IN THIS RUN
ARE STORED ON A PERMANENT FILE. WHAT IS THE NAME OF THIS FILE?
(9 CHARACTERS OR LESS, PLEASE, AND ONE WORD.)

 PERMANENT FILE NAME :
PERMANENT FILE NAME :SAMPLEDEC.DAT

IS PART OR ALL OF THE INPUT FOR THIS CASE STORED ON
THIS FILE YET?
Y

DO YOU WISH TO CHANGE THE TITLE OF THIS CASE...
N
DO YOU WANT MORE INFORMATION ON THIS PROGRAM?
N


DO YOU WISH TO CHANGE THE LOADS OR THE FACTOR PHI
N

DO YOU WANT TO MAKE THE PANEL FLAT...
N

YOU CAN DO TWO TYPES OF ANALYSIS WITH PANDA:

    1. A BUCKLING ANALYSIS OF A FIXED DESIGN (NO OPTIMIZATION)
    2. AN OPTIMIZATION ANALYSIS

DO YOU WANT TO DO A BUCKLING ANALYSIS OF A FIXED DESIGN?
Y


DO YOU WISH TO CHANGE SOME OF THE STRUCTURAL DIMENSIONS
OR WINDING ANGLES..
N


WHEN YOUR TERMINAL SAYS

            READY

  PLEASE TYPE THE COMMAND

            -PANCON
```

```
$ RUN PANCON                          (do simple buckling analysis)

  BUCKLING OF UNSTIFFENED CYLINDER WITH TWO LAYERS


 DO YOU WANT TO SEE THE WALL STIFFNESS MATRICES C(I,J)
 FOR THE SKIN ALONE AND FOR THE PANEL WITH SMEARED STIFFENERS...
 N

 PANEL WEIGHT=  1.2560E+04
 DO YOU WISH TO PRINT OUT A SUMMARY OF DESIGN INFORMATION. . .

 Y

  BUCKLING OF UNSTIFFENED CYLINDER WITH TWO LAYERS


 ******************************************************
 PANEL WEIGHT =                                  1.2560E+04

 AXIAL LOAD/(LENGTH OF CIRCUMFERENCE), NX =     -1.0000E+03
 CIRC. LOAD/(LENGTH OF GENERATOR),     NY =     -2.0000E+03
 IN-PLANE SHEAR STRESS RESULTANT,      NXY =     2.2361E-02

 FIXED AXIAL STRESS RESULTANT,     NXFIXED =     0.0000E+00
 FIXED CIRC. STRESS RESULTANT,     NYFIXED =     0.0000E+00

 DECISION VARIABLES FOLLOW...


         (M=AXIAL, N=CIRC.) HALF-WAVES OVER ENTIRE PANEL (AXIAL,CIRC.)
 GENERAL INSTABILITY EIGENVALUE(M,N)=          3.2383E+00(    1,    6)
 ******************************************************


 DO YOU WANT TO PRINT OUT MORE INFORMATION ABOUT THE
 CURRENT DESIGN...
 N

 DO YOU WANT TO STORE OUTPUT DESIGN INFORMATION ON A
 PERMANENT FILE?
 N
```

```
$ RUN DECIDE      (choose decision variables for optimization analysis)

  BUCKLING OF UNSTIFFENED CYLINDER WITH TWO LAYERS


 INPUT DATA SUPPLIED INTERACTIVELY BY YOU IN THIS RUN
 ARE STORED ON A PERMANENT FILE. WHAT IS THE NAME OF THIS FILE?
 (9 CHARACTERS OR LESS, PLEASE, AND ONE WORD.)

  PERMANENT FILE NAME =
PERMANENT FILE NAME =SAMPLEDC2.DAT

 IS PART OR ALL OF THE INPUT FOR THIS CASE STORED ON
 THIS FILE YET?
 Y

 DO YOU WISH TO CHANGE THE TITLE OF THIS CASE...
 Y
 TYPE A NEW TITLE...
  OPTIMIZATION OF UNSTIFFENED CYLINDER OF TWO LAYERS

 DO YOU WANT MORE INFORMATION ON THIS PROGRAM?
 N


 DO YOU WISH TO CHANGE THE LOADS OR THE FACTOR PHI
 N

 DO YOU WANT TO MAKE THE PANEL FLAT...
 N

 YOU CAN DO TWO TYPES OF ANALYSIS WITH PANDA:

     1. A BUCKLING ANALYSIS OF A FIXED DESIGN (NO OPTIMIZATION)
     2. AN OPTIMIZATION ANALYSIS

 DO YOU WANT TO DO A BUCKLING ANALYSIS OF A FIXED DESIGN?
 N


 DO YOU WISH TO CHANGE SOME OF THE STRUCTURAL DIMENSIONS
 OR WINDING ANGLES..
 N

 NOTE... DEFAULT VALUES FOR LOWER AND UPPER BOUNDS OF A
 DECISION VARIABLE X ARE...

             LOWER BOUND = X/100
             UPPER BOUND = X*100

 IN WHICH X IS THE CURRENT VALUE OF THE DECISION VARIABLE.

 ARE ANY OF THE SHELL WALL LAYER THICKNESSES DECISION VARIABLES...
 Y
```

Table 2a (continued)

```
DO YOU WANT TO USE DEFAULT VALUES FOR LOWER AND UPPER BOUNDS
OF SHELL WALL LAYER THICKNESSES...
Y

IS THE THICKNESS OF LAYER NO. 1 A DECISION VARIABLE.
Y
(LOWER,UPPER) BOUNDS FOR THICKNESS OF LAYER NO. 1 =
(   5.000E-03 ,   5.000E+01)

IS THE THICKNESS OF LAYER NO. 2 A DECISION VARIABLE.
Y
(LOWER,UPPER) BOUNDS FOR THICKNESS OF LAYER NO. 2 =
(   5.000E-03 ,   5.000E+01)

ARE ANY OF THE LAYER WINDING ANGLES DECISION VARIABLES
N


WHEN YOUR TERMINAL SAYS

            READY

  PLEASE TYPE THE COMMAND

            -PANCON
```

```
$ RUN PANCON                    (Perform the optimization analysis)

  OPTIMIZATION OF UNSTIFFENED CYLINDER OF TWO LAYERS


 PANEL WEIGHT=  1.2560E+04

 PANEL WEIGHT=  8.3906E+03

 PANEL WEIGHT=  6.5349E+03

 PANEL WEIGHT=  5.7286E+03

 PANEL WEIGHT=  5.2393E+03

 PANEL WEIGHT=  4.9426E+03
 DO YOU WISH TO PRINT OUT A SUMMARY OF DESIGN INFORMATION. . .

 N

 DO YOU WISH TO DO MORE ITERATIONS WITH THE SAME DECISION
 VARIABLES...
 Y

 PANEL WEIGHT=  4.9426E+03

 PANEL WEIGHT=  4.7624E+03

 PANEL WEIGHT=  4.6767E+03

 PANEL WEIGHT=  4.6272E+03

 PANEL WEIGHT=  4.5963E+03

 PANEL WEIGHT=  4.5734E+03
 DO YOU WISH TO PRINT OUT A SUMMARY OF DESIGN INFORMATION. . .

 N
```

```
DO YOU WISH TO DO MORE ITERATIONS WITH THE SAME DECISION
VARIABLES...
Y

PANEL WEIGHT=  4.5734E+03

PANEL WEIGHT=  4.5581E+03

PANEL WEIGHT=  4.5464E+03

PANEL WEIGHT=  4.5492E+03

PANEL WEIGHT=  4.5414E+03

PANEL WEIGHT=  4.5362E+03
DO YOU WISH TO PRINT OUT A SUMMARY OF DESIGN INFORMATION. . .

Y

 OPTIMIZATION OF UNSTIFFENED CYLINDER OF TWO LAYERS


**********************************************************
PANEL WEIGHT =                                  4.5362E+03

AXIAL LOAD/(LENGTH OF CIRCUMFERENCE), NX =     -1.0000E+03
CIRC. LOAD/(LENGTH OF GENERATOR),     NY =     -2.0000E+03
IN-PLANE SHEAR STRESS RESULTANT,      NXY =     2.2361E-02

FIXED AXIAL STRESS RESULTANT,     NXFIXED =     0.0000E+00
FIXED CIRC. STRESS RESULTANT,     NYFIXED =     0.0000E+00

DECISION VARIABLES FOLLOW...
THICKNESS OF PANEL SKIN LAYER NO. 1 =           6.8305E-01
THICKNESS OF PANEL SKIN LAYER NO. 2 =           1.3092E-02


        (M=AXIAL, N=CIRC.) HALF-WAVES OVER ENTIRE PANEL (AXIAL,CIRC.)
GENERAL INSTABILITY EIGENVALUE(M,N)=          9.9974E-01(   1,   7)
**********************************************************


DO YOU WISH TO DO MORE ITERATIONS WITH THE SAME DECISION
VARIABLES...
N
```

```
DO YOU WANT TO PRINT OUT MORE INFORMATION ABOUT THE
CURRENT DESIGN...
Y


OPTIMIZATION OF UNSTIFFENED CYLINDER OF TWO LAYERS


CURRENT DESIGN FOLLOWS....
 PANEL RADIUS OF CURVATURE     =    1.000E+02
 PANEL AXIAL, CIRC. LENGTHS    =    2.000E+02   3.140E+02
 PANEL AXIAL PRESTRESS,  NXP   =    0.000E+00 (NOT AN EIGENPARAM)
 PANEL CIRC. PRESTRESS,  NYP   =    0.000E+00 (NOT AN EIGENPARAM)
 PANEL TOTAL THICKNESS         =    6.961E-01
 PANEL LAYER THICKNESSES       =    6.831E-01   1.309E-02
 PANEL LAYER WINDING ANGLES    =    0.000E+00   0.000E+00
 PANEL LAYER MATERIAL TYPES    =          1           2
MODULI (E1, E2, G) OF MATL  1 =    1.000E+07   1.000E+07   3.846E+06
POISSON RAT., DENSITY MATL  1 =    3.000E-01   1.000E-01
MODULI (E1, E2, G) OF MATL  2 =    2.000E+07   2.000E+07   7.692E+06
POISSON RAT., DENSITY MATL  2 =    3.000E-01   3.000E-01

THE TOTAL PANEL WEIGHT        =   4.536E+03
 THE PANEL SKIN WEIGHT        =    4.536E+03
 THE TOTAL STIFFENER WEIGHT   =    0.000E+00

GENERAL INSTABILITY QUANIITIES (STIFFENERS SMEARED OUT)...
 AXIAL STRESS RESULTANT, NX    =  -1.000E+03 (AN EIGENPARAMETER)
 CIRC. STRESS RESULTANT, NY    =  -2.000E+03 (AN EIGENPARAMETER)
 SHEAR STRESS RESULTANT, NXY   =   2.236E-02 (AN EIGENPARAMETER)
 AXIAL HALF WAVES OVER PANEL   =     1
 CIRC. HALF WAVES OVER PANEL   =     7
 SLOPE OF BUCKLING NODAL LINES=    0.000E+00
GENERAL INSTABILITY MULTIPLIER=    9.997E-01   (EIGENVALUE)

AVERAGE AXIAL STRAIN           =  -5.640E-05
AVERAGE MIDBAY HOOP STRAIN     =  -2.397E-04
AVERAGE SHEAR STRAIN           =   8.197E-09
FIBER STRAINS AT EACH LAYER CENTER=
                                  -5.640E-05  -5.640E-05
STRAINS NORMAL TO FIBERS IN LAYERS=
                                  -2.397E-04  -2.397E-04
SHEAR STRAINS IN MATERIAL COORDS  =
                                   8.133E-09   8.133E-09
EFFECTIVE STRAINS AT LAYER CENTERS =
                                   2.117E-04   2.117E-04

DO YOU WANT TO STORE OUTPUT DESIGN INFORMATION ON A
PERMANENT FILE?
Y
 NAME OF PERMANENT FILE (9 CHAR. OR LESS) =
PERMANENT FILE NAME =OPTMUMCYL.DAT
DO YOU WISH TO PRINT OUT A SUMMARY OF DESIGN INFORMATION. . .
```

Table 2a (continued)

```
Y

DO YOU WANT TO PRINT OUT MORE INFORMATION ABOUT THE
CURRENT DESIGN...
Y

(Because the previous two questions were answered "YES" (Y),
 the file "OPTMUMCYL.DAT" will contain the same information
 that is printed after the last set of design iterations. In
 interactive runs this design information is presented on the
 terminal only.  If the user wants to obtain a "hard" copy
 he must answer "Y" to these last two questions.  He can then
 print out the file "OPTMUMCYL.DAT" on any device he chooses.)
```

Table 2b

LIST OF USER-PROVIDED RESPONSES TO QUESTIONS ASKED IN "BEGIN"

(The following constitutes the file "SAMPLECYL.DAT" which can be edited if the user wishes to modify the case without having to answer all of the questions in BEGIN again.)

```
BUCKLING OF UNSTIFFENED CYLINDER WITH TWO LAYERS

N           WANT MORE INFORMATION?
N           WANT LONG PROMPTS?
N           IS PANEL FLAT?
0.100E+04 AXIAL STRESS RESULTANT
Y           IS NX COMPRESSIVE?
Y           IS PREVIOUS NUMERICAL ENTRY OK?
0.200E+04 CIRCUMFERENTIAL STRESS RESULTANT
Y           IS NY COMPRESSIVE?
Y           IS PREVIOUS NUMERICAL ENTRY OK?
0.000E+00 IN-PLANE SHEAR STRESS RESULTANT
Y           IS PREVIOUS NUMERICAL ENTRY OK?
N           WANT TO INPUT NXFIXED,NYFIXED?
 100.       CYLINDER RADIUS
Y           IS PREVIOUS NUMERICAL ENTRY OK?
 200.       AXIAL LENGTH OF PANEL
Y           IS PREVIOUS NUMERICAL ENTRY OK?
 314.       CIRCUMFERENTIAL LENGTH OF PANEL
Y           IS PREVIOUS NUMERICAL ENTRY OK?
   2        NUMBER OF LAYERS IN PANEL SKIN
Y           IS PREVIOUS NUMERICAL ENTRY OK?
0.500         TLAYER
Y           IS PREVIOUS NUMERICAL ENTRY OK?
0.500         TLAYER
Y           IS PREVIOUS NUMERICAL ENTRY OK?
0.000E+00     ALPHA
Y           IS PREVIOUS NUMERICAL ENTRY OK?
0.000E+00     ALPHA
Y           IS PREVIOUS NUMERICAL ENTRY OK?
   1            MATL
Y           IS PREVIOUS NUMERICAL ENTRY OK?
   2            MATL
Y           IS PREVIOUS NUMERICAL ENTRY OK?
N           IS THE PANEL STIFFENED?
0.100E+08 MODULUS IN FIBER DIRECTION
Y           IS PREVIOUS NUMERICAL ENTRY OK?
Y           IS THIS MATERIAL ISOTROPIC?
0.300       POISSONS RATIO
Y           IS PREVIOUS NUMERICAL ENTRY OK?
0.100       WEIGHT DENSITY
Y           IS PREVIOUS NUMERICAL ENTRY OK?
N           WANT TO INPUT STRESS-STRAIN?
Y           WANT TO INPUT EFFECTIVE STRESS?
0.500E+05 MAXIMUM EFFECTIVE STRESS
```

```
Y          IS PREVIOUS NUMERICAL ENTRY OK?
N          DO MATERIAL PROPERTIES AGAIN?
0.200E+08  MODULUS IN FIBER DIRECTION
Y          IS PREVIOUS NUMERICAL ENTRY OK?
Y          IS THIS MATERIAL ISOTROPIC?
0.300      POISSONS RATIO
Y          IS PREVIOUS NUMERICAL ENTRY OK?
0.300      WEIGHT DENSITY
Y          IS PREVIOUS NUMERICAL ENTRY OK?
N          WANT TO INPUT STRESS-STRAIN?
Y          WANT TO INPUT EFFECTIVE STRESS?
0.100E+06  MAXIMUM EFFECTIVE STRESS
Y          IS PREVIOUS NUMERICAL ENTRY OK?
N          DO MATERIAL PROPERTIES AGAIN?
N          IS LOCAL/GENERAL NOT = UNITY?
```

Table 2c

LIST OF USER-PROVIDED RESPONSES TO QUESTIONS ASKED IN "DECIDE" CORRESPONDING TO A CASE IN WHICH A SIMPLE BUCKLING ANALYSIS IS DESIRED

(The following constitutes the file "SAMPLEDEC.DAT", which can be edited if the user wishes to modify the case without having to answer all of the questions in DECIDE again.)

```
N          CHANGE TITLE?
N          WANT MORE INFORMATION?
N          CHANGE LOADING?
N          MAKE PANEL FLAT OR CURVED?
Y          DO BUCKLING ONLY?
N          CHANGE DIMENSIONS?
```

Table 2d

LIST OF USER-PROVIDED RESPONSES TO QUESTIONS ASKED IN "DECIDE"

(The following constitutes the file "SAMPLEDC2.DAT", which can be edited if the user wishes to modify the case without having to answer all of the questions in DECIDE again.)

```
Y          CHANGE TITLE?
OPTIMIZATION OF UNSTIFFENED CYLINDER OF TWO LAYERS

N          WANT MORE INFORMATION?
N          CHANGE LOADING?
N          MAKE PANEL FLAT OR CURVED?
N          DO BUCKLING ONLY?
N          CHANGE DIMENSIONS?
Y          ANY t(i) DECISION VARIABLES?
Y          WANT DEFAULT BOUNDS ON t(i)?
Y          IS t(i) A DECISION VARIABLE?
Y          IS t(i) A DECISION VARIABLE?
N          ANY phi(i) DECISION VAR.?
```

Table 3 Buckling of Monocoque Cylindrical Panels under Pure Shear

Case	$Z = \frac{a^2(1-\nu^2)^{1/2}}{Rt}$ (t = 1.0)	R	a/b	$[k_x^o]^*$	$k_s = N_{xy}^{cr}\, a^2 12(1-\nu^2)/(\pi^2 Et^3)$	
					PANDA ($\bar{m},\bar{n}$,c or d)	Simitses [61]
1	10	100	0.187	0	8.15 (1,7,d=1.47)	7.90
2	100	100	0.187	0	29.41 (1,17,d=2.11)	29.01
3	1000	2000	0.187	0	159.8 (1,36,d=3.65)	162.00
4	2000	2000	0.187	0	268.9 (1,43,d=4.38)	266.00
5	100	100	1.000	0	29.22 (1,3,d=2.114)	34.73
6	100	100	5.000	0	163.93 (4,1,c=0.681)	148.30
7	100	100	10.00	0	577.8 (8,1,c=0.681)	564.90
8	1000	2000	10.00	0	950.9 (4,1,c=0.981)	700.00
9	1	100	0.667	-1.8	2.0045 (1,1,d=2.537)	2.956
10	1	100	0.667	+1.8	8.0853 (1,2,d=1.468)	9.572

* $k_x^o = N_{XPRE}\, a^2\, 12(1-\nu^2)/(\pi^2 Et^3)$

Table 4 Buckling Predictions with PANDA and STAGSC-1 for Complete Cylindrical Shells and Cylindrical Panels under Pure Shear

Case	Case Description	Buckling Load Factors, λ from PANDA	Buckling Load Factors, λ from STAGSC-1
1	Unstiffened, composite cylinder with unbalanced laminate, 3 layers, with (+60°, 0, -60°) windings (see Fig. 15) $N^{o}_{xy} = \pm 1.0$	Positive N_{xy}: 156.7(1,8,3.05)[a]	160,5 (1,8,-)
		Negative N_{xy}: 234.2(1,9,-2.11)	222.2 (1,8,-)
2	Ring and stringer-stiffened cylindrical shell analyzed by Simitses and Giri (Ref. [63], Fig. 20). Design load, N^{o}_{xy} = 418.5 lb/in.	General instability: 4.74(1,11,7.57)	4.61 (-,10,-)
		Local skin buckling: 1.41(1,6,1.47)	Not calculated
		Between rings, smeared stringers: 1550.3(1,919,25.0)	Not calculated
		Between stringers, smeared rings: 1.144(24,1,0.394)	1.096 (25,2,-)
3	Shallow panel with J-stringers; design load, N^{o}_{xy} = 1500 lb/in. (see Fig. 21)	General instability, smeared stringers: 1.120(1,3,5.26)	1.00 (1,3,-)
		General instability, discrete stringers: Not calculated	0.684 (1,3,-)
		Local skin buckling: 1.177(3,1,0.681)	Not calculated

[a] Numbers in parentheses are:
axial half-waves, circumferential $\left\{\begin{matrix}\text{full waves if complete cyl.} \\ \text{half-waves if panel}\end{matrix}\right\}$,
slope of buckling mode nodal lines).

Table 5 Comparison of PANDA Buckling Load Predictions with Those of Other Analyses for an Axially-Compressed Cylinder with Smeared Rings and Stringers (Fig. 23)

Case	Position of Stiffeners	NORMALIZED BUCKLING LOAD, $(N_x/E\bar{t})$ [a]		
		PANDA	NASA-TND-2960 [65]	Kicher & Wu [66]
1	Rings External Stringers External	0.004225(2,8) [b]	0.004137(3,8)	0.004270(-,7)
2	Rings Internal Stringers External	0.003544(3,8)	0.003574(3,8)	0.003562(-,8)
3	Rings External Stringers Internal	0.003025(3,8)	----------	0.003022(-,8)
4	Rings Internal Stringers Internal	0.002729(3,8)	0.002779(2,8)	0.002787(-,8)

[a] $\bar{t} = t_{shell} + (Area_{stringer}/b_{stringer}) = 0.244$ in.

[b] Numbers in parentheses are (axisl half-waves, circumferential full waves) over cylinder.

Table 6 Buckling Load Factors for Axially-Compressed, Blade-Stiffened Composite Plate with Length a = 76 cm and N_x^o = 15730 N/m (Geometry and Material Properties Shown in Fig. 25)

Type of Buckling	Buckling Load Factor	Axial Half-Waves	Governing Equations	Is a Point Plotted in Fig. 25?
General instability	1.332	1	57 (smeared srtinger)	Yes
Local skin buckling	1.135	7	57 (no stiffeners)	Yes
Buckling of stringer seg. 1	1.207	7	79	No
Local rolling with skin buckling between stringers	1.029	5	57 (with 96 and 97)	Yes
Rolling of stringers, no skin buckling	1.834	6	112	No

Table 7 Buckling Load Factors for Externally-Pressurized, Ring-Stiffened Cylinder with Length 100 in., $N_x^o = 0$, $N_y^o = 5.218$ lb/in. (Geometry Shown in Fig. 26)

Type of Buckling	Buckling Load Factor	Circ. Full Waves	Governing Equations	Is a Point Plotted in Fig. 26?
General instability	438	2	57 (smeared rings)	Yes
Local skin buckling	246000	36	57 (no rings)	No
Buckling of ring seg. 1	2920	48	71 (web buckling)	No
Buckling of ring seg. 2	17605	48	79 (flange buckling)	No
Buckling of ring seg. 3	17605	48	79 (flange buckling)	No
Local rolling with skin buckling between rings	159490	36	57 (with 96 and 97)	No
Rolling of rings, no skin buckling	1826	10	112 (web), 119 (flange)	Yes
Axisymmetric rolling of rings, no skin buckling	4819	0	112 and 119, $\bar{n} = 0$	No

Table 8 Buckling Load Factors for Hydrostatically-Compressed, Ring-Stiffened Cylinder with Length = 23.2 in., N_x^o = 10.21, N_y^o = 20.42 lb/in. (Geometry Shown in Fig. 27)

Type of Buckling	Buckling Load Factor	Circ. Full Waves	Governing Equations	Is a Point Plotted in Fig. 27?
General instability	14638	3	57 (smeared rings)	No
Local skin buckling	12023	9	57 (no rings)	No
Buckling of ring seg. 1	4747	17	71 (web buckling)	Yes
Buckling of ring seg. 2	46671	17	79 (flange buckling)	No
Buckling of ring seg. 3	46671	17	79 (flange buckling)	No
Local rolling with skin buckling between rings	10852	5	57 (with 96 and 97)	No
Rolling of rings, no skin buckling	3217	1	112 (web), 119 (flange)	Yes
Axisymmetric rolling of rings, no skin buckling	3179	0	112 (web), 119 (flange)	Yes

Table 9 Buckling Load Factors for Externally-Pressurized, Ring-Stiffened Cylinder with Radius = 100 in., Thickness = 1.0 in., Length = 200 in., $N_x^o = 0$, $N_y^o = 1$ lb/in. (Geometry Shown in Fig. 28)

Type of Buckling	Buckling Load Factor	Circ. Full Waves	Governing Equations	Is a Point Plotted in Fig. 28?
General instability	949	3	57 (smeared rings)	Yes
Local skin buckling	738	16	57 (no rings)	Yes
Buckling of ring seg. 1	1113	39	71 (web buckling)	No
Buckling of ring seg. 2	3645	39	79 (flange buckling)	No
Buckling of ring seg. 3	3645	39	79 (flange buckling)	No
Local rolling with skin buckling between rings	707	15	57 (with 96 and 97)	Yes
Rolling of rings, no skin buckling	811	6	112 (web), 119 (flange)	Yes
Axisymmetric rolling of rings, no skin buckling	1320	0	112 (web), 119 (flange)	Yes

Table 10 Buckling Load Factors for Axially-Compressed Ring and Stringer-Stiffened Cylindrical Shell with N_x^o = 1.0 lb/in., N_y = 0 (Geometry Shown in Figure 9)

Type of Buckling	Buckling Load Factor	Axial Half-Waves	Circ. Full Waves	STAGSC-1 Buckling Load Predictions (See Fig. 29)
General instability	105600	8	1	106200
Local skin buckling	58149	21	59	Not calculated
Buckling between rings with smeared stringers	67083	7	24	Not calculated
Buckling between stringers with smeared rings	507420	92	59	Not calculated
Buckling of stringer seg. 1	331940	21		Not calculated
Local rolling with skin buckling between stiffeners	70919	21	59	70000
Rolling of stringers, no skin buckling	995440	84		Not calculated
Axisymmetric rolling of rings, no skin buckling	10899000	0	0	Not calculated
Rolling mode with smeared stringers	68015	7	24	66000
Rolling mode with smeared rings	509270	92	59	Not calculated

Table 1 Effect of Plastic Buckling of an Axially Compressed Ring and Stringer Stiffened Cylindrical Shell (Eqs. 4, 30)

APPLIED AXIAL COMPRESSION (LB/IN)

(a) N_x^o = 440185

(M=AXIAL, N=CIRC.) HALF-WAVES OVER ENTIRE PANEL (AXIAL,CIRC.)			
GENERAL INSTABILITY EIGENVALUE(M,N)=	2.6278E+00	8,	1)
LOCAL SKIN (BUCKLING/PHI) (M,N) =	1.4470E+00	21,	59)
BUCKLING BETWEEN RINGS WITH SMEARD STRINGRS=	1.6694E+00	7,	24)
BUCKLING BETWEEN STRINGRS WITH SMEARD RINGS=	1.2627E+01	92,	59)
BUCKLING/PHI (M) OF STRINGER SEGMENT NO. 1=	8.2605E+00	21)	
LOCAL ROLLING WITH SKIN BUCKLING BETWN STIF=	1.7642E+00	21,	59)
ROLLING OF STRINGERS(M,0), NO SKIN BUCKLING=	2.4772E+01	84,	0)
AXISYMMETRIC ROLLING OF RINGS, NO SKIN BUCK=	2.7436E+02	0,	0)
BUCKLING(ROLLING) MODE WITH SMEARD STRINGRS=	1.6925E+00	7,	24)
BUCKLING(ROLLING) MODE WITH SMEARED RINGS =	1.2673E+01	92,	59)

(b) N_x^o = -40200

(M=AXIAL, N=CIRC.) HALF-WAVES OVER ENTIRE PANEL (AXIAL,CIRC.)			
GENERAL INSTABILITY EIGENVALUE(M,N)=	5.6817E-01	19,	1)
LOCAL SKIN (BUCKLING/PHI) (M,N) =	1.4465E+00	21,	59)
BUCKLING BETWEEN RINGS WITH SMEARD STRINGRS=	4.7837E-01	7,	24)
BUCKLING BETWEEN STRINGRS WITH SMEARD RINGS=	1.2622E+01	92,	59)
BUCKLING/PHI (M) OF STRINGER SEGMENT NO. 1=	7.9054E+00	21)	
LOCAL ROLLING WITH SKIN BUCKLING BETWN STIF=	1.7582E+00	21,	59)
ROLLING OF STRINGERS(M,0), NO SKIN BUCKLING=	1.0983E+01	169,	0)
AXISYMMETRIC ROLLING OF RINGS, NO SKIN BUCK=	2.7425E+02	0,	0)
BUCKLING(ROLLING) MODE WITH SMEARD STRINGRS=	4.9652E-01	7,	24)
BUCKLING(ROLLING) MODE WITH SMEARED RINGS =	1.2570E+01	92,	59)

(c) N_x^o = -40600

(M=AXIAL, N=CIRC.) HALF-WAVES OVER ENTIRE PANEL (AXIAL,CIRC.)			
GENERAL INSTABILITY EIGENVALUE(M,N)=	1.4200E-01	15,	1)
LOCAL SKIN (BUCKLING/PHI) (M,N) =	1.0217E+00	28,	59)
BUCKLING BETWEEN RINGS WITH SMEARD STRINGRS=	6.8279E-02	14,	1)
BUCKLING BETWEEN STRINGRS WITH SMEARD RINGS=	6.0797E+00	137,	59)
BUCKLING/PHI (M) OF STRINGER SEGMENT NO. 1=	6.8279E+00	28)	
LOCAL ROLLING WITH SKIN BUCKLING BETWN STIF=	1.3154E+00	28,	59)
ROLLING OF STRINGERS(M,0), NO SKIN BUCKLING=	9.4625E+00	169,	0)
AXISYMMETRIC ROLLING OF RINGS, NO SKIN BUCK=	2.2815E+02	0,	0)
BUCKLING(ROLLING) MODE WITH SMEARD STRINGRS=	6.8305E-02	14,	1)
BUCKLING(ROLLING) MODE WITH SMEARED RINGS =	6.1224E+00	137,	59)

(d) N_x^o = -41200

(M=AXIAL, N=CIRC.) HALF-WAVES OVER ENTIRE PANEL (AXIAL,CIRC.)			
GENERAL INSTABILITY EIGENVALUE(M,N)=	1.3280E-01	16,	1)
LOCAL SKIN (BUCKLING/PHI) (M,N) =	7.3740E-01	35,	59)
BUCKLING BETWEEN RINGS WITH SMEARD STRINGRS=	6.1802E-02	14,	1)
BUCKLING BETWEEN STRINGRS WITH SMEARD RINGS=	5.0759E+00	147,	59)
BUCKLING/PHI (M) OF STRINGER SEGMENT NO. 1=	4.8150E+00	35)	
LOCAL ROLLING WITH SKIN BUCKLING BETWN STIF=	1.0073E+00	35,	59)
ROLLING OF STRINGERS(M,0), NO SKIN BUCKLING=	6.6879E+00	169,	0)
AXISYMMETRIC ROLLING OF RINGS, NO SKIN BUCK=	1.5702E+02	0,	0)
BUCKLING(ROLLING) MODE WITH SMEARD STRINGRS=	6.1827E-02	14,	1)
BUCKLING(ROLLING) MODE WITH SMEARED RINGS =	5.0978E+00	147,	59)

Table 12 Comparison of Optimum Designs Obtained from PANDA and from the Analysis of Ref. [14] for a Hydrostatically Compressed Ring and Stringer Stiffened Cylindrical Shell

Cylinder radius, R = 60 in.; cylinder length, L = 90 in.; cylinder thickness, t = 0.05;
Axial, circumferential resultants, N_x^o = -1200 lb/in.; N_y^o = -2400 lb/in.;
Young's Modulus, E = 10^7 psi; Poisson's ratio, NU = 0.3; density = 0.10 lb/in^3
Maximum height of stiffeners = 0.025 R;
Maximum height/thickness of stiffeners = 15.0;
Stringers external; rings internal; rings and stringers have rectangular cross sections.

OPTIMUM DESIGN AND BUCKLING LOAD FACTORS AND MODES:	FROM PANDA	FROM REF. [14]
PANEL WEIGHT (180° OF CYLINDER)	2.1738E+02	2.2821E+02
DESIGN VARIABLES FOR ITERATION NUMBER FOLLOW...		
THICKNESS OF PANEL SKIN LAYER NO. 1 =	5.0000E-02	5.0000E-02
STRINGER SPACING, B =	6.1548E-01	7.4000E-01
THICKNESS OF STRINGER SEGMENT NO. 1 =	2.1020E-02	4.6000E-02
WIDTH, BS(I), OF STRINGER SEGMENT 1 =	2.9850E-01	2.4000E-01
RING SPACING, A =	2.2078E+00	2.5000E+00
THICKNESS OF RING SEGMENT NO. 1 =	1.0000E-01	1.1600E-01
WIDTH, BR(I), OF RING SEGMENT 1 =	1.5001E+00	1.5000E+00
(M=AXIAL, N=CIRC.) HALF-WAVES OVER ENTIRE PANEL (AXIAL,CIRC.)		(AXIAL,CIRC.
GENERAL INSTABILITY EIGENVALUE(M,N)=	9.9682E-01(1, 5)	9.8094E-01(12, 8)
LOCAL SKIN (BUCKLING/PHI) (M,N) =	2.7118E+00(40, 306)	1.9298E+00(36, 254)
BUCKLING BETWEEN RINGS WITH SMEARD STRINGRS=	2.1990E+00(40, 186)	1.7535E+00(36, 154)
BUCKLING BETWEEN STRINGRS WITH SMEARD RINGS=	3.9201E+02(1209, 306)	2.9303E+02(1012, 254)
BUCKLING/PHI (M) OF STRINGER SEGMENT NO. 1=	1.4405E+00(40)	1.1292E+01(36)
BUCKLING/PHI (N) OF RING SEGMENT NO. 1 =	1.4442E+01(306)	1.3945E+01(254)
LOCAL ROLLING WITH SKIN BUCKLING BETWN STIF=	9.5930E+00(40, 306)	8.3512E+00(36, 254)
ROLLING OF STRINGERS(M,0), NO SKIN BUCKLING=	4.3647E+00(186, 0)	3.4900E+01(226, 0)
ROLLING OF RINGS (0,N), NO SKIN BUCKLING=	3.0671E+00(0, 76)	4.1577E+00(0, 76)
AXISYMMETRIC ROLLING OF RINGS, NO SKIN BUCK=	7.1292E+01(0, 0)	9.6649E+01(0, 0)
BUCKLING(ROLLING) MODE WITH SMEARD STRINGRS=	2.6909E+00(40, 101)	2.4717E+00(36, 79)
BUCKLING(ROLLING) MODE WITH SMEARED RINGS =	3.6137E+02(1209, 306)	2.8657E+02(911, 254)

Table 13 Comparison of Optimum Designs Obtained from PANDA and from the Analysis of Ref. [33] for an Axially Compressed Ring and Stringer Stiffened Cylindrical Shell

CYLINDER RADIUS, R = 95.5 in.; CYLINDER LENGTH, L = 291 in.;
AXIAL RESULTANT, N_x^o = -800 lb/in.;
YOUNG'S MODULUS, E = 10.5 x 10^6 psi; POISSON'S RATIO, NU = 0.33; DENSITY = 0.101 lb/in^3;
MINIMUM GAGE OF ANY THICKNESS = 0.02 in.
BOTH STRINGERS AND RINGS INTERNAL AND OF RECTANGULAR CROSS SECTION

OPTIMUM DESIGN AND BUCKLING LOAD FACTORS AND MODES:	FROM PANDA	FROM REF. [33]
PANEL WEIGHT (180° OF CYLINDER) =	3.4893E+02	3.7796E+02
DESIGN VARIABLES FOR ITERATION NUMBER 0 FOLLOW...		
THICKNESS OF PANEL SKIN LAYER NO. 1 =	2.1701E-02	2.2105E-02
STRINGER SPACING, B =	8.9191E-01	9.1985E-01
THICKNESS OF STRINGER SEGMENT NO. 1 =	2.6267E-02	3.2620E-02
WIDTH, BS(I), OF STRINGER SEGMENT 1 =	4.5089E-01	4.4210E-01
RING SPACING, A =	9.4767E+00	9.3871E+00
THICKNESS OF RING SEGMENT NO. 1 =	2.0000E-02	2.2720E-02
WIDTH, BR(I), OF RING SEGMENT 1 =	2.1766E+00	2.1000E+00
(M=AXIAL, N=CIRC.) HALF-WAVES OVER ENTIRE PANEL	(AXIAL,CIRC.)	(AXIAL,CIRC.)
GENERAL INSTABILITY EIGENVALUE(M,N)=	9.9691E-01(18, 9)	1.0432E+00(17, 9)[a]
LOCAL SKIN (BUCKLING/PHI) (M,N) =	9.9299E-01(337, 336)	1.0425E+00(309, 326)[a]
BUCKLING BETWEEN RINGS WITH SMEARD STRINGRS=	1.0012E+00(30, 36)	1.1181E+00(30, 36)[a]
BUCKLING BETWEEN STRINGRS WITH SMEARD RINGS=	4.3916E+01(3057, 336)	4.5582E+01(2946, 326)
BUCKLING/PHI (M) OF STRINGER SEGMENT NO. 1=	1.0004E+00(337)	1.6029E+00(309)
LOCAL ROLLING WITH SKIN BUCKLING BETWN STIF=	6.2211E+00(276, 336)	6.2724E+00(247, 326)
ROLLING OF STRINGERS(M,0), NO SKIN BUCKLING=	1.9307E+00(404, 0)	3.3449E+00(404, 0)
AXISYMMETRIC ROLLING OF RINGS, NO SKIN BUCK=	1.0000E+23(0, 0)	1.0000E+23(0, 0)
BUCKLING(ROLLING) MODE WITH SMEARD STRINGRS=	1.0098E+00(30, 36)	1.1271E+00(30, 34)
BUCKLING(ROLLING) MODE WITH SMEARED RINGS =	3.9001E+01(2752, 336)	4.4407E+01(2358, 326)

[a] These loads and modes are predicted by PANDA for the optimum design obtained by the computer analysis described in [33]. The load factors and modes predicted by the Ref. [33] are, respectively, 1.000(18,9), 1.048(-,-), and 1.109(30,36).

Table 14 Comparison of Optimum Designs Obtained from PANDA and from the Analysis of Ref. [63] for a Ring and Stringer Stiffened Cylindrical Shell under Pure Torsion

CYLINDER RADIUS, R = 85.0 in.; CYLINDER LENGTH, L = 100 in.;
SHEAR STRESS RESULTANT, N^{o}_{xy} = 418.5 lb/in.;
YOUNG'S MODULUS, E = 10.5 x 10^{6} psi; POISSON'S RATIO, NU = 0.33; DENSITY = 0.101 lb/in^{3};
MINIMUM GAGE OF ANY THICKNESS = 0.05 in.;
INTERNAL STRINGERS WITH T-SHAPED CROSS SECTION; INTERNAL RINGS WITH RECTANGULAR CROSS SECTION

OPTIMUM DESIGN AND BUCKLING LOAD FACTORS AND MODES:	FROM PANDA	FROM REF. [63]
PANEL WEIGHT (180° OF CYLINDER) =	1.5701E+02	2.0362E+02
DESIGN VARIABLES FOR ITERATION NUMBER 0 FOLLOW...		
THICKNESS OF PANEL SKIN LAYER NO. 1 =	5.0000E-02	5.0480E-02
STRINGER SPACING, B =	2.4993E+01	2.4276E+01
THICKNESS OF STRINGER SEGMENT NO. 1 =	5.0000E-02	5.0314E-02
THICKNESS OF STRINGER SEGMENT NO. 2 =	5.0000E-02	5.8110E-02
WIDTH, BS(I), OF STRINGER SEGMENT 1 =	3.6046E-01	5.2459E+00
WIDTH, BS(I), OF STRINGER SEGMENT 2 =	4.9186E-02	1.3115E+00
RING SPACING, A =	4.2999E+00	3.5714E+00
THICKNESS OF RING SEGMENT NO. 1 =	5.0000E-02	5.5709E-02
WIDTH, BR(I), OF RING SEGMENT 1 =	6.2807E-01	5.0480E-01
(M=AXIAL, N=CIRC.) HALF-WAVES OVER ENTIRE PANEL (AXIAL,CIRC.)		(AXIAL,CIRC.)
GENERAL INSTABILITY EIGENVALUE(M,N)=	9.9992E-01(1, 18)	4.7410E+00(1, 11)[a]
LOCAL SKIN (BUCKLING/PHI) (M,N) =	9.9825E-01(23, 64)	1.4135E+00(28, 65)[a]
BUCKLING BETWEEN RINGS WITH SMEARD STRINGRS=	2.9042E+00(23, 94)	1.5503E+03(28, 919)[a]
BUCKLING BETWEEN STRINGRS WITH SMEARD RINGS=	1.2722E+00(24, 10)	1.1439E+00(24, 10)[b]
BUCKLING/PHI (M) OF STRINGER SEGMENT NO. 1=	9.2125E+06(255)	5.8334E+04(0)
BUCKLING/PHI (M) OF STRINGER SEGMENT NO. 2=	5.2682E+07(255)	1.4622E+05(0)
BUCKLING/PHI (M) OF STRINGER SEGMENT NO. 3=	5.2682E+07(255)	1.4622E+05(0)
ROLLING OF STRINGERS(M,0), NO SKIN BUCKLING=	2.7265E+06(114, 0)	2.7543E+05(1, 0)
AXISYMMETRIC ROLLING OF RINGS, NO SKIN BUCK=	1.0000E+23(0, 0)	1.0000E+23(0, 0)

[a] These loads and modes are predicted by PANDA for the optimum design obtained by the analysis described in [63]. The load factors and modes predicted by the analysis of Ref. [63] are, respectively, 1.0(1,11), 1.267(-,-), and 1332(28,869).
[b] Not included in the analysis of Ref. [63].

Table 15 Comparison of Optimum Designs Obtained from PANDA and from the Analysis of Ref. [61] for a Ring and Stringer-Stiffened Cylindrical Shell under Combined Axial Compression and Torsion

CYLINDER RADIUS, R = 85.0 in.; CYLINDER LENGTH, L = 100 in.;
AXIAL, SHEAR STRESS RESULTANTS, N_x^o = -2700 lb/in.; N_{xy}^o = 418.5 lb/in.;
YOUNG'S MODULUS, E = 10.5 x 10^6 psi; POISSON'S RATIO, NU = 0.33; DENSITY = 0.101 lb/in^3;
MAXIMUM STRESS = 45 ksi; MINIMUM GAGE OF ANY THICKNESS = 0.05 in.;
INTERNAL STRINGERS WITH T-SHAPED CROSS SECTION; INTERNAL RINGS WITH RECTANGULAR CROSS SECTION.

OPTIMUM DESIGN AND BUCKLING LOAD FACTORS AND MODES:	FROM PANDA	FROM REF. [61]
PANEL WEIGHT (180° OF CYLINDER) =	2.2961E+02	2.4301E+02
DESIGN VARIABLES FOR ITERATION NUMBER 0 FOLLOW...		
THICKNESS OF PANEL SKIN LAYER NO. 1 =	5.0000E-02	5.0000E-02
STRINGER SPACING, B =	1.6054E+00	1.6086E+00
THICKNESS OF STRINGER SEGMENT NO. 1 =	5.0000E-02	5.0120E-02
THICKNESS OF STRINGER SEGMENT NO. 2 =	7.3997E-02	5.0120E-02
WIDTH, BS(I), OF STRINGER SEGMENT 1 =	7.1470E-01	6.5738E-01
WIDTH, BS(I), OF STRINGER SEGMENT 2 =	1.9535E-02	9.8605E-02
RING SPACING, A =	1.2284E+01	9.0909E+00
THICKNESS OF RING SEGMENT NO. 1 =	5.0000E-02	5.1630E-02
WIDTH, BR(I), OF RING SEGMENT 1 =	2.7232E+00	2.3750E+00
(M=AXIAL, N=CIRC.) HALF-WAVES OVER ENTIRE PANEL (AXIAL,CIRC.)		(AXIAL,CIRC.)
GENERAL INSTABILITY EIGENVALUE(M,N)=	9.9963E-01(1, 8)	1.0121E+00(1, 8)[a]
LOCAL SKIN (BUCKLING/PHI) (M,N) =	9.9984E-01(65, 166)	1.0285E+00(65, 165)[a]
BUCKLING BETWEEN RINGS WITH SMEARD STRINGRS=	1.0062E+00(8, 26)	2.0912E+00(10, 28)[a]
BUCKLING BETWEEN STRINGRS WITH SMEARD RINGS=	2.5461E+01(436, 166)	2.5254E+01(428, 165)
BUCKLING/PHI (M) OF STRINGER SEGMENT NO. 1=	5.3301E+00(138)	6.5595E+00(142)
BUCKLING/PHI (M) OF STRINGER SEGMENT NO. 2=	1.5940E+03(138)	3.1326E+01(142)
BUCKLING/PHI (M) OF STRINGER SEGMENT NO. 3=	1.5940E+03(138)	3.1326E+01(142)
LOCAL ROLLING WITH SKIN BUCKLING BETWN STIF=	1.1231E+00(56, 166)	1.5011E+00(43, 165)
ROLLING OF STRINGERS(M,0), NO SKIN BUCKLING=	1.5450E+00(84, 0)	3.0057E+00(45, 0)
AXISYMMETRIC ROLLING OF RINGS, NO SKIN BUCK=	1.0000E+23(0, 0)	1.0000E+23(0, 0)
BUCKLING(ROLLING) MODE WITH SMEARD STRINGRS=	1.0170E+00(8, 26)	2.1131E+00(10, 28)
BUCKLING(ROLLING) MODE WITH SMEARED RINGS =	1.3474E+01(393, 166)	2.5362E+01(278, 165)
MARGIN FOR EFFECTIVE STRESS IN LAYER 1 =	1.1795E+00	1.2174E+00
MARGIN FOR COMP. STRAIN IN STRINGER SEG. 1=	1.2642E+00	1.3100E+00
MARGIN FOR COMP. STRAIN IN STRINGER SEG. 2=	1.2642E+00	1.3100E+00
MARGIN FOR COMP. STRAIN IN STRINGER SEG. 3=	1.2642E+00	1.3100E+00

[a]The analysis of Ref. [61] yields, respectively, for these modes: 1.0(1,8), 1.048(-,-), & 20.8(10,30)

Table 16 Comparison of Optimum Designs Obtained from PANDA and from the Analysis of Ref. [61] for the Same Case as Described in Table 15, except that Internal Pressure of 14.7 psi is Present. The internal pressure is treated as a constant prestress (not an eigenparameter to which the load factors shown below apply).

AXIAL, SHEAR STRESS RESULTANTS (EIGENPARAMETERS): N_x^o = -2700 lb/in.; N_{xy}^o = 418.5 lb/in.;
AXIAL, HOOP STRESS RESULTANTS (NOT EIGENPARAMETERS) FROM INTERNAL PRESSURE:
N_{xpre} = +625 lb/in.; N_{ypre} = +1250 lb/in.

OPTIMUM DESIGN AND BUCKLING LOAD FACTORS AND MODES:	FROM PANDA	FROM REF. [61]
PANEL WEIGHT (180° OF CYLINDER) =	1.9349E+02	2.1292E+02
DESIGN VARIABLES FOR ITERATION NUMBER 0 FOLLOW...		
THICKNESS OF PANEL SKIN LAYER NO. 1 =	5.5142E-02	5.0000E-02
STRINGER SPACING, B =	2.7593E+00	1.9281E+00
THICKNESS OF STRINGER SEGMENT NO. 1 =	5.0000E-02	5.0060E-02
THICKNESS OF STRINGER SEGMENT NO. 2 =	5.0000E-02	5.0060E-02
WIDTH, BS(I), OF STRINGER SEGMENT 1 =	6.7642E-01	5.4782E-01
WIDTH, BS(I), OF STRINGER SEGMENT 2 =	1.1372E-01	8.2175E-02
RING SPACING, A =	7.6665E+00	6.2500E+00
THICKNESS OF RING SEGMENT NO. 1 =	5.0000E-02	5.2320E-02
WIDTH, BR(I), OF RING SEGMENT 1 =	3.5431E-02	1.2500E+00
(M=AXIAL, N=CIRC.) HALF-WAVES OVER ENTIRE PANEL (AXIAL,CIRC.)		(AXIAL,CIRC.)
GENERAL INSTABILITY EIGENVALUE(M,N)=	1.0004E+00(1, 13)	1.0101E+00(1, 10)
LOCAL SKIN (BUCKLING/PHI) (M,N) =	1.0087E+00(52, 96)	1.2304E+00(80, 138)
BUCKLING BETWEEN RINGS WITH SMEARD STRINGRS=	2.7087E+00(13, 20)	2.7341E+00(16, 25)
BUCKLING BETWEEN STRINGRS WITH SMEARD RINGS=	1.0014E+00(59, 96)	7.8836E+00(245, 138)
BUCKLING/PHI (M) OF STRINGER SEGMENT NO. 1=	5.7329E+00(143)	8.5091E+00(176)
BUCKLING/PHI (M) OF STRINGER SEGMENT NO. 2=	2.1858E+01(143)	4.0243E+01(176)
BUCKLING/PHI (M) OF STRINGER SEGMENT NO. 3=	2.1858E+01(143)	4.0243E+01(176)
LOCAL ROLLING WITH SKIN BUCKLING BETWN STIF=	1.0013E+00(52, 96)	1.3691E+00(64, 138)
ROLLING OF STRINGERS(M,0), NO SKIN BUCKLING=	2.9343E+00(40, 0)	3.4762E+00(56, 0)
AXISYMMETRIC ROLLING OF RINGS, NO SKIN BUCK=	1.0000E+23(0, 0)	1.0000E+23(0, 0)
BUCKLING(ROLLING) MODE WITH SMEARD STRINGRS=	2.7087E+00(13, 20)	2.7434E+00(16, 25)
BUCKLING(ROLLING) MODE WITH SMEARED RINGS =	1.0074E+00(53, 96)	7.7418E+00(221, 138)
MARGIN FOR EFFECTIVE STRESS IN LAYER 1 =	1.0022E+00	1.0306E+00
MARGIN FOR COMP. STRAIN IN STRINGER SEG. 1=	1.3051E+00	1.3029E+00
MARGIN FOR COMP. STRAIN IN STRINGER SEG. 2=	1.3051E+00	1.3029E+00
MARGIN FOR COMP. STRAIN IN STRINGER SEG. 3=	1.3051E+00	1.3029E+00
MARGIN FOR TENSILE STRAIN IN RING SEG. 1=	1.4350E+00	1.5931E+00

Table 17 Comparison of Optimum Designs Obtained from PANDA and from the Analysis of Ref. [6] for a Waffle-Stiffened Plate under Combined Axial Compression, Lateral Compression, and Shear.

PANEL AXIAL LENGTH, a = 40 in.; PANEL WIDTH, b = 30 in.;
STRESS RESULTANTS, N_x^o = -300 lb/in.; N_y^o = -400 lb/in.; N_{xy}^o = 200 lb/in.;
YOUNG'S MODULUS, E = 10.5 x 10^6 psi; POISSON'S RATIO, NU = 0.32; DENSITY = 0.101 lb/in^3;
MAXIMUM HEIGHT OF STIFFENERS = 0.8 in.; MINIMUM SPACING OF STIFFENERS = 2.0 in.;
HEIGHT OF "STRINGERS" EQUALS HEIGHT OF "RINGS"; "STRINGERS" AND "RINGS" ON THE SAME SIDE OF THE SHEET AND HAVE RECTANGULAR CROSS SECTIONS.

OPTIMUM DESIGN AND BUCKLING LOAD FACTORS AND MODES:	FROM PANDA	FROM REF. [6]
PANEL WEIGHT (180° OF CYLINDER) =	8.9324E+00	9.6049E+00
DESIGN VARIABLES FOR ITERATION NUMBER 0 FOLLOW...		
THICKNESS OF PANEL SKIN LAYER NO. 1 =	3.9257E-02	3.5500E-02
STRINGER SPACING, B =	2.0000E+00	2.0000E+00
THICKNESS OF STRINGER SEGMENT NO. 1 =	2.2549E-02	2.6000E-02
WIDTH, BS(I), OF STRINGER SEGMENT 1 =	8.0000E-01	7.4720E-01
RING SPACING, A =	2.0000E+00	2.0000E+00
THICKNESS OF RING SEGMENT NO. 1 =	6.3558E-02	9.1100E-02
WIDTH, BR(I), OF RING SEGMENT 1 =	8.0000E-01	7.4720E-01
(M=AXIAL, N=CIRC.) HALF-WAVES OVER ENTIRE PANEL	(AXIAL,CIRC.)	(AXIAL,CIRC.)
GENERAL INSTABILITY EIGENVALUE(M,N)=	1.0011E+00(1, 1)	1.0429E+00(1, 1)[a]
LOCAL SKIN (BUCKLING/PHI) (M,N) =	1.0018E+00(20, 15)	7.8969E-01(20, 15)[a]
BUCKLING BETWEEN RINGS WITH SMEARD STRINGRS=	1.9789E+01(20, 65)	1.8459E+01(20, 65)
BUCKLING BETWEEN STRINGRS WITH SMEARD RINGS=	3.5881E+01(103, 15)	3.6672E+01(127, 15)
BUCKLING/PHI (M) OF STRINGER SEGMENT NO. 1=	1.0004E+00(20)	1.3147E+00(20)[a]
BUCKLING/PHI (N) OF RING SEGMENT NO. 1 =	7.1739E+00(15)	1.7406E+01(15)[a]
LOCAL ROLLING WITH SKIN BUCKLING BETWN STIF=	1.5265E+00(20, 15)	2.1342E+00(20, 15)
ROLLING OF STRINGERS(M,0), NO SKIN BUCKLING=	2.3102E+00(29, 0)	3.1445E+00(32, 0)
ROLLING OF RINGS (0,N), NO SKIN BUCKLING=	1.6558E+01(0, 23)	4.1722E+01(0, 23)
AXISYMMETRIC ROLLING OF RINGS, NO SKIN BUCK=	1.0000E+23(0, 0)	1.0000E+23(0, 0)
BUCKLING(ROLLING) MODE WITH SMEARD STRINGRS=	2.2416E+01(20, 54)	2.8992E+01(20, 45)
BUCKLING(ROLLING) MODE WITH SMEARED RINGS =	3.3959E+01(103, 15)	3.4848E+01(115, 15)

[a] These loads and modes are predicted by PANDA for the optimum design obtained in Ref. [6]. The load factors predicted by the analysis of Ref. [6] are, respectively, 1.0, 1.0, 1.013, and 14.1.

Table 18 Comparison of Optimum Designs Obtained from PANDA and from the Analysis of Ref. [47] for a Hydrostatically-Compressed Ring-Stiffened Cylindrical Shell (T-Shaped Rings).

CYLINDER RADIUS, R = 198 in.; CYLINDER LENGTH, L = 594 in.;
AXIAL, CIRCUMFERENTIAL STRESS RESULTANTS, N_x^o = -88900 lb/in.; N_y^o = -177800 lb/in.; (p_o = 898 psi)
YOUNG'S MODULUS, E = 30 x 10^6 psi; POISSON'S RATIO, NU = 0.33; DENSITY = 0.282 lb/in^3;
MAXIMUM STRESS = 180000 psi.

OPTIMUM DESIGN AND BUCKLING LOAD FACTORS AND MODES:	FROM PANDA	FROM REF. [47]
PANEL WEIGHT (180° OF CYLINDER) =	1.3878E+05	1.3796E+05
DESIGN VARIABLES FOR ITERATION NUMBER 0 FOLLOW...		
THICKNESS OF PANEL SKIN LAYER NO. 1 =	1.0032E+00	7.0870E-01
RING SPACING, A =	2.0480E+01	1.2638E+01
THICKNESS OF RING SEGMENT NO. 1 =	3.8197E-01	4.9840E-01
THICKNESS OF RING SEGMENT NO. 2 =	3.1177E-01	4.9840E-01
WIDTH, BR(I), OF RING SEGMENT 1 =	1.2034E+01	9.3258E+00
WIDTH, BR(I), OF RING SEGMENT 2 =	3.4259E+00	3.1400E+00
(M=AXIAL, N=CIRC.) HALF-WAVES OVER ENTIRE PANEL	(AXIAL,CIRC.)	(AXIAL,CIRC.)
GENERAL INSTABILITY EIGENVALUE(M,N)=	9.9982E-01(1, 3)	5.3866E-01(28, 5)[a]
LOCAL SKIN (BUCKLING/PHI) (M,N) =	1.0000E+00(29, 17)	7.9293E-01(47, 1)
BUCKLING/PHI (N) OF RING SEGMENT NO. 1 =	9.9914E-01(51)	2.7570E+00(66)
BUCKLING/PHI (N) OF RING SEGMENT NO. 2 =	1.0027E+00(51)	3.1656E+00(66)
BUCKLING/PHI (N) OF RING SEGMENT NO. 3 =	1.0027E+00(51)	3.1656E+00(66)
LOCAL ROLLING WITH SKIN BUCKLING BETWN STIF=	1.0019E+00(29, 9)	7.6497E-01(47, 6)
ROLLING OF RINGS (0,N), NO SKIN BUCKLING=	1.5167E+00(0, 4)	2.8512E+00(0, 7)
AXISYMMETRIC ROLLING OF RINGS, NO SKIN BUCK=	1.7691E+00(0, 0)	4.2475E+00(0, 0)
MARGIN FOR EFFECTIVE STRESS IN LAYER 1 =	1.4338E+00	1.2781E+00
MARGIN FOR COMP. STRAIN IN RING SEG. 1=	1.6789E+00	1.6223E+00
MARGIN FOR COMP. STRAIN IN RING SEG. 2=	1.6789E+00	1.6223E+00
MARGIN FOR COMP. STRAIN IN RING SEG. 3=	1.6789E+00	1.6223E+00

[a] The load factor and mode from the analysis of Ref. [47] are 1.0(27,5).

Table 19 Comparison of Optimum Designs Obtained from PANDA and from the Analysis of Ref. [44] for Elastic-Plastic Hydrostatically-Compressed Cylindrical Shell with Rings of Rectangular Cross Section.

CYLINDER RADIUS, R = 44.625 in.; CYLINDER LENGTH, L = 172 in.;
AXIAL, CIRCUMFERENTIAL STRESS RESULTANTS, N_x^o = -90720 lb/in.; N_y^o = -181440 lb/in.; (p_o=4066 psi)
YOUNG'S MODULUS, E = 18 x 10^6 psi; POISSON'S RATIO, NU = 0.3; DENSITY = 0.16 lb/in^3;
STRESS-STRAIN CURVE: STRESS (ksi): 0.,70.,80.,90.,96.,100.,103.5,107.,115.,118.,124.,125.
STRAIN (%): 0.,0.38889,0.46,0.54,0.6,0.65,0.7,0.78,0.9,1.2,1.8,2.2
RINGS INTERNAL AND OF RECTANGULAR CROSS SECTION.

OPTIMUM DESIGN AND BUCKLING LOAD FACTORS AND MODES:	FROM PANDA	FROM REF. [44]
PANEL WEIGHT (180° OF CYLINDER) =	6.5005E+03	6.5065E+03
DESIGN VARIABLES FOR ITERATION NUMBER 0 FOLLOW...		
THICKNESS OF PANEL SKIN LAYER NO. 1 =	1.2617E+00	1.2880E+00
RING SPACING, A =	1.7200E+01	1.2290E+01
THICKNESS OF RING SEGMENT NO. 1 =	9.0375E-01	8.8200E-01
WIDTH, BR(I), OF RING SEGMENT 1 =	8.0539E+00	5.5520E+00
(M=AXIAL, N=CIRC.) HALF-WAVES OVER ENTIRE PANEL	(AXIAL,CIRC.)	(AXIAL,CIRC.)
GENERAL INSTABILITY EIGENVALUE(M,N)=	1.0029E+00(1, 2)	7.3273E-01(1, 2)[b]
LOCAL SKIN (BUCKLING/PHI) (M,N) =	1.1802E+00(10, 9)[a]	2.5964E+00(13, 8)[c]
BUCKLING/PHI (N) OF RING SEGMENT NO. 1 =	1.2471E+00(9)	1.9067E+00(8)[d]
LOCAL ROLLING WITH SKIN BUCKLING BETWN STIF=	1.1841E+00(10, 8)	2.5480E+00(13, 8)
ROLLING OF RINGS (0,N), NO SKIN BUCKLING=	2.5336E+00(0, 10)	4.5300E+00(0, 16)
AXISYMMETRIC ROLLING OF RINGS, NO SKIN BUCK=	7.0305E+00(0, 0)	1.9126E+01(0, 0)

[a,b,c,d] Because the material is stressed beyond its proportional limit at the applied loads N_x^o and N_y^o given above, the load factors times this load do not give the actual buckling load predicted by PANDA. The critical pressures for (a,b,c,d) are, respectively, 4257, 3648, 4862, and 4885 psi. The axial and circumferential resultants corresponding to these pressures yield, respectively, load factors (a,b,c,d) equal to unity.

Table 20 Optimum Designs of Hydrostatically-Compressed, Ring-Stiffened Cylinders Derived by PANDA. Radius to Shell Middle Surface = 44.625 in.; Length = 172 in.; Material Properties are Given in Table 19; T-Shaped Internal Rings.

Pressure P_o (psi)	Weight (lbs)	Thickness of Shell (inches)	Ring Spacing (inches)	WEB		FLANGE	
				Thickness (inches)	Height (inches)	Thickness (inches)	Height (inches)
677	2898	0.289	5.93	0.112	3.44	0.077	1.65
1355	4951	0.493	9.05	0.202	5.03	0.131	2.51
2032	6835	0.688	11.47	0.276	6.21	0.177	3.17
2710	8662	0.807	11.47	0.351	6.95	0.262	4.51
2710*	8724	0.822	11.47	0.346	6.85	0.261	4.46
3388	10694	0.998	13.23	0.460	7.82	0.310	4.97
4066	12682	1.244	15.65	0.560	7.96	0.377	4.75
4743	14667	1.519	19.11	0.651	8.42	0.394	4.60

* Model in which the shell wall is treated as if it consists of five identical layers, in order to account for the variation of midbay prebuckling axial strain through the wall thickness.

Table 21 Buckling Pressure Factors and Modes for Various Types of Instability Predicted by PANDA

Design Pressure, p_o (psi)	General Instability	Local Skin Buckling	Buckling of Web	Buckling of Flange	Rolling with Skin Buckling	Rolling, No Skin Buckling	Axisymmetric Rolling
677	1.0011(1,2)[a]	1.0003(1,16)	1.0(40)	1.0(40)	1.0(1,10)	1.11(4)	1.21(0)
1355	1.0(1,2)	1.0(1,13)	1.0(29)	1.0(29)	1.0(1,9)	1.05(3)	1.10(0)
2032	1.0(1,2)	1.0(1,12)	1.0(24)	1.0(24)	1.0(1,8)	1.01(2)	1.03(0)
2710	1.0(1,2)	1.0(1,11)	1.0(22)	1.0(22)	1.01(1,6)	1.00(1)	1.00(0)
2710[b]	1.0(1,2)	1.0(1,10)	1.0(22)	1.0(22)	0.999(1,5)	1.01(2)	1.02(0)
3388	1.02(1,2)	1.03(1,10)	1.06(19)	1.04(19)	1.03(1,6)	1.03(2)	1.04(0)
4066	1.0(1,2)	1.07(1,9)	1.10(19)	1.11(19)	1.06(1,7)	1.07(2)	1.08(0)
4743	1.0(1,2)	1.07(1,8)			1.06(1,7)	1.07(3)	1.08(0)

[a] Numbers in parentheses are (axial, circumferential) waves in buckling pattern (axial halfwaves, circ. full waves). For local skin buckling and rolling with skin buckling the axial half-wave-index refers to the number of half-waves between adjacent rings. Where only one number is given, it refers to the number of full circumferential waves.

[b] 5-layered model.

Table 22 Effect on Local Shell Instability of Treatment in PANDA of Shell as if It Had Five Layers

Design Pressure, p_o (psi)	LOCAL INSTABILITY PRESSURE MULTIPLIER		
	PANDA Results		
	One-Layered Shell	Five-Layered Shell	BOSOR5 Result
677	1.0	0.975	0.945
1355	1.0	0.966	0.959
2033	1.0	0.961	0.965
2710	1.0	0.971	0.960
3388	1.02	0.989	0.980
4066	1.06	1.017	1.021
4743	1.06	1.027	1.032

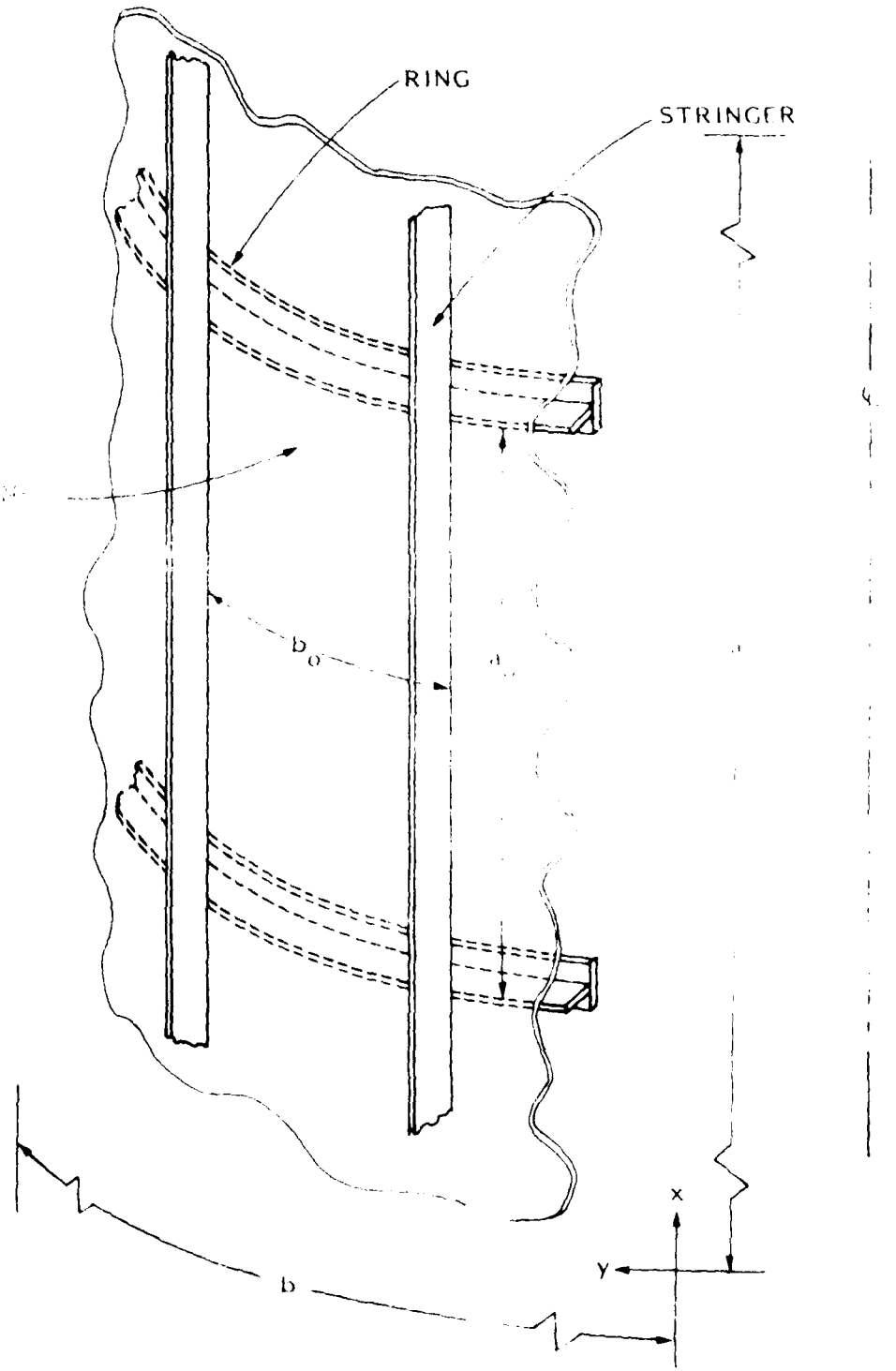

Figure 1. Stiffened cylindrical panel with overall dimensions (a,b), ring spacing (a_o), and stringer spacing (b_o)

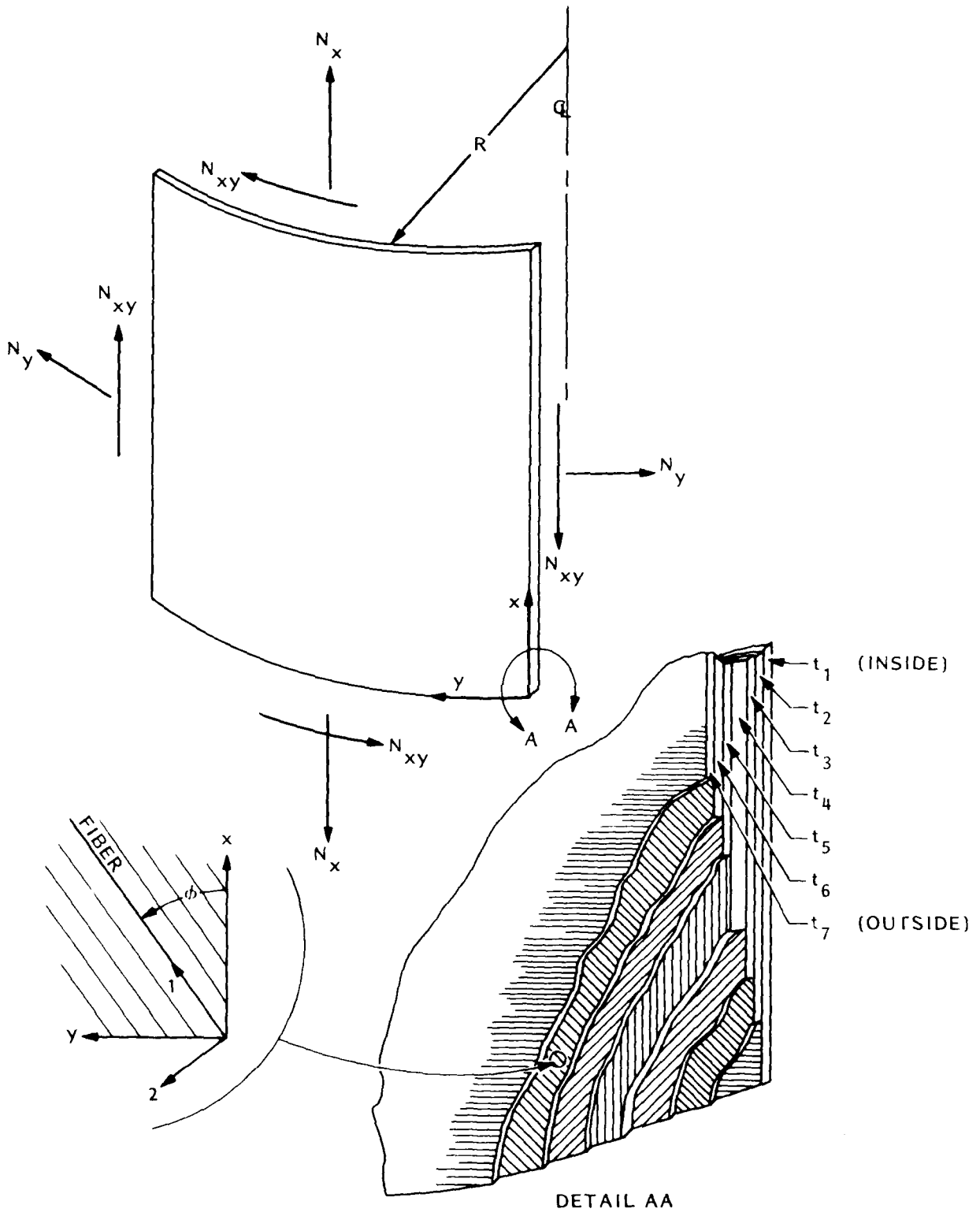

Figure 2. Coordinates, loading, and wall construction

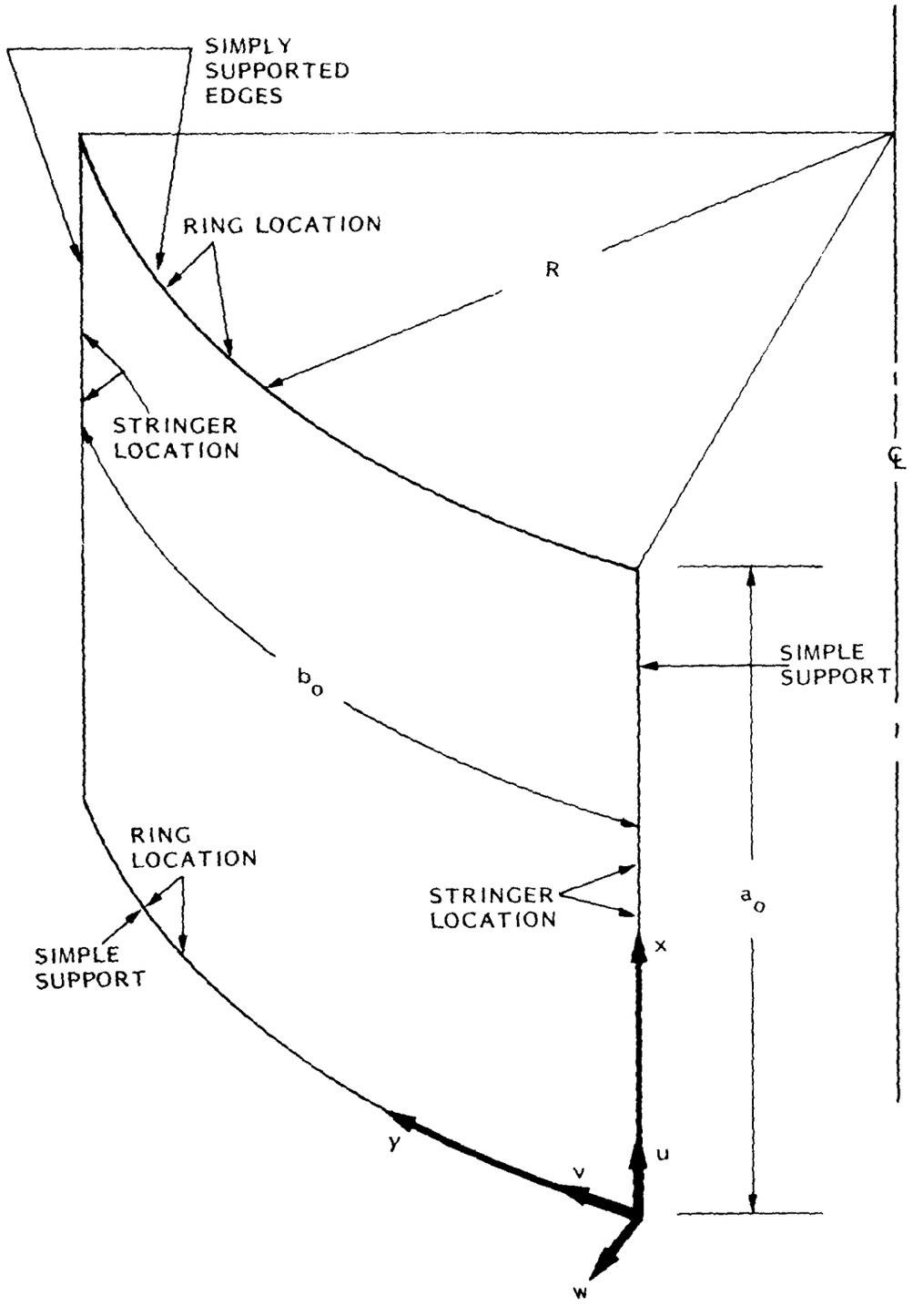

Figure 3. Cylindrical panel between stiffeners: displacement components u, v, w, and coordinates for local skin buckling

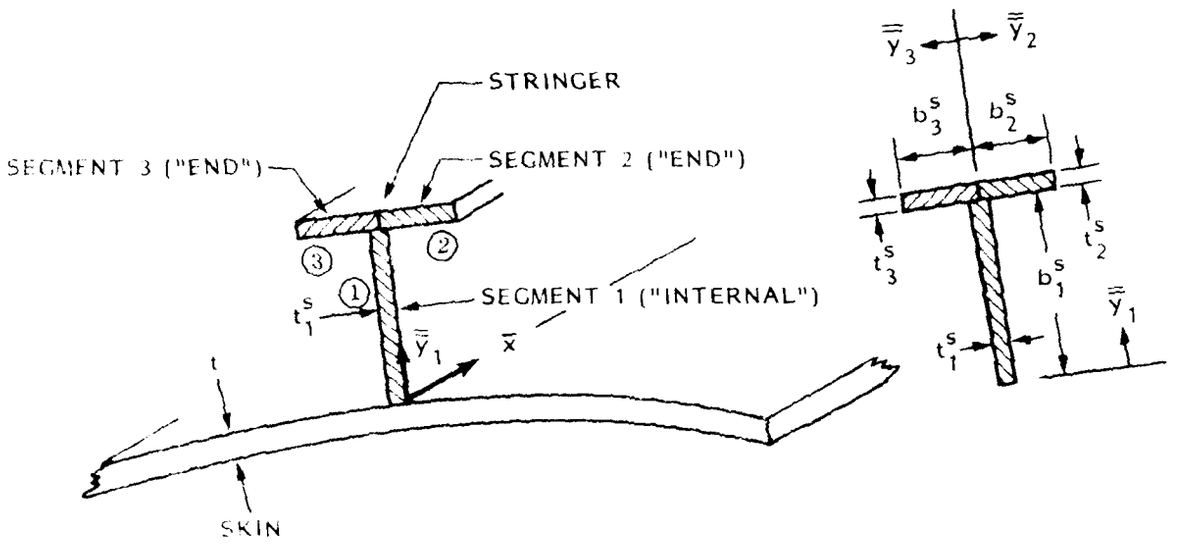

(a) A "T" shaped stiffener must be treated as if it consists of three segments, one "internal" and two "ends".

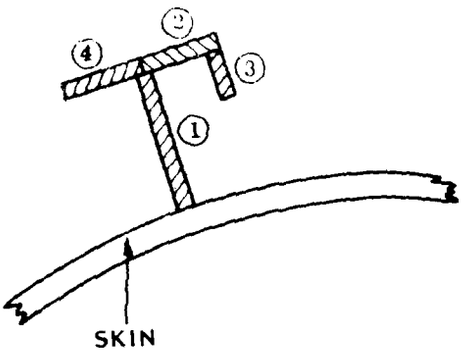

(b) Segments (1) and (2) are "internal"; (3) and (4) are "ends".

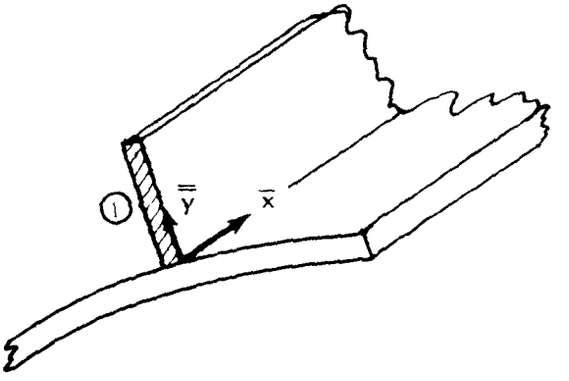

(c) Segment (1) is an "end".

Figure 4. Stiffener nomenclature and local coordinates $\bar{x}$ and $\bar{\bar{y}}_i$

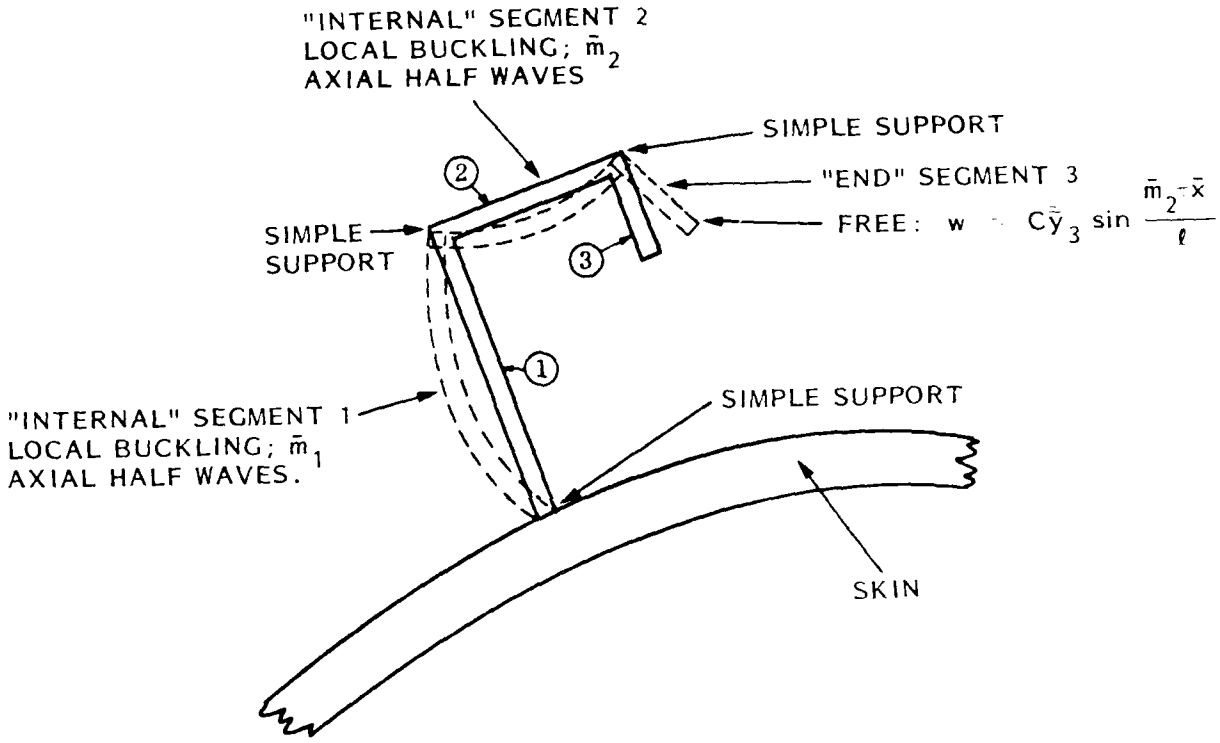

EACH "INTERNAL" STIFFENER SEGMENT IS ASSUMED TO BE SIMPLY-SUPPORTED AT ITS EDGES. THE "END" SEGMENT REMAINS STRAIGHT IN THE WIDTH COORDINATE AS SEGMENTS 2 AND 3 BUCKLE TOGETHER WITH THE SAME $\bar{m} = \bar{m}_2$.

Figure 5. Local buckling of stiffener segments

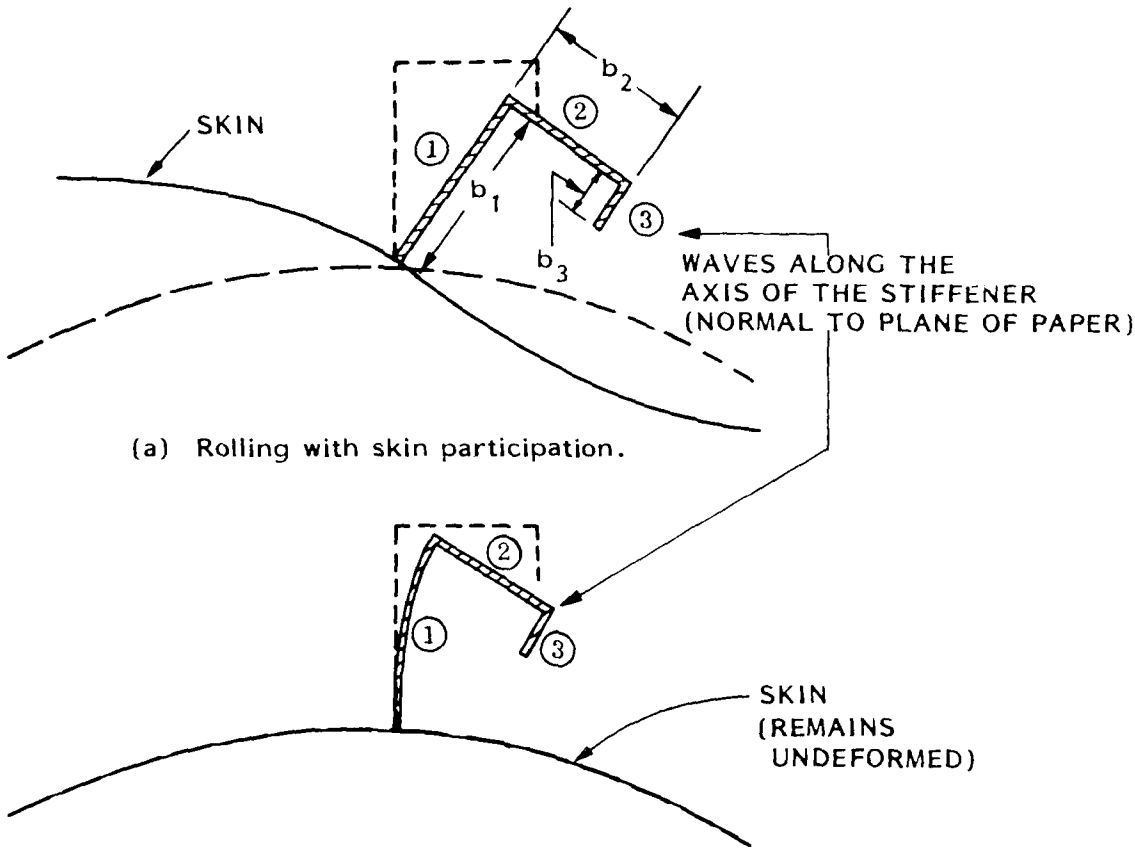

(a) Rolling with skin participation.

(b) No skin participation, wavy buckles.

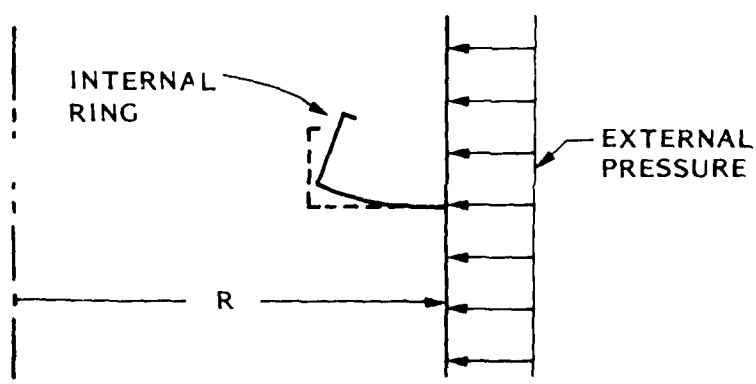

(c) No skin participation; axisymmetric sidesway.

Figure 6. Three types of "rolling" of a stiffener

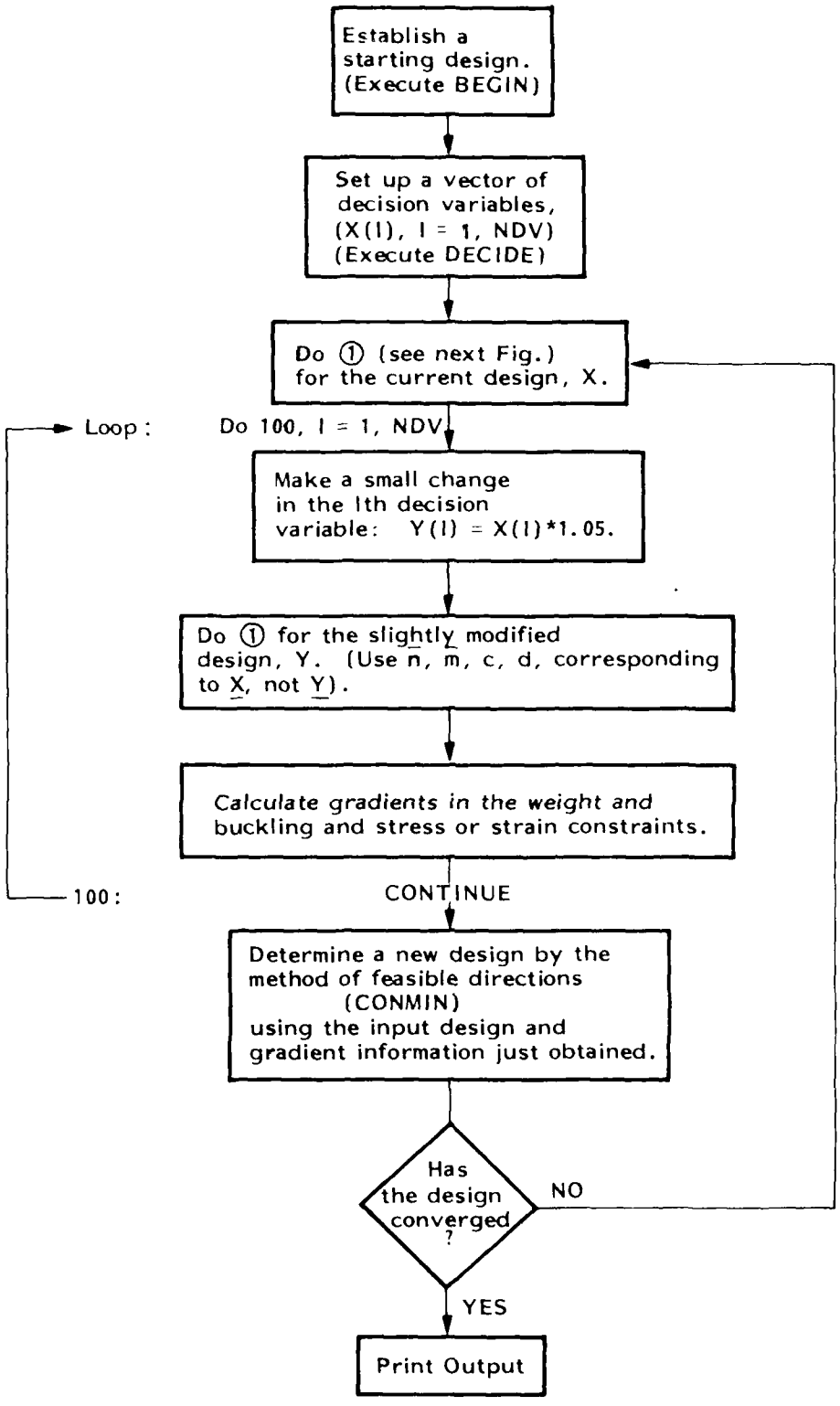

Figure 7. Flow of calculations in PANDA for an optimization analysis.

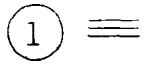

1. Calculate prebuckling state, Eqs. (4-41),

2. Calculate constitutive coefficients governing stability for all possible modes of buckling, Eqs. (37-45).

3. Calculate buckling load factors for all possible modes of buckling, Eqs. (46-123):

   (1) shell general, semi-general, and local, Eqs. (46-65).

   (2) stiffener segment crippling, Eqs. (66-80).

   (3) rolling with skin participation, Eqs. (81-97).

   (4) stiffener rolling without skin participation, Eqs. (98-123).

4. Set up a vector of constraint conditions which include:

   (1) buckling margins for all possible modes of buckling.

   (2) stress or strain margins in each shell wall layer and and in each stiffener segment.

5. Calculate weight.

Figure 8. The structural analysis module of PANDA. This module is embedded in the executable processor PANCON.

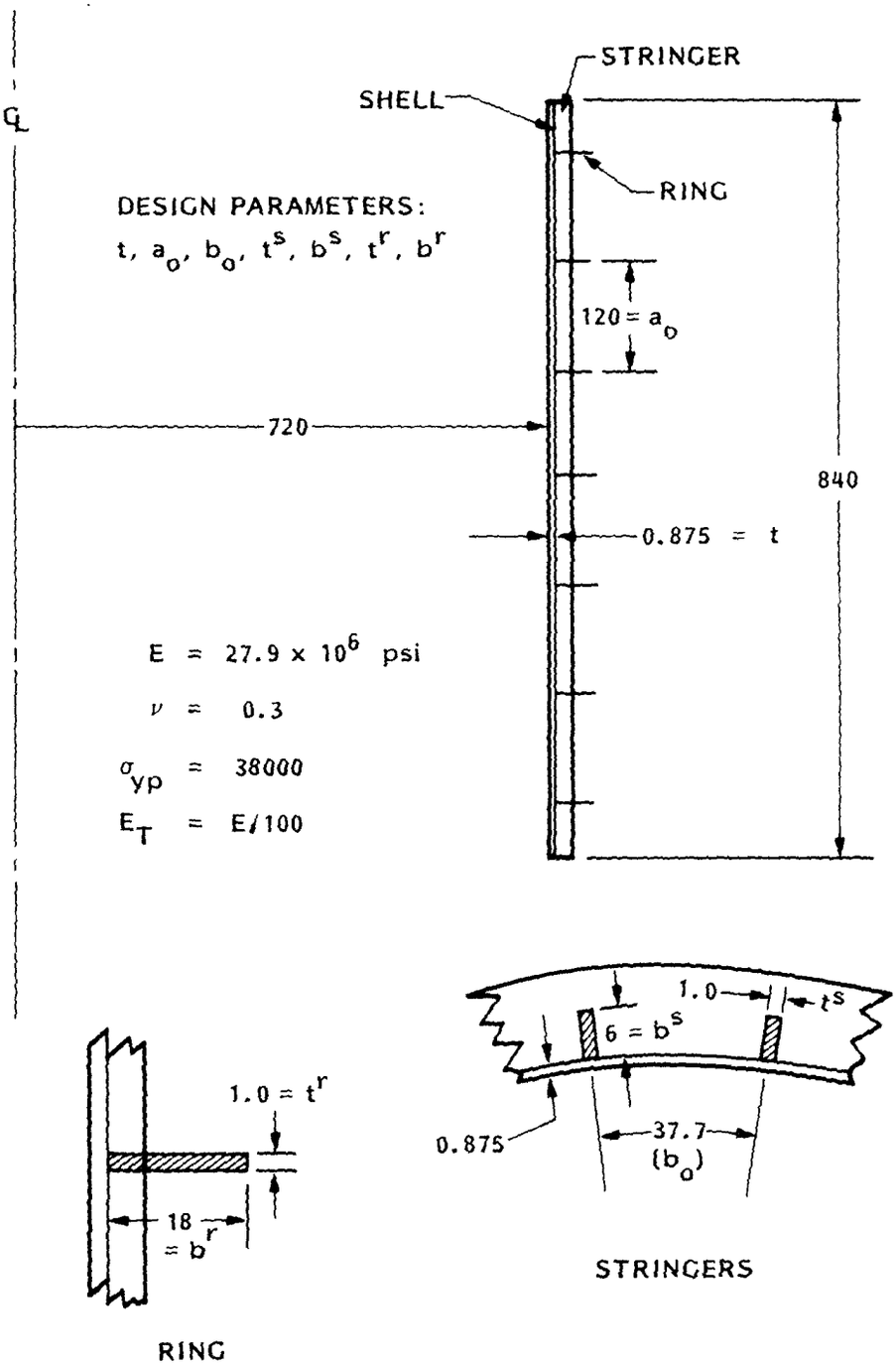

Figure 9. Ring and stringer stiffened cylindrical shell with dimensions typical of a large containment vessel for a nuclear reactor. Buckling load factors from PANDA are listed in Tables 10 and 11.

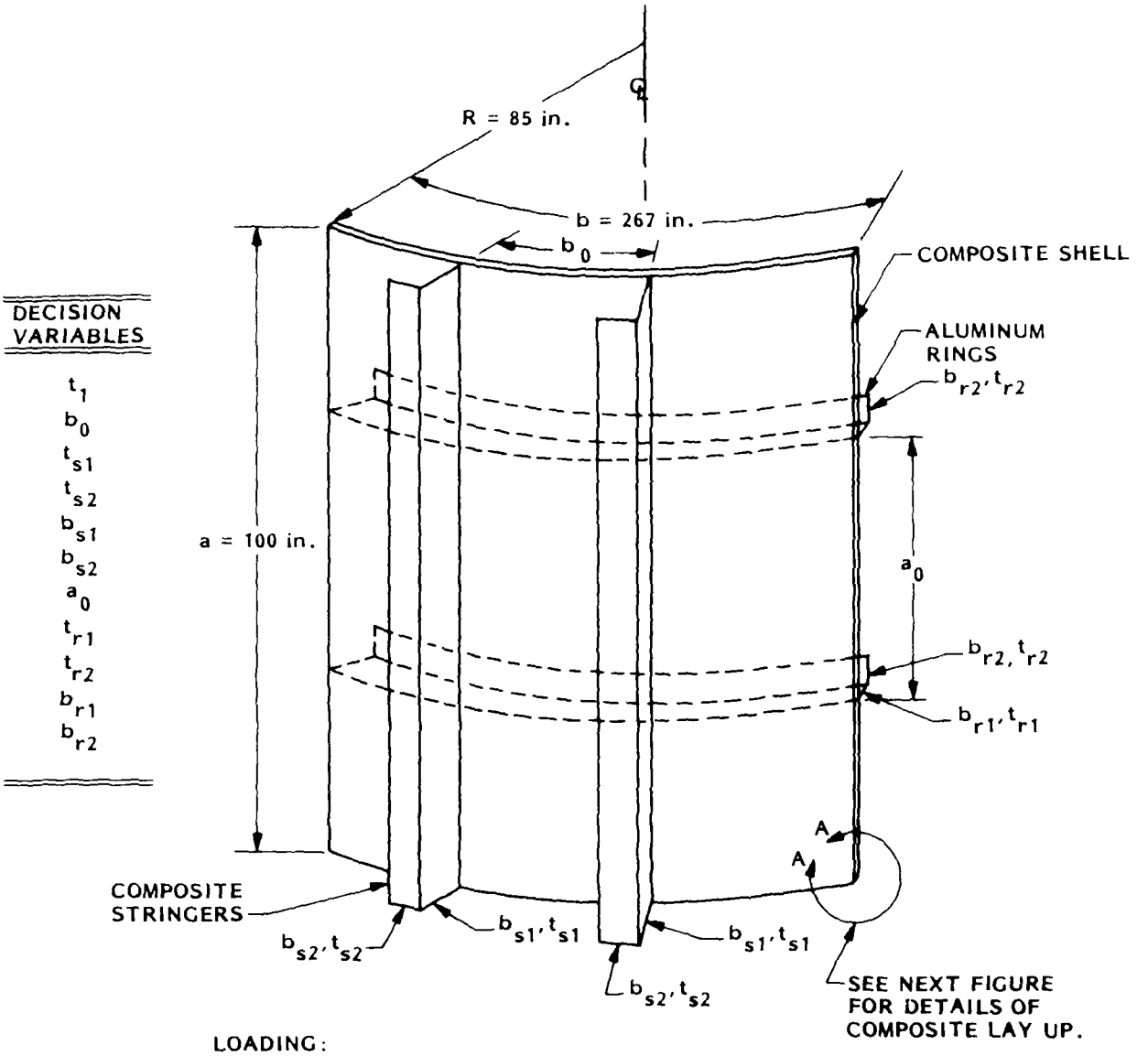

LOADING:

(a) EIGENVALUE PARAMETERS:	(b) FIXED PRELOAD:
N_x^o = -2700 lb/in.	N_{xfixed} = 625 lb/in.
N_y^o = 0 lb.in.	N_{yfixed} = 1250 lb/in.
N_{xy}^o = 420 lb/in.	

Figure 10. Composite cylindrical shell (180 deg.) with dimensions and loading typical of the fuselage of an air transport. Results from PANDA for this case are listed in the appendix.

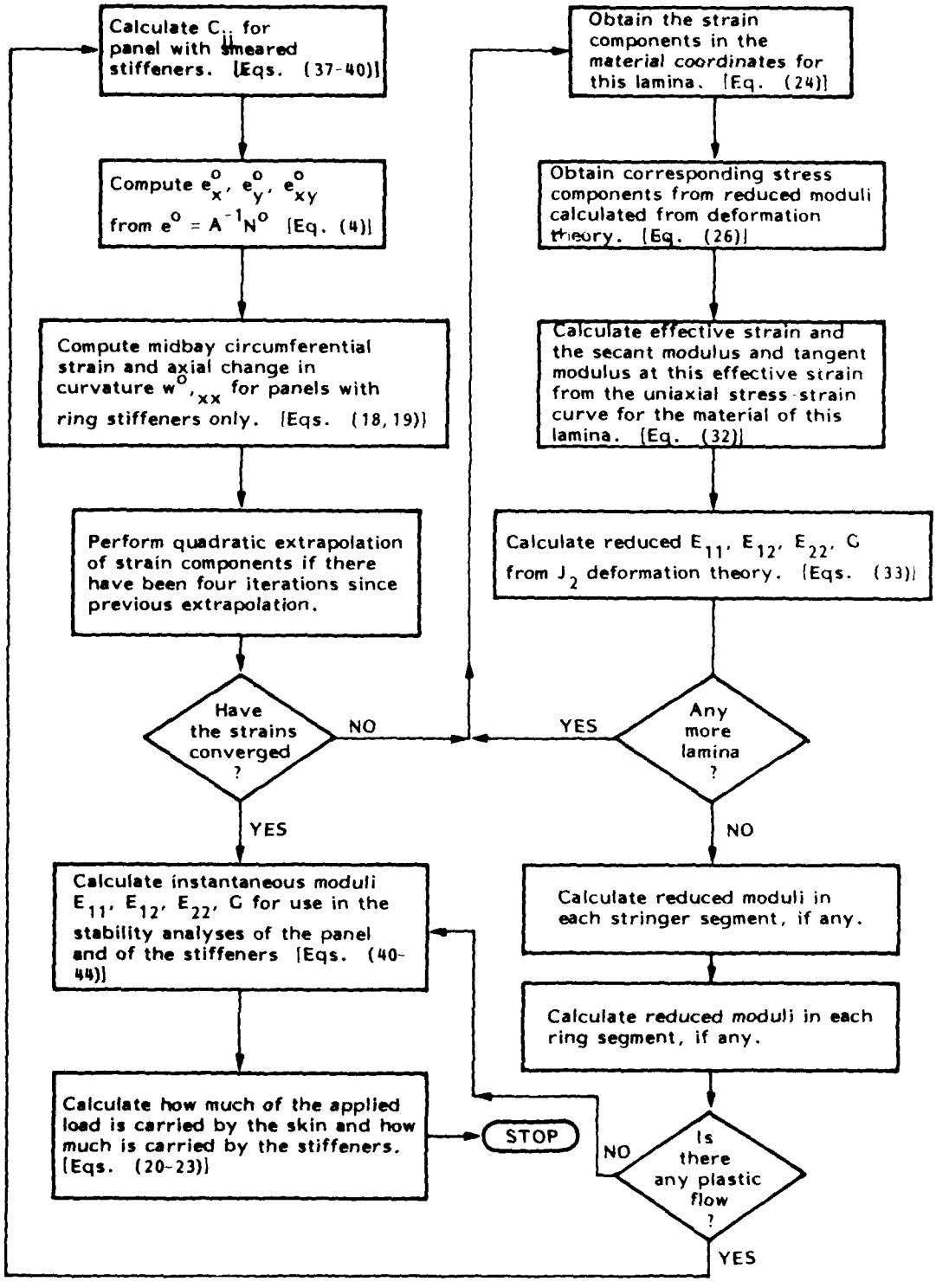

Figure 12. Flow of calculations for elastic-plastic prebuckling analysis in PANDA

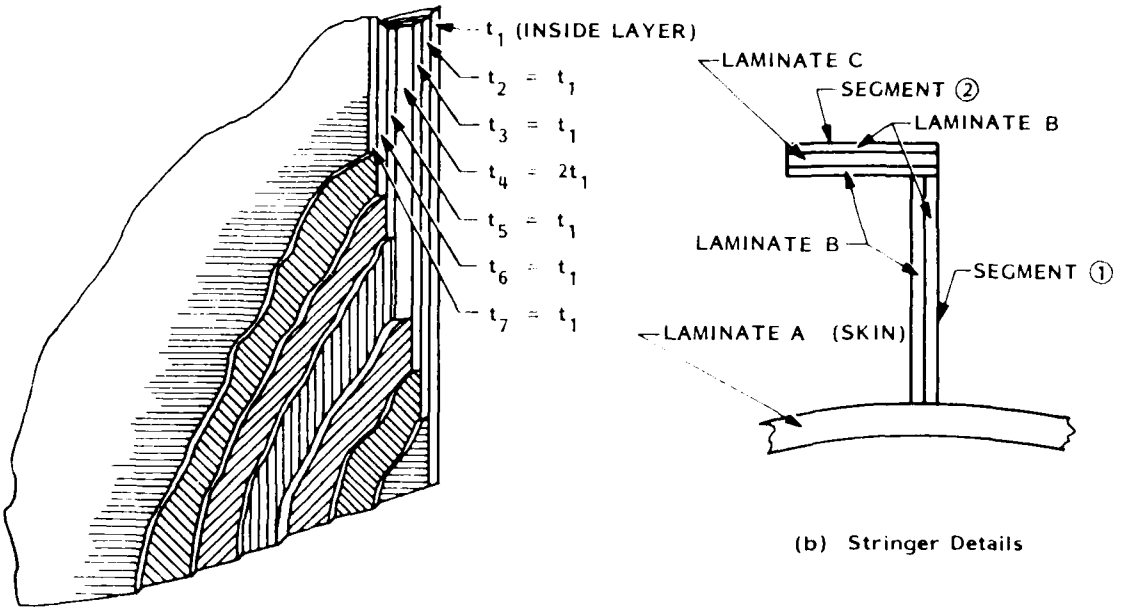

(a) Detail AA
(Panel Skin = Laminate A)

(b) Stringer Details

STACKING SEQUENCE OF THE PANEL SKIN (LAMINATE A):

$$\phi = (90, \pm 45, 0_2, \mp 45, 90)$$

STACKING SEQUENCE OF LAMINATE B OF STRINGER:

$$\phi = (90, \pm 45, 0)_s$$

STACKING SEQUENCE OF LAMINATE C OF STRINGER

$$\phi = (0_{20})$$

MATERIAL PROPERTIES OF EACH LAMINA OF THE LAMINATES A, B, AND C:

MODULI AND POISSON'S RATIO IN (1,2) DIRECTIONS:		MAXIMUM STRAINS IN (1,2) DIRECTIONS:	
E_1	$= 23 \times 10^6$ psi	e_1 (TENSION)	.00565
E_2	$= 1.7 \times 10^6$ psi	e_1 (COMPRESSION)	.00452
G	$= 0.94 \times 10^6$ psi	e_2 (TENSION)	.0032
ν	$= 0.304$	e_2 (COMPRESSION)	.0125
ρ	$= 0.056$ lb/in.^{3}	e_{12} (IN PLANE SHEAR)	.0125

Figure 11. Wall construction and material properties for the stiffened cylindrical shell shown in Fig. 10

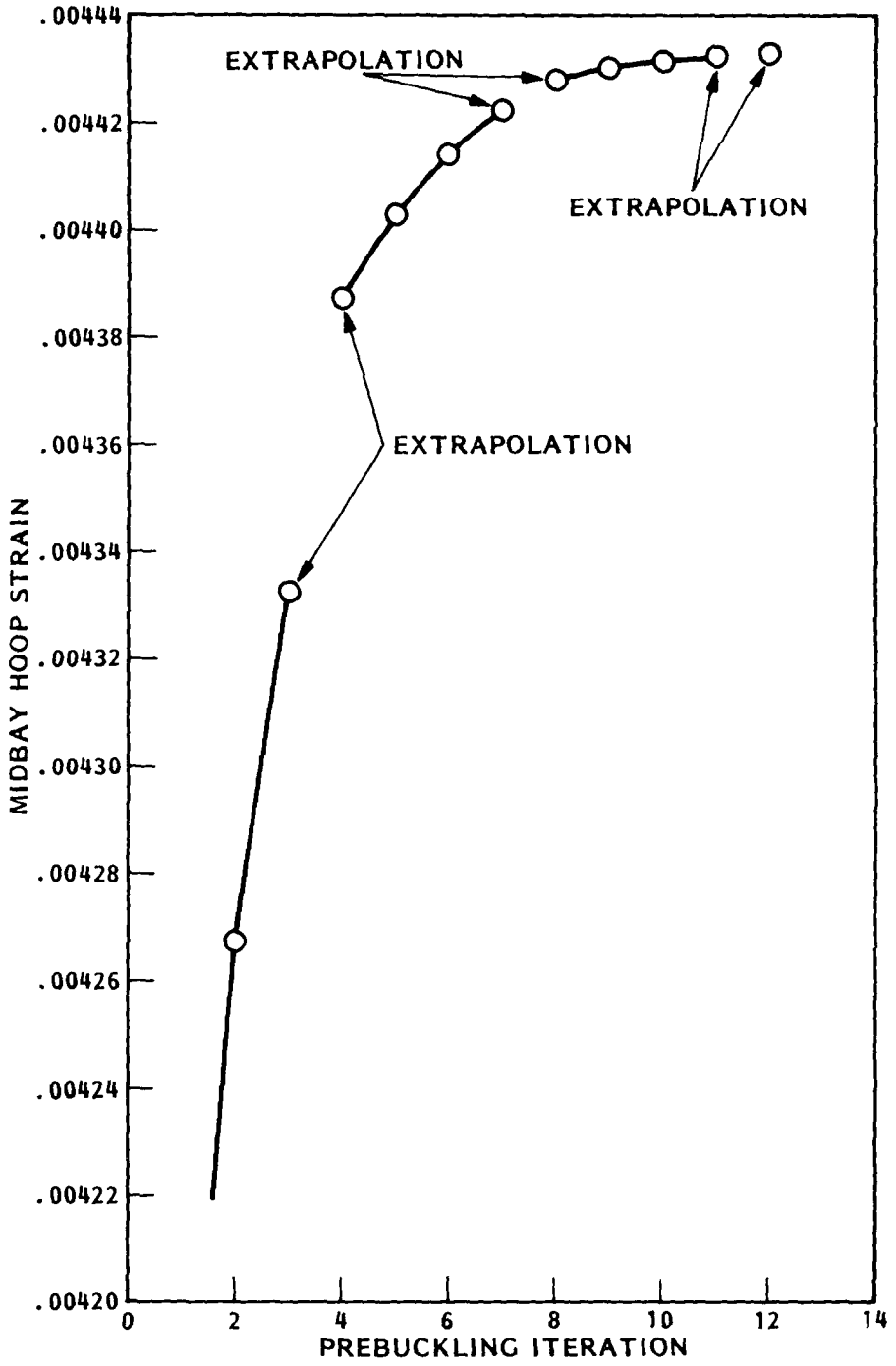

Figure 13. Typical convergence of the prebuckling strain in the plastic region. This case corresponds to a hydrostatically compressed, ring stiffened cylindrical shell.

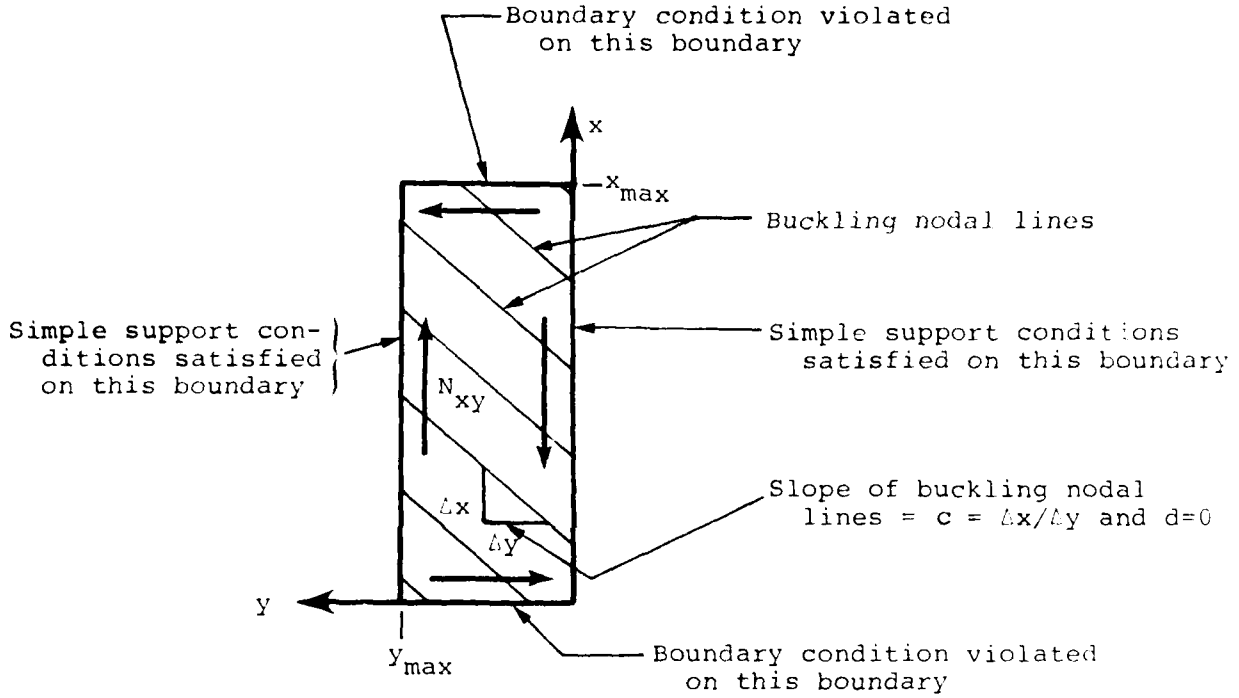

(a) Assumed buckling mode for panel that is "long" in the x-direction: $w = C \sin(ny)\sin[m(x-cy)]$

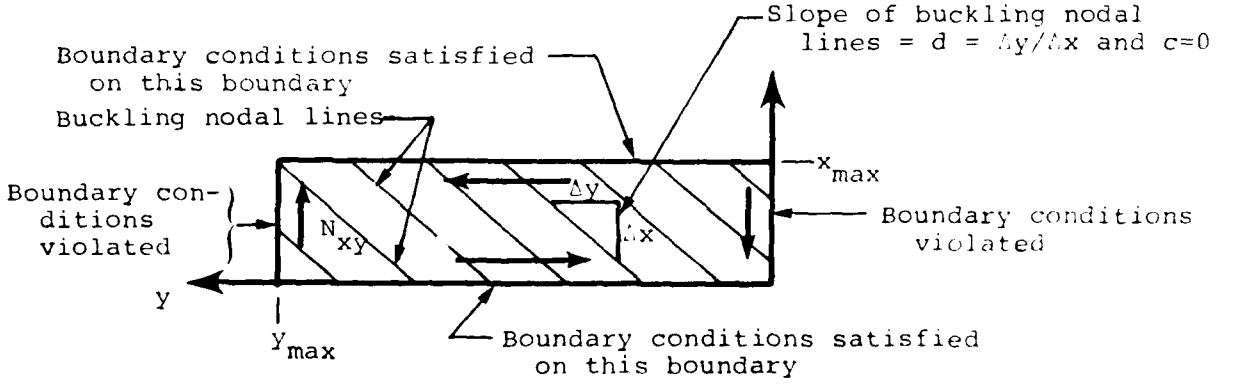

(b) Assumed buckling mode for panel that is "long" in the y-direction: $w = \sin[n(y-dx)]\sin(mx)$

Figure 14. Assumed buckling modal patterns with shear and/or unbalanced laminates present

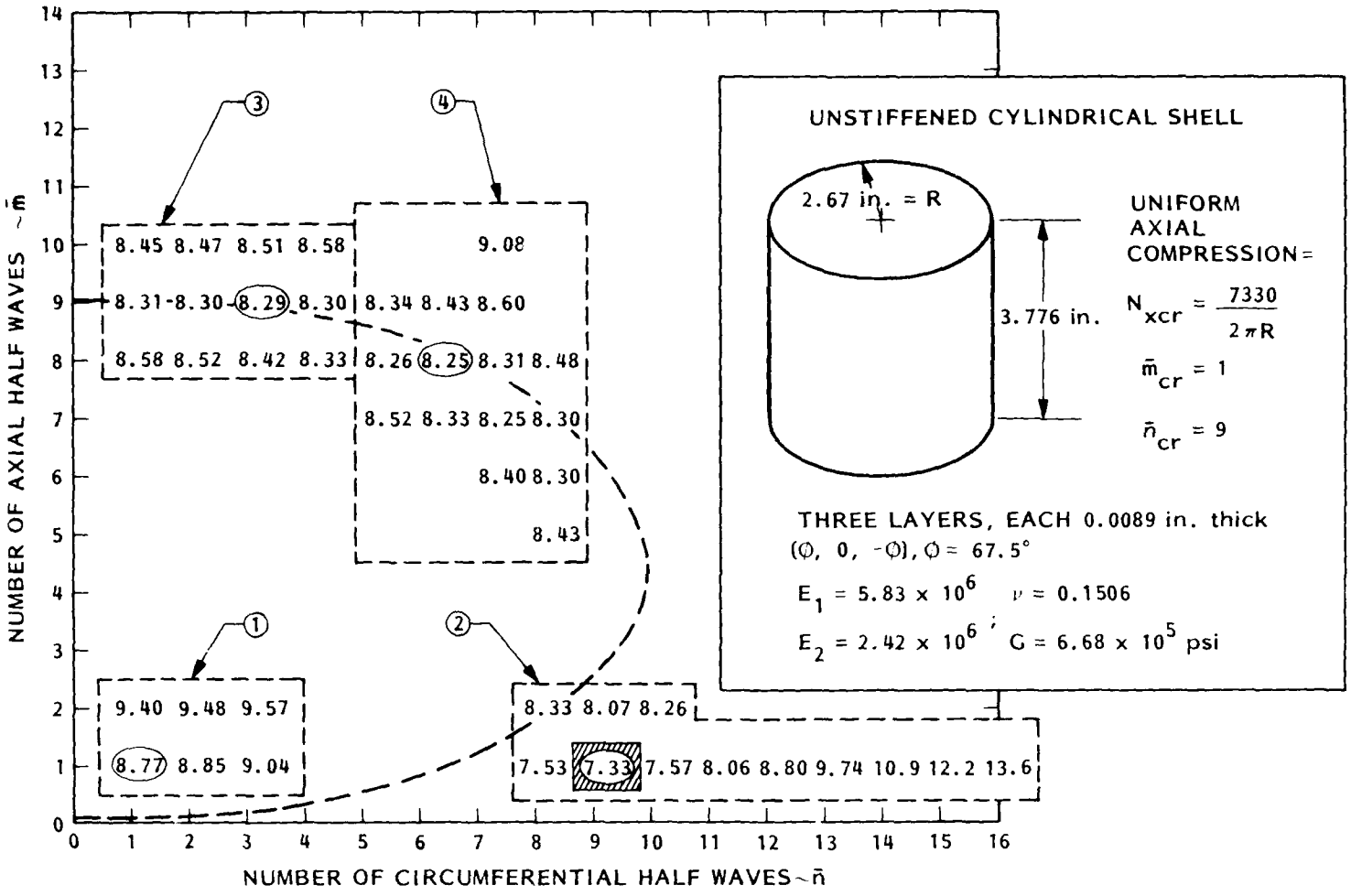

Figure 15. Buckling loads for axially compressed composite cylindrical shell with an unbalanced laminate $(\phi, 0, -\phi)$: Four regions, ①, ②, ③, ④, are shown in which minimum critical load multipliers λ_{cr} $(\bar{m}_{cr}, \bar{n}_{cr})$ are sought. The numbers in the dashed boxes are buckling loads in thousands of pounds for each $(\bar{m}, \bar{n})$ combination investigated by PANDA.

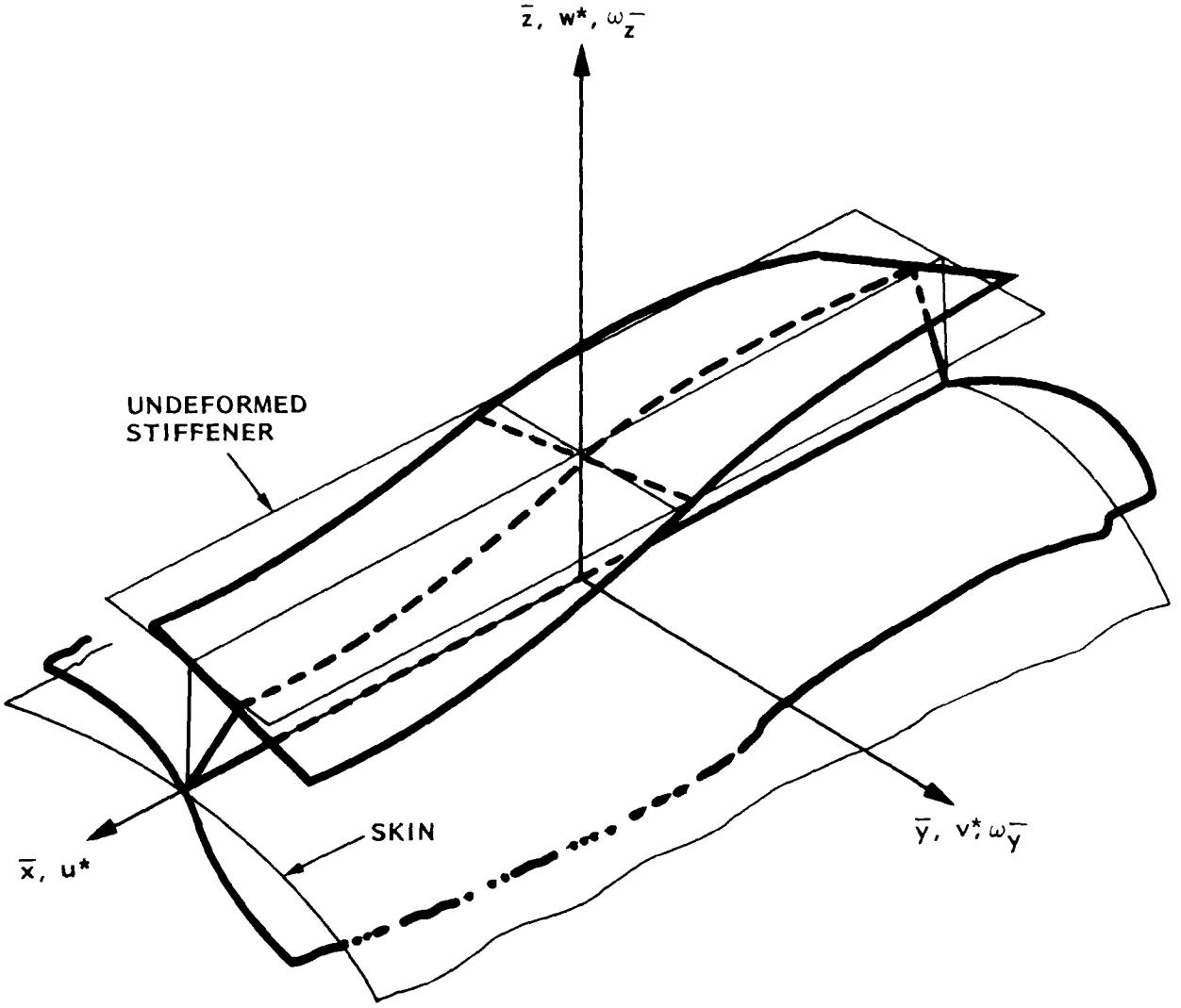

Figure 16. Rolling of stiffener as in Figure 6a

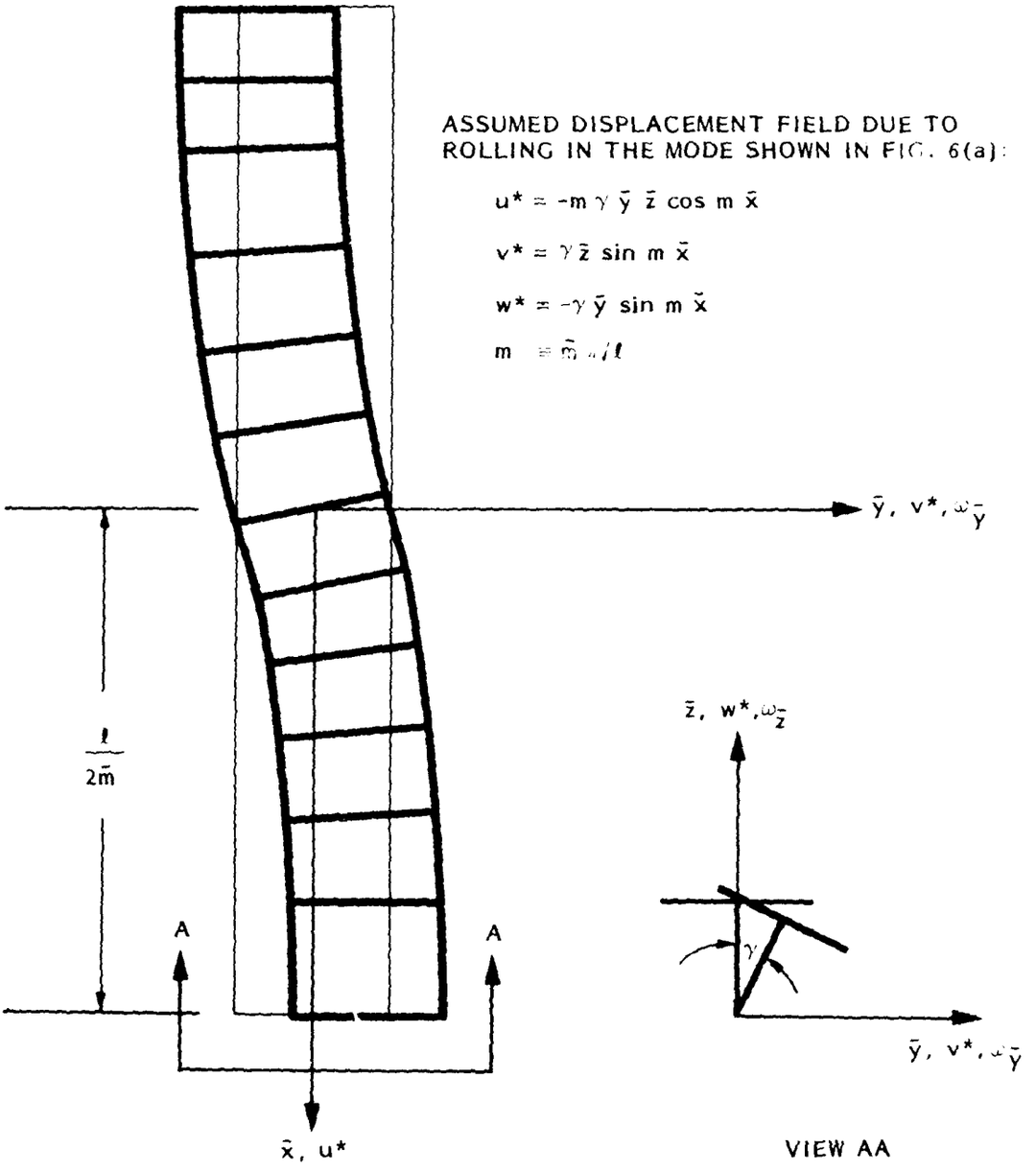

Figure 17. In-plane bending of a flange induced by rolling of the stiffener in the mode shown in Figure 6a

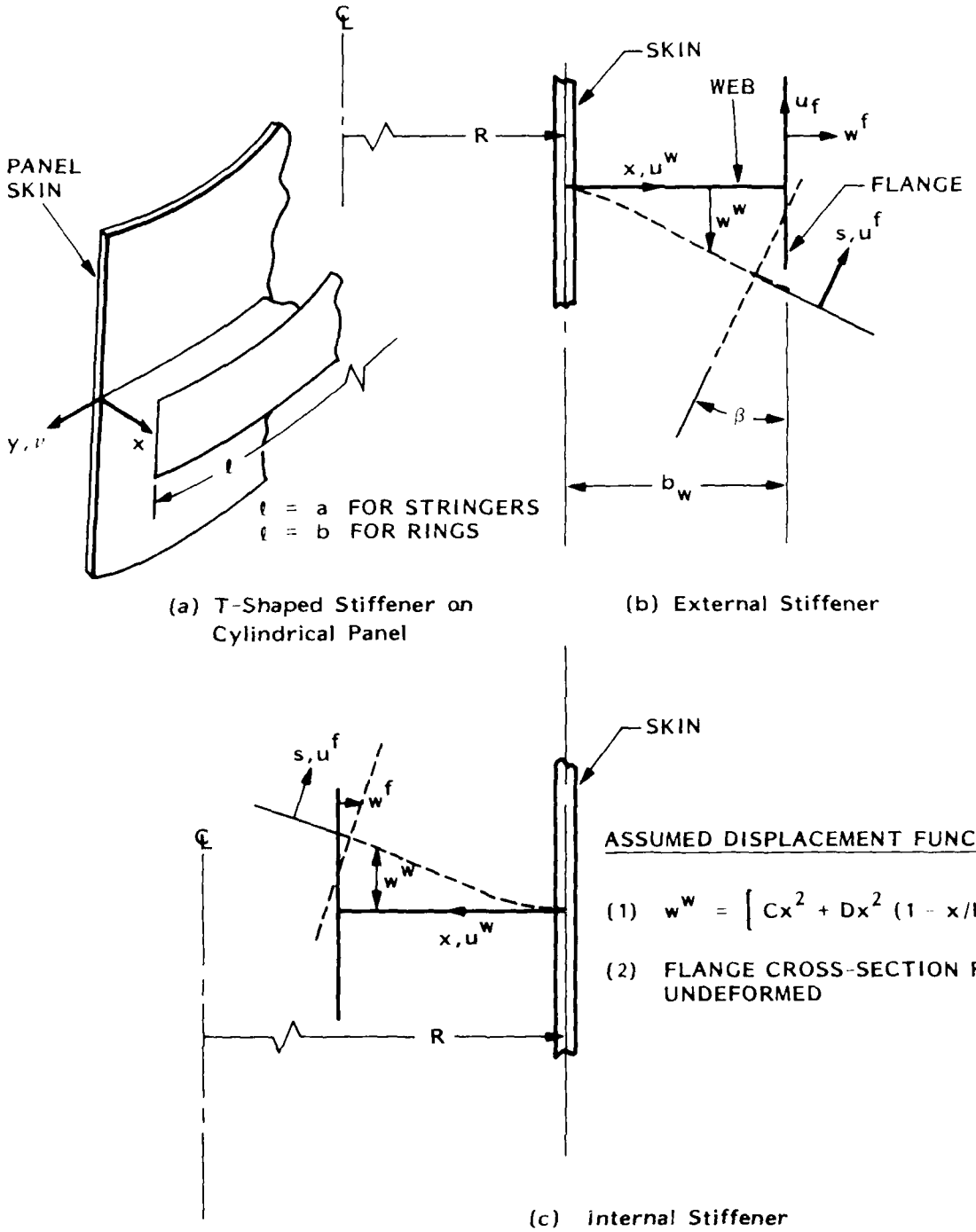

Figure 18. Stiffener coordinates and displacement components for rolling analysis of the types shown in Figs 6b and 6c (no participation of the panel skin)

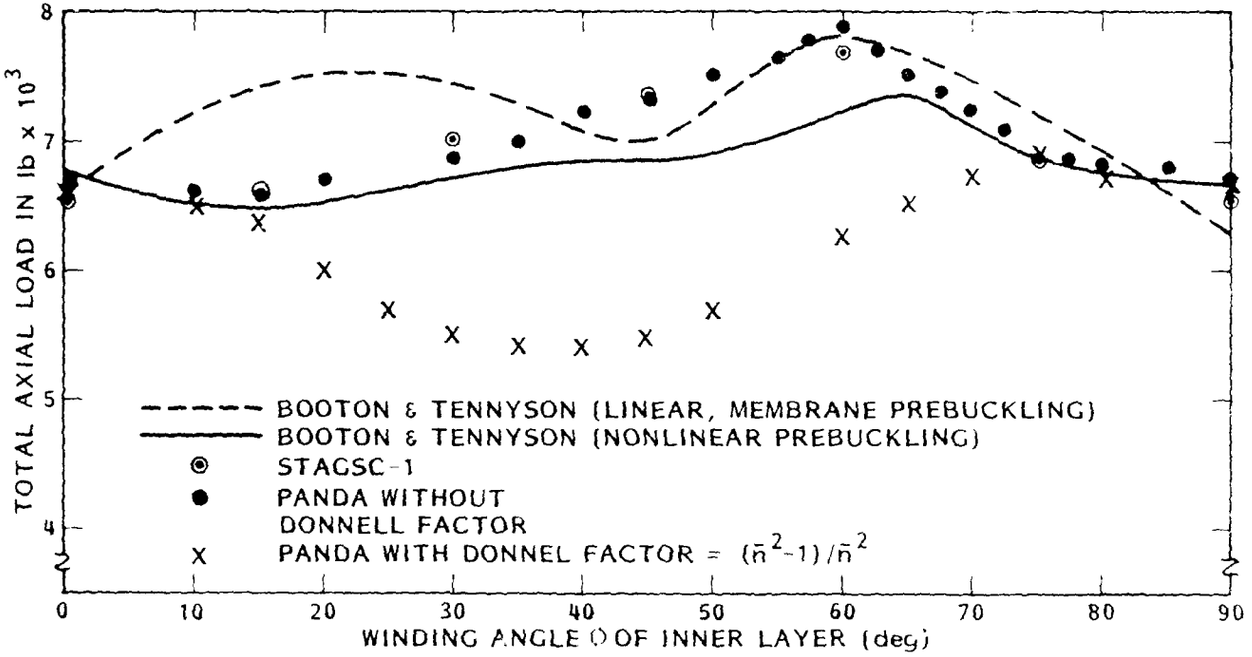

CYLINDER GEOMETRY AND MATERIAL PROPERTIES GIVEN IN FIG. 15.
WINDING ANGLES OF INNER, MIDDLE, OUTER LAYERS = Θ, 0, -Θ.

Figure 19. Buckling loads of a composite, axially compressed cylindrical shell with an unbalanced laminate (Θ, 0, -Θ). Comparison of results from PANDA, STAGSC-1 [62], and Booton and Tennyson [57].

AD-A110 963 LOCKHEED MISSILES AND SPACE CO INC PALO ALTO CA PALO --ETC F/G 1/3
PANEL OPTIMIZATION WITH INTEGRATED SOFTWARE (POIS). VOLUME I. P--ETC(U)
JUL 81 D BUSHNELL F33615-76-C-3105

UNCLASSIFIED AFWAL-TR-81-3073-VOL-1 NL

3 OF 3
AD A
110963

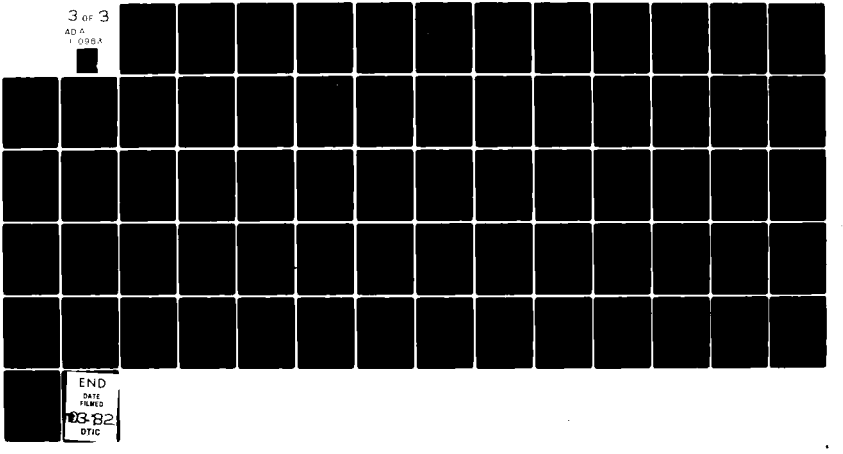

END
DATE FILMED
03-82
DTIC

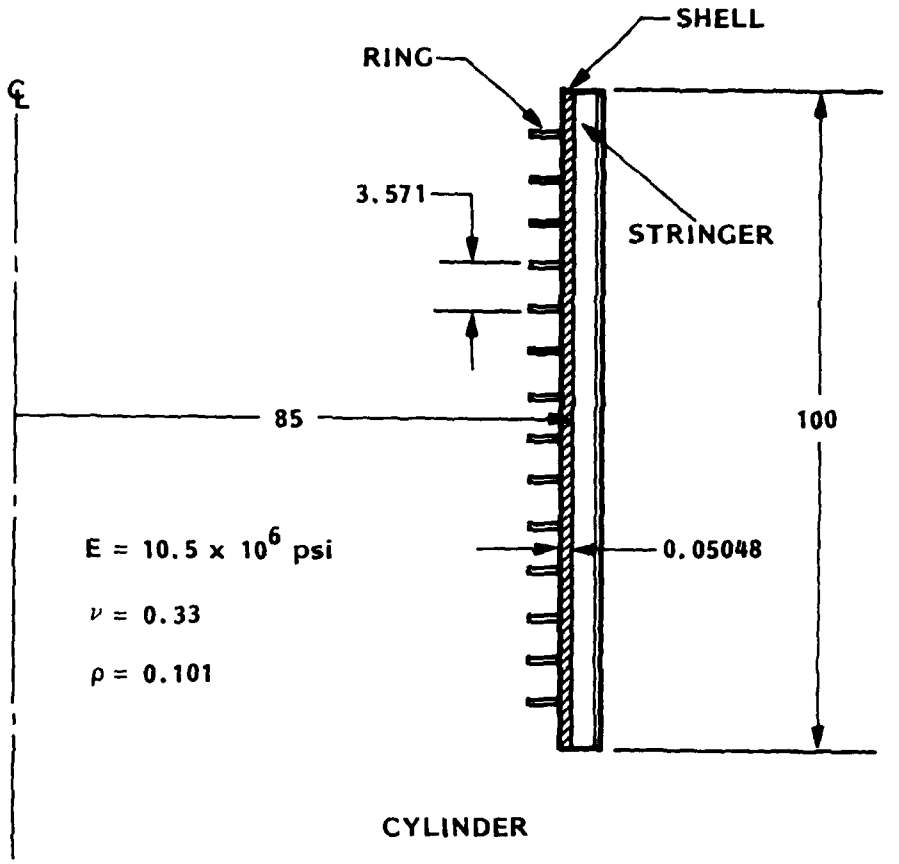

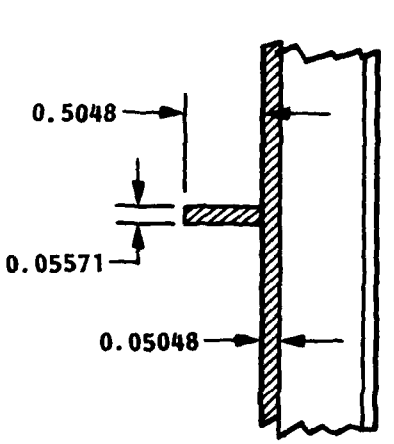

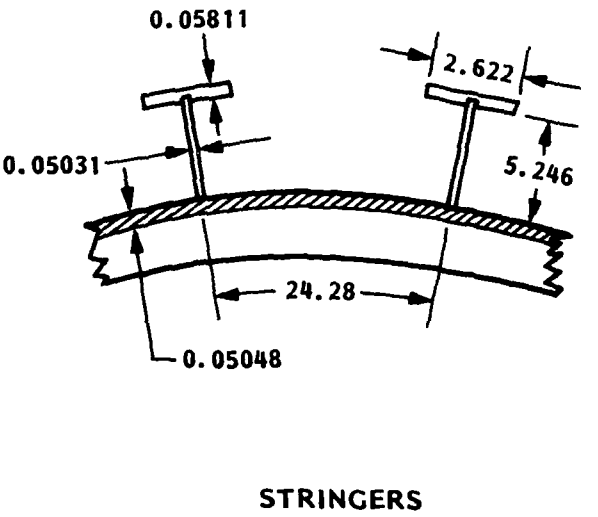

Figure 20. Ring and stringer stiffened cylindrical shell under pure torsion. The dimensions correspond to an optimum design obtained by Simitses and Giri [63] (See Table 4, Case 2)

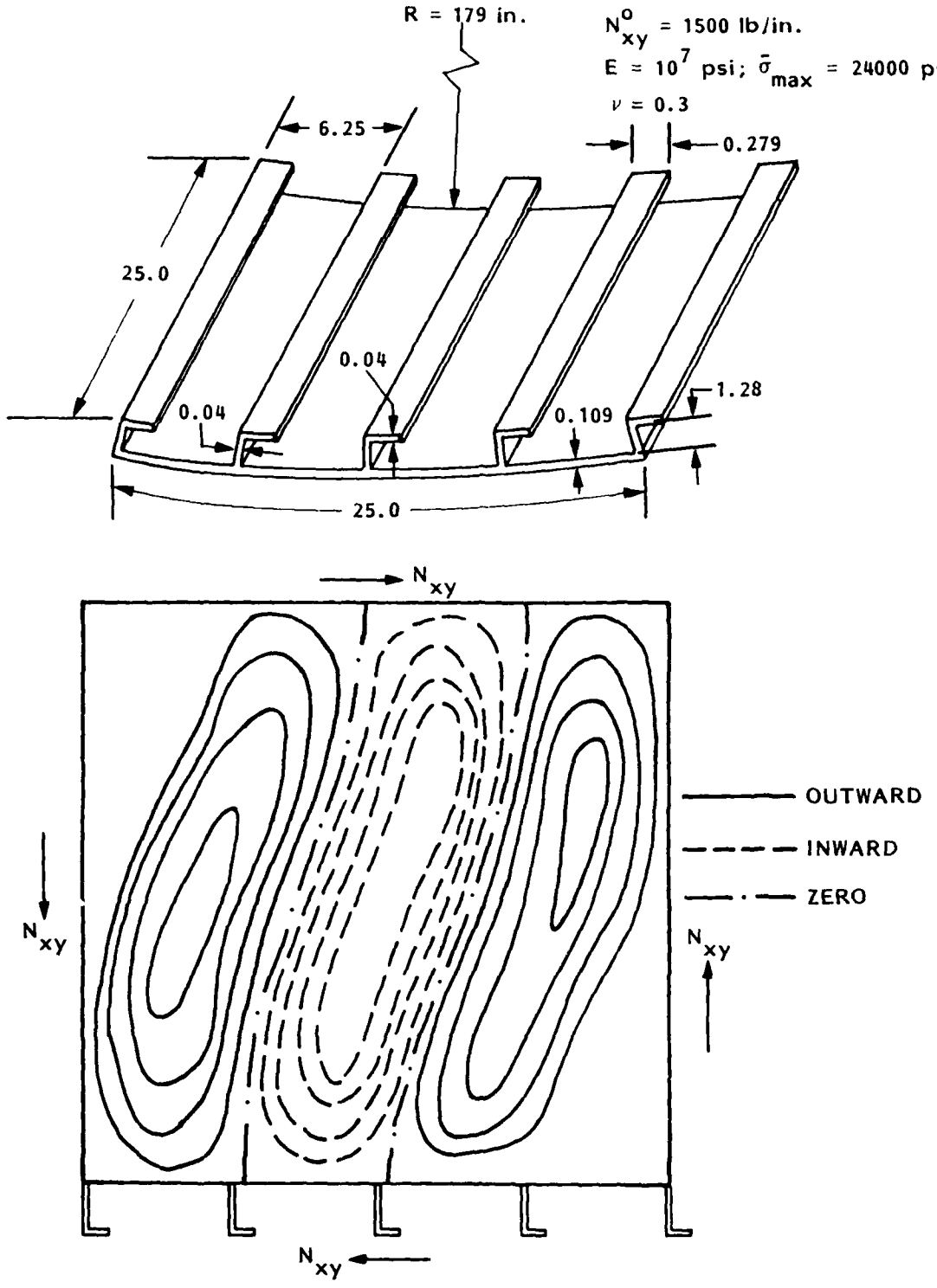

Figure 21. Shallow curved panel under pure in-plane shear. Bottom portion shows bifurcation buckling pattern predicted by STAGSC-1 [62]. (See Table 4, Case 3)

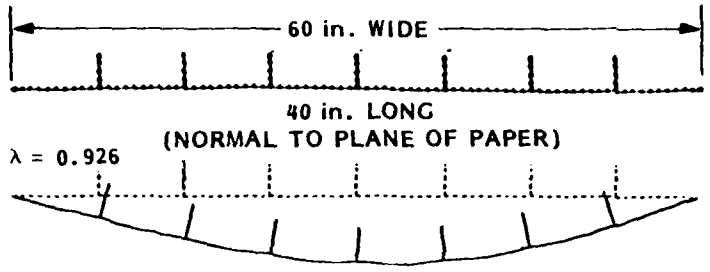

PANDA PREDICTS $\lambda = 1.0$

BOSOR4 PREDICTS $\lambda = 0.926$ (a)

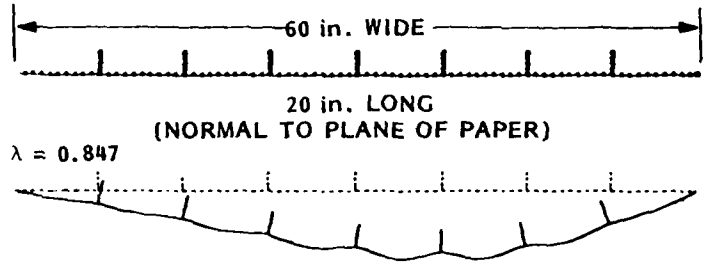

PANDA PREDICTS $\lambda = 1.0$

BOSOR4 PREDICTS $\lambda = 0.847$ (b)

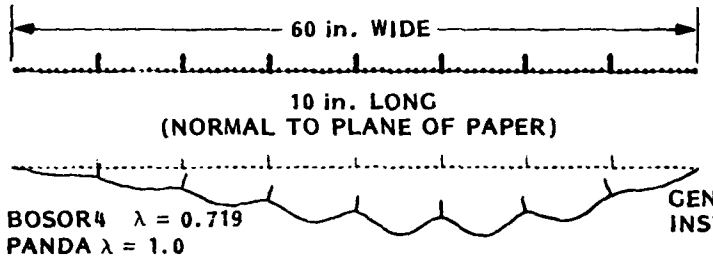

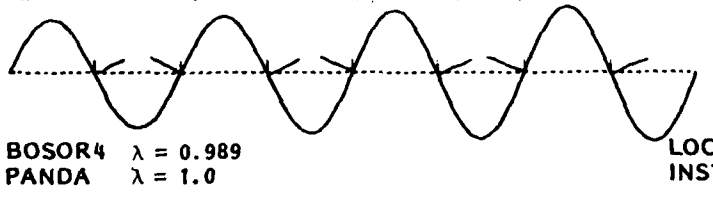

Figure 22. Buckling modes predicted by BOSOR4 for axially compressed panels of lengths (a) 40 in., (b) 20 in., (c,d) 10 in. Dimensions of the cross sections were obtained by optimization analyses with PANDA.

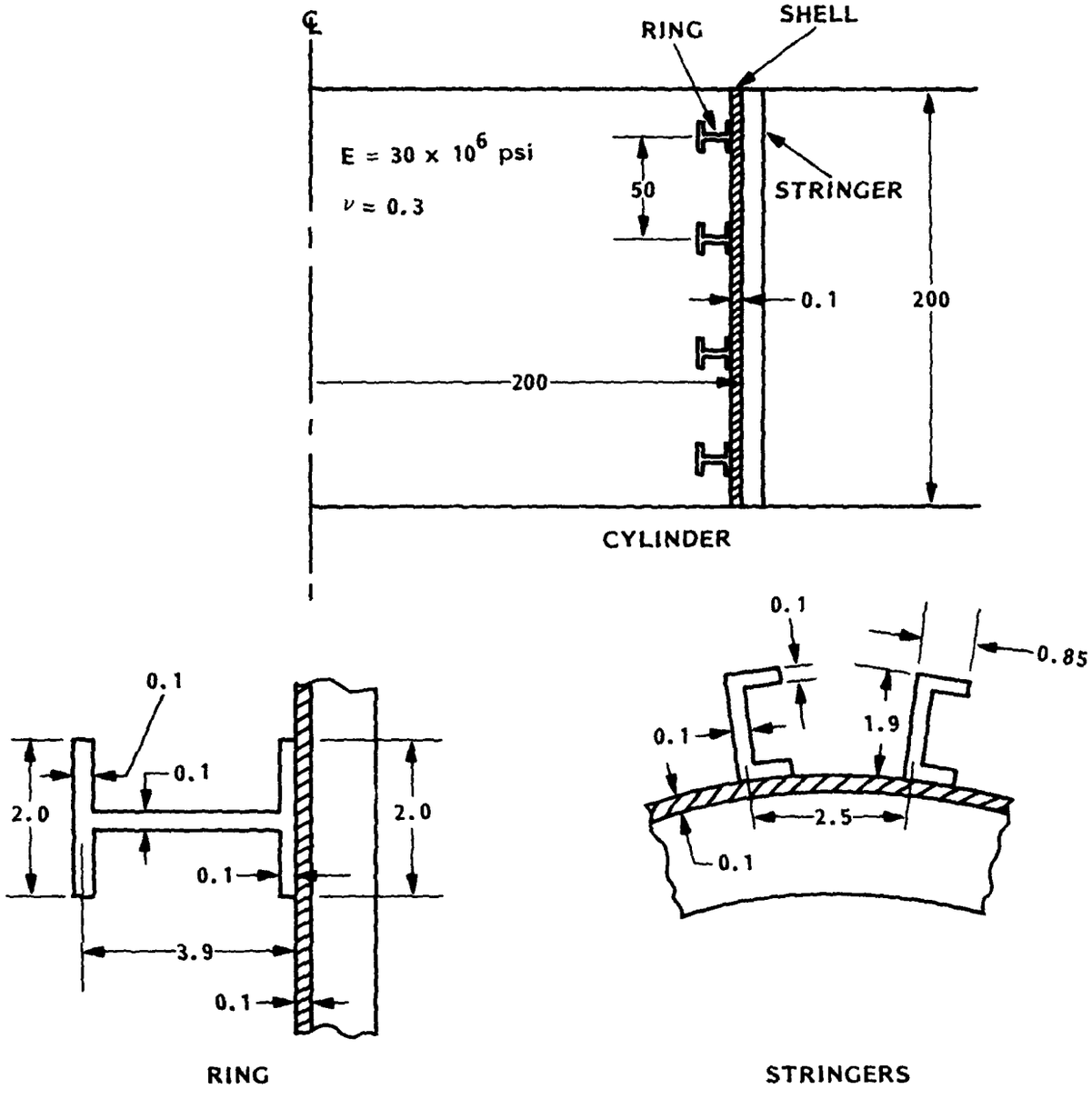

Figure 23. Axially compressed ring and stringer stiffened cylindrical shell analysed by Block, Card, and Mikulas [65] and by Kicher and Wu [66]. (See Table 5)

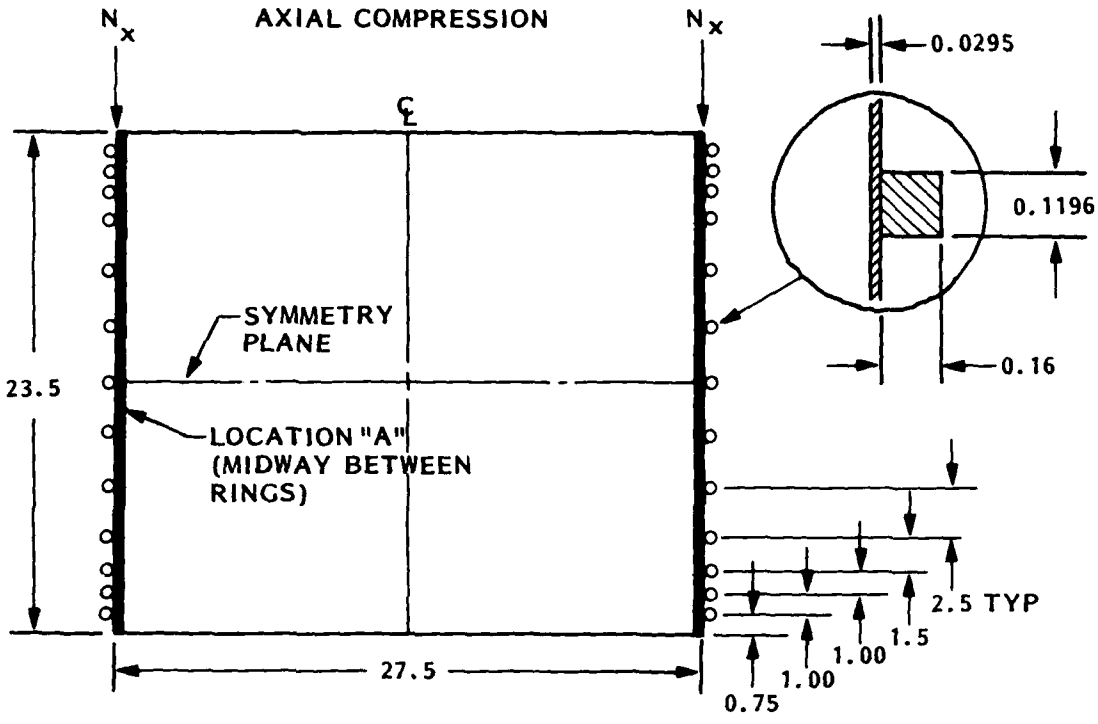

(a) Ring Stiffened Axially Compressed Cylindrical Shell (dimensions in inches)

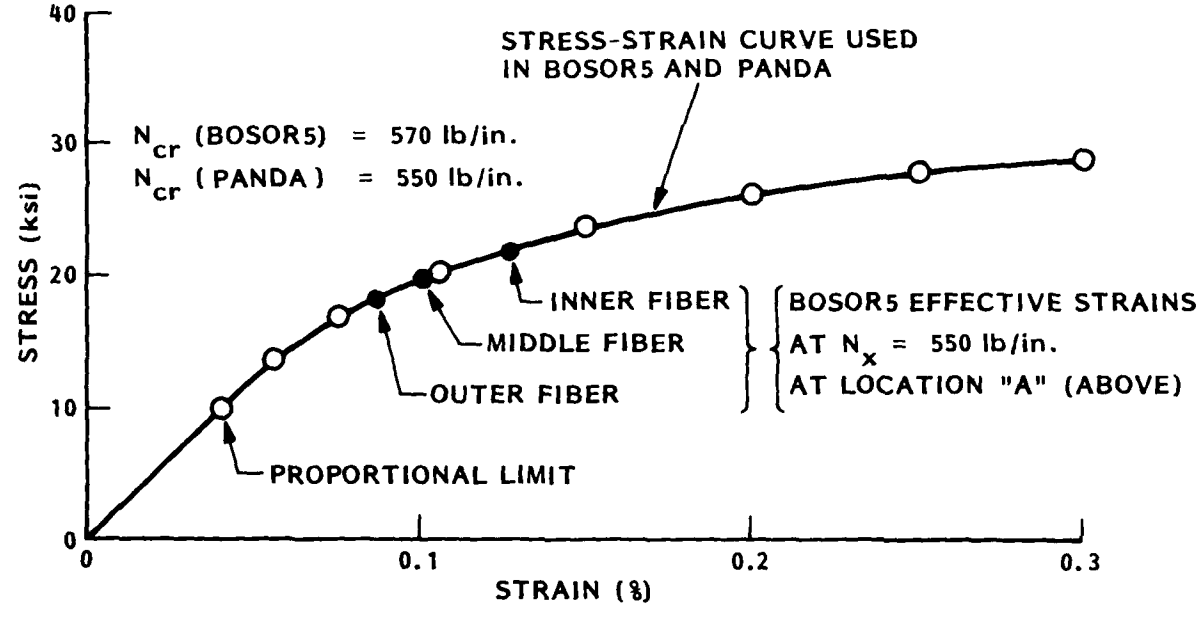

(b) Stress-Strain Curve and Maximum Effective Strain at Collapse

Figure 24. Axially compressed, elastic-plastic, ring stiffened cylindrical shell. Comparison of critical loads from PANDA and from BOSOR5 [59].

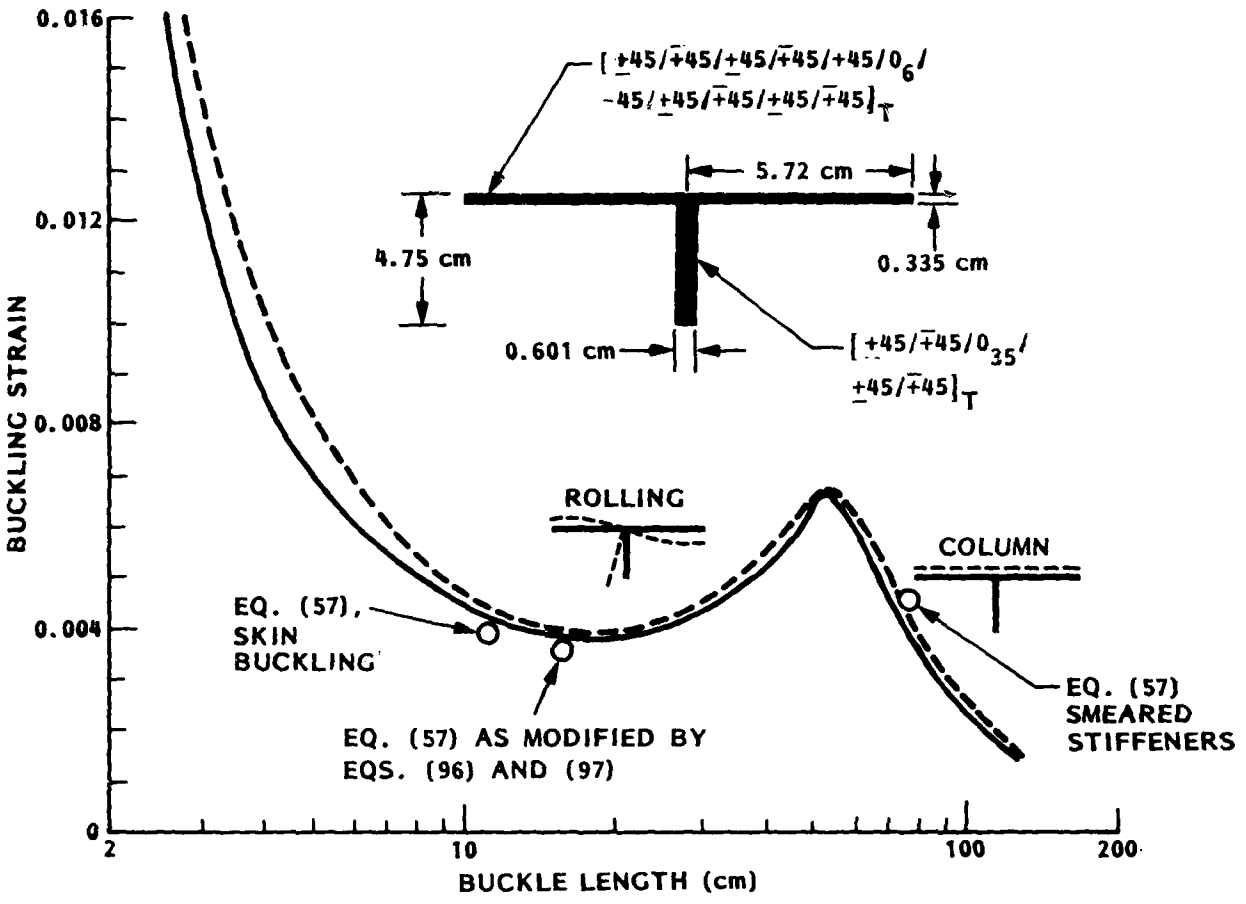

MATERIAL PROPERTIES:

E_1 = 131 GPa $\quad \nu_{12}$ = 0.038
E_2 = 13 GPa $\quad \rho$ = 1522 kg/m^3
G = 6.41 GPa

O PANDA
------ SIMPLIFIED ANALYSIS (REF. 24)
——— EXACT ANALYSIS (REF. 24)

Figure 25. Buckling of axially compressed composite panel with composite stringers. Comparison of results from PANDA and the analyses of Williams and Stein [24]. (See Table 6)

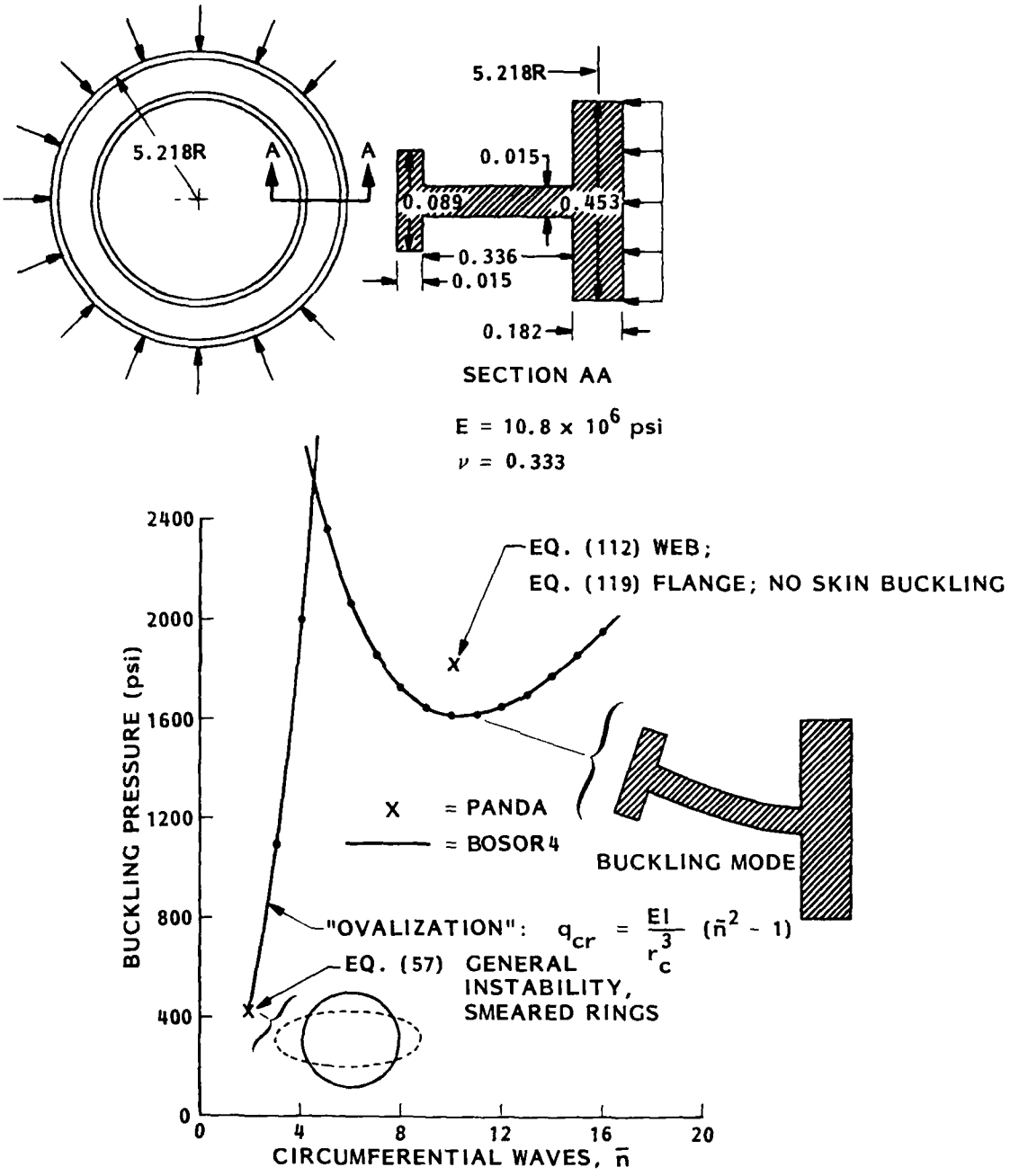

Figure 26. General (ring) instability of long, ring stiffened cylindrical shell under uniform external lateral pressure, and local instability (nonsymmetric sidesway or "tripping") of ring. Comparison of results from PANDA and results from BOSOR4 [58]. (See Table 7)

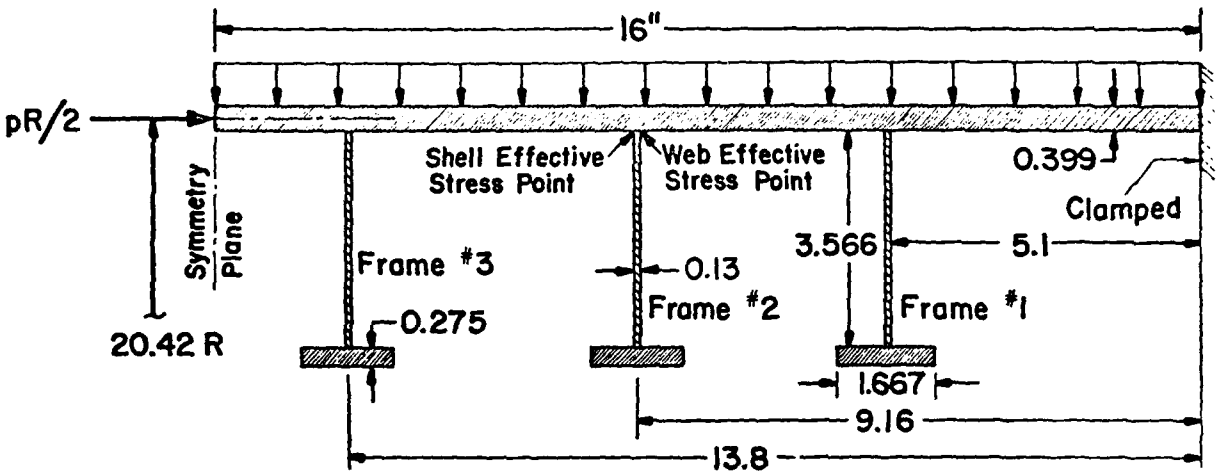

(a)

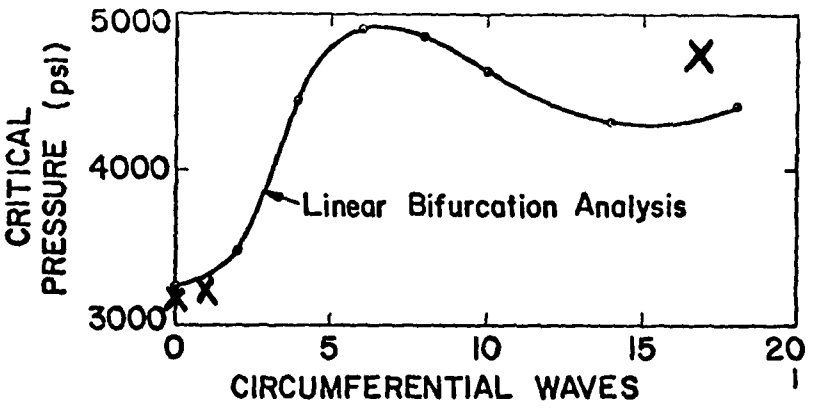

(b)

Figure 27. Externally pressurized ring stiffened cylindrical shell that fails by axisymmetric sidesway of the deep rings; (a) geometry, (b) results of linear bifurcation analyses with BOSOR4 (solid line) and PANDA (x's). (See Table 8)

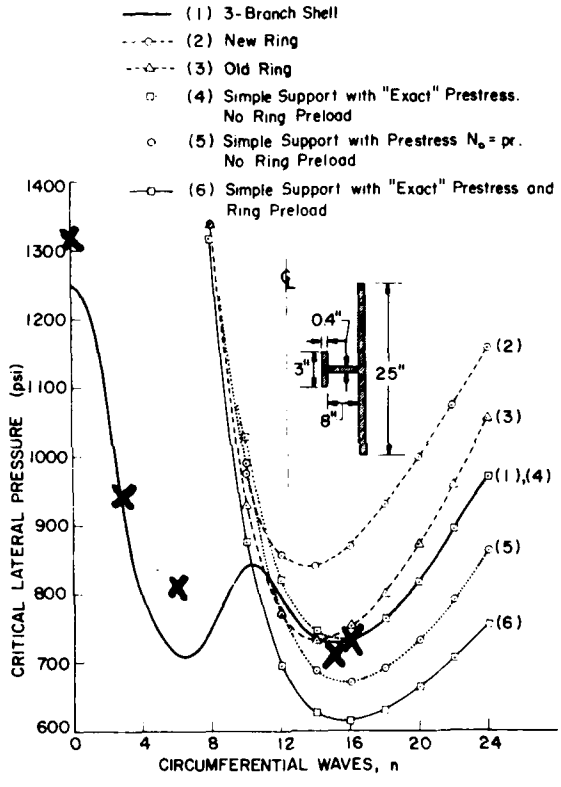

Figure 28. Local and general buckling of ring stiffened cylinder under uniform lateral external pressure. Solid line is from BOSOR4 predictions; x's are from PANDA. (See Table 9)

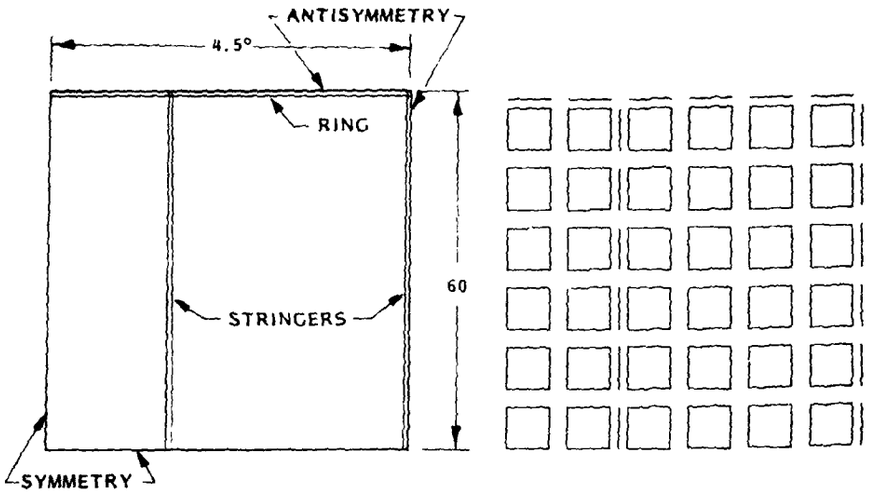

(a) Small STAGSC1 model for local buckling of the cylindrical shell shown in Fig. 9

(b) Finite element discretization corresponding to a 7 x 7 grid. The ring and the two stringers are shown as line segments

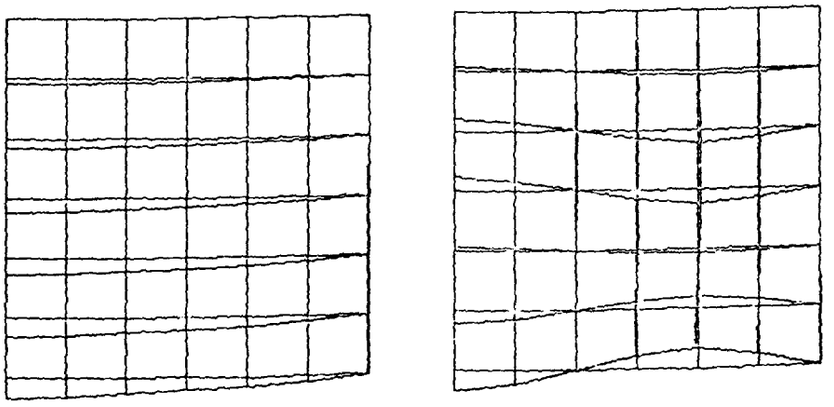

(c) First eigenvector for a 7 x 7 grid. Panel instability (between rings) is indicated (66 kips/in.)

(d) Second eigenvector for the 7 x 7 grid. Local buckling is indicated (70 kips/in.)

Figure 29. Finite element model for local buckling under axial compression of a portion of the ring and stringer stiffened cylindrical shell shown in Fig. 9. Linear bifurcation buckling load factors and an elastic-plastic collapse load were obtained through use of the STAGSC-1 program [62]. (See Table 10)

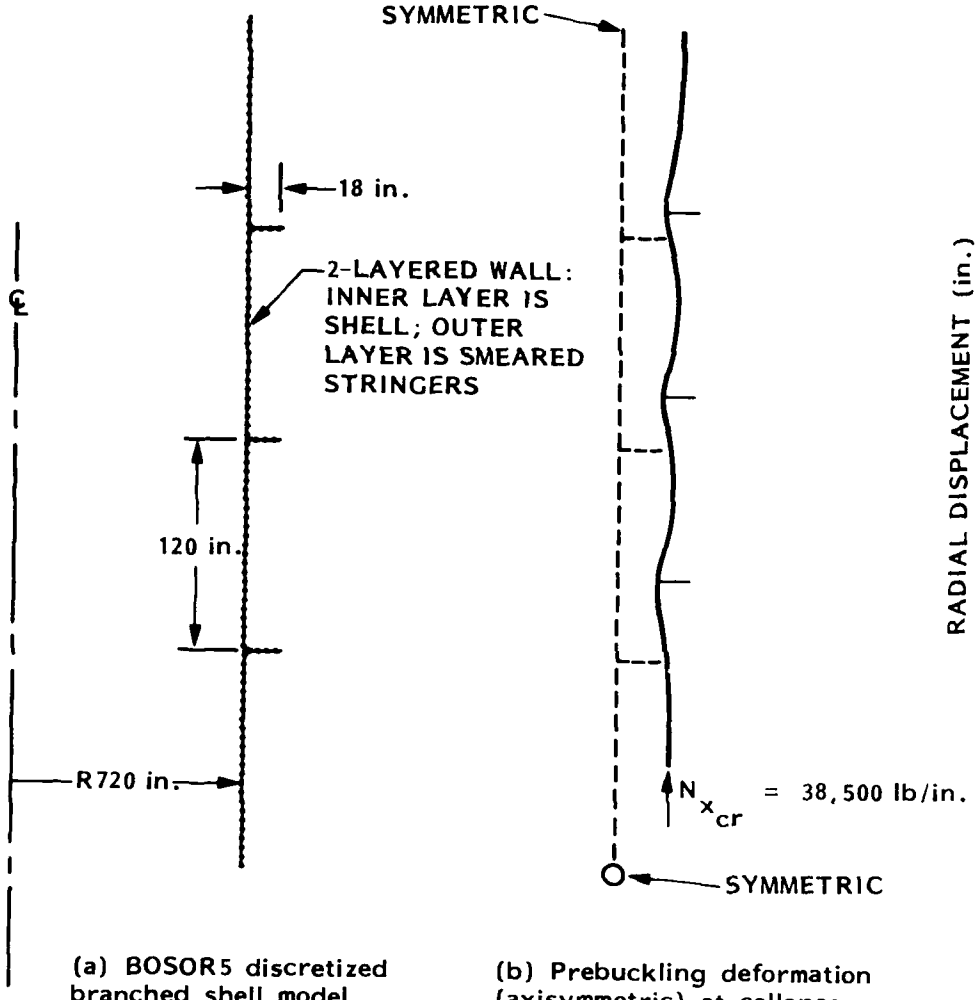

(a) BOSOR5 discretized branched shell model (stringers are smeared).

(b) Prebuckling deformation (axisymmetric) at collapse load. $N_{x_{cr}}$ = 38,500 lb/in.

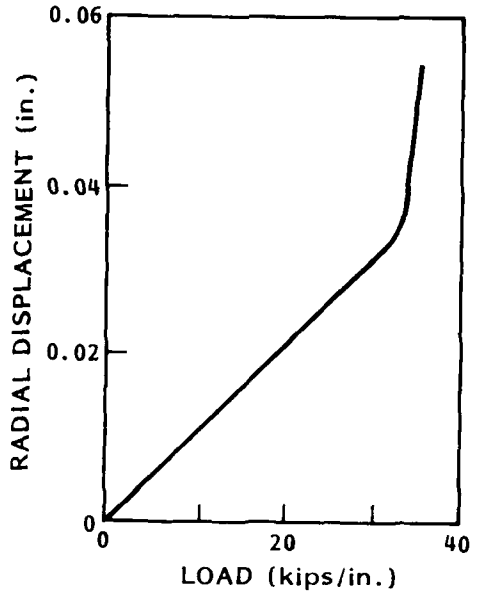

(c) Load-displacement curve for inelastic collapse analysis with STAGSC1 and the portion of the stiffened cylinder shown in Fig. 29 (a).

Figure 30. Elastic-plastic collapse of the axially compressed cylindrical shell shown in Figure 9, as predicted by BOSOR5 [59] and STAGSC-1 [62] (See Table 11)

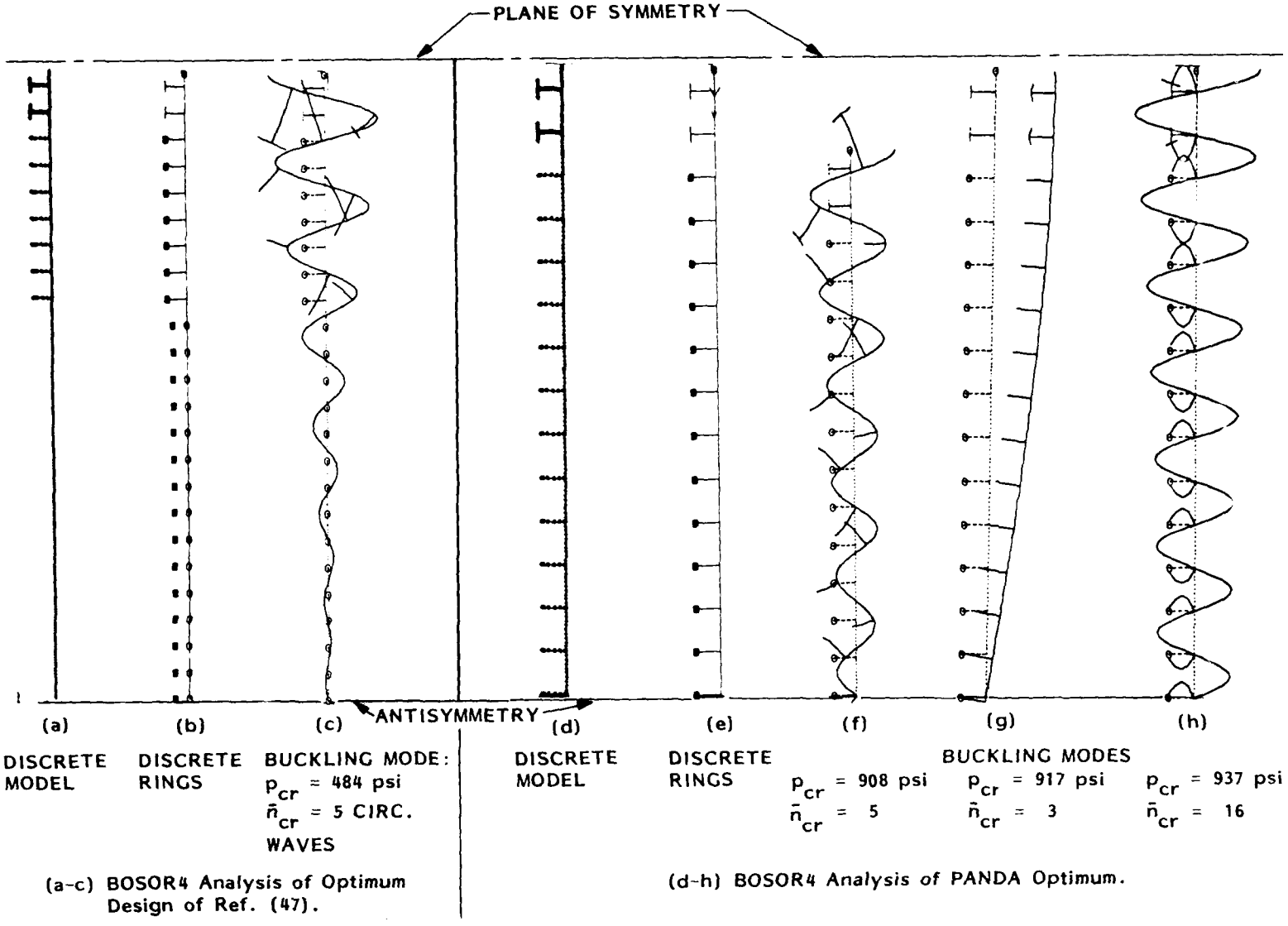

Figure 31. Buckling modes obtained with BOSOR4 corresponding to optimum designs of hydrostatically compressed, ring stiffened cylindrical shells. The configuration (a) was obtained by Pappas and Allentuch [47]. The configuration (d) was obtained by PANDA. Design pressure p_o = 898 psi. (See Table 18)

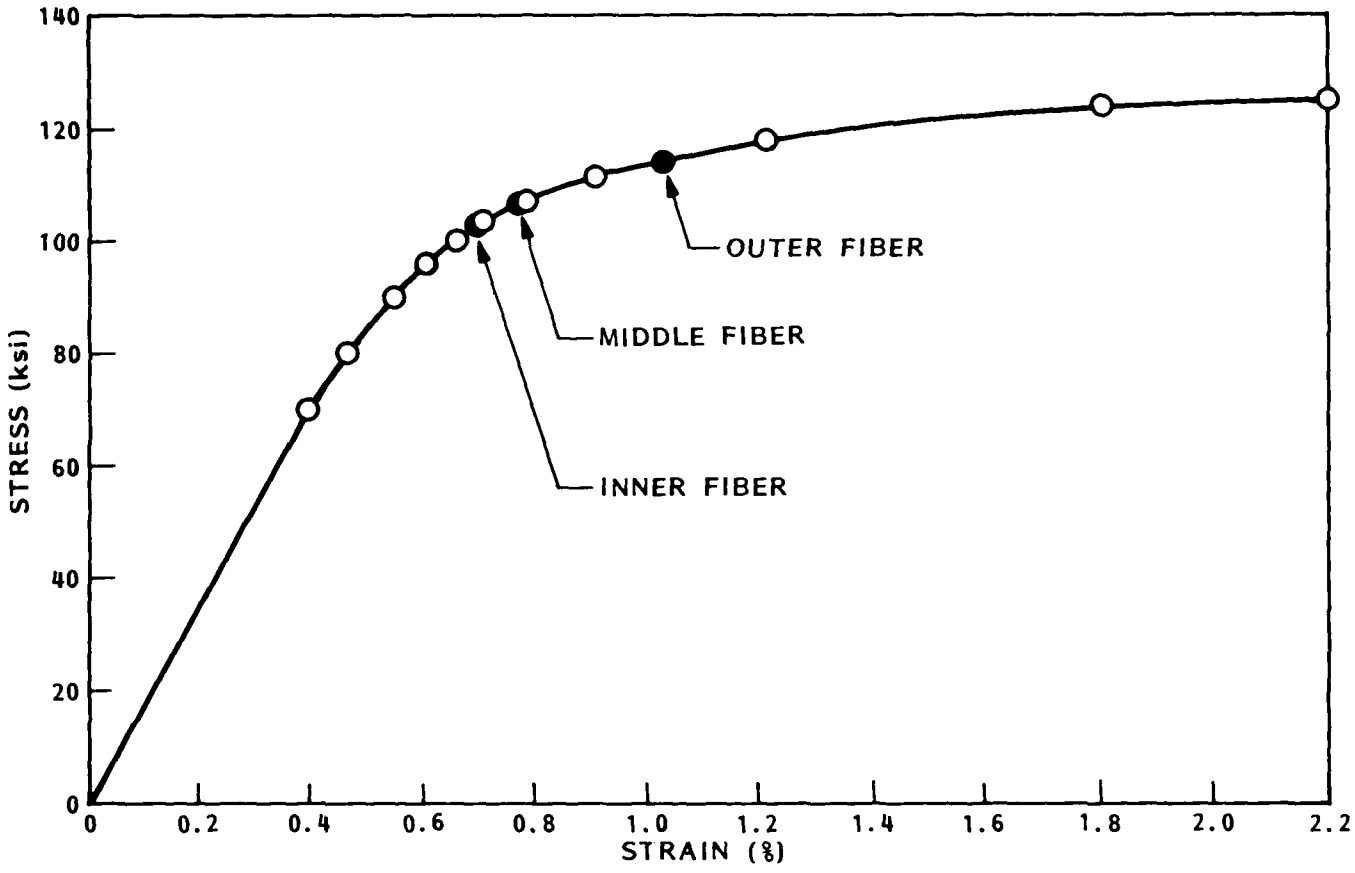

Figure 32. Effective strains midway between adjacent rings at the buckling pressure for a hydrostatically compressed cylindrical shell with internal rectangular stiffeners. Configuration is shown in Fig. 34. Design pressure p_o = 4066 psi. (See Table 19)

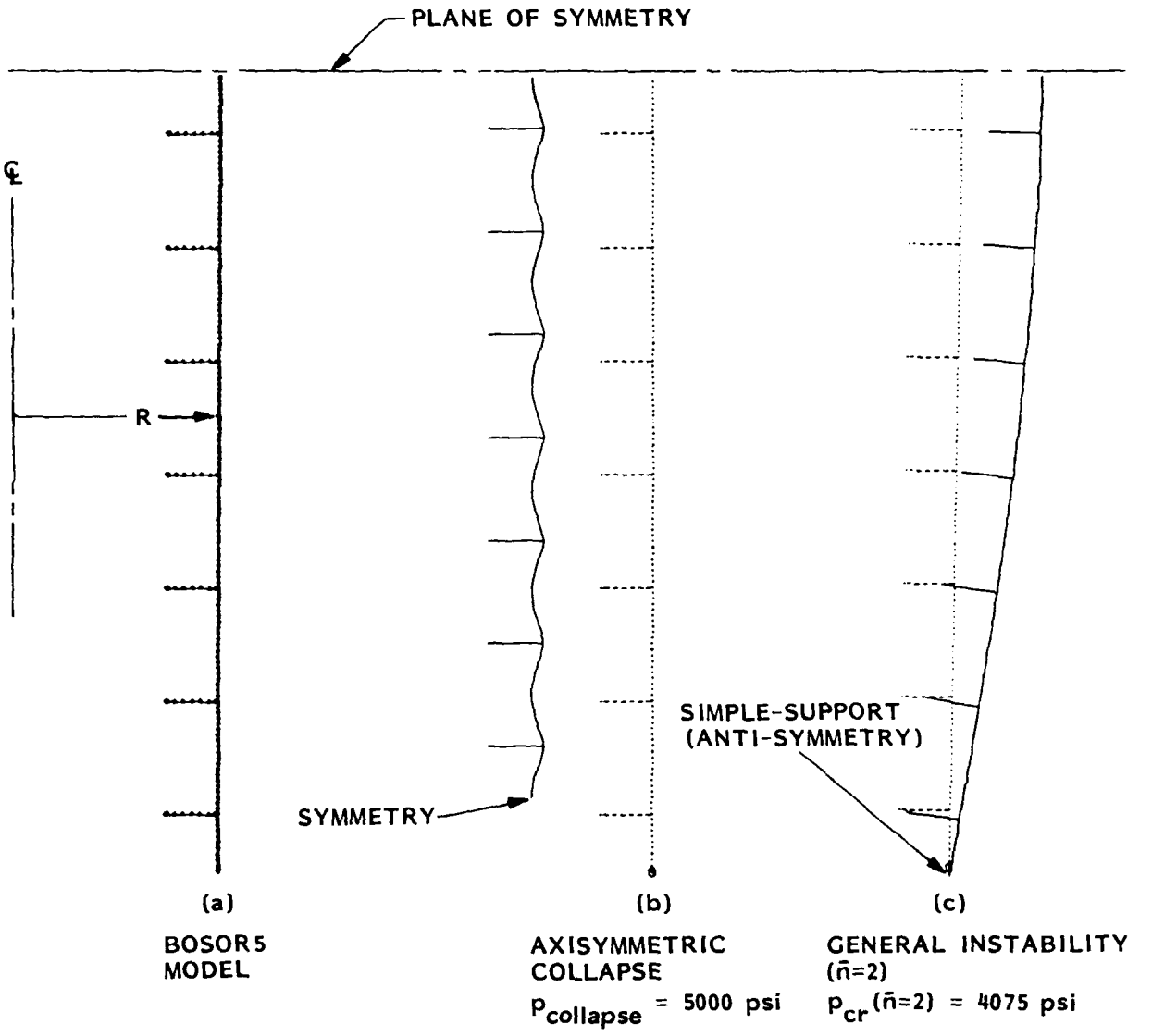

Figure 33. Hydrostatically compressed, internally ring stiffened cylindrical shell: BOSOR5 model and predicted buckling modes and pressures corresponding to the analysis of *Renzi* [44]. (See Table 19)

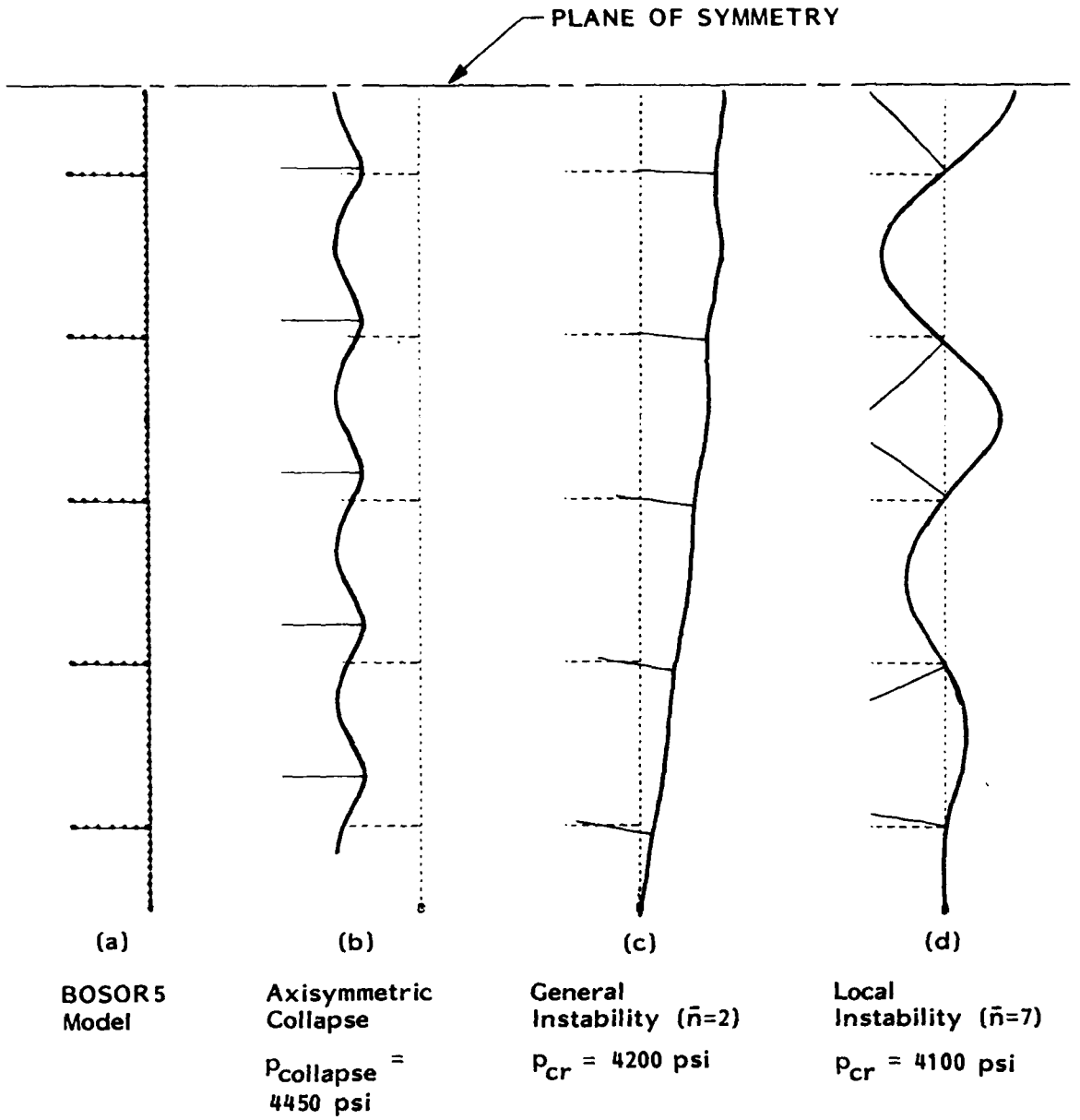

Figure 34. Hydrostatically compressed, internally ring stiffened cylindrical shell: BOSOR5 model and predicted buckling modes and pressures corresponding to the optimum design determined by PANDA. (See Table 19)

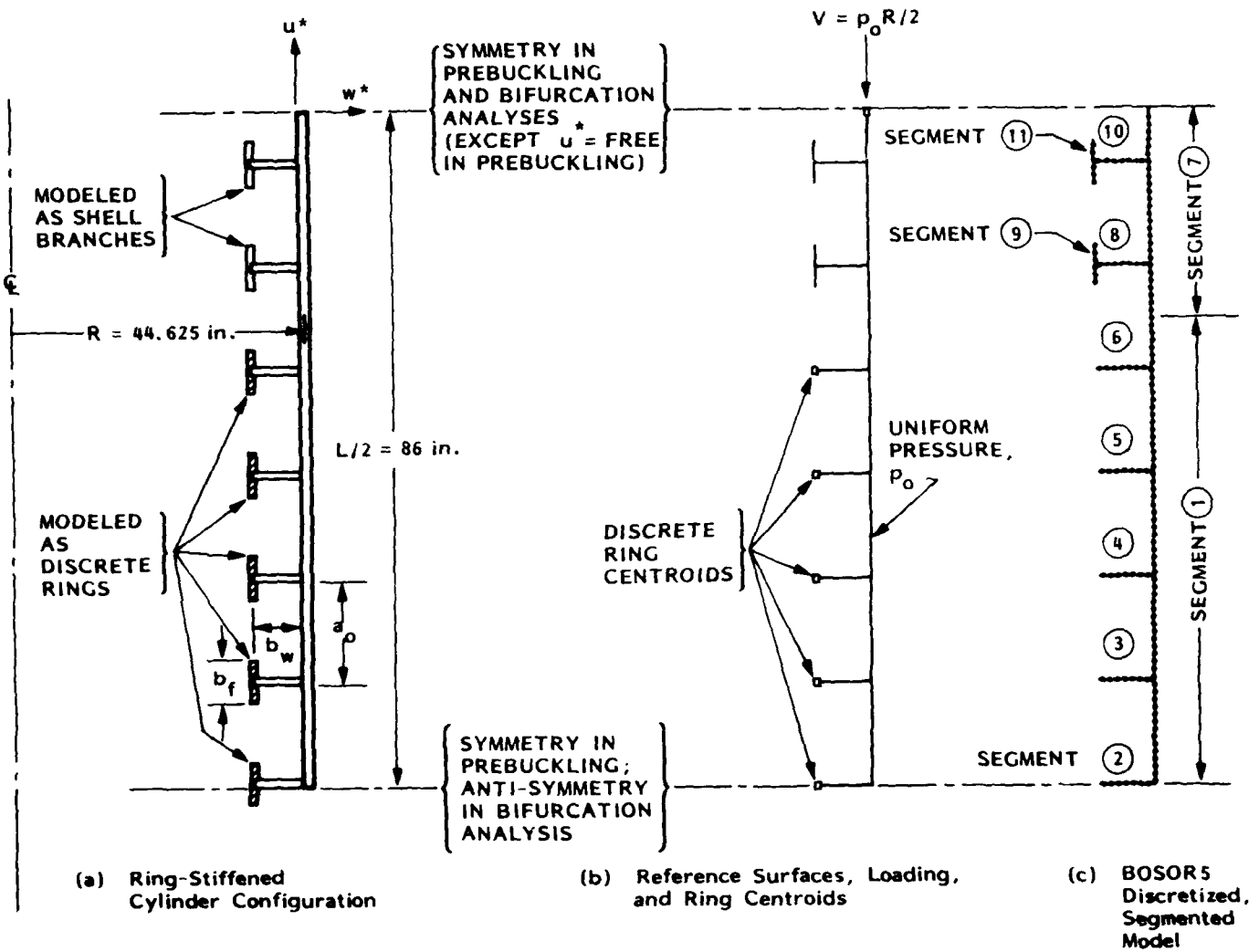

Figure 35. Hydrostatically compressed, internally ring stiffened cylindrical shells: Modeling strategy for BOSOR5 analyses of the minimum weight designs obtained by PANDA for design pressures p_o ranging from p_o = 677 psi to p_o = 4743 psi. (See Table 20 for dimensions)

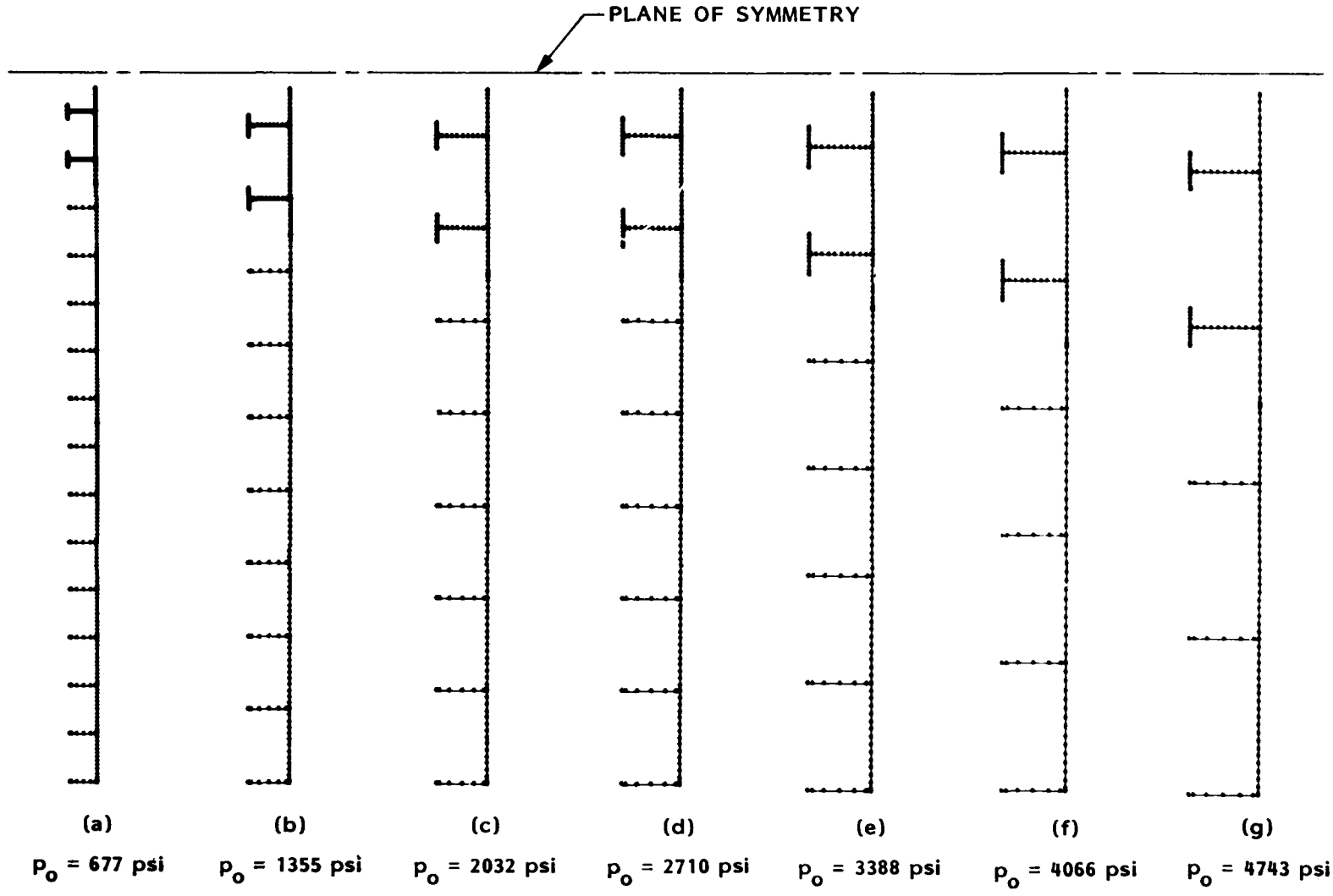

Figure 36. Hydrostatically compressed, internally ring stiffened cylindrical shells: BOSOR5 discretized models corresponding to minimum weight designs obtained by PANDA for design pressures ranging from 677 psi to 4743 psi. (See Table 20)

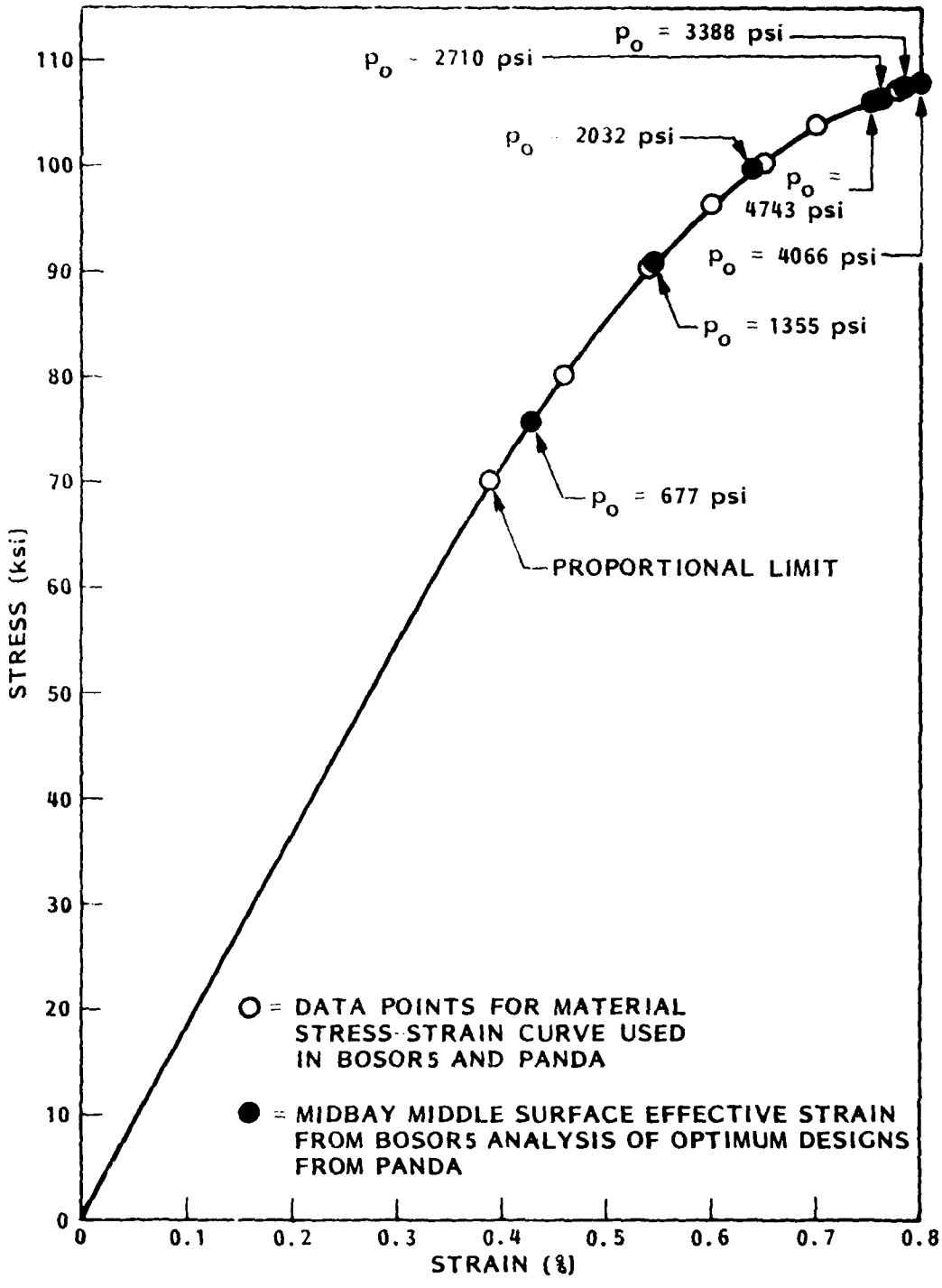

Figure 37. Hydrostatically compressed, internally ring stiffened cylindrical shells: Midbay effective membrane strains at the design pressures for the optimized configurations shown in Figure 36.

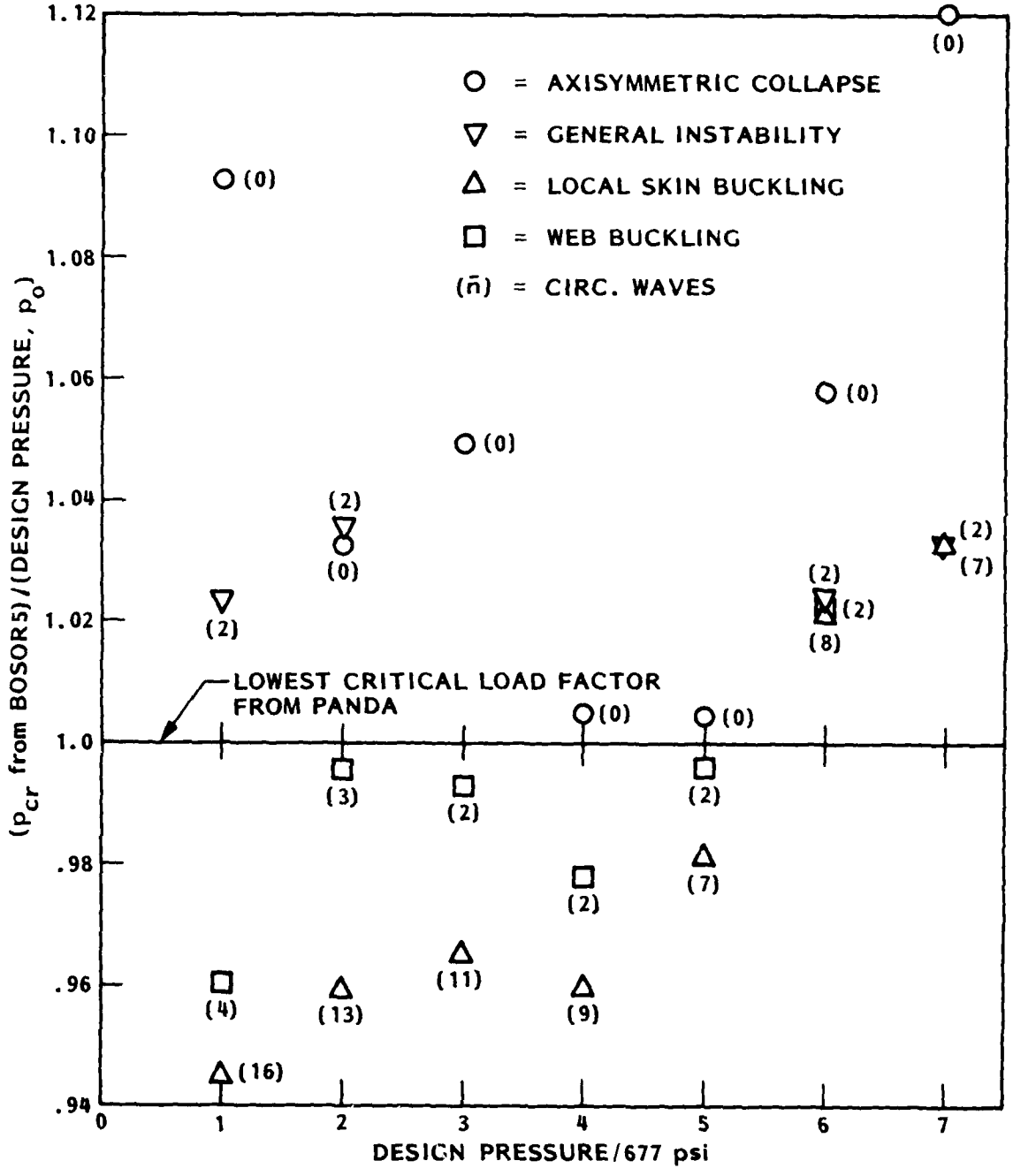

Figure 38. Hydrostatically compressed, internally ring stiffened cylindrical shells: Comparison of buckling loads obtained from PANDA and from BOSOR5. This is a comparison because the critical loads from PANDA are all very near unity, as seen from Table 21.

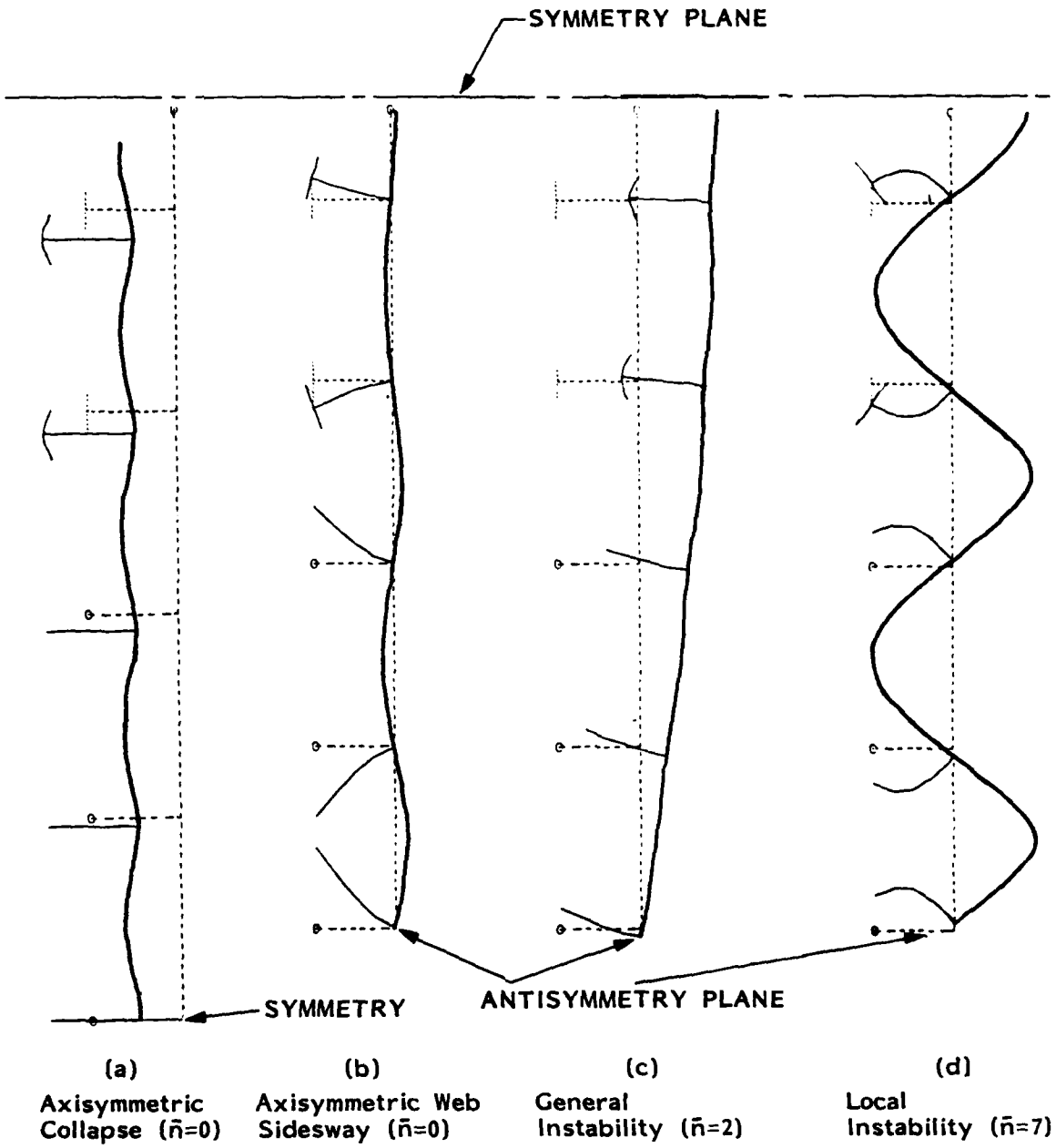

Figure 39. Buckling modes predicted by BOSOR5 for the optimum design corresponding to p_o = 4743 psi.

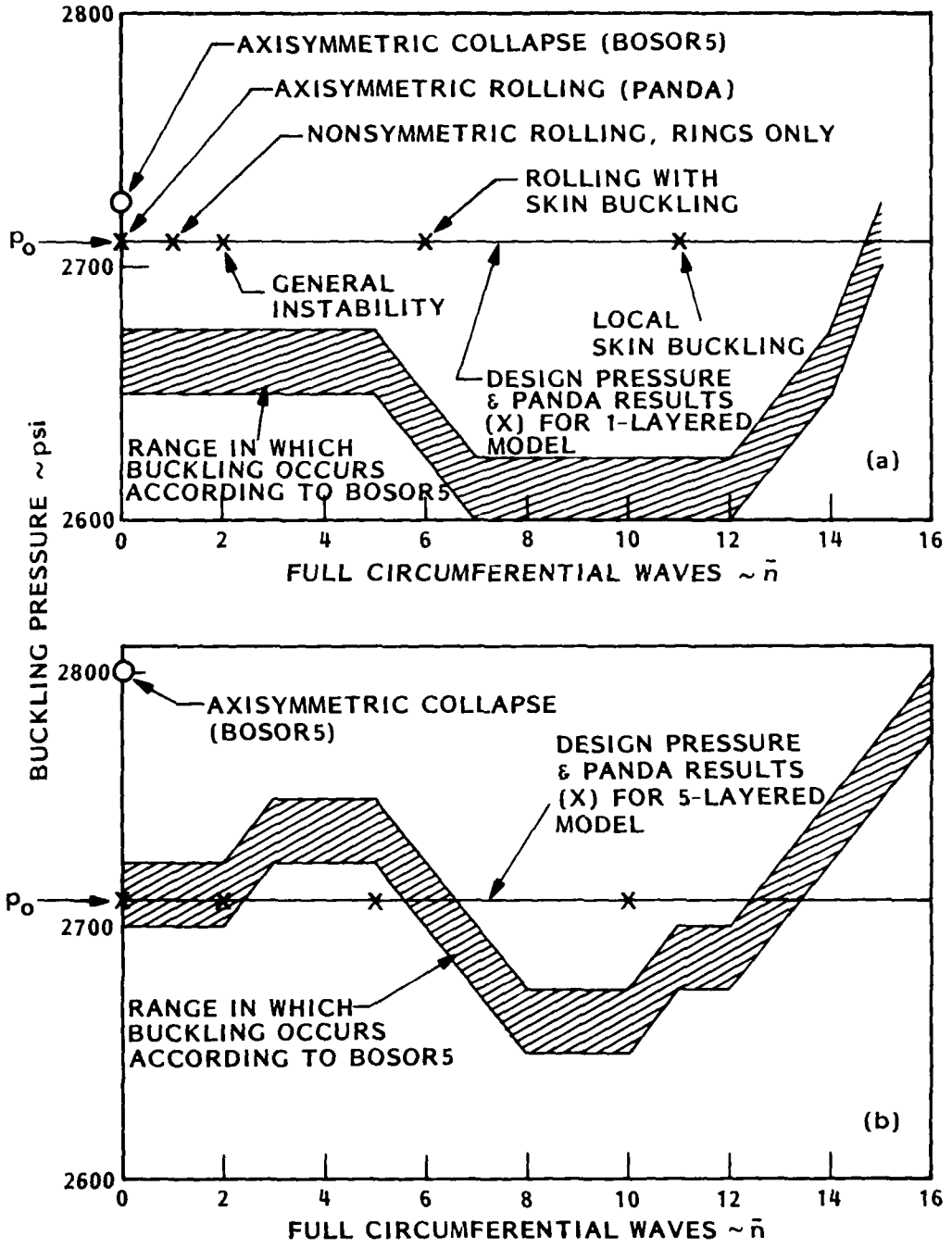

Figure 40. Hydrostatically compressed, internally ring-stiffened cylindrical shells optimized by PANDA for a design pressure of 2710 psi. Comparisons of buckling predictions from BOSOR5 and PANDA: (a) minimum weight design corresponding to a one-layered model in PANDA; (b) minimum weight design corresponding to a 5-layered model in PANDA.

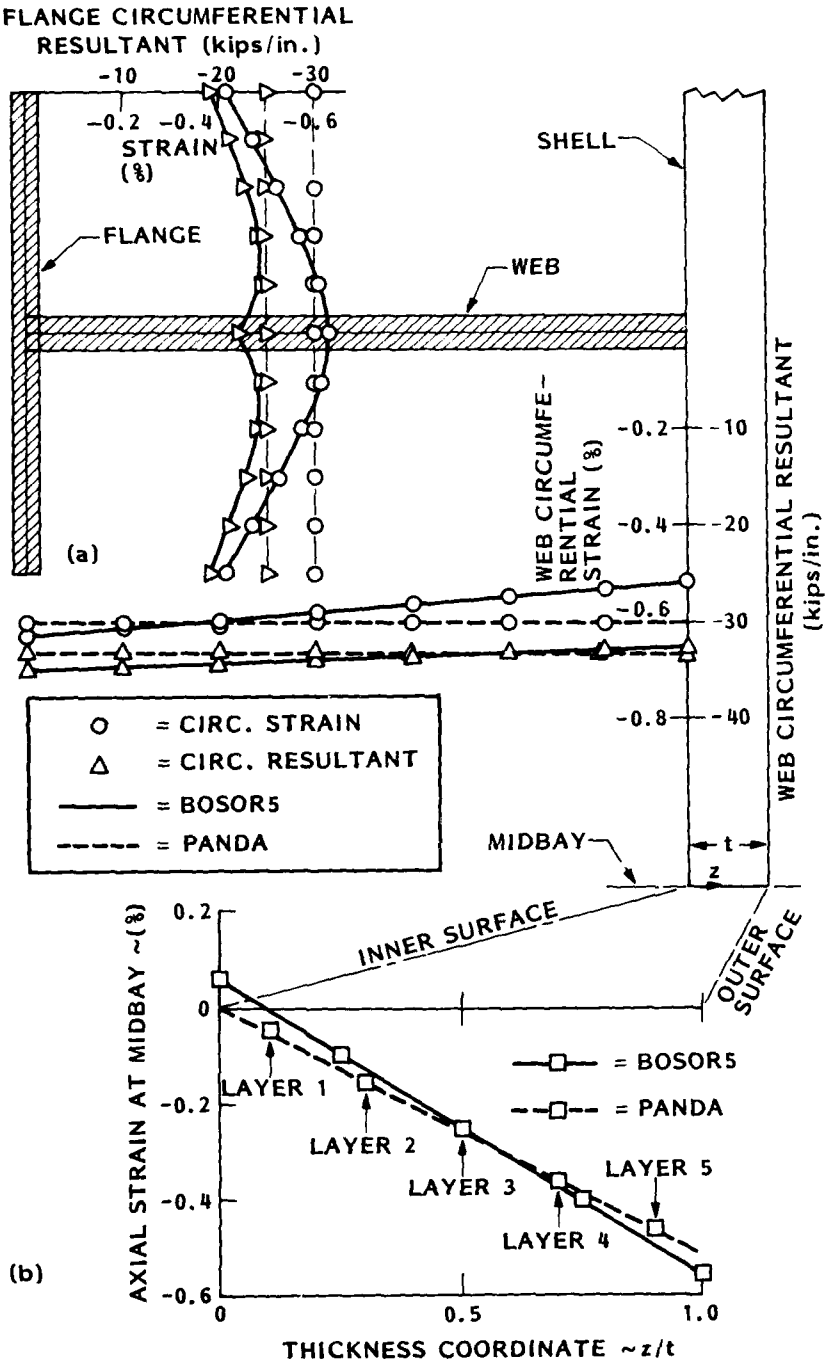

Figure 41. Hydrostatically compressed internally ring-stiffened cylindrical shell optimized by PANDA (5-layered model) for a design pressure of 2710 psi: Comparisons between BOSOR5 and PANDA of the prebuckling state (a) in the ring; (b) in the skin midway between rings.

APPENDIX

PANDA RUNSTREAM FOR

COMPLEX CASE ILLUSTRATED

IN FIGURES 10 AND 11

```
$ RUN BEGIN                    (provide initial design)

 THE INPUT DATA PROVIDED BY YOU DURING EXECUTION
 OF THIS PROGRAM ARE SAVED ON A PERMANENT FILE. PLEASE
 PROVIDE THE NAME (9 CHARACTERS OR LESS AND ONE WORD) FOR THIS
 FILE.

 PERMANENT FILE NAME =
 PERMANENT FILE NAME =PANDACASE.DAT

 IS PART OR ALL OF THE INPUT FOR THIS CASE STORED ON
 THIS FILE YET?
 Y

 PLEASE TYPE A SHORT TITLE ON THE NEXT LINE..
  COMPOSITE STIFF. CYL., FIXED INT. PRESS., NX =-2700, NXY=420 LB/IN.

  DO YOU WANT MORE INFORMATION ABOUT PANDA (Y or N)
 Y


 WELCOME TO *** -BEGIN ***.

     THE OBJECTIVE IS TO DETERMINE CERTAIN DESIGN VARIABLES OF
 A CYLINDRICAL OR FLAT PANEL WITH STRINGERS AND RINGS.
 THE PANEL CAN BE LOADED BY ANY COMBINATION OF UNIFORM
 IN-PLANE AXIAL, CIRCUMFERENTIAL, AND SHEAR STRESS RESULTANTS.

 LOCAL AND GENERAL INSTABILITY AND MAXIMUM STRESS OR
 STRAIN CRITERIA ACT AS CONSTRAINTS ON THE OPTIMUM DESIGN CON-
 FIGURATION.  ELASTIC-PLASTIC BEHAVIOR IS INCLUDED FOR CERTAIN
 MATERIAL TYPES.

  WANT MORE INFORMATION?
 Y


     THE OVERALL DIMENSIONS OF THE PANEL (LENGTH,
 WIDTH, AND RADIUS OF CURVATURE) ARE FIXED.  THE PANEL SKIN
 CONSISTS OF LAYERS OF ORTHOTROPIC MATERIAL, EACH LAYER WITH
 ITS OWN ANGLE OF ORTHOTROPICITY (COMPOSITE LAYUP).
 PLASTICITY IS INCLUDED FOR ISOTROPIC OR UNIDIRECTIONAL
 MATERIALS. DEFORMATION THEORY IS USED FOR THIS.

  WANT MORE INFORMATION?
 Y
     ALL STRINGERS ARE IDENTICAL AND ARE EQUALLY SPACED.
 SAME GOES FOR RINGS.  STRINGER CROSS SECTION AND SPACING CAN
 DIFFER FROM RING CROSS SECTION AND SPACING.  THE FOLLOWING
 INFORMATION APPLIES TO BOTH STRINGERS AND RINGS (CALLED STIF-
 FENERS/).

  WANT MORE INFORMATION?
 Y
```

EACH STIFFENER CROSS SECTION IS BUILT UP OF A NUMBER OF RECTANGULAR SEGMENTS (UP TO 5 PER CROSS SECTION). EACH RECTANGULAR SEGMENT IS ORIENTED EITHER NORMAL OR PARALLEL TO THE PLANE OF THE PANEL SURFACE AT THE LINE OF ATTACHMENT TO THE PANEL. AS OF NOW, THE ASSEMBLAGES OF RECTANGULAR SEGMENTS FORMING THE CROSS SECTIONS OF THE STIFFENERS CANNOT ENCLOSE AREAS. IN THE ANALYSIS THE SEGMENT CROSS SECTIONS ARE ASSUMED TO BE SLENDER, THAT IS, THEIR WIDTHS ARE MUCH GREATER THAN THEIR THICKNESSES.

WANT MORE INFORMATION?
Y

LOCAL BUCKLING OF INDIVIDUAL STIFFENER SEGMENTS IS INCLUDED IN THE ANALYSIS, AS WELL AS LOCAL BUCKLING OF THE SKIN BETWEEN STIFFENERS AND GENERAL INSTABILITY. CERTAIN PANEL INSTABILITY MODES, IDENTIFIED LATER, ARE ALSO INCLUDED.

WANT MORE INFORMATION?
Y

LAMINATED STIFFENER SEGMENTS ARE TREATED IN THE FOLLOWING WAY... THE PROGRAM ASKS FOR THE LAYER THICKNESSES, WINDING ANGLES, AND MATERIAL PROPERTY INDICES, JUST AS IT DOES FOR THE PANEL SKIN. HOWEVER, UNLIKE THE ANALYSIS FOR THE SKIN, WHICH IS TREATED MORE RIGOROUSLY, THE PROGRAM CALCULATES FROM THE SUM OF THE LAMINAE PROPERTIES, EFFECTIVE MODULI, POISSON RATIO, AND DENSITY FOR THE ENTIRE STIFFENER SEGMENT LAMINATE. THE STIFFENER SEGMENT LAMINATE IS THENCEFORTH TREATED AS A MONOCOQUE ORTHOTROPIC MATERIAL OF THICKNESS EQUAL TO THE LAMINATE THICKNESS. THIS TOTAL THICKNESS CAN BE A DECISION VARIABLE IN THE OPTIMIZATION PROCESS. INDIVIDUAL LAMINA THICKNESSES AND WINDING ANGLES IN THE STIFFENER SEGMENT ARE NOT DECISION VARIABLES.

STIFFENER SEGMENT PLASTICITY IS INCLUDED IF THE SEGMENT IS MONOCOQUE AND ISOTROPIC.

WANT MORE INFORMATION?
Y

THE PANEL DESIGN ITERATIONS ARE CARRIED OUT WITH THE ASSUMPTIONS THAT THE PREBUCKLING NORMAL STRAINS (AXIAL AND CIRCUMFERENTIAL) ARE UNIFORM THROUGH THE PANEL SKIN THICKNESS AND UNIFORM (ALTHOUGH POSSIBLY DIFFERENT FROM THE SKIN STRAIN) OVER THE STIFFENER CROSS SECTIONS. THE PREBUCKLING IN-PLANE SHEAR RESULTANT IS CARRIED ONLY BY THE PANEL SKIN

WANT MORE INFORMATION?
Y
FOR CYLINDRICAL PANELS STIFFENED BY RINGS, THE
FACT THAT THE HOOP STRAIN IS GREATER MIDWAY BETWEEN
RINGS THAN AT THE RINGS IS ACCOUNTED FOR

COMPLETE CYLINDRICAL SHELLS MAY BE TREATED
WIDTH OF THE PANEL EQUAL TO

```
THIS CORRESPONDS TO HALF (180 DEG.) OF THE CYLINDER.  HOWEVER,
THE NUMBER OF HALF-WAVES AROUND HALF OF THE FULL (360 DEG.)
CIRCUMFERENCE IS THE SAME AS THE NUMBER OF FULL WAVES AROUND
THE FULL CIRCUMFERENCE.  REMEMBER TO MULTIPLY THE WEIGHT OB-
TAINED BY PANDA BY TWO IF YOU WANT THE WEIGHT OF THE FULL
CYLINDER.

 WANT MORE INFORMATION?
Y


    OPTIMUM DESIGNS ARE DERIVED THROUGH EXECUTION OF
THREE INTERACTIVE COMPUTER PROGRAMS.  THE EXECUTION MODE OF
EACH PROGRAM IS ENTERED WHEN THE USER TYPES THE ENTRIES AS
GIVEN ON THE LEFT BELOW...

      USER TYPES                        IN ORDER TO
      ----------                        -----------

      RUN BEGIN                 PROVIDE INITIAL LOADS, DIMENSIONS,
                                AND MATERIAL PROPERTIES.


      RUN DECIDE                MODIFY LOADING AND/OR DIMENSIONS,
                                DECIDE WHETHER TO DO...
                                 (1) A SIMPLE BUCKLING ANALYSIS OR
                                 (2) AN OPTIMIZATION ANALYSIS
                                AND IF (2) CHOOSE WHICH OF THE
                                DESIGN PARAMETERS ARE DECISION
                                VARIABLES IN THE OPTIMIZATION PROCESS.


      RUN PANCON                PERFORM THE SIMPLE BUCKLING ANALY-
                                SIS OR THE OPTIMIZATION ANALYSIS

 WANT MORE INFORMATION?
Y

THE USUAL SEQUENCE OF PROGRAM EXECUTIONS IS...

      -BEGIN
      -DECIDE
      -PANCON

FOLLOWED BY ADDITIONAL PAIRS

      -DECIDE
      -PANCON

AS A GIVEN DESIGN CONCEPT IS EXPLORED.  (E.G. CYLINDRICAL
SHELL OF GIVEN MATERIAL WITH T-SHAPED RINGS OF GIVEN MATERIAL)
 DO YOU WANT LONG PROMPTS?
Y

IS THE PANEL FLAT  (YES OR NO)...
```

```
N

STRESS RESULTANTS - - AXIAL = NX, CIRCUMFEREN-
TIAL = NY, SHEAR = NXY --(NOTE THAT POSITIVE NX AND NY COR-
RESPOND TO TENSION, POSITIVE NXY IS IN THE +Y COORDINATE DIR-
ECTION ON THE EDGE OF THE PANEL THAT CORRESPONDS TO THE MAX-
IMUM VALUE OF X.--SEE FIG. 2-- .  THE UNITS OF NX, NY, AND
NXY ARE FORCE/LENGTH (e.g. LB/IN).

    YOU WILL FIRST BE ASKED TO
PROVIDE THREE RESULTANTS, (NX,NY, AND NXY), WHICH ARE CON-
SIDERED TO BE BUCKLING PARAMETERS.  THEN YOU WILL BE ASKED TO
PROVIDE TWO RESULTANTS (NXFIXED, NYFIXED), WHICH REPRESENT A
FIXED STATE OF PRESTRESS.  THE TOTAL IN-PLANE STRESS RESULT-
ANTS AT BUCKLING (FOR A LINEAR MATERIAL OR FOR EIGENVALUES=1)
ARE GIVEN BY...

      NXTOT(CRIT) = NXFIXED + EIGENVALUE*NX
      NYTOT(CRIT) = NYFIXED + EIGENVALUE*NY
      NXYTOT(CRIT)=           EIGENVALUE*NXY

NOTE THAT FOR HYDROSTATIC PRESSURE NX = PRESSURE*RADIUS/2
AND NY = PRESSURE*RADIUS.


 AXIAL RESULTANT, NX =
 IS THE AXIAL LOAD COMPRESSIVE...(Y or N)
Y
NX =-0.270E+04
 IS  NX  OKAY...(Y or N)
Y
 CIRCUMFERENTIAL RESULTANT, NY =
 IS THE CIRCUMFERENTIAL LOAD COMPRESSIVE...(Y or N)
Y
NY = 0.000E+00
 IS  NY  OKAY...(Y or N)
Y
 IN-PLANE SHEAR RESULTANT, NXY =
NXY =  420.
 IS  NXY  OKAY...(Y or N)
Y

DO YOU WANT TO READ VALUES FOR AXIAL RESULTANT AND
HOOP RESULTANT  (NXFIXED, NYFIXED) WHICH ARE NOT BUCKLING
PARAMETERS BUT REPRESENT A FIXED PRESTRESSED STATE...
(THE USUAL ANSWER IS NO)
Y
 FIXED AXIAL RESULTANT, NXFIXED =
 IS NXFIXED COMPRESSIVE...
N
NXFIXED =  625.
 IS  NXFIXED  OKAY...(Y or N)
Y
 FIXED CIRCUMFERENTIAL RESULTANT, NYFIXED =
 IS NYFIXED COMPRESSIVE...
```

```
N
NYFIXED = 0.125E+04
 IS  NYFIXED  OKAY...(Y or N)
Y

CYLINDRICAL PANEL RADIUS OF CURVATURE=
CYLINDRICAL PANEL RADIUS, R=  85.0
 IS  THE PANEL RADIUS R OKAY...(Y or N)
Y
 AXIAL LENGTH OF PANEL =
AXIAL LENGTH OF PANEL =  100.
 IS THE AXIAL LENGTH OKAY...(Y or N)
Y
 CIRCUMFERENTIAL LENGTH OF PANEL =
CIRCUMFERENTIAL LENGTH OF PANEL =  267.
 IS THE CIRCUMFERENTIAL LENGTH OKAY...(Y or N)
Y

NUMBER OF LAYERS IN PANEL SKIN=
NUMBER OF LAYERS IN PANEL SKIN=  ?
 IS THE NUMBER OF LAYERS OKAY...(Y or N)
Y

PANEL SKIN LAYER THICKNESSES (INNER LAYER IS FIRST)

TLAYER( 1) = ...
TLAYER( 1) =  5.000E-03
IS TLAYER( 1) OKAY....(Y or N)
Y

TLAYER( 2) = ...
TLAYER( 2) =  5.000E-03
IS TLAYER( 2) OKAY....(Y or N)
Y

TLAYER( 3) = ...
TLAYER( 3) =  5.000E-03
IS TLAYER( 3) OKAY....(Y or N)
Y

TLAYER( 4) = ...
TLAYER( 4) =  1.000E-02
IS TLAYER( 4) OKAY....(Y or N)
Y

TLAYER( 5) = ...
TLAYER( 5) =  5.000E-03
IS TLAYER( 5) OKAY....(Y or N)
Y

TLAYER( 6) = ...
TLAYER( 6) =  5.000E-03
IS TLAYER( 6) OKAY....(Y or N)
Y
```

```
TLAYER( 7) = ...
TLAYER( 7) =  5.000E-03
IS TLAYER( 7) OKAY....(Y or N)
Y

PANEL SKIN LAYER WINDING ANGLES (DEGREES)

 ALPHA( 1) = ...
 ALPHA( 1) =   90.0
IS  ALPHA( 1) OKAY....(Y or N)
Y

 ALPHA( 2) = ...
 ALPHA( 2) =   45.0
IS  ALPHA( 2) OKAY....(Y or N)
Y

 ALPHA( 3) = ...
 ALPHA( 3) =  -45.0
IS  ALPHA( 3) OKAY....(Y or N)
Y

 ALPHA( 4) = ...
 ALPHA( 4) =  0.000E+00
IS  ALPHA( 4) OKAY....(Y or N)
Y

 ALPHA( 5) = ...
 ALPHA( 5) =  -45.0
IS  ALPHA( 5) OKAY....(Y or N)
Y

 ALPHA( 6) = ...
 ALPHA( 6) =   45.0
IS  ALPHA( 6) OKAY....(Y or N)
Y

 ALPHA( 7) = ...
 ALPHA( 7) =   90.0
IS  ALPHA( 7) OKAY....(Y or N)
Y

PANEL SKIN LAYER MATERIAL TYPES (1, 2, 3, ...)

  MATL( 1) = ...
  MATL( 1) =   1
IS   MATL( 1) OKAY....(Y or N)
Y

  MATL( 2) = ...
  MATL( 2) =   1
IS   MATL( 2) OKAY....(Y or N)
Y

  MATL( 3) = ...
```

```
  MATL( 3) =   1
IS   MATL( 3) OKAY....(Y or N)
Y

  MATL( 4) = ...
  MATL( 4) =   1
IS   MATL( 4) OKAY....(Y or N)
Y

  MATL( 5) = ...
  MATL( 5) =   1
IS   MATL( 5) OKAY....(Y or N)
Y

  MATL( 6) = ...
  MATL( 6) =   1
IS   MATL( 6) OKAY....(Y or N)
Y

  MATL( 7) = ...
  MATL( 7) =   1
IS   MATL( 7) OKAY....(Y or N)
Y

IS THE PANEL STIFFENED...  (YES OR NO)
Y
```

STIFFENERS OF ARBITRARY CROSS SECTION GEOMETRY ARE BUILT UP OF AS MANY AS 5 RECTANGULAR SEGMENTS, EACH WITH ITS OWN THICKNESS AND WIDTH. THE THEORY IS VALID IF THE THICKNESS IS LESS THAN ABOUT ONE QUARTER OF THE WIDTH. (WE USE THE TERM --WIDTH-- HERE INSTEAD OF --LENGTH-- IN ORDER TO AVOID CONFUSION WITH THE LENGTH OF THE STIFFENER, WHICH IS ,OF COURSE, EQUAL TO ONE OF THE DIMENSIONS OF THE PANEL. WE ARE REFERRING HERE TO THE STIFFENER CROSS SECTION DIMENSIONS.)

YOU WILL BE ASKED TO PROVIDE DATA FOR..

1. THE NUMBER OF SEGMENTS IN THE STIFFENER CROSS SECTION
   (CALLED --NPARTS-- FOR STRINGERS AND
   --NPARTR-- FOR RINGS,

2. STIFFENER SEGMENT WIDTHS AND THICKNESSES,
   (LAMINA THICKNESSES, WINDING ANGLES, AND MATERIAL TYPES
   IF THE SEGMENT IS OF COMPOSITE MATERIAL)

3. ANGULAR ORIENTATIONS OF THE RECTANGULAR SEGMENTS WITH
   RESPECT TO THE NORMAL TO THE PANEL AT THE STIFFENER
   LINE OF ATTACHMENT,

4. HOW THE SEGMENTS ARE CONNECTED TO EACH OTHER AND TO THE
   PANEL SKIN,

5. WHETHER OR NOT EACH SEGMENT HAS A FREE END,

```
  6. MATERIAL TYPE INDICATORS FOR EACH SEGMENT.

 WANT MORE INFORMATION?
Y

     NOTE THAT STIFFENER SEGMENTS MUST BE JOINED END TO END.
THEREFORE, A T-SHAPED STIFFENER MUST HAVE THREE SEGMENTS, AS
SHOWN BELOW.  AN I-SHAPED STIFFENER MUST HAVE FIVE SEGMENTS.
```

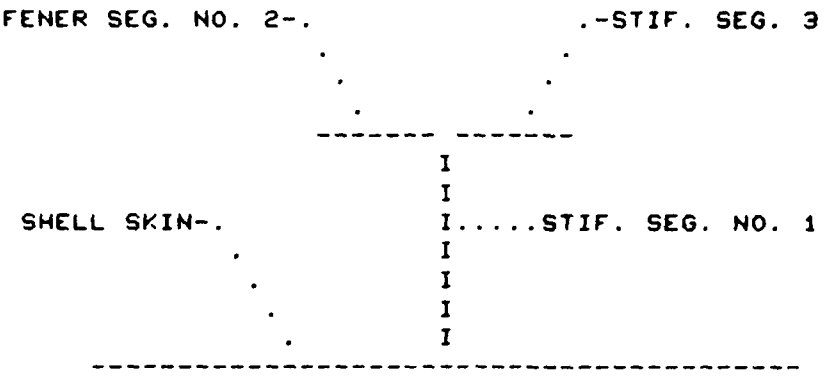


```
DOES THE PANEL HAVE STRINGERS (AXIAL STIFFENERS)
Y



NEXT PROVIDE INPUT DATA FOR STRINGERS...
ARC LENGTH, B0, BETWEEN ADJACENT STRINGERS =
ARC LENGTH BETWEEN STRINGERS, B0=  10.0
 IS  THE STRINGER SPACING, B0,   OKAY...(Y or N)
Y
YOU MUST NOW SPECIFY WHETHER THESTRINGERS ARE INTERNAL OR EXTERNAL.
ARE THESTRINGERS INTERNAL?
N
WHAT TYPE OF CROSS SECTION DO THESTRINGERS HAVE?

CHOOSE ONE OF THE FOLLOWING...
RECTANGULAR (please type the letter R)
T-SHAPED (FLANGE AWAY FROM PANEL SKIN) (type the letter T)
INVERTED T (FLANGE NEXT TO PANEL SKIN)  (type T2)
Z-SHAPED    (type the letter Z)
I-SHAPED    (type the letter I)
C-SHAPED (CHANNEL)     (please type C)
L-SHAPED (ANGLE) (FLANGE AWAY FROM SKIN) (please type L)
INVERTED L (ANGLE) (FLANGE NEXT TO SKIN) (please type L2)
OTHER    (please type the word OTHER)

STRINGERS CROSS SECTION INDICATOR=L
  IS THE CROSS SECTION INDICATOR OKAY? (Y or N)
```

```
Y


 STIFFENER SEG. NO. 2-.
                        .
                         .
                          .
                        --------
                               I
                               I
      SHELL SKIN-.             I.....STIF. SEG. NO. 1
                  .            I
                   .           I
                    .          I
                     .         I
           ----------------------------------------

WHILE PROVIDING THE FOLLOWING INPUT DATA, PLEASE REFER
TO THE SKETCH ABOVE FOR A DIAGRAM OF THE STRINGER CROSS SEC-
TION AND THE STRINGER SEGMENT NUMBERING SCHEME.

ARE ANY OF THE STRINGER SEGMENTS MADE OF
LAYERED OR COMPOSITE MATERIAL...
Y

NUMBER OF LAYERS IN STRINGER SEGMENT 1 =
NUMBER OF LAYERS IN CURRENT STRINGER SEGMENT= 16
 IS THE NUMBER OF LAYERS OKAY...(Y or N)
Y

THICKNESSES OF EACH OF THE16 LAYERS IN STRINGER
SEGMENT NO. 1

STRINGER SEGMENT LAYER THICKNESSES

TLAYER( 1) = ...
TLAYER( 1) =  5.000E-03
IS TLAYER( 1) OKAY....(Y or N)
Y

TLAYER( 2) = ...
TLAYER( 2) =  5.000E-03
IS TLAYER( 2) OKAY....(Y or N)
Y

TLAYER( 3) = ...
TLAYER( 3) =  5.000E-03
IS TLAYER( 3) OKAY....(Y or N)
Y

TLAYER( 4) = ...
TLAYER( 4) =  5.000E-03
IS TLAYER( 4) OKAY....(Y or N)
Y
```

```
TLAYER( 5) = ...
TLAYER( 5) =  5.000E-03
IS TLAYER( 5) OKAY....(Y or N)
Y

TLAYER( 6) = ...
TLAYER( 6) =  5.000E-03
IS TLAYER( 6) OKAY....(Y or N)
Y

TLAYER( 7) = ...
TLAYER( 7) =  5.000E-03
IS TLAYER( 7) OKAY....(Y or N)
Y

TLAYER( 8) = ...
TLAYER( 8) =  5.000E-03
IS TLAYER( 8) OKAY....(Y or N)
Y

TLAYER( 9) = ...
TLAYER( 9) =  5.000E-03
IS TLAYER( 9) OKAY....(Y or N)
Y

TLAYER(10) = ...
TLAYER(10) =  5.000E-03
IS TLAYER(10) OKAY....(Y or N)
Y

TLAYER(11) = ...
TLAYER(11) =  5.000E-03
IS TLAYER(11) OKAY....(Y or N)
Y

TLAYER(12) = ...
TLAYER(12) =  5.000E-03
IS TLAYER(12) OKAY....(Y or N)
Y

TLAYER(13) = ...
TLAYER(13) =  5.000E-03
IS TLAYER(13) OKAY....(Y or N)
Y

TLAYER(14) = ...
TLAYER(14) =  5.000E-03
IS TLAYER(14) OKAY....(Y or N)
Y

TLAYER(15) = ...
TLAYER(15) =  5.000E-03
IS TLAYER(15) OKAY....(Y or N)
Y
```

```
TLAYER(16) = ...
TLAYER(16) =  5.000E-03
IS TLAYER(16) OKAY....(Y or N)
Y

WINDING ANGLES OF EACH OF THE 16 LAYERS IN
STRINGER SEGMENT NO. 1
NOTE.. ZERO WINDING ANGLE MEANS FIBERS RUNNING ALONG
THE AXIS OF THE STRINGER.)

STRINGER SEGMENT LAYER WINDING ANGLES (DEGREES)

 ALPHA( 1) = ...
 ALPHA( 1) =   90.0
IS  ALPHA( 1) OKAY....(Y or N)
Y

 ALPHA( 2) = ...
 ALPHA( 2) =   45.0
IS  ALPHA( 2) OKAY....(Y or N)
Y

 ALPHA( 3) = ...
 ALPHA( 3) =  -45.0
IS  ALPHA( 3) OKAY....(Y or N)
Y

 ALPHA( 4) = ...
 ALPHA( 4) =  0.000E+00
IS  ALPHA( 4) OKAY....(Y or N)
Y

 ALPHA( 5) = ...
 ALPHA( 5) =  0.000E+00
IS  ALPHA( 5) OKAY....(Y or N)
Y

 ALPHA( 6) = ...
 ALPHA( 6) =  -45.0
IS  ALPHA( 6) OKAY....(Y or N)
Y

 ALPHA( 7) = ...
 ALPHA( 7) =   45.0
IS  ALPHA( 7) OKAY....(Y or N)
Y

 ALPHA( 8) = ...
 ALPHA( 8) =   90.0
IS  ALPHA( 8) OKAY....(Y or N)
Y

 ALPHA( 9) = ...
 ALPHA( 9) =   90.0
IS  ALPHA( 9) OKAY....(Y or N)
```

```
Y

 ALPHA(10) = ...
 ALPHA(10) =   45.0
IS  ALPHA(10) OKAY....(Y or N)
Y

 ALPHA(11) = ...
 ALPHA(11) =  -45.0
IS  ALPHA(11) OKAY....(Y or N)
Y

 ALPHA(12) = ...
 ALPHA(12) =  0.000E+00
IS  ALPHA(12) OKAY....(Y or N)
Y

 ALPHA(13) = ...
 ALPHA(13) =  0.000E+00
IS  ALPHA(13) OKAY....(Y or N)
Y

 ALPHA(14) = ...
 ALPHA(14) =  -45.0
IS  ALPHA(14) OKAY....(Y or N)
Y

 ALPHA(15) = ...
 ALPHA(15) =   45.0
IS  ALPHA(15) OKAY....(Y or N)
Y

 ALPHA(16) = ...
 ALPHA(16) =   90.0
IS  ALPHA(16) OKAY....(Y or N)
Y

MATERIAL TYPES OF EACH OF THE 16 LAYERS IN
STRINGER SEGMENT NO. 1

STRINGER SEGMENT LAYER MATERIAL TYPES (1, 2, 3,...)

  MATL( 1) = ...
  MATL( 1) =   1
IS   MATL( 1) OKAY....(Y or N)
Y

  MATL( 2) = ...
  MATL( 2) =   1
IS   MATL( 2) OKAY....(Y or N)
Y

  MATL( 3) = ...
  MATL( 3) =   1
IS   MATL( 3) OKAY....(Y or N)
```

```
Y

  MATL( 4) = ...
  MATL( 4) =   1
IS   MATL( 4) OKAY....(Y or N)
Y

  MATL( 5) = ...
  MATL( 5) =   1
IS   MATL( 5) OKAY....(Y or N)
Y

  MATL( 6) = ...
  MATL( 6) =   1
IS   MATL( 6) OKAY....(Y or N)
Y

  MATL( 7) = ...
  MATL( 7) =   1
IS   MATL( 7) OKAY....(Y or N)
Y

  MATL( 8) = ...
  MATL( 8) =   1
IS   MATL( 8) OKAY....(Y or N)
Y

  MATL( 9) = ...
  MATL( 9) =   1
IS   MATL( 9) OKAY....(Y or N)
Y

  MATL(10) = ...
  MATL(10) =   1
IS   MATL(10) OKAY....(Y or N)
Y

  MATL(11) = ...
  MATL(11) =   1
IS   MATL(11) OKAY....(Y or N)
Y

  MATL(12) = ...
  MATL(12) =   1
IS   MATL(12) OKAY....(Y or N)
Y

  MATL(13) = ...
  MATL(13) =   1
IS   MATL(13) OKAY....(Y or N)
Y

  MATL(14) = ...
  MATL(14) =   1
IS   MATL(14) OKAY....(Y or N)
```

```
Y

  MATL(15) = ...
  MATL(15) =   1
IS   MATL(15) OKAY....(Y or N)
Y

  MATL(16) = ...
  MATL(16) =   1
IS   MATL(16) OKAY....(Y or N)
Y

NUMBER OF LAYERS IN STRINGER SEGMENT 2 =
NUMBER OF LAYERS IN CURRENT STRINGER SEGMENT= 17
 IS THE NUMBER OF LAYERS OKAY...(Y or N)
Y

THICKNESSES OF EACH OF THE17 LAYERS IN STRINGER
SEGMENT NO. 2

STRINGER SEGMENT LAYER THICKNESSES

TLAYER( 1) = ...
TLAYER( 1) =  5.000E-03
IS TLAYER( 1) OKAY....(Y or N)
Y

TLAYER( 2) = ...
TLAYER( 2) =  5.000E-03
IS TLAYER( 2) OKAY....(Y or N)
Y

TLAYER( 3) = ...
TLAYER( 3) =  5.000E-03
IS TLAYER( 3) OKAY....(Y or N)
Y

TLAYER( 4) = ...
TLAYER( 4) =  5.000E-03
IS TLAYER( 4) OKAY....(Y or N)
Y

TLAYER( 5) = ...
TLAYER( 5) =  5.000E-03
IS TLAYER( 5) OKAY....(Y or N)
Y

TLAYER( 6) = ...
TLAYER( 6) =  5.000E-03
IS TLAYER( 6) OKAY....(Y or N)
Y

TLAYER( 7) = ...
TLAYER( 7) =  5.000E-03
IS TLAYER( 7) OKAY....(Y or N)
```

```
Y

TLAYER( 8) = ...
TLAYER( 8) =  5.000E-03
IS TLAYER( 8) OKAY....(Y or N)
Y

TLAYER( 9) = ...
TLAYER( 9) =  0.100
IS TLAYER( 9) OKAY....(Y or N)
Y

TLAYER(10) = ...
TLAYER(10) =  5.000E-03
IS TLAYER(10) OKAY....(Y or N)
Y

TLAYER(11) = ...
TLAYER(11) =  5.000E-03
IS TLAYER(11) OKAY....(Y or N)
Y

TLAYER(12) = ...
TLAYER(12) =  5.000E-03
IS TLAYER(12) OKAY....(Y or N)
Y

TLAYER(13) = ...
TLAYER(13) =  5.000E-03
IS TLAYER(13) OKAY....(Y or N)
Y

TLAYER(14) = ...
TLAYER(14) =  5.000E-03
IS TLAYER(14) OKAY....(Y or N)
Y

TLAYER(15) = ...
TLAYER(15) =  5.000E-03
IS TLAYER(15) OKAY....(Y or N)
Y

TLAYER(16) = ...
TLAYER(16) =  5.000E-03
IS TLAYER(16) OKAY....(Y or N)
Y

TLAYER(17) = ...
TLAYER(17) =  5.000E-03
IS TLAYER(17) OKAY....(Y or N)
Y

WINDING ANGLES OF EACH OF THE 17 LAYERS IN
STRINGER SEGMENT NO. 2
NOTE.. ZERO WINDING ANGLE MEANS FIBERS RUNNING ALONG
```

```
THE AXIS OF THE STRINGER.)

STRINGER SEGMENT LAYER WINDING ANGLES (DEGREES)

 ALPHA( 1) = ...
 ALPHA( 1) =   90.0
IS  ALPHA( 1) OKAY....(Y or N)
Y

 ALPHA( 2) = ...
 ALPHA( 2) =   45.0
IS  ALPHA( 2) OKAY....(Y or N)
Y

 ALPHA( 3) = ...
 ALPHA( 3) =  -45.0
IS  ALPHA( 3) OKAY....(Y or N)
Y

 ALPHA( 4) = ...
 ALPHA( 4) =  0.000E+00
IS  ALPHA( 4) OKAY....(Y or N)
Y

 ALPHA( 5) = ...
 ALPHA( 5) =  0.000E+00
IS  ALPHA( 5) OKAY....(Y or N)
Y

 ALPHA( 6) = ...
 ALPHA( 6) =  -45.0
IS  ALPHA( 6) OKAY....(Y or N)
Y

 ALPHA( 7) = ...
 ALPHA( 7) =   45.0
IS  ALPHA( 7) OKAY....(Y or N)
Y

 ALPHA( 8) = ...
 ALPHA( 8) =   90.0
IS  ALPHA( 8) OKAY....(Y or N)
Y

 ALPHA( 9) = ...
 ALPHA( 9) =  0.000E+00
IS  ALPHA( 9) OKAY....(Y or N)
Y

 ALPHA(10) = ...
 ALPHA(10) =   90.0
IS  ALPHA(10) OKAY....(Y or N)
Y

 ALPHA(11) = ...
```

```
 ALPHA(11) =   45.0
IS  ALPHA(11) OKAY....(Y or N)
Y

 ALPHA(12) = ...
 ALPHA(12) =  -45.0
IS  ALPHA(12) OKAY....(Y or N)
Y

 ALPHA(13) = ...
 ALPHA(13) =  0.000E+00
IS  ALPHA(13) OKAY....(Y or N)
Y

 ALPHA(14) = ...
 ALPHA(14) =  0.000E+00
IS  ALPHA(14) OKAY....(Y or N)
Y

 ALPHA(15) = ...
 ALPHA(15) =  -45.0
IS  ALPHA(15) OKAY....(Y or N)
Y

 ALPHA(16) = ...
 ALPHA(16) =   45.0
IS  ALPHA(16) OKAY....(Y or N)
Y

 ALPHA(17) = ...
 ALPHA(17) =   90.0
IS  ALPHA(17) OKAY....(Y or N)
Y

MATERIAL TYPES OF EACH OF THE 17 LAYERS IN
STRINGER SEGMENT NO. 2

STRINGER SEGMENT LAYER MATERIAL TYPES (1, 2, 3,...)

  MATL( 1) = ...
  MATL( 1) =   1
IS   MATL( 1) OKAY....(Y or N)
Y

  MATL( 2) = ...
  MATL( 2) =   1
IS   MATL( 2) OKAY....(Y or N)
Y

  MATL( 3) = ...
  MATL( 3) =   1
IS   MATL( 3) OKAY....(Y or N)
Y

  MATL( 4) = ...
```

```
  MATL( 4) =    1
IS    MATL( 4) OKAY....(Y or N)
Y

  MATL( 5) = ...
  MATL( 5) =    1
IS    MATL( 5) OKAY....(Y or N)
Y

  MATL( 6) = ...
  MATL( 6) =    1
IS    MATL( 6) OKAY....(Y or N)
Y

  MATL( 7) = ...
  MATL( 7) =    1
IS    MATL( 7) OKAY....(Y or N)
Y

  MATL( 8) = ...
  MATL( 8) =    1
IS    MATL( 8) OKAY....(Y or N)
Y

  MATL( 9) = ...
  MATL( 9) =    1
IS    MATL( 9) OKAY....(Y or N)
Y

  MATL(10) = ...
  MATL(10) =    1
IS    MATL(10) OKAY....(Y or N)
Y

  MATL(11) = ...
  MATL(11) =    1
IS    MATL(11) OKAY....(Y or N)
Y

  MATL(12) = ...
  MATL(12) =    1
IS    MATL(12) OKAY....(Y or N)
Y

  MATL(13) = ...
  MATL(13) =    1
IS    MATL(13) OKAY....(Y or N)
Y

  MATL(14) = ...
  MATL(14) =    1
IS    MATL(14) OKAY....(Y or N)
Y

  MATL(15) = ...
```

```
  MATL(15) =   1
IS   MATL(15) OKAY....(Y or N)
Y

  MATL(16) = ...
  MATL(16) =   1
IS   MATL(16) OKAY....(Y or N)
Y

  MATL(17) = ...
  MATL(17) =   1
IS   MATL(17) OKAY....(Y or N)
Y

STRINGER SEGMENT WIDTHS (HEIGHT, NOT THICKNESS)

    BS( 1) = ...
    BS( 1) =   1.00
IS     BS( 1) OKAY....(Y or N)
Y

    BS( 2) = ...
    BS( 2) =  0.500
IS     BS( 2) OKAY....(Y or N)
Y


 REVIEW OF STRINGER INPUT DATA FOR 2 STRINGER SEGS.
SEG.   BS(I)     ANGLES(I)  THICKNESS    CONNECT.  FREE END  MATL TYPE
 1    1.00E+00   0.00E+00   8.00E-02          0       NO        9999
 2    5.00E-01   9.00E+01   1.80E-01          1      YES        9999

DO YOU WANT ANOTHER CHANCE TO PROVIDE STRINGER INPUT DATA(YES OR NO)
N

DOES THE PANEL HAVE RINGS
Y



NEXT PROVIDE NUMERICAL INPUT DATA FOR RINGS...
SPACING, A, BETWEEN ADJACENT RINGS =
SPACING BETWEEN RINGS=  10.0
 IS THE RING SPACING, A0, OKAY...(Y or N)
Y
YOU MUST NOW SPECIFY WHETHER THE  RINGS   ARE INTERNAL OR EXTERNAL.
ARE THE  RINGS   INTERNAL?
Y
WHAT TYPE OF CROSS SECTION DO THE  RINGS   HAVE?

CHOOSE ONE OF THE FOLLOWING...
RECTANGULAR (please type the letter R)
T-SHAPED (FLANGE AWAY FROM PANEL SKIN) (type the letter T)
INVERTED T (FLANGE NEXT TO PANEL SKIN)  (type T2)
Z-SHAPED    (type the letter Z)
```

```
I-SHAPED    (type the letter I)
[-SHAPED (CHANNEL)     (please type C)
L-SHAPED (ANGLE) (FLANGE AWAY FROM SKIN) (please type L)
INVERTED L (ANGLE) (FLANGE NEXT TO SKIN) (please type L2)
OTHER    (please type the word OTHER)

 RINGS   CROSS SECTION INDICATOR=L
 IS THE CROSS SECTION INDICATOR OKAY? (Y or N)
Y


 STIFFENER SEG. NO. 2-.
                          .
                           .
                            .
                          --------
                                 I
                                 I
      SHELL SKIN-.               I.....STIF. SEG. NO. 1
                  .              I
                   .             I
                    .            I
                     .           I
           ------------------------------------------

WHILE PROVIDING THE FOLLOWING INPUT DATA, PLEASE
REFER TO THE SKETCH ABOVE FOR A DIAGRAM OF THE RING CROSS
SECTION AND THE SEGMENT NUMBERING SCHEME.

ARE ANY OF THE RING SEGMENTS MADE OF
LAYERED OR COMPOSITE MATERIAL...
N

RING SEGMENT THICKNESSES

    TR( 1) = ...
    TR( 1) =  5.000E-02
IS      TR( 1) OKAY....(Y or N)
Y

    TR( 2) = ...
    TR( 2) =  5.000E-02
IS      TR( 2) OKAY....(Y or N)
Y

RING SEGMENT WIDTHS (HEIGHT, NOT THICKNESS)

    BR( 1) = ...
    BR( 1) =   1.00
IS      BR( 1) OKAY....(Y or N)
Y

    BR( 2) = ...
    BR( 2) =  0.500
IS      BR( 2) OKAY....(Y or N)
```

```
Y

RING SEGMENT MATERIAL TYPES (1, 2, 3,...)

  MATL( 1) = ...
  MATL( 1) =   2
IS   MATL( 1) OKAY....(Y or N)
Y

  MATL( 2) = ...
  MATL( 2) =   2
IS   MATL( 2) OKAY....(Y or N)
Y


  REVIEW OF RING INPUT DATA FOR 2 RING SEGMENTS
SEG.   BR(I)     ANGLES(I)  THICKNESS    CONNECT.  FREE END  MATL TYPE
 1   1.00E+00    1.80E+02   5.00E-02          0        NO          2
 2   5.00E-01    9.00E+01   5.00E-02          1       YES          2

DO YOU WANT ANOTHER CHANCE TO PROVIDE RING INPUT DATA (YES OR NO)
N

YOU WILL NOW BE ASKED TO PROVIDE MATERIAL PROPERTIES
CORRESPONDING TO THE MATERIAL TYPES THAT YOU HAVE ALREADY IN-
DICATED.  IN THE FOLLOWING E1 DENOTES THE MODULUS ALONG THE
FIBER AXIS FOR EACH LAYER OF A COMPOSITE LAMINATE OR IN THE
CASE OF NON-LAYERED STIFFENERS E1 IS THE MODULUS ALONG THE
STIFFENER AXIS FOR EACH STIFFENER SEGMENT.  (FOR EXAMPLE, IN
THE CASE OF A RING THE STIFFENER AXIS RUNS IN THE PANEL CIR-
CUMFERENTIAL DIRECTION.)  E2 IS THE MODULUS FOR THE DIRECTION
NORMAL TO THE E1-DIRECTION.
NUMBER OF DIFFERENT MATERIALS SPECIFIED = 2

MATERIAL PROPERTIES FOR MATERIAL TYPE 1
MODULI E1, E2, AND G; POISSONS RATIO NU; AND
DENSITY RHO ARE TO BE PROVIDED NOW FOR MATERIAL TYPE NO.  1

 MODULUS E1 IN MATL FIBER DIRECTION OR STIFFENER AXIS=
MATERIAL TYPE  1 AND  E1( 1) = 0.230E+08
 IS  THE MODULUS E1  OKAY...(Y or N)
Y
 IS THIS MATERIAL ISOTROPIC?
N
 MODULUS E2 IN DIRECTION PERPENDICULAR TO E1 =
MATERIAL TYPE  1 AND  E2( 1) = 0.170E+07
 IS THE MODULUS  E2  OKAY...
Y
 IN-PLANE SHEAR MODULUS G =
MATERIAL TYPE  1 AND   G( 1) = 0.940E+06
 IS THE SHEAR MODULUS  G  OKAY...
Y

NOTE THAT THE POISSONS RATIO THAT YOU ARE TO PROVIDE
IS ASSUMED TO SATISFY THE EQUATION..
```

```
       NU(INPUT)  =  NU12  =  NU21 * E2/E1


 POISSONS RATIO NU =
MATERIAL TYPE  1 AND  NU( 1) = 0.225E-01
 IS POISSONS RATIO NU OKAY...
Y
 WEIGHT DENSITY (e.g. LB/CUBIC INCH), RHO =
MATERIAL TYPE  1 AND RHO( 1) = 0.560E-01
 IS THE DENSITY RHO OKAY...
Y
DO YOU WANT TO PROVIDE A STRESS-STRAIN CURVE FOR THIS MATERIAL..

N
FOR THIS MATERIAL YOU MAY SPECIFY EITHER A SINGLE
MAXIMUM ALLOWABLE EFFECTIVE STRESS  OR  FIVE ULTIMATE
STRAIN COMPONENTS.


DO YOU WANT TO SPECIFY A SINGLE MAXIMUM ALLOWABLE
EFFECTIVE STRESS...(Y or N)
N
NOW PROVIDE 5 ULTIMATE STRAIN COMPONENTS...
EPS1(TENSION), EPS1(COMPRESSION), EPS2(+), EPS2(-), EPS12(SHEAR) =
 MAX. TENSILE STRAIN IN E1-DIRECTION =
MATERIAL TYPE  1 AND MAX.  EPS1(  TENSION  ) = 0.565E-02
 IS THE MAXIMUM VALUE OF EPS1(TENSION) OKAY...
Y
 MAX. COMPRESSIVE STRAIN IN E1-DIRECTION =
MATERIAL TYPE  1 AND MAX.  EPS1(COMPRESSION) = 0.452E-02
 IS THE MAXIMUM VALUE OF EPS1(COMPRESSION) OKAY...
Y
 MAX. TENSILE STRAIN IN E2-DIRECTION =
MATERIAL TYPE  1 AND MAX.  EPS2(  TENSION  ) = 0.320E-02
 IS THE MAXIMUM VALUE OF EPS2(TENSION) OKAY...
Y
 MAX. COMPRESSIVE STRAIN IN E2-DIRECTION =
MATERIAL TYPE  1 AND MAX.  EPS2(COMPRESSION) = 0.125E-01
 IS THE MAXIMUM VALUE OF EPS2(COMPRESSION) OKAY...
Y
 MAX. IN-PLANE SHEAR STRAIN =
MATERIAL TYPE  1 AND MAX. EPS12(  SHEAR    ) = 0.125E-01
 IS THE MAXIMUM VALUE OF EPS12(SHEAR) OKAY...
Y

DO YOU WANT ANOTHER CHANCE TO PROVIDE MATERIAL
PROPERTIES FOR THIS MATERIAL TYPE..
N

MATERIAL PROPERTIES FOR MATERIAL TYPE 2
MODULI E1, E2, AND G; POISSONS RATIO NU; AND
DENSITY RHO ARE TO BE PROVIDED NOW FOR MATERIAL TYPE NO.  2

 MODULUS E1 IN MATL FIBER DIRECTION OR STIFFENER AXIS=
```

```
MATERIAL TYPE  2 AND  E1( 2) = 0.100E+08
 IS  THE MODULUS E1  OKAY...(Y or N)
Y
 IS THIS MATERIAL ISOTROPIC?
Y
 POISSONS RATIO NU =
MATERIAL TYPE  2 AND  NU( 2) = 0.300
 IS POISSONS RATIO NU OKAY...
Y
 WEIGHT DENSITY (e.g. LB/CUBIC INCH), RHO =
MATERIAL TYPE  2 AND RHO( 2) = 0.100
 IS THE DENSITY RHO OKAY...
Y
DO YOU WANT TO PROVIDE A STRESS-STRAIN CURVE FOR THIS MATERIAL..

N
FOR THIS MATERIAL YOU MAY SPECIFY EITHER A SINGLE
MAXIMUM ALLOWABLE EFFECTIVE STRESS  OR  FIVE ULTIMATE
STRAIN COMPONENTS.


DO YOU WANT TO SPECIFY A SINGLE MAXIMUM ALLOWABLE
EFFECTIVE STRESS...(Y or N)
Y
MAXIMUM ALLOWABLE EFFECTIVE STRESS =
MATL TYPE  2. MAX EFFECTIVE STRESS = 0.400E+05
 IS THE MAXIMUM VALUE OF EFFECTIVE STRESS OKAY...
Y

DO YOU WANT ANOTHER CHANCE TO PROVIDE MATERIAL
PROPERTIES FOR THIS MATERIAL TYPE..
N

MATERIAL PROPERTIES FOR STRINGER SEGMENT 1
MATERIAL TYPE  3  E1  E2, G, NU, RHO =
  9.002E+06   9.002E+06   3.449E+06   3.052E-01   5.600E-02

MAXIMUM ALLOWABLE TENSILE AND COMPRESSIVE
STRAINS IN STRINGER SEGMENT 1 (MATERIAL TYPE  3)
MAX. TENSILE STRAIN      =   3.200E-03
MAX. COMPRESSIVE STRAIN =   -4.520E-03

MATERIAL PROPERTIES FOR STRINGER SEGMENT 2
MATERIAL TYPE  4  E1, E2, G, NU, RHO =
  1.678E+07   5.208E+06   2.055E+06   9.469E-02   5.600E-02

MAXIMUM ALLOWABLE TENSILE AND COMPRESSIVE
STRAINS IN STRINGER SEGMENT 2 (MATERIAL TYPE  4)
MAX. TENSILE STRAIN      =   3.200E-03
MAX. COMPRESSIVE STRAIN =   -4.520E-03

IT MAY SOMETIMES BE ADVISABLE TO DESIGN A PANEL SUCH
THAT LOCAL BUCKLING OCCURS AT A DIFFERENT LOAD FROM GENERAL
INSTABILITY.  IN THIS PROGRAM WE ALLOW FOR A FACTOR, PHI, TO
BE PROVIDED BY YOU, SUCH THAT
```

```
    (LOCAL INSTABILITY LOAD) = PHI*(GENERAL INSTABILITY LOAD)
DO YOU WISH TO PROVIDE A VALUE FOR PHI DIFFERENT FROM UNITY
N
```

WHEN YOUR TERMINAL SAYS

READY

PLEASE TYPE THE COMMAND

-DECIDE

(*The following is the input data file PANDACASE.DAT generated by execution of BEGIN. If any errors were made during interactive input, they can be corrected by editing of this file, rather than having to answer all the questions posed by BEGIN again.*)

```
COMPOSITE STIFF. CYL., FIXED INT. PRESS., NX =-2700, NXY=420
LB/IN.
Y           WANT MORE INFORMATION?
Y           WANT MORE INFORMATION?
Y           WANT MORE INFORMATION?
Y           WANT MORE INFORMATION?
Y           WANT MORE INFORMATION?
Y           WANT MORE INFORMATION?
Y           WANT MORE INFORMATION?
Y           WANT MORE INFORMATION?
Y           WANT MORE INFORMATION?
Y           WANT MORE INFORMATION?
Y           WANT LONG PROMPTS?
N           IS PANEL FLAT?
0.270E+04   AXIAL STRESS RESULTANT
Y           IS NX COMPRESSIVE?
Y           IS PREVIOUS NUMERICAL ENTRY OK?
0.000E+00   CIRCUMFERENTIAL STRESS RESULTANT
Y           IS NY COMPRESSIVE?
Y           IS PREVIOUS NUMERICAL ENTRY OK?
 420.       IN-PLANE SHEAR STRESS RESULTANT
Y           IS PREVIOUS NUMERICAL ENTRY OK?
Y           WANT TO INPUT NXFIXED,NYFIXED?
 625.       FIXED PORTION OF AXIAL RESULTANT
N           IS NXFIXED COMPRESSIVE?
Y           IS PREVIOUS NUMERICAL ENTRY OK?
0.125E+04   FIXED PART OF CIRCUMF. RESULTANT
N           IS NYFIXED COMPRESSIVE?
Y           IS PREVIOUS NUMERICAL ENTRY OK?
 85.0       CYLINDER RADIUS
Y           IS PREVIOUS NUMERICAL ENTRY OK?
 100.       AXIAL LENGTH OF PANEL
Y           IS PREVIOUS NUMERICAL ENTRY OK?
 267.       CIRCUMFERENTIAL LENGTH OF PANEL
Y           IS PREVIOUS NUMERICAL ENTRY OK?
   7        NUMBER OF LAYERS IN PANEL SKIN
Y           IS PREVIOUS NUMERICAL ENTRY OK?
0.500E-02     TLAYER
Y           IS PREVIOUS NUMERICAL ENTRY OK?
0.500E-02     TLAYER
Y           IS PREVIOUS NUMERICAL ENTRY OK?
0.500E-02     TLAYER
Y           IS PREVIOUS NUMERICAL ENTRY OK?
0.100E-01     TLAYER
Y           IS PREVIOUS NUMERICAL ENTRY OK?
0.500E-02     TLAYER
Y           IS PREVIOUS NUMERICAL ENTRY OK?
0.500E-02     TLAYER
Y           IS PREVIOUS NUMERICAL ENTRY OK?
```

```
0.500E-02   TLAYER
Y           IS PREVIOUS NUMERICAL ENTRY OK?
 90.0         ALPHA
Y           IS PREVIOUS NUMERICAL ENTRY OK?
 45.0         ALPHA
Y           IS PREVIOUS NUMERICAL ENTRY OK?
-45.0         ALPHA
Y           IS PREVIOUS NUMERICAL ENTRY OK?
0.000E+00     ALPHA
Y           IS PREVIOUS NUMERICAL ENTRY OK?
-45.0         ALPHA
Y           IS PREVIOUS NUMERICAL ENTRY OK?
 45.0         ALPHA
Y           IS PREVIOUS NUMERICAL ENTRY OK?
 90.0         ALPHA
Y           IS PREVIOUS NUMERICAL ENTRY OK?
   1            MATL
Y           IS PREVIOUS NUMERICAL ENTRY OK?
   1            MATL
Y           IS PREVIOUS NUMERICAL ENTRY OK?
   1            MATL
Y           IS PREVIOUS NUMERICAL ENTRY OK?
   1            MATL
Y           IS PREVIOUS NUMERICAL ENTRY OK?
   1            MATL
Y           IS PREVIOUS NUMERICAL ENTRY OK?
   1            MATL
Y           IS PREVIOUS NUMERICAL ENTRY OK?
   1            MATL
Y           IS PREVIOUS NUMERICAL ENTRY OK?
Y           IS THE PANEL STIFFENED?
Y           WANT MORE INFORMATION?
Y           ARE THERE STRINGERS?
 10.0       STRINGER SPACING
Y           IS PREVIOUS NUMERICAL ENTRY OK?
N           IS THE STIFFENER INTERNAL?
L           CROSS SECTION TYPE FOR THESTRINGERS
Y           IS CROSS-SECTION CHOICE OKAY?
Y           ANY STR. SEGS OF COMPOSITE MAT?
  16        NO. OF LAYERS IN STRINGER SEG.
Y           IS PREVIOUS NUMERICAL ENTRY OK?
0.500E-02   TLAYER
Y           IS PREVIOUS NUMERICAL ENTRY OK?
0.500E-02   TLAYER
Y           IS PREVIOUS NUMERICAL ENTRY OK?
0.500E-02   TLAYER
Y           IS PREVIOUS NUMERICAL ENTRY OK?
0.500E-02   TLAYER
Y           IS PREVIOUS NUMERICAL ENTRY OK?
0.500E-02   TLAYER
Y           IS PREVIOUS NUMERICAL ENTRY OK?
0.500E-02   TLAYER
Y           IS PREVIOUS NUMERICAL ENTRY OK?
```

```
0.500E-02   TLAYER
Y          IS PREVIOUS NUMERICAL ENTRY OK?
0.500E-02   TLAYER
Y          IS PREVIOUS NUMERICAL ENTRY OK?
0.500E-02   TLAYER
Y          IS PREVIOUS NUMERICAL ENTRY OK?
0.500E-02   TLAYER
Y          IS PREVIOUS NUMERICAL ENTRY OK?
0.500E-02   TLAYER
Y          IS PREVIOUS NUMERICAL ENTRY OK?
0.500E-02   TLAYER
Y          IS PREVIOUS NUMERICAL ENTRY OK?
0.500E-02   TLAYER
Y          IS PREVIOUS NUMERICAL ENTRY OK?
0.500E-02   TLAYER
Y          IS PREVIOUS NUMERICAL ENTRY OK?
0.500E-02   TLAYER
Y          IS PREVIOUS NUMERICAL ENTRY OK?
 90.0         ALPHA
Y          IS PREVIOUS NUMERICAL ENTRY OK?
 45.0         ALPHA
Y          IS PREVIOUS NUMERICAL ENTRY OK?
-45.0         ALPHA
Y          IS PREVIOUS NUMERICAL ENTRY OK?
0.000E+00     ALPHA
Y          IS PREVIOUS NUMERICAL ENTRY OK?
0.000E+00     ALPHA
Y          IS PREVIOUS NUMERICAL ENTRY OK?
-45.0         ALPHA
Y          IS PREVIOUS NUMERICAL ENTRY OK?
 45.0         ALPHA
Y          IS PREVIOUS NUMERICAL ENTRY OK?
 90.0         ALPHA
Y          IS PREVIOUS NUMERICAL ENTRY OK?
 90.0         ALPHA
Y          IS PREVIOUS NUMERICAL ENTRY OK?
 45.0         ALPHA
Y          IS PREVIOUS NUMERICAL ENTRY OK?
-45.0         ALPHA
Y          IS PREVIOUS NUMERICAL ENTRY OK?
0.000E+00     ALPHA
Y          IS PREVIOUS NUMERICAL ENTRY OK?
0.000E+00     ALPHA
Y          IS PREVIOUS NUMERICAL ENTRY OK?
-45.0         ALPHA
Y          IS PREVIOUS NUMERICAL ENTRY OK?
 45.0         ALPHA
Y          IS PREVIOUS NUMERICAL ENTRY OK?
 90.0         ALPHA
Y          IS PREVIOUS NUMERICAL ENTRY OK?
    1           MATL
Y          IS PREVIOUS NUMERICAL ENTRY OK?
    1           MATL
Y          IS PREVIOUS NUMERICAL ENTRY OK?
    1           MATL
```

```
Y           IS PREVIOUS NUMERICAL ENTRY OK?
    1          MATL
Y           IS PREVIOUS NUMERICAL ENTRY OK?
    1          MATL
Y           IS PREVIOUS NUMERICAL ENTRY OK?
    1          MATL
Y           IS PREVIOUS NUMERICAL ENTRY OK?
    1          MATL
Y           IS PREVIOUS NUMERICAL ENTRY OK?
    1          MATL
Y           IS PREVIOUS NUMERICAL ENTRY OK?
    1          MATL
Y           IS PREVIOUS NUMERICAL ENTRY OK?
    1          MATL
Y           IS PREVIOUS NUMERICAL ENTRY OK?
    1          MATL
Y           IS PREVIOUS NUMERICAL ENTRY OK?
    1          MATL
Y           IS PREVIOUS NUMERICAL ENTRY OK?
    1          MATL
Y           IS PREVIOUS NUMERICAL ENTRY OK?
    1          MATL
Y           IS PREVIOUS NUMERICAL ENTRY OK?
    1          MATL
Y           IS PREVIOUS NUMERICAL ENTRY OK?
    1          MATL
Y           IS PREVIOUS NUMERICAL ENTRY OK?
   17       NO. OF LAYERS IN STRINGER SEG.
Y           IS PREVIOUS NUMERICAL ENTRY OK?
0.500E-02     TLAYER
Y           IS PREVIOUS NUMERICAL ENTRY OK?
0.500E-02     TLAYER
Y           IS PREVIOUS NUMERICAL ENTRY OK?
0.500E-02     TLAYER
Y           IS PREVIOUS NUMERICAL ENTRY OK?
0.500E-02     TLAYER
Y           IS PREVIOUS NUMERICAL ENTRY OK?
0.500E-02     TLAYER
Y           IS PREVIOUS NUMERICAL ENTRY OK?
0.500E-02     TLAYER
Y           IS PREVIOUS NUMERICAL ENTRY OK?
0.500E-02     TLAYER
Y           IS PREVIOUS NUMERICAL ENTRY OK?
0.500E-02     TLAYER
Y           IS PREVIOUS NUMERICAL ENTRY OK?
0.100         TLAYER
Y           IS PREVIOUS NUMERICAL ENTRY OK?
0.500E-02     TLAYER
Y           IS PREVIOUS NUMERICAL ENTRY OK?
0.500E-02     TLAYER
Y           IS PREVIOUS NUMERICAL ENTRY OK?
0.500E-02     TLAYER
Y           IS PREVIOUS NUMERICAL ENTRY OK?
0.500E-02     TLAYER
Y           IS PREVIOUS NUMERICAL ENTRY OK?
```

```
0.500E-02   TLAYER
Y          IS PREVIOUS NUMERICAL ENTRY OK?
0.500E-02   TLAYER
Y          IS PREVIOUS NUMERICAL ENTRY OK?
0.500E-02   TLAYER
Y          IS PREVIOUS NUMERICAL ENTRY OK?
0.500E-02   TLAYER
Y          IS PREVIOUS NUMERICAL ENTRY OK?
 90.0         ALPHA
Y          IS PREVIOUS NUMERICAL ENTRY OK?
 45.0         ALPHA
Y          IS PREVIOUS NUMERICAL ENTRY OK?
-45.0         ALPHA
Y          IS PREVIOUS NUMERICAL ENTRY OK?
0.000E+00     ALPHA
Y          IS PREVIOUS NUMERICAL ENTRY OK?
0.000E+00     ALPHA
Y          IS PREVIOUS NUMERICAL ENTRY OK?
-45.0         ALPHA
Y          IS PREVIOUS NUMERICAL ENTRY OK?
 45.0         ALPHA
Y          IS PREVIOUS NUMERICAL ENTRY OK?
 90.0         ALPHA
Y          IS PREVIOUS NUMERICAL ENTRY OK?
0.000E+00     ALPHA
Y          IS PREVIOUS NUMERICAL ENTRY OK?
 90.0         ALPHA
Y          IS PREVIOUS NUMERICAL ENTRY OK?
 45.0         ALPHA
Y          IS PREVIOUS NUMERICAL ENTRY OK?
-45.0         ALPHA
Y          IS PREVIOUS NUMERICAL ENTRY OK?
0.000E+00     ALPHA
Y          IS PREVIOUS NUMERICAL ENTRY OK?
0.000E+00     ALPHA
Y          IS PREVIOUS NUMERICAL ENTRY OK?
-45.0         ALPHA
Y          IS PREVIOUS NUMERICAL ENTRY OK?
 45.0         ALPHA
Y          IS PREVIOUS NUMERICAL ENTRY OK?
 90.0         ALPHA
Y          IS PREVIOUS NUMERICAL ENTRY OK?
   1           MATL
Y          IS PREVIOUS NUMERICAL ENTRY OK?
   1           MATL
Y          IS PREVIOUS NUMERICAL ENTRY OK?
   1           MATL
Y          IS PREVIOUS NUMERICAL ENTRY OK?
   1           MATL
Y          IS PREVIOUS NUMERICAL ENTRY OK?
   1           MATL
Y          IS PREVIOUS NUMERICAL ENTRY OK?
   1           MATL
Y          IS PREVIOUS NUMERICAL ENTRY OK?
   1           MATL
```

```
Y           IS PREVIOUS NUMERICAL ENTRY OK?
   1           MATL
Y           IS PREVIOUS NUMERICAL ENTRY OK?
   1           MATL
Y           IS PREVIOUS NUMERICAL ENTRY OK?
   1           MATL
Y           IS PREVIOUS NUMERICAL ENTRY OK?
   1           MATL
Y           IS PREVIOUS NUMERICAL ENTRY OK?
   1           MATL
Y           IS PREVIOUS NUMERICAL ENTRY OK?
   1           MATL
Y           IS PREVIOUS NUMERICAL ENTRY OK?
   1           MATL
Y           IS PREVIOUS NUMERICAL ENTRY OK?
   1           MATL
Y           IS PREVIOUS NUMERICAL ENTRY OK?
   1           MATL
Y           IS PREVIOUS NUMERICAL ENTRY OK?
   1           MATL
Y           IS PREVIOUS NUMERICAL ENTRY OK?
 1.00             BS
Y           IS PREVIOUS NUMERICAL ENTRY OK?
0.500             BS
Y           IS PREVIOUS NUMERICAL ENTRY OK?
N           DO STRINGER STUFF AGAIN?
Y           ARE THERE RINGS?
 10.0       RING SPACING
Y           IS PREVIOUS NUMERICAL ENTRY OK?
Y           IS THE STIFFENER INTERNAL?
L           CROSS SECTION TYPE FOR THE  RINGS
Y           IS CROSS-SECTION CHOICE OKAY?
N           ANY RING SEGS OF COMPOSITE MAT?
0.500E-01         TR
Y           IS PREVIOUS NUMERICAL ENTRY OK?
0.500E-01         TR
Y           IS PREVIOUS NUMERICAL ENTRY OK?
 1.00             BR
Y           IS PREVIOUS NUMERICAL ENTRY OK?
0.500             BR
Y           IS PREVIOUS NUMERICAL ENTRY OK?
   2           MATL
Y           IS PREVIOUS NUMERICAL ENTRY OK?
   2           MATL
Y           IS PREVIOUS NUMERICAL ENTRY OK?
N           WANT TO DO RING STUFF AGAIN?
0.230E+08 MODULUS IN FIBER DIRECTION
Y           IS PREVIOUS NUMERICAL ENTRY OK?
N           IS THIS MATERIAL ISOTROPIC?
0.170E+07 MODULUS NORMAL TO E1-DIRECTION
Y           IS PREVIOUS NUMERICAL ENTRY OK?
0.940E+06 IN-PLANE SHEAR MODULUS
Y           IS PREVIOUS NUMERICAL ENTRY OK?
0.225E-01 POISSONS RATIO
Y           IS PREVIOUS NUMERICAL ENTRY OK?
```

```
0.560E-01 WEIGHT DENSITY
Y         IS PREVIOUS NUMERICAL ENTRY OK?
N         WANT TO INPUT STRESS-STRAIN?
N         WANT TO INPUT EFFECTIVE STRESS?
0.565E-02 MAX TENSILE STRAIN, E1-DIRECTION
Y         IS PREVIOUS NUMERICAL ENTRY OK?
0.452E-02 MAX COMP. STRAIN,  E1-DIRECTION
Y         IS PREVIOUS NUMERICAL ENTRY OK?
0.320E-02 MAX TENSILE STRAIN, E2-DIRECTION
Y         IS PREVIOUS NUMERICAL ENTRY OK?
0.125E-01 MAX COMP. STRAIN,  E2-DIRECTION
Y         IS PREVIOUS NUMERICAL ENTRY OK?
0.125E-01 MAX IN-PLANE SHEAR STRAIN
Y         IS PREVIOUS NUMERICAL ENTRY OK?
N         DO MATERIAL PROPERTIES AGAIN?
0.100E+08 MODULUS IN FIBER DIRECTION
Y         IS PREVIOUS NUMERICAL ENTRY OK?
Y         IS THIS MATERIAL ISOTROPIC?
0.300     POISSONS RATIO
Y         IS PREVIOUS NUMERICAL ENTRY OK?
0.100     WEIGHT DENSITY
Y         IS PREVIOUS NUMERICAL ENTRY OK?
N         WANT TO INPUT STRESS-STRAIN?
Y         WANT TO INPUT EFFECTIVE STRESS?
0.400E+05 MAXIMUM EFFECTIVE STRESS
Y         IS PREVIOUS NUMERICAL ENTRY OK?
N         DO MATERIAL PROPERTIES AGAIN?
N         IS LOCAL/GENERAL NOT = UNITY?
```

```
$ RUN DECIDE                    (choose decision variables for optimization)

 COMPOSITE STIFF. CYL., FIXED INT. PRESS., NX =-2700, NXY=420 LB/IN.


INPUT DATA SUPPLIED INTERACTIVELY BY YOU IN THIS RUN
ARE STORED ON A PERMANENT FILE. WHAT IS THE NAME OF THIS FILE?
(9 CHARACTERS OR LESS, PLEASE, AND ONE WORD.)

 PERMANENT FILE NAME =
PERMANENT FILE NAME =PANDADECI.DAT

IS PART OR ALL OF THE INPUT FOR THIS CASE STORED ON
THIS FILE YET?
Y

DO YOU WISH TO CHANGE THE TITLE OF THIS CASE...
N
DO YOU WANT MORE INFORMATION ON THIS PROGRAM?
Y
    THE FOLLOWING TERMS ARE USED IN THIS PROGRAM, AND
IT IS VERY IMPORTANT THAT YOU UNDERSTAND THEIR MEANING...

**********************************************************
**********************************************************

 (1)  DESIGN PARAMETER-- ANY STRUCTURAL DIMENSION OR WINDING
                         ANGLE.

 (2)  DECISION VARIABLE- A DESIGN PARAMETER WHICH HAS BEEN
                         SELECTED AS A PRIMARY VARIABLE IN THE
                         OPTIMIZATION PROCESS.

 (3)  LINKED VARIABLE--  A DESIGN PARAMETER WHICH HAS BEEN
                         SELECTED AS A SECONDARY VARIABLE IN
                         THE OPTIMIZATION PROCESS.   A LINKED
                         VARIABLE IS PROPORTIONAL TO ONE OF
                         THE DECISION VARIABLES, BUT IS NOT A
                         MEMBER OF THE VECTOR  OF DECISION
                         VARIABLES, (X(I),I=1,NDV).

**********************************************************
**********************************************************


 DO YOU WANT MORE INFORMATION?
Y

     FIRST YOU DECIDE WHICH OF THE DESIGN PARAMETERS
(DIMENSIONS AND WINDING ANGLES) ARE TO BE DECISION VARIABLES
IN THE OPTIMIZATION PROCESS.  YOU CAN SELECT AS DECISION
VARIABLES ANY SUBSET OF DESIGN PARAMETERS YOU WISH.   OTHER
DESIGN PARAMETERS CAN BE SELECTED AS BEING LINKED TO DECISION
VARIABLES.  A LINKED VARIABLE Y WILL VARY IN PROPORTION TO A
USER-SELECTED DECISION VARIABLE X, AS FOLLOWS...
```

```
    Y(A LINKED VARIABLE) = C * X(A DECISION VARIABLE)

IN WHICH YOU CHOOSE THE CONSTANT OF PROPORTIONALITY  C  AND
WHICH DECISION VARIABLE  X  THAT  Y  IS LINKED TO.   THE
OPTIMUM DESIGN IS OBTAINED ITERATIVELY BY THE METHOD OF
FEASIBLE DIRECTIONS  (VANDERPLAATS).   SEE THE LOCKHEED
REPORT          AND ITS REFERENCES FOR FURTHER DETAILS.


DO YOU WISH TO CHANGE THE LOADS OR THE FACTOR PHI
N

DO YOU WANT TO MAKE THE PANEL FLAT...
N

YOU CAN DO TWO TYPES OF ANALYSIS WITH PANDA:

    1. A BUCKLING ANALYSIS OF A FIXED DESIGN (NO OPTIMIZATION)
    2. AN OPTIMIZATION ANALYSIS

DO YOU WANT TO DO A BUCKLING ANALYSIS OF A FIXED DESIGN?
N


DO YOU WISH TO CHANGE SOME OF THE STRUCTURAL DIMENSIONS
OR WINDING ANGLES..
N

NOTE... DEFAULT VALUES FOR LOWER AND UPPER BOUNDS OF A
DECISION VARIABLE X ARE...

           LOWER BOUND = X/100
           UPPER BOUND = X*100

IN WHICH X IS THE CURRENT VALUE OF THE DECISION VARIABLE.

ARE ANY OF THE SHELL WALL LAYER THICKNESSES DECISION VARIABLES...
Y

DO YOU WANT TO USE DEFAULT VALUES FOR LOWER AND UPPER BOUNDS
OF SHELL WALL LAYER THICKNESSES...
N

IS THE THICKNESS OF LAYER NO. 1 A DECISION VARIABLE.
Y

LOWER BOUND FOR THICKNESS OF LAYER NO. 1 =

UPPER BOUND FOR THICKNESS OF LAYER NO. 1 =
(LOWER,UPPER) BOUNDS FOR THICKNESS OF LAYER NO. 1 =
(   5.000E-03 ,   1.500E-02)

IS THE THICKNESS OF LAYER NO. 2 A DECISION VARIABLE.
```

```
N

IS THE THICKNESS OF LAYER NO. 2 LINKED TO THE THICKNESS
OF A PREVIOUS LAYER IN THE SKIN...
(NOTE THAT THIS PREVIOUS LAYER THICKNESS
MUST BE A DECISION VARIABLE)
Y

WHICH PREVIOUS LAYER...
THE THICKNESS OF LAYER NO. 2 IS LINKED TO THAT OF LAYER 1
SUPPOSE THAT THE THICKNESS, T, OF LAYER NO. 2 =

        T( 2) = C * T( 1).              WHAT IS C...
THICKNESS, T( 2) =  1.00E+00 * T( 1).
T( 1) IS A DECISION VARIABLE.

IS THE THICKNESS OF LAYER NO. 3 A DECISION VARIABLE.
N

IS THE THICKNESS OF LAYER NO. 3 LINKED TO THE THICKNESS
OF A PREVIOUS LAYER IN THE SKIN...
Y

WHICH PREVIOUS LAYER...
THE THICKNESS OF LAYER NO. 3 IS LINKED TO THAT OF LAYER 1
SUPPOSE THAT THE THICKNESS, T, OF LAYER NO. 3 =

        T( 3) = C * T( 1).              WHAT IS C...
THICKNESS, T( 3) =  1.00E+00 * T( 1).
T( 1) IS A DECISION VARIABLE.

IS THE THICKNESS OF LAYER NO. 4 A DECISION VARIABLE.
N

IS THE THICKNESS OF LAYER NO. 4 LINKED TO THE THICKNESS
OF A PREVIOUS LAYER IN THE SKIN...
Y

WHICH PREVIOUS LAYER...
THE THICKNESS OF LAYER NO. 4 IS LINKED TO THAT OF LAYER 1
SUPPOSE THAT THE THICKNESS, T, OF LAYER NO. 4 =

        T( 4) = C * T( 1).              WHAT IS C...
THICKNESS, T( 4) =  2.00E+00 * T( 1).
T( 1) IS A DECISION VARIABLE.

IS THE THICKNESS OF LAYER NO. 5 A DECISION VARIABLE.
N

IS THE THICKNESS OF LAYER NO. 5 LINKED TO THE THICKNESS
OF A PREVIOUS LAYER IN THE SKIN...
Y

WHICH PREVIOUS LAYER...
THE THICKNESS OF LAYER NO. 5 IS LINKED TO THAT OF LAYER 1
```

```
SUPPOSE THAT THE THICKNESS, T, OF LAYER NO. 5 =

        T( 5) = C * T( 1).              WHAT IS C...
THICKNESS, T( 5) =  1.00E+00 * T( 1).
T( 1) IS A DECISION VARIABLE.

IS THE THICKNESS OF LAYER NO. 6 A DECISION VARIABLE.
N

IS THE THICKNESS OF LAYER NO. 6 LINKED TO THE THICKNESS
OF A PREVIOUS LAYER IN THE SKIN...
Y

WHICH PREVIOUS LAYER...
THE THICKNESS OF LAYER NO. 6 IS LINKED TO THAT OF LAYER 1
SUPPOSE THAT THE THICKNESS, T, OF LAYER NO. 6 =

        T( 6) = C * T( 1).              WHAT IS C...
THICKNESS, T( 6) =  1.00E+00 * T( 1).
T( 1) IS A DECISION VARIABLE.

IS THE THICKNESS OF LAYER NO. 7 A DECISION VARIABLE.
N

IS THE THICKNESS OF LAYER NO. 7 LINKED TO THE THICKNESS
OF A PREVIOUS LAYER IN THE SKIN...
Y

WHICH PREVIOUS LAYER...
THE THICKNESS OF LAYER NO. 7 IS LINKED TO THAT OF LAYER 1
SUPPOSE THAT THE THICKNESS, T, OF LAYER NO. 7 =

        T( 7) = C * T( 1).              WHAT IS C...
THICKNESS, T( 7) =  1.00E+00 * T( 1).
T( 1) IS A DECISION VARIABLE.

ARE ANY OF THE LAYER WINDING ANGLES DECISION VARIABLES
N

IS THE STRINGER SPACING A DECISION VARIABLE...
Y

DO YOU WANT TO USE DEFAULT VALUES FOR LOWER AND UPPER BOUNDS
OF STRINGER SPACING...
N

LOWER BOUND FOR STRINGER SPACING=

UPPER BOUND FOR STRINGER SPACING=
(LOWER,UPPER) BOUNDS FOR STRINGER SPACING=
(   3.000E+00 ,   3.000E+01)

ARE ANY OF THE STRINGER SEGMENT THICKNESSES DECISION VARIABLES..
Y
```

```
DO YOU WANT TO USE DEFAULT VALUES FOR LOWER AND UPPER BOUNDS
OF STRINGER SEGMENT THICKNESSES...
N

IS THE THICKNESS OF STRINGER SEG. NO. 1 A DECISION VARIABLE..
Y

LOWER BOUND FOR THICKNESS OF STRINGER SEGMENT NO. 1=

UPPER BOUND FOR THICKNESS OF STRINGER SEGMENT NO. 1=
(LOWER,UPPER) BOUNDS FOR THICKNESS OF STRINGER SEGMENT NO. 1=
(    8.000E-02 ,    3.200E-01)

IS THE THICKNESS OF STRINGER SEG. NO. 2 A DECISION VARIABLE..
Y

LOWER BOUND FOR THICKNESS OF STRINGER SEGMENT NO. 2=

UPPER BOUND FOR THICKNESS OF STRINGER SEGMENT NO. 2=
(LOWER,UPPER) BOUNDS FOR THICKNESS OF STRINGER SEGMENT NO. 2=
(    8.000E-02 ,    4.200E-01)

ARE ANY OF THE STRINGER SEG. WIDTHS DECISION VARIABLES...
Y

DO YOU WANT TO USE DEFAULT VALUES FOR LOWER AND UPPER BOUNDS
OF STRINGER SEGMENT  WIDTHS...
Y

IS THE  WIDTH BS(I) OF STRINGER SEGMENT NO. 1
A DECISION VARIABLE...
Y
(LOWER,UPPER) BOUNDS FOR WIDTHS OF STRINGER SEG. 1=
(    1.000E-02 ,    1.000E+02)

IS THE  WIDTH BS(I) OF STRINGER SEGMENT NO. 2
A DECISION VARIABLE...
Y
(LOWER,UPPER) BOUNDS FOR WIDTHS OF STRINGER SEG. 2=
(    5.000E-03 ,    5.000E+01)

IS THE   RING   SPACING A DECISION VARIABLE...
Y

DO YOU WANT TO USE DEFAULT VALUES FOR LOWER AND UPPER BOUNDS
OF RING SPACING...
N

LOWER BOUND FOR   RING   SPACING=

UPPER BOUND FOR   RING   SPACING=
(LOWER,UPPER) BOUNDS FOR RING SPACING=
(    3.000E+00 ,    3.000E+01)

ARE ANY OF THE   RING   SEGMENT THICKNESSES DECISION VARIABLES..
```

```
Y

DO YOU WANT TO USE DEFAULT VALUES FOR LOWER AND UPPER BOUNDS
OF RING SEGMENT THICKNESSES...
N

IS THE THICKNESS OF   RING   SEG. NO. 1 A DECISION VARIABLE..
Y

LOWER BOUND FOR THICKNESS OF   RING   SEGMENT NO. 1=

UPPER BOUND FOR THICKNESS OF   RING   SEGMENT NO. 1=
(LOWER,UPPER) BOUNDS FOR THICKNESS OF RING SEGMENT NO. 1=
(   5.000E-02 ,   3.000E-01)

IS THE THICKNESS OF   RING   SEG. NO. 2 A DECISION VARIABLE..
Y

LOWER BOUND FOR THICKNESS OF   RING   SEGMENT NO. 2=

UPPER BOUND FOR THICKNESS OF   RING   SEGMENT NO. 2=
(LOWER,UPPER) BOUNDS FOR THICKNESS OF RING SEGMENT NO. 2=
(   5.000E-02 ,   3.000E-01)

ARE ANY OF THE RING SEG. WIDTHS DECISION VARIABLES...
Y

DO YOU WANT TO USE DEFAULT VALUES FOR LOWER AND UPPER BOUNDS
OF RING SEGMENT  WIDTHS...
Y

IS THE  WIDTH BR(I)  OF  RING   SEGMENT NO. 1
A DECISION VARIABLE...
Y
(LOWER,UPPER) BOUNDS FOR  WIDTHS OF RING SEG. 1=
(   1.000E-02 ,   1.000E+02)

IS THE  WIDTH BP(I)  OF  RING   SEGMENT NO. 2
A DECISION VARIABLE...
Y
(LOWER,UPPER) BOUNDS FOR  WIDTHS OF RING SEG. 2=
(   5.000E-03 ,   5.000E+01)


WHEN YOUR TERMINAL SAYS

            READY

  PLEASE TYPE THE COMMAND

            -PANCON
```

```
(The following is the input data file PANDADECI.DAT generated by
 execution of DECIDE.  If any errors were made during
 interactive
 input, they can be corrected by editing of this file, rather
 than having to answer all the questions posed by DECIDE again.
 Note that in order to use this file as is for execution by
 DECIDE, it will be necessary to rerun BEGIN with the file
 PANDACASE.DAT)

 N           CHANGE TITLE?
 Y           WANT MORE INFORMATION?
 Y           WANT MORE INFORMATION?
 N           CHANGE LOADING?
 N           MAKE PANEL FLAT OR CURVED?
 N           DO BUCKLING ONLY?
 N           CHANGE DIMENSIONS?
 Y           ANY t(i) DECISION VARIABLES?
 N           WANT DEFAULT BOUNDS ON t(i)?
 Y           IS t(i) A DECISION VARIABLE?
 0.500E-02 LOWER BOUND FOR THICKNESS OF LAYER NO.   1
 0.150E-01 UPPER BOUND FOR THICKNESS OF LAYER NO.   1
 N           IS t(i) A DECISION VARIABLE?
 Y           IS t(i) LINKED TO PREVIOUS t?
    1           t( 2) LINKED TO t( 1)
  1.00       LINKING FACTOR OF PROPORTIONALITY
 N           IS t(i) A DECISION VARIABLE?
 Y           IS t(i) LINKED TO PREVIOUS t?
    1           t( 3) LINKED TO t( 1)
  1.00       LINKING FACTOR OF PROPORTIONALITY
 N           IS t(i) A DECISION VARIABLE?
 Y           IS t(i) LINKED TO PREVIOUS t?
    1           t( 4) LINKED TO t( 1)
  2.00       LINKING FACTOR OF PROPORTIONALITY
 N           IS t(i) A DECISION VARIABLE?
 Y           IS t(i) LINKED TO PREVIOUS t?
    1           t( 5) LINKED TO t( 1)
  1.00       LINKING FACTOR OF PROPORTIONALITY
 N           IS t(i) A DECISION VARIABLE?
 Y           IS t(i) LINKED TO PREVIOUS t?
    1           t( 6) LINKED TO t( 1)
  1.00       LINKING FACTOR OF PROPORTIONALITY
 N           IS t(i) A DECISION VARIABLE?
 Y           IS t(i) LINKED TO PREVIOUS t?
    1           t( 7) LINKED TO t( 1)
  1.00       LINKING FACTOR OF PROPORTIONALITY
 N           ANY a(i) DECISION VARIABLES?
 Y           IS bo A DECISION VARIABLE?
 N           WANT DEFAULT BOUNDS ON bo?
  3.00       LOWER BOUND OF STRINGER SPACING
  30.0       UPPER BOUND OF STRINGER SPACING
 Y           ANY ts(i) DECISION VARIABLES?
 N           WANT DEFAULT BOUNDS ON ts(i)?
 Y           IS ts(i) A DECISION VARIABLE?
 0.800E-01 LOWER BOUND OF THICKNESS, STRINGER SEG.  1
```

```
0.320       UPPER BOUND OF THICKNESS, STRINGER SEG. 1
Y           IS ts(i) A DECISION VARIABLE?
0.800E-01 LOWER BOUND OF THICKNESS, STRINGER SEG. 2
0.420       UPPER BOUND OF THICKNESS, STRINGER SEG. 2
Y           ANY bs(i) DECISION VARIABLES?
Y           WANT DEFAULT BOUNDS ON bs(i)?
Y           IS bs(i) A DECISION VARIABLE?
Y           IS bs(i) A DECISION VARIABLE?
Y           IS ao A DECISION VARIABLE?
N           WANT DEFAULT BOUNDS ON ao?
 3.00       LOWER BOUND OF RING SPACING
 30.0       UPPER BOUND OF RING SPACING
Y           ANY tr(i) DECISION VARIABLES?
N           WANT DEFAULT BOUNDS ON tr(i)?
Y           IS tr(i) A DECISION VARIABLE?
0.500E-01 LOWER BOUND OF tr OF RING SEGMENT NO. 1
0.300       UPPER BOUND OF tr OF RING SEGMENT NO. 1
Y           IS tr(i) A DECISION VARIABLE?
0.500E-01 LOWER BOUND OF tr OF RING SEGMENT NO. 2
0.300       UPPER BOUND OF tr OF RING SEGMENT NO. 2
Y           ANY br(i) DECISION VARIABLES?
Y           WANT DEFAULT BOUNDS ON br(i)?
Y           IS br(i) A DECISION VARIABLE?
Y           IS br(i) A DECISION VARIABLE?
```

```
$ RUN PANCON                                    (perform the optimization analysis)

COMPOSITE STIFF. CYL.,FIXED INT. PRESS., NX=-2700, NXY=420 LB/IN.

PANEL WEIGHT=  1.0525E+02

PANEL WEIGHT=  1.1578E+02

PANEL WEIGHT=  1.2735E+02

PANEL WEIGHT=  1.4009E+02

PANEL WEIGHT=  1.5410E+02

PANEL WEIGHT=  1.6951E+02

PANEL WEIGHT=  1.8646E+02

PANEL WEIGHT=  2.0511E+02

PANEL WEIGHT=  3.2261E+02

PANEL WEIGHT=  2.7252E+02

PANEL WEIGHT=  2.2967E+02

PANEL WEIGHT=  2.0718E+02

PANEL WEIGHT=  1.9705E+02
DO YOU WISH TO PRINT OUT A SUMMARY OF DESIGN INFORMATION. . .

NO

DO YOU WISH TO DO MORE ITERATIONS WITH THE SAME DECISION
VARIABLES...
YES

PANEL WEIGHT=  1.9705E+02

PANEL WEIGHT=  1.8745E+02

PANEL WEIGHT=  1.7955E+02

PANEL WEIGHT=  1.6090E+02

PANEL WEIGHT=  1.4400E+02

PANEL WEIGHT=  1.3715E+02
```

```
DO YOU WISH TO PRINT OUT A SUMMARY OF DESIGN INFORMATION. . .

NO

DO YOU WISH TO DO MORE ITERATIONS WITH THE SAME DECISION
VARIABLES...
YES

PANEL WEIGHT=  1.3715E+02

PANEL WEIGHT=  1.3361E+02

PANEL WEIGHT=  1.3323E+02

PANEL WEIGHT=  1.3315E+02

PANEL WEIGHT=  1.3302E+02

PANEL WEIGHT=  1.3300E+02
DO YOU WISH TO PRINT OUT A SUMMARY OF DESIGN INFORMATION. . .

NO

DO YOU WISH TO DO MORE ITERATIONS WITH THE SAME DECISION
VARIABLES...
YES

PANEL WEIGHT=  1.3300E+02

PANEL WEIGHT=  1.3299E+02

PANEL WEIGHT=  1.3297E+02

PANEL WEIGHT=  1.3287E+02

PANEL WEIGHT=  1.3281E+02

PANEL WEIGHT=  1.3281E+02
```

```
DO YOU WISH TO PRINT OUT A SUMMARY OF DESIGN INFORMATION. . .

YES

 COMPOSITE STIFF. CYL.,FIXED INT. PRESS., NX=-2700, NXY=420 LB/IN.


**********************************************************
PANEL WEIGHT =                                    1.3281E+02
DESIGN VARIABLES FOR ITERATION NUMBER  5 FOLLOW...
THICKNESS OF PANEL SKIN LAYER NO. 1 =             8.7963E-03
STRINGER SPACING, B =                             3.0000E+00
THICKNESS OF STRINGER SEGMENT NO. 1 =             8.0000E-02
THICKNESS OF STRINGER SEGMENT NO. 2 =             9.7748E-02
WIDTH, BS(I), OF STRINGER SEGMENT 1 =             3.6710E-01
WIDTH, BS(I), OF STRINGER SEGMENT 2 =             2.5251E-01
RING SPACING, A =                                 1.4072E+01
THICKNESS OF RING SEGMENT NO. 1 =                 5.0000E-02
THICKNESS OF RING SEGMENT NO. 2 =                 5.0000E-02
WIDTH, BR(I), OF RING SEGMENT 1 =                 5.2489E-02
WIDTH, BR(I), OF RING SEGMENT 2 =                 1.6261E-02


        (M=AXIAL, N=CIRC.) HALF-WAVES OVER ENTIRE PANEL (AXIAL,CIRC.)
GENERAL INSTABILITY EIGENVALUE(M,N)=          9.9798E-01(   1,  12)
LOCAL SKIN (BUCKLING/PHI)  (M,N) =            9.9885E-01(  63,  88)
BUCKLING BETWEEN RINGS WITH SMEARD STRINGRS=  1.1330E+00(   7,   7)
BUCKLING BETWEEN STRINGRS WITH SMEARD RINGS=  1.0057E+00(  61,  88)
BUCKLING/PHI (M) OF STRINGER SEGMENT NO. 1=   5.5507E+01( 270)
BUCKLING/PHI (M) OF STRINGER SEGMENT NO. 2=   2.4750E+01( 270)
LOCAL ROLLING WITH SKIN BUCKLING BETWN STIF=  1.4840E+00(  42,  88)
ROLLING OF STRINGERS(M,0), NO SKIN BUCKLING=  1.7808E+01(  40,   0)
AXISYMMETRIC ROLLING OF RINGS, NO SKIN BUCK=  1.0000E+23(   0,   0)
BUCKLING(ROLLING) MODE WITH SMEARD STRINGRS=  1.1330E+00(   7,   7)
BUCKLING(ROLLING) MODE WITH SMEARED RINGS =   1.4927E+00(  43,  88)
MARGIN FOR STRAIN  -EPS1  IN LAYER 4 =         1.5992E+00
MARGIN FOR STRAIN  +EPS2  IN LAYER 4 =         1.2104E+00
MARGIN FOR   COMP. STRAIN IN STRINGER SEG. 1=  1.5992E+00
MARGIN FOR   COMP. STRAIN IN STRINGER SEG. 2=  1.5992E+00
MARGIN FOR TENSILE STRAIN IN   RING   SEG. 1=  1.5198E+00
MARGIN FOR TENSILE STRAIN IN   RING   SEG. 2=  1.5198E+00
**********************************************************


DO YOU WISH TO DO MORE ITERATIONS WITH THE SAME DECISION
VARIABLES...
NO


DO YOU WANT TO PRINT OUT MORE INFORMATION ABOUT THE
CURRENT DESIGN...  (ABOUT ONE PAGE)
YES
```

COMPOSITE STIFF. CYL.,FIXED INT. PRESS., NX=-2700, NXY=420 LB/IN.

COMMENT ABOUT PRESTRESS AND CRITICAL LOAD COMBINATION...
IN THE FOLLOWING TWO INSTANCES...

1. MATERIAL STRESSED IN THE ELASTIC REGIME OR
2. IF, REGARDLESS OF ANY PLASTICITY, THE EIGENVALUE, LAMBDA, EQUALS UNITY

THE CRITICAL IN-PLANE RESULTANTS ARE GIVEN BY...

NX(CRIT) = NXP + LAMBDA*NX
NY(CRIT) = NYP + LAMBDA*NY
NXY(CRIT) = 0.0 + LAMBDA*NXY

IN WHICH	(NXP, NYP) =	6.250E+02	1.250E+03	
AND	(NX, NY, NXY) =	-2.700E+03	0.000E+00	4.200E+02

AND LAMBDA REPRESENTS ANY OF THE EIGENVALUES PRINTED IN THE FOLLOWING...

CURRENT DESIGN FOLLOWS....

PANEL RADIUS OF CURVATURE	=	8.500E+01		
PANEL AXIAL, CIRC. LENGTHS	=	1.000E+02	2.670E+02	
PANEL AXIAL PRESTRESS, NXP	=	6.250E+02	(NOT AN EIGENPARAM)	
PANEL CIRC. PRESTRESS, NYP	=	1.250E+03	(NOT AN EIGENPARAM)	
PANEL TOTAL THICKNESS	=	7.037E-02		
PANEL LAYER THICKNESSES	=	8.796E-03	8.796E-03	8.796E-03
		1.759E-02	8.796E-03	8.796E-03
		8.796E-03		
PANEL LAYER WINDING ANGLES	=	9.000E+01	4.500E+01	-4.500E+01
		0.000E+00	-4.500E+01	4.500E+01
		9.000E+01		
PANEL LAYER MATERIAL TYPES	=	1	1	1
		1	1	1
		1		

STRINGER DESIGN DATA FOLLOWS...

STRINGER SPACING, B	=	3.000E+00	
STRINGER SEGMENT THICKNESSES	=	8.000E-02	9.775E-02
STRINGER SEGMENT WIDTHS	=	3.671E-01	2.525E-01
STRINGER SEGMENT ANGLES	=	0.000E+00	9.000E+01
STRINGER SEG. MATERIAL TYPES	=	3	4

RING DESIGN DATA FOLLOWS...

RING SPACING, A	=	1.407E+01	
RING SEGMENT THICKNESSES	=	5.000E-02	5.000E-02
RING SEGMENT WIDTHS	=	5.249E-02	1.626E-02
RING SEGMENT ANGLES	=	1.800E+02	9.000E+01
RING SEGMENT MATERIAL TYPES	=	2	2

```
MODULI (E1, E2, G) OF MATL  1 =   2.300E+07   1.700E+06   9.400E+05
POISSON RAT., DENSITY MATL  1 =   2.250E-02   5.600E-02
MODULI (E1, E2, G) OF MATL  2 =   1.000E+07   1.000E+07   3.846E+06
POISSON RAT., DENSITY MATL  2 =   3.000E-01   1.000E-01
MODULI (E1, E2, G) OF MATL  3 =   9.002E+06   9.002E+06   3.449E+06
POISSON RAT., DENSITY MATL  3 =   3.052E-01   5.600E-02
MODULI (E1, E2, G) OF MATL  4 =   1.678E+07   5.208E+06   2.055E+06
POISSON RAT., DENSITY MATL  4 =   9.469E-02   5.600E-02

THE TOTAL PANEL WEIGHT       =   1.328E+02
 THE PANEL SKIN WEIGHT       =   1.052E+02
 THE TOTAL STIFFENER WEIGHT  =   2.759E+01

GENERAL INSTABILITY QUANIITIES (STIFFENERS SMEARED OUT)...
 AXIAL STRESS RESULTANT, NX  =  -2.700E+03 (AN EIGENPARAMETER)
 CIRC. STRESS RESULTANT, NY  =   0.000E+00 (AN EIGENPARAMETER)
 SHEAR STRESS RESULTANT, NXY =   4.200E+02 (AN EIGENPARAMETER)
 AXIAL HALF WAVES OVER PANEL =    1
 CIRC. HALF WAVES OVER PANEL =   12
 SLOPE OF BUCKLING NODAL LINES=  7.081E-01
GENERAL INSTABILITY MULTIPLIER=  9.980E-01   (EIGENVALUE)

LOCAL INSTABILITY QUANTITIES (BUCKLING BETWEEN STIFFENERS)...
 AXIAL RESULTANT IN SKIN     =  -1.997E+03 (AN EIGENPARAMETER)
 CIRC. RESULTANT IN SKIN     =  -8.949E+00 (AN EIGENPARAMETER)
 SHEAR RESULTANT IN SKIN     =   4.200E+02 (AN EIGENPARAMETER)
AXIAL HALF WAVES BETWEEN RINGS=    9
CIRC. HALF WAVES BET STRINGERS=    1
SLOPE OF BUCKLING NODAL LINES =   1.320E-01
LOCAL INSTABILITY MULTIPLIER  =   9.989E-01   (EIGENVALUE)

INSTABILITY WITH SMEARED STRINGERS, BETWEEN RINGS...
 AXIAL RESULTANT IN PANEL    =  -2.700E+03 (AN EIGENPARAMETER)
 CIRC. RESULTANT IN SKIN     =  -8.949E+00 (AN EIGENPARAMETER)
 SHEAR RESULTANT IN SKIN     =   4.200E+02 (AN EIGENPARAMETER)
AXIAL HALF WAVES BETWEEN RINGS=    1
CIRC. HALF WAVES OVER PANEL   =    7
SLOPE OF BUCKLING NODAL LINES =   9.091E+00
SMEARED STRINGER EIGENVALUE   =   1.133E+00   (EIGENVALUE)

INSTABILITY WITH SMEARED RINGS, BETWEEN STRINGERS...
 AXIAL RESULTANT IN SKIN     =  -1.997E+03 (AN EIGENPARAMETER)
 CIRC. RESULTANT IN PANEL    =   0.000E+00 (AN EIGENPARAMETER)
 SHEAR RESULTANT IN SKIN     =   4.200E+02 (AN EIGENPARAMETER)
AXIAL HALF WAVES OVER PANEL   =   61
CIRC. HALF WAVES BET STRINGERS=    1
SLOPE OF BUCKLING NODAL LINES =   1.320E-01
SMEARED   RING   EIGENVALUE   =   1.006E+00   (EIGENVALUE)
```

```
AVERAGE AXIAL STRAIN          =  -2.826E-03
AVERAGE MIDBAY HOOP STRAIN    =   2.644E-03
AVERAGE SHEAR STRAIN          =   1.731E-03
FIBER STRAINS AT EACH LAYER CENTER=
                                   2.644E-03   7.731E-04  -9.572E-04
                                  -2.826E-03  -9.561E-04   7.750E-04
                                   2.644E-03
STRAINS NORMAL TO FIBERS IN LAYERS=
                                  -2.829E-03  -9.576E-04   7.735E-04
                                   2.644E-03   7.746E-04  -9.557E-04
                                  -2.824E-03
SHEAR STRAINS IN MATERIAL COORDS  =
                                  -1.731E-03   5.472E-03  -5.471E-03
                                   1.731E-03  -5.469E-03   5.468E-03
                                  -1.731E-03
AVERAGE STRAIN IN RINGS       =   2.633E-03
RADIUS(CYL.)/RADIUS(RING C.G.)=   1.000E+00

THE ABOVE STRAIN COMPONENTS RESULT FROM THE COMBINED
IN-PLANE RESULTANTS ..

                     NXP + NX =  -2.075E+03
                     NYP + NY =   1.250E+03
                          NXY =   4.200E+02


STRESS RESULTANTS IN THE STIFFENER SEGMENTS CONSIST OF
TWO PARTS.. A FIXED PRESTRESS WHICH ARISES FROM NXP AND NYP
AND AN ADDITIONAL STRESS (EIGENSTRESS) THAT ARISES FROM NX AND
NY.  THE CRITICAL RESULTANT IN THE ISEG TH SEGMENT OF EITHER
STRINGERS OR RINGS IS GIVEN BY...

   NCRIT(ISEG) = PRESTRESS(ISEG) + LAMBDA * EIGENSTRESS(ISEG)

IN WHICH LAMBDA IS ANY OF THE EIGENVALUES PRINTED ABOVE OR IN
THE FOLLOWING...


PRESTRESS(LB/IN) IN STRING.SEGS=   2.036E+02   4.637E+02
EIGENSTRESS IN STRINGER SEGS.  =  -2.239E+03  -5.099E+03
PRESTRESS(LB/IN) IN RING SEGS. =   8.465E+02   8.465E+02
EIGENSTRESS IN   RING   SEGS.  =   4.700E+02   4.700E+02

LOCAL ROLLING MODE EIGENVALUE =   1.484E+00
CORRESPONDING TO    6 AXIAL HALF WAVES BETWEEN RINGS AND
CORRESPONDING TO    1 CIRC. HALF WAVES BETWEEN STRINGERS

SMEARED STRINGER ROLLING MODE EIGENVALUE=   1.133E+00
CORRESPONDING TO    1 AXIAL HALF WAVES BETWEEN RINGS AND
CORRESPONDING TO    7 CIRC. HALF WAVES OVER PANEL

SMEARED   RING   ROLLING MODE EIGENVALUE=   1.493E+00
CORRESPONDING TO   43 AXIAL HALF WAVES OVER PANEL AND
CORRESPONDING TO    1 CIRC. HALF WAVES BETWEEN STRINGERS
```

```
STRINGER ROLLING MODE
 (NO BUCKLING OF SKIN)          =    1.781E+01
NUMBER OF AXIAL HALF WAVES =    40


AXISYMMETRIC(N=0) RING WEB BUCKLING=  1.0000E+23


DO YOU WISH TO SAVE THIS DESIGN ON THE CATALOGUED FILE...
YES
```


☆U.S.Government Printing Office: 1982 — 559-005/40[illegible]

END

DATE
FILMED

03-82

DTIC